

MODELING OF STEADY STATE HEAT RELEASE,
OXYGEN PROFILE AND TEMPERATURE PROFILE IN
CIRCULATING FLUIDIZED BED COMBUSTORS

By

Dale Wen-Ching Ju

B.A.Sc., University of British Columbia, 1989

A THESIS SUBMITTED IN PARTIAL FULFILLMENT OF
THE REQUIREMENTS FOR THE DEGREE OF
MASTER OF APPLIED SCIENCE

in

THE FACULTY OF GRADUATE STUDIES
Department of Chemical Engineering

We accept this thesis as conforming
to the required standard

THE UNIVERSITY OF BRITISH COLUMBIA

May 1995

© Dale Wen-Ching Ju, 1995

In presenting this thesis in partial fulfilment of the requirements for an advanced degree at the University of British Columbia, I agree that the Library shall make it freely available for reference and study. I further agree that permission for extensive copying of this thesis for scholarly purposes may be granted by the head of my department or by his or her representatives. It is understood that copying or publication of this thesis for financial gain shall not be allowed without my written permission.

Department of Chemical Engineering

The University of British Columbia
Vancouver, Canada

Date May 25, 1995

ABSTRACT

A computer model, using the Monte Carlo method, was developed to predict heat release, oxygen profiles and temperature profiles in Circulating Fluidized Bed (CFB) combustors. The model includes initial devolatilization of the coal feed, a correction in the evolved volatiles region based on the plume model, char combustion, an oxygen mass balance to determine the oxygen profile, and an energy balance to determine the temperature profile. The highly non-linear energy balance equation includes conduction, particle and gas convection and radiative heat transfer terms.

A number of studies were conducted to observe how the model's prediction changes with superficial gas velocities of 6 m/s and 7 m/s, and solids recirculation rates of 15, 30 and 50 kg/m²s, for both the UBC CFB and the Studsvik CFB.

A validation of the model's partial pressure of oxygen profile predictions compared to experimental data was made for the UBC CFB test case.

TABLE OF CONTENTS

	<u>Page</u>
<u>ABSTRACT</u>	ii
<u>LIST OF TABLES</u>	vii
<u>LIST OF FIGURES</u>	viii
<u>ACKNOWLEDGMENT</u>	xi
CHAPTER 1 <u>INTRODUCTION</u>	1
1.1 DESCRIPTION OF CIRCULATING FLUIDIZED BEDS	6
CHAPTER 2 <u>PREVIOUS MODELS OF CFBs</u>	11
2.1 INTRODUCTION	11
2.2 OVERALL MODELS	11
2.3 HYDRODYNAMICS	13
2.3.1 Senior's Hydrodynamic Model	15
2.3.1.1 Assumptions	16
2.4 HEAT TRANSFER	22
2.4.1 Film Theory	22
2.4.2 General Comments on the Film Theory	24
2.4.3 Penetration Theory	25
2.4.4 Gas Film - Emulsion Packet Theory	28
2.4.5 Radiative Heat Transfer	28
2.4.5.1 Chen's Model	31
2.4.5.2 Radiative Contribution in Heat Transfer Model	34
2.4.6 Heat Transfer in Overall Model	35
CHAPTER 3 <u>MODELLING OF HEAT RELEASE, OXYGEN PROFILES</u> <u>AND TEMPERATURE PROFILES OF CFBs</u>	37
3.1 MODEL ASSUMPTIONS	37

3.2	DESCRIPTION OF MODEL APPROACH AND SUBROUTINE EQUATIONS	39
3.2.1	Devolatilization.....	39
3.2.2	Plume Model.....	42
3.2.3	Char Combustion	44
3.2.4	Monte Carlo Approach	47
3.2.5	Comparison of Monte Carlo Approach with Analytic Technique	48
3.2.6	Monte Carlo Approach within the Program.....	48
3.2.7	Heat Transfer Model.....	52
3.2.7.1	Cell to Cell Heat Transfer	52
3.2.7.2	Differences with Chen's Model.....	54
3.2.7.3	Finite Difference Formulation	56
3.2.7.4	Wall to Cell Heat Transfer Equation	58
3.2.7.5	Cyclone and Standpipe	58
3.3	DESCRIPTION OF MODEL PROGRAM	59
3.3.1	Input and Output Files.....	59
3.3.2	Program Steps	61
3.3.3	Model Tuning	64
3.3.4	Discontinuity of Temperature Profile.....	66
3.3.5	Convergence	69
3.3.6	Numerical Stability of Partial Pressure of Oxygen Profile	69
3.3.7	Run Time.....	72
CHAPTER 4	<u>DISCUSSION OF RESULTS AND VALIDATION</u>	75
4.1	INTRODUCTION.....	75
4.1.1	Initial Test Runs.....	76
4.2	STUDSVIK CFB	79
4.2.1	General Description	79
4.2.2	Sensitivity Analysis	79
4.2.3	Results.....	83
4.2.3.1	Heat Release Profiles	83
4.2.3.2	Partial Pressure Profiles	87
4.2.3.3	Temperature Profiles	92
4.3	UBC PILOT CFB.....	95

4.3.1	Description	95
4.3.2	Test Run	98
4.3.3	Results	98
4.4	VALIDATION	108
CHAPTER 5 <u>CONCLUSION AND RECOMMENDATIONS</u>		111
5.1	CONCLUSION	111
5.2	RECOMMENDATIONS FOR FUTURE WORK	112
<u>NOMENCLATURE</u>		113
<u>REFERENCES</u>		115
APPENDIX A	<u>PROGRAM LISTING</u>	119
APPENDIX B	<u>SAMPLE INPUT FILES</u>	154
B.1	HYDRODYNAMIC INPUT FILE LISTING	154
B.2	USER INPUT FILE LISTING	157
APPENDIX C	<u>OUTPUT FILES</u>	158
	sh0	159
	sh1	165
	sh2	171
	sh3	177
	sh4	183
	sh5	189
	sh2b	195
	sh700	201
	sh900	207
	uh0	213
	sh6	219
APPENDIX D	<u>LIST OF VARIABLES</u>	225
D.1	INPUT FILE FROM HYDRODYNAMIC MODEL	225
D.2	USER INPUT FILE	226
D.3	PROGRAM VARIABLES	226

APPENDIX E ENTHALPY BALANCE SPREADSHEETS.....228

LIST OF TABLES

	<u>Page</u>
Table 1.1 Comparison of CFB With Other Types of Boilers [Basu and Fraser, 1991].....	4
Table 2.1 Predictions of Overall CFB Models [Sanderson, 1993]	12
Table 3.1 Comparison of Predicted Burnout Times with Particle Diameters.....	46
Table 3.2 Description of Convergence Loops and Tolerances used in Program.....	61
Table 4.1 Characteristics of Highvale Coal [Grace et al., 1989]	81
Table 4.2 Particle Size Distribution of Highvale Coal and Bed.....	81
Table 4.3 Major Parameters in the Sensitivity Analysis Cases (Studsvik CFB, base case sh0)	82
Table 4.4 Parameters in Baseline Test	99

LIST OF FIGURES

	<u>Page</u>
Figure 1.1	Coal Production and Consumption in Canada, 1986 [Energy, Mines and Resources Canada, 1987]2
Figure 1.2	Heat Transfer Surfaces of a CFB Boiler [Basu and Fraser, 1991].....5
Figure 1.3	A Typical Commercial CFB [Kullendorf and Andersson, 1985]8
Figure 1.4	Various CFB Configurations [Yang, 1992]9
Figure 1.5	Common Non-Mechanical Valves [Yang, 1992] 10
Figure 2.1	Illustration of Solids Distribution in a CFB Riser [Senior, 1992] 14
Figure 2.2	Regions and Flow Patterns Assumed by a 2-Zone Core/Annulus Modelling Approach in a CFB [Brereton, 1987].....17
Figure 2.3	Observed Gas and Solid Flow Patterns in a Sharp CFB Riser Exit [Brereton, 1987].....20
Figure 2.4	Apparent Suspension Density Profile as a Function of Riser Exit Geometries [Senior, 1992].....21
Figure 2.5	Film Theory23
Figure 2.6	Penetration Theory26
Figure 2.7	Gas Film - Emulsion Packet Theory29
Figure 2.8	Radiative Heat Transfer Model [Chen, 1988].....32
Figure 2.9	Schematic Cross-Section of a Membrane Waterwall Surface [Bowen et al., 1991]36
Figure 3.1	Devolatilization Time as a Function of Temperature Predicted by Equation 3.140
Figure 3.2	Plume Model of Volatiles Dispersion [Stubington, 1980]43
Figure 3.3	Probability of a Particle Leaving a Cell.....50
Figure 3.4	Particle Paths in a Riser51

Figure 3.5	Direction Convention used in Cell to Cell Heat Transfer Equation.....	55
Figure 3.6	Model Algorithm.....	60
Figure 3.7	Net Mass Flowrate From the Core to the Streamer vs Height for the UBC CFB	67
Figure 3.8	Temperature Distribution of Core Cells (before and after curve smoothing)	68
Figure 3.9	Temperature Convergence for Various Initial Temp. Guesses (Studsvik CFB, case sh0)	70
Figure 3.10	Temperature Profile of Case sh0 (for various initial temperature guesses).....	71
Figure 3.11	Partial Pressure of O ₂ vs Height (Studsvik CFB, Combustion of Highvale Coal with U=7 m/s and G _s =15 kg/m ² s).....	73
Figure 4.1	Pressure of Cells at a Height of 1 m Above Secondary Air (Studsvik CFB; case sh0).....	78
Figure 4.2	Schematic of Studsvik CFB [Kobro, 1984]	80
Figure 4.3	Volatiles Heat Release vs Height (Combustion of Highvale Coal with U = 7 m/s; Studsvik CFB; cases sh0, sh1 & sh2)	84
Figure 4.4	Char Heat Release vs Height (Combustion of Highvale Coal with U = 7 m/s; Studsvik CFB; cases sh0, sh1 & sh2)	85
Figure 4.5	Char Heat Release vs Height (Combustion of Highvale Coal with U = 6 m/s; Studsvik CFB; cases sh3, sh4 & sh5)	86
Figure 4.6	Changes in Core Density in Secondary Zone for Various Solids Recirculation Rates - Primary Zone Density = 315 kg/m ³ (Combustion of Highvale Coal with U = 7 m/s; Studsvik CFB; cases sh0, sh1 & sh2).....	88
Figure 4.7	Char Heat Release Distribution vs Height (Combustion of Highvale Coal, Studsvik CFB; cases sh0 and sh3)	89
Figure 4.8	Partial Pressure of O ₂ vs Height (Combustion of Highvale Coal with U = 7 m/s; Studsvik CFB; cases sh0, sh1 & sh2)	90
Figure 4.9	Partial Pressure of O ₂ vs Height (Combustion of Highvale Coal with U = 6 m/s; Studsvik CFB; cases sh3, sh4 & sh5)	91
Figure 4.10	Temperature vs Height (Combustion of Highvale Coal with U = 7 m/s; Studsvik CFB; cases sh0, sh1 & sh2)	93
Figure 4.11	Temperature vs Height (Combustion of Highvale Coal with	

	U = 6 m/s; Studsvik CFB; cases sh3, sh4 & sh5).....	94
Figure 4.12	Comparison of Wall Temperature Gradient at a Height of 2.4 m Above Secondary Air with Other Experimental and Theoretical Works	96
Figure 4.13	Simplified Schematic Diagram of UBC Pilot-Scale CFB.....	97
Figure 4.14	Volatile Heat Release (Combustion of Highvale Coal with U = 7 m/s and Gs = 30 kg/m ² s)	100
Figure 4.15	Char Heat Release (Combustion of Highvale Coal with U = 7 m/s and Gs = 30 kg/m ² s)	101
Figure 4.16	Char Heat Release for Various Mean Particle Diameters (UBC CFB, Combustion of Highvale Coal with U = 7 m/s)..	103
Figure 4.17	Partial Pressure of O ₂ vs Height (Combustion of Highvale Coal with U = 7 m/s and Gs = 30 kg/m ² s)	104
Figure 4.18	Temperature vs Height (Combustion of Highvale Coal with U = 7 m/s; UBC CFB; case uh0).....	106
Figure 4.19	Enthalpy Balance for Core Cell at Height = 3.36 m (UBC CFB, case uh0).....	107
Figure 4.20	Oxygen Concentration Profiles for Highvale Coal Conditions: Zhao (T=891 °C, U=8.26 m/s, O ₂ in flue gas=2.9%) Anthony (T=830 °C, U=7 m/s, O ₂ in flue gas=3.7%) Agarwal & Davidson (T=830 °C, U=7 m/s, O ₂ in flue gas=3.7%)	109

ACKNOWLEDGMENT

I would like to thank Dr. Clive Brereton for his continual guidance and encouragement throughout the course of this work. The success of this thesis could not have been achieved without his invaluable insights and support. I would also like to thank Dr. John Grace, Dr. Jim Lim and Dr. Serge Julien for their prompt comments given the short notice. The financial support of ABB Combustion is also gratefully acknowledged.

Most of all, thank You Jesus! To You be the Glory, forever.

CHAPTER 1

INTRODUCTION

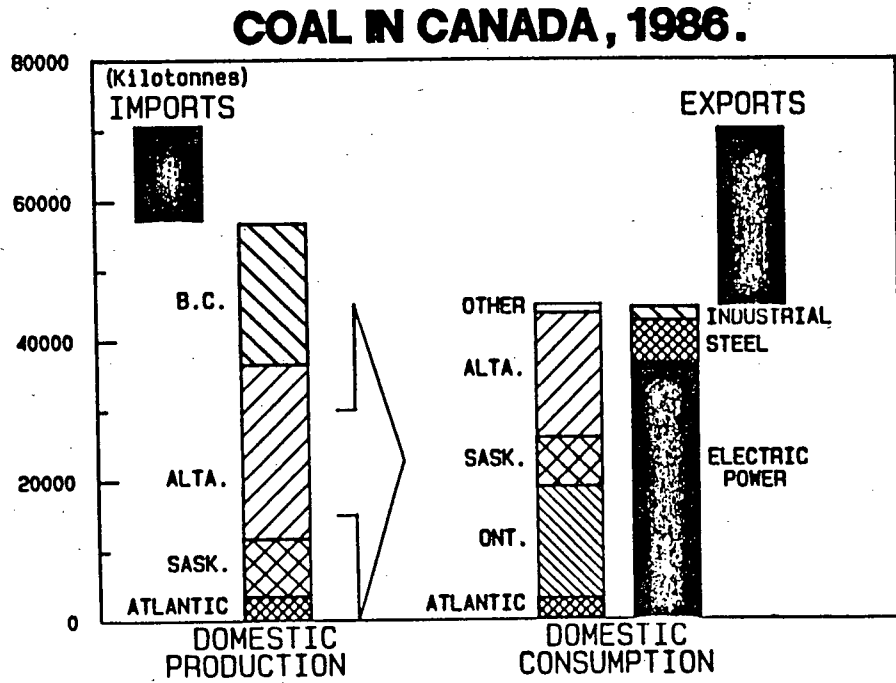
In Canada, the major uses of coal are for the generation of electricity and for coking coal in the steel industry. Because coal is very expensive to transport compared to its energy value, its popularity as an energy source is usually only for the provinces with substantial coal reserves. In addition to transportation costs, environmental concerns are also a factor in coal's competitiveness. Combustion of coal releases sulfurous gases, NO_x, unburnt trace elements [Energy, Mines and Resources Canada, 1987], and more carbon dioxide than the combustion of natural gas.

Since 1973, coal production in Canada has steadily increased. In 1985, coal production was estimated to be 60.7 million tonnes, 94% of which was mined in Western Canada. Presently, coal is Canada's third largest mineral export, after oil and natural gas. Coal consumption as a fuel in power generation is mainly in four provinces, Alberta, Saskatchewan, Ontario and Nova Scotia, with Alberta consuming the largest percentage at 47%. In fact, 92% of Alberta's electrical energy production is from the consumption of coal. See Figure 1.1 [Energy, Mines and Resources Canada, 1987].

The future outlook of coal consumption shows Canada with a large remaining reserve of coal, which is 1.5 times as large as oil and gas reserves. At the present rate of coal production, the proven reserves will last more than 100 years. The major competition for thermal coal is from nuclear sources, since nuclear energy production releases little or no gas emissions. Therefore, the challenge in using thermal coal is to develop more cost effective clean coal technologies.

Circulating Fluidized Bed Boilers (CFBBs) have a number of advantages over other solid fuel fired boilers. Some of these advantages include fuel flexibility, high combustion efficiency, in-situ and low cost sulphur removal, low NO_x emissions and load turndown capabilities. In addition, CFBs are part of some advanced cycles, such as

Figure 1.1 Coal Production and Consumption in Canada, 1986
[Energy, Mines and Resources Canada, 1987]



topping cycles, which have higher cycle efficiency. Less coal is used for the same amount of thermal energy production; therefore, less carbon dioxide is released.

There are very good gas-solid and solid-solid mixing in CFBs and there are many inert solids present in the bed; therefore, fuels that enter CFBs quickly mix with the bed solids without a significant drop in the bed temperature. This results in CFBs' ability to burn many different fuels without the support of auxiliary fuel.

Compared to bubbling beds, which have combustion efficiencies of 90% to 96%, CFBs have a combustion efficiency of approximately 97.5% to 99.5% [Basu and Fraser, 1991]. The high combustion efficiencies are mainly due to good gas-solid mixing and the fact that unburnt fuel is returned back into the riser. Sulphur capture in CFBs is also better than in bubbling beds. CFBs can capture approximately 90% of the sulphur dioxide released during combustion, using less sorbent than in bubbling beds, where in both cases the beds are made up of sorbent. Sulphur capture reaction is slow; therefore, the longer residence time of particles in the CFB, approximately 3 to 4 sec., makes it more effective compared to 1 to 2 sec. in an average combustion zone.

CFBs also have low NO_x emissions. CFBs have the capability to provide the combustion air in stages. Fuel nitrogen is usually released with the volatiles near the base of the riser. If not enough oxygen is supplied in the primary air, the fuel nitrogen will form molecular nitrogen before it reaches the secondary air and form NO_x. Once molecular nitrogen is formed, it will not normally form NO_x at the relatively low CFB temperatures of 850 °C.

Finally, the ability to control heat absorption allows the CFB to respond quickly to changes in loads. Therefore, CFBs are known to have good turndown capabilities.

All of the mentioned advantages make CFB's ideal for certain operations, depending on the type of fuel available and environmental concerns. Table 1.1 shows a comparison of a typical CFB with other types of boilers.

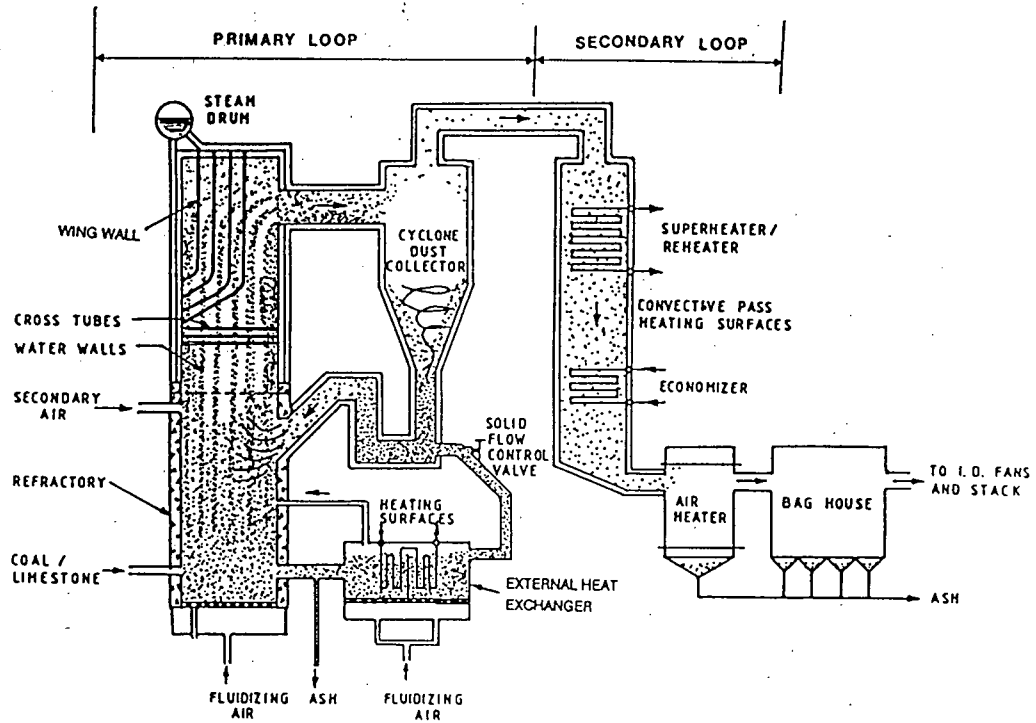
Table 1.1 Comparison of CFB With Other Types of Boilers [Basu and Fraser, 1991]

Characteristics	Stoker	Bubbling	CFB	Pulverized
Height (m)	0.2	1 - 2	15 - 40	27 - 45
U (m/s)	1.2	1.5 - 2.5	4 - 8	4 - 6
Excess air (%)	20 - 30	20 - 25	10 - 20	15 - 30
Grate Heat Release Rate (MW/m ²)	0.5 - 1.5	0.5 - 1.5	3 - 5	4 - 6
Coal size (mm)	6 - 32	0 - 6	0 - 6	<0.001
Turndown ratio	4 : 1	3 : 1	3 - 4 : 1	
Efficiency (%)	85 - 90	90 - 96	95 - 99	99
NO _x emission (ppm)	400 - 600	300 - 400	50 - 200	400 - 600
SO ₂ capture (%)	none	80 - 90	80 - 90	small

There are several possible locations and arrangements of heat transfer surfaces in a typical CFB boiler, some of which are shown in Figure 1.2 [Basu and Fraser, 1991]. Generally, heat is removed through vertical membrane wall surfaces, located around the outer reactor wall above the secondary air. For large commercial CFBs, additional internal heat transfer tubes may be added in the reactor or heat may be removed from the cyclone or external heat exchangers.

In order to design an appropriate CFB, designers need to know the heat transfer coefficients for varying operating condition; however, experimental data for CFB operations are few and fundamental understanding of CFBs trails considerably behind commercial advances, making scale-up from pilot plant data a difficult task. Therefore, there is a need for a better understanding of the hydrodynamics and heat transfer mechanism in CFBs.

Figure 1.2 Heat Transfer Surfaces of a CFB Boiler
 [Basu and Fraser, 1991]



CFBs dynamics are complex and many variables affect heat transfer to the membrane walls, some of which include particle size distribution, thermal conductivity of the particle and gas, heat capacity of the particle and gas and wall surface temperature, just to name a few. There are actually more than 31 variables that affect heat transfer in CFBs [Wu, 1989].

It is the goal of this thesis work to develop a model to predict heat release, partial pressure of oxygen profiles and temperature profiles in a CFB given the geometry and hydrodynamic properties of the CFB and the physical and chemical properties of the fuel. This model will also be used to observe changes in the CFB's operating conditions when variables such as superficial gas velocity and solids recirculation rate are changed. This model will aid in selecting the appropriate locations for heat transfer surfaces in CFBs, so that a CFB unit can be optimized for turndown and fuel flexibility.

This thesis consists of the results of a literature search into various overall models of CFBCs heat transfer and hydrodynamics, including a description of Senior's hydrodynamic model, described in chapter 2. Chapter 3 consists of a detailed discussion of a model, which was developed in this thesis to predict heat release and heat transfer in CFBs. In addition, this chapter includes a discussion of the various assumptions and convergence problems encountered throughout the model's development stages. And finally in chapter 4, there is brief discussion of the test results from the model and a qualitative comparison of the predicted results with measured experimental data for the UBC CFB. The findings from this research work are then summarized in chapter 5.

1.1 Description of Circulating Fluidized Beds

CFBs are a subset of fluidization operations, called fast fluidization, that lie between turbulent fluidization and pneumatic transport regimes. In other words, the superficial gas velocity through the bed is larger than the transport velocity of the

particles, but is small enough that some particles travel downwards or fall back in a region close to the outer wall of the CFB. Figure 1.3 shows a schematic of a typical CFB.

A CFB consists of a "riser", where combustion principally occurs. It is a tall column of relatively small cross sectional area compared to stoker and bubbling bed boilers. Combustion air is normally split into a primary and a secondary air feed. The primary air enters the base of the riser and the secondary air is injected anywhere from 1 m to 10 m above the base. The region below the secondary air ports is usually called the primary zone and the region above the primary zone is called the secondary zone. The superficial gas velocity in the primary zone ranges from 2 m/s to 6 m/s. In the secondary zone, gas velocities range from 5 m/s to 10 m/s. The total height of the riser can range anywhere from 10 m to 20 m or higher, and the mean particle size is approximately 50 μm to 500 μm . There are many different arrangements of CFB systems. A few of the more common configurations can be seen in Figure 1.4.

Solids in a CFB are comprised mainly of ash, sand during startup and fresh calcined and spent sorbent. There is considerable carryover of particles from the riser, depending on the exit geometry. Therefore, solid separators such as cyclones are used to separate the solids from the riser exit gas stream. The solids from the cyclone are returned continuously through a return leg near the base of the riser. Most return legs include a non-mechanical valve such as L-valve, J-valve, V-valve and seal pot, shown in Figure 1.5. Non-mechanical valves do not contain any moving parts. The solids that flow through the return leg are controlled by aeration and the geometry of the pipe.

The primary zone can be designed to have different geometries, such as a tapered or a constant cross-sectional area, which will affect the acceleration of particles in the primary zone as well as fuel mixing.

Figure 1.3 A Typical Commercial CFB [Kullendorf and Andersson, 1985]

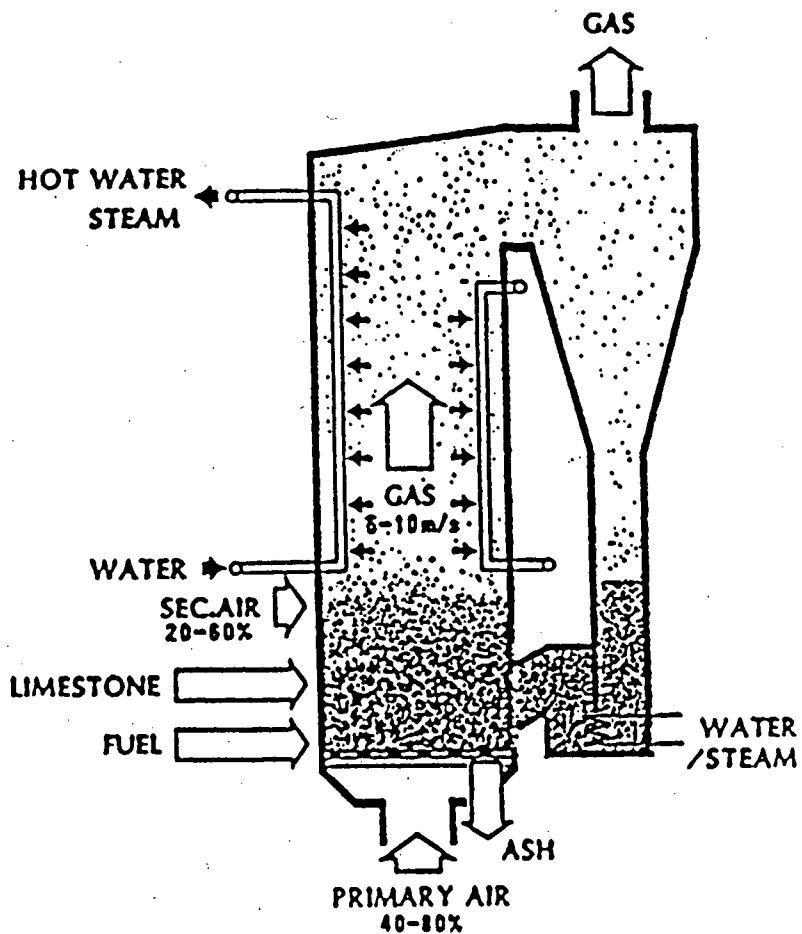
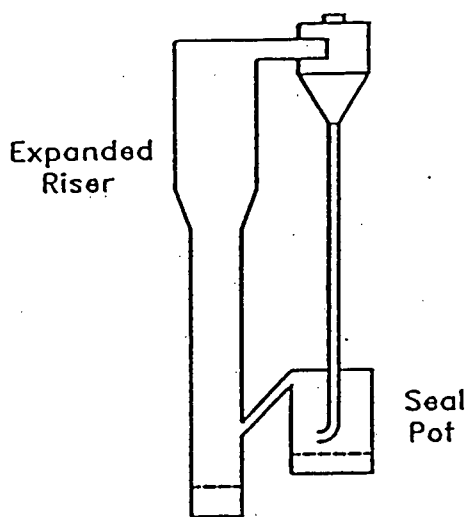
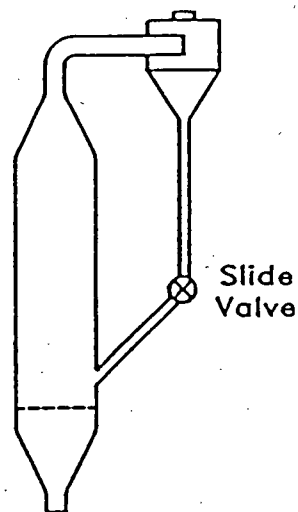


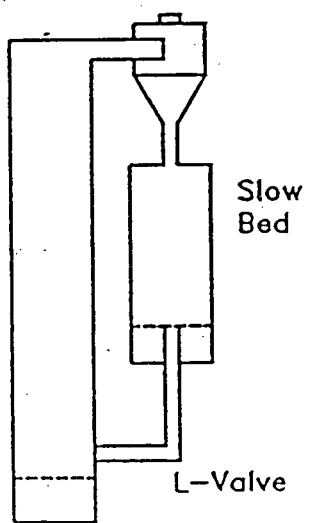
Figure 1.4 Various CFB Configurations
[Yang, 1992]



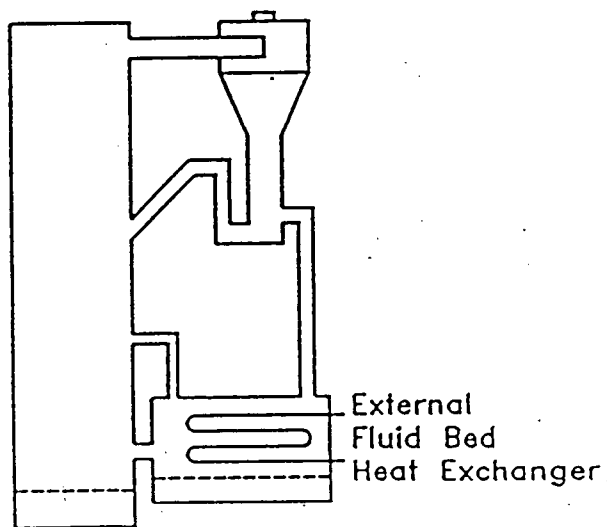
CFB with Seal Pot & Expanded Section



CFB with Mechanical Valve

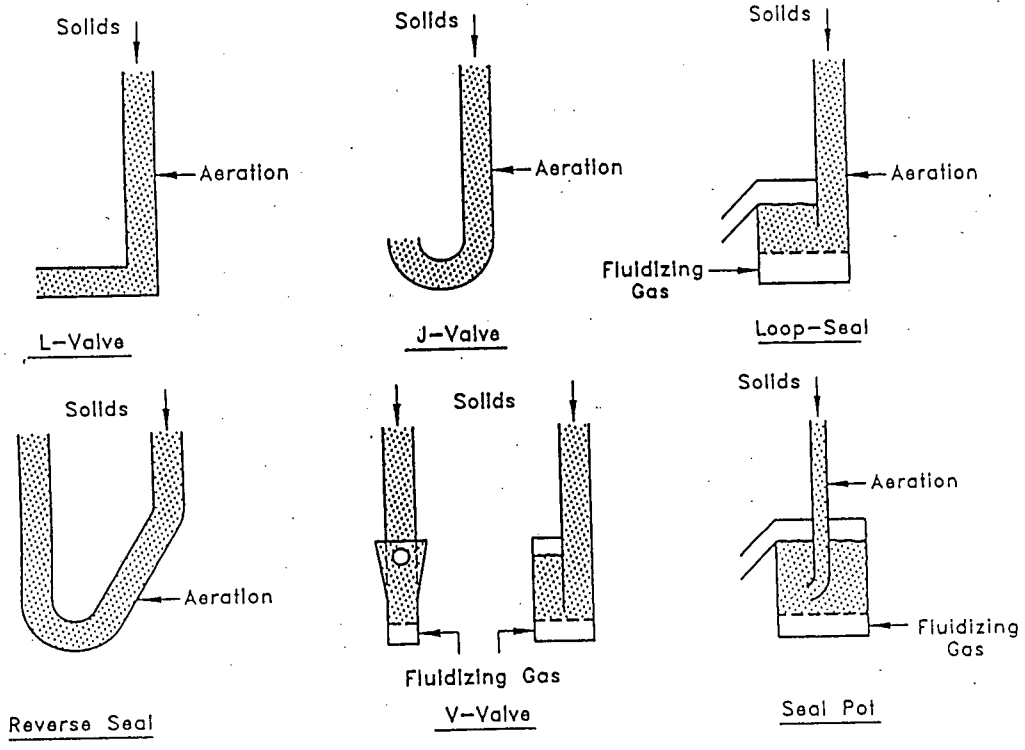


CFB with Slow Bed and L-Valve



CFB with External Heat Exchanger

Figure 1.5 Common Non-Mechanical Valves
[Yang, 1992]



5

CHAPTER 2

PREVIOUS MODELS OF CFBs

2.1 INTRODUCTION

There have been several models of fluidized beds and CFBCs developed within the last 10 years. A summary of fluidized bed models can be found in [Saxena et al., 1981] and a summary of CFB models can be found in [Sanderson, 1993]. These models describe various fluidized bed phenomena, in order to gain a better understanding of CFB operations and to predict transient behavior and control of disturbances.

A practical model can be as complex as the power of one's computing system; however, a more complex model does not necessarily mean a more accurate one. In fact, the philosophy of modeling is to include only enough detail to adequately predict the important parameters, since it is usually unrealistic to study all possible parameters. Therefore, deciding the level of complexity needed to obtain an adequate model is highly subjective and depends on what variables the model intends to predict.

2.2 OVERALL MODELS

Overall models of CFBC are complex in nature, since there are many interrelated processes taking place. Generally, a complete overall model will include hydrodynamics, combustion reactions and heat transfer. In addition, the cyclone, particle size distribution, attrition, agglomeration and exit/inlet geometries should be taken into account.

Several overall models, listed in Table 2.1 [Sanderson, 1993], will be briefly described. The assumptions that each model has made in regards to their hydrodynamics and heat transfer models will be mentioned in the following sections. These models vary in complexity and in the variables they predict, such as

hydrodynamics, combustion, pollutant emissions, temperature and response to disturbances.

Model 1 focuses mainly on predicting combustion efficiencies, while model 2 is concerned with predicting operating parameters such as hydrodynamics, heat transfer, chemical reaction kinetics and cyclone performance. Model 3 focuses on predicting pollutant emissions and model 4 considers hydrodynamics and oxygen concentration profiles. Models 7 and 9 are steady state models while models 5, 6, 8 and 10 describe static and dynamic behaviors.

Table 2.1 Predictions of Overall CFB Models [Sanderson, 1993]

	1	2	3	4	5	6	7	8	9	10
Hydrodynamics	x	x	x	x	x	x	x	x	x	x
Combustion	x	x	x	x	x	x	x	x	x	x
Emissions	x	x	x	x	x	x	x	x	x	x
Heat Transfer		x	x		x	x	x	x		x
Miscellaneous (e.g. L-valve, additional heat exchanger)					x	x	x	x		x

Models:

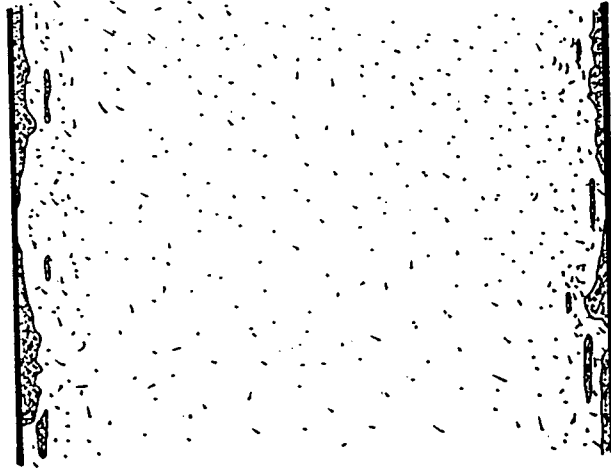
- 1 Ahlstrom Pyroflow (1987)
- 2 Basu (1991)
- 3 IST (1993)
- 4 Halder & Datta (1993)
- 5 Zhang (1991)
- 6 Xu & Mao (1993)
- 7 IEA (1993)
- 8 Mori (1991)
- 9 Lin & Li (1993)
- 10 Siegen (1987)

2.3 HYDRODYNAMICS

In order to predict heat release and heat transfer in CFBs, knowledge of the flow patterns of solids within the riser must be known. Experimental observations have shown some characteristic hydrodynamics found in CFBs. Some of these observations are a downward flow of dense streamers near the walls of the riser, otherwise known as the annulus region, and an upward flow of dilute suspension in the middle of the riser, known as the core region [Yerushalmi et al., 1978], [Brereton et al., 1986] and [Yang et al., 1991], shown in Figure 2.1. It has also been observed that the core has regions of higher and lower voidages, which seem to suggest "clustering". Clustering is the phenomenon where a group of particles are loosely locked in some random configuration and engulfed in gas. The cluster, sometimes referred to as a "packet" or "streamer", acts as an individual entity, occasionally losing and gaining a few particles.

Models 1, 2, 3, 4 and 6, noted in the previous section, use the core/annulus structure of the riser. The overall models that did not use the core/annulus structure characterized a section of the CFB riser at a given height as a lumped-parameter section. In other words, gas and solids are ideally mixed in each cell and each cell has

Figure 2.1 Illustration of Solids Distribution in a CFB Riser [Senior, 1992]



chemical reactions, particle attrition and cell to wall heat transfer occurring. None of the models simulated the clustering phenomena.

From previous experimental and modelling work, it was found that reactor geometry affects the hydrodynamics [Senior, 1992]. Sharp riser exits result in a higher suspension density at the top of the riser. In addition, the presence of a membrane heat transfer surface will affect the thickness of the streamers formed near the wall. It has also been shown that the position of the solids return entry and the shape of the primary zone tapering affects the solids acceleration in the developing zone. None of the CFB models incorporate reactor geometry effects.

2.3.1 Senior's Hydrodynamic Model

The heat release and heat transfer model developed in this thesis work is based on a mechanistic model of CFB hydrodynamics by Senior [1992]. This hydrodynamic model predicts the suspension density profiles and hydrodynamics of the wall and core regions. The accuracy of the predicted suspension density profile is approximately $\pm 20\%$ and was based on comparisons with experimental data, obtained from the UBC pilot CFB and the Studsvik CFB. For the UBC CFB, experimental data were measured for superficial gas velocities of 6 m/s to 10 m/s, solids recirculation rates of 20 kg/m²s to 170 kg/m²s and for various primary/secondary air splits. For the Studsvik CFB, experimental data were collected for superficial gas velocities of 4 m/s to 8 m/s, solids recirculation rates of 40 kg/m²s to 90 kg/m²s and for various air splits.

Although solids flow in a two-dimensional or a three-dimensional model will be more representative of an actual CFB riser, than a simple core/annulus model, increased dimensional models are more complex, significantly more difficult to solve and may not necessarily give more accurate results than a lower dimensional model. It was found that a model where the riser was split into a one-dimensional core and an annulus region, which is called the two-zone, core/annulus approach, gave reasonable

trends. The two zones interact with one another by radial interchange of solids across the zone boundary, see Figure 2.2.

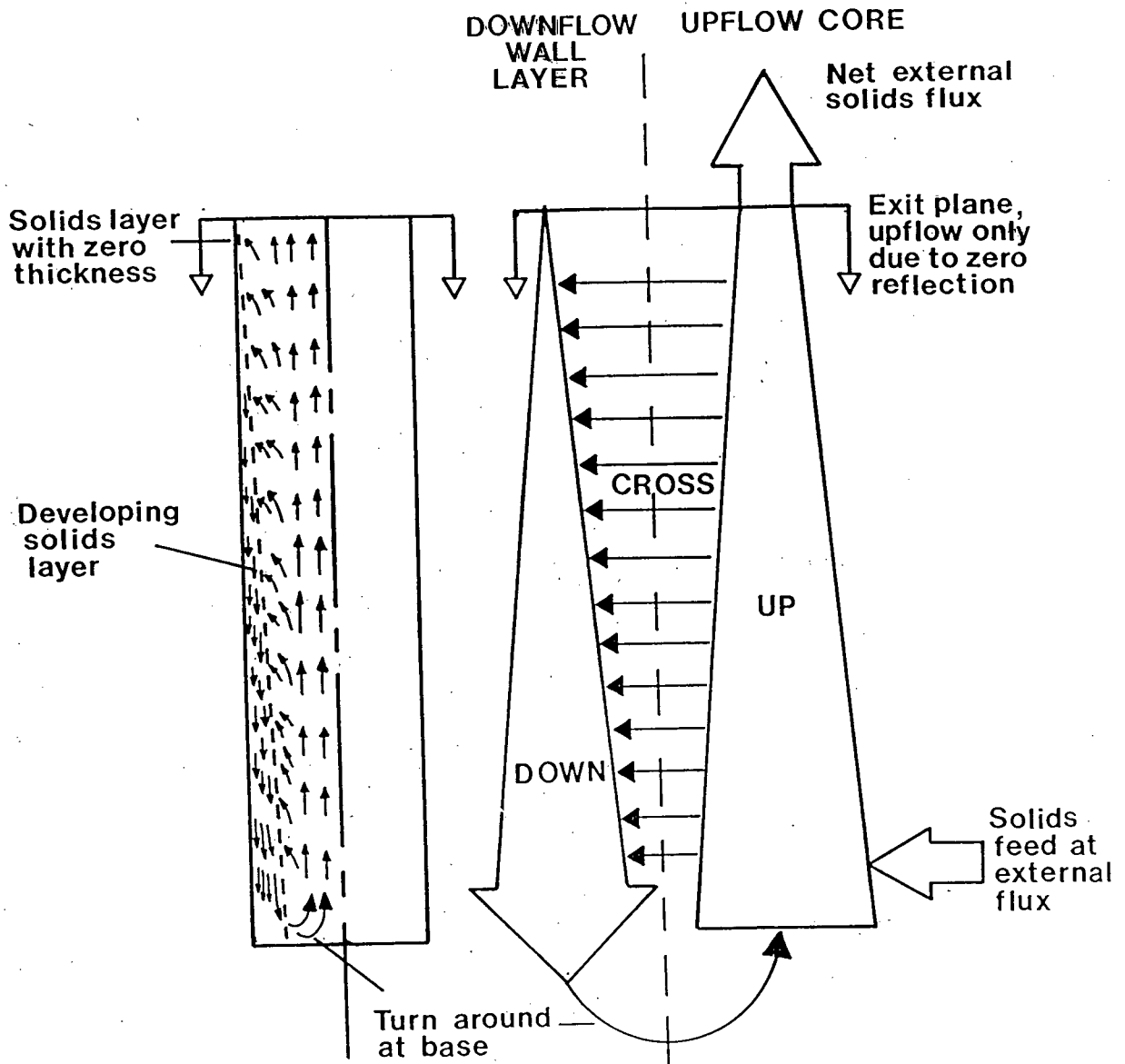
Axially, Senior's CFB model was divided into 20 core cells and 20 annulus cells along the height of the riser, above the secondary air. The primary zone is represented as a single cell. The hydrodynamic results from Senior's models show that fewer cells can be used near the middle section of the riser, where suspension densities are quite uniform; however, the top and the bottom of the riser may be regions of steep suspension density gradients and more cells may be needed to accurately predict the densities. Comparing this model to the overall models shows that the overall models had different number of cells along the height of the riser. Some models divided the riser into 2, 3 or many cells, and one model (IEA) took the entire riser as being one cell. Some of the model differences result from different number of cells being needed to predict different phenomena. For example, a riser where the solids are well mixed will require only a single cell to sufficiently predict the overall solids mixing. However, to understand the details of the density profile, more axial cells may be needed.

2.3.1.1 Assumptions

The assumptions made in Senior's model are:

- (i) The hydrodynamics is represented by a two-zone, core/annulus flow structure, which is described above.
- (ii) The riser is isothermal. Typically, a riser's temperature ranges from 850 °C to 1000 °C, and is not isothermal in practice; however, these temperature variations will not significantly affect the hydrodynamics but will affect heat release and heat transfer in the riser. Test runs conducted using Senior's model and varying bed temperatures from 850 °C to 1000 °C show less than a 10%

Figure 2.2 Regions and Flow Patterns Assumed by a 2-Zone Core/Annulus Modelling Approach in a CFB [Brereton, 1987]



difference in the mass flowrate of air; therefore, the hydrodynamic results are almost the same.

- (iii) Gas and solid densities are constant. The solid suspension densities, however, vary along the height of the riser and in each zone.
- (iv) The behavior of the particles is represented by particles with the sauter mean particle size.
- (v) The particles in the fully-developed region in the core travel up the riser at a constant velocity. This velocity is equal to the superficial gas velocity minus the sauter mean particle terminal velocity. This assumption is valid for dilute systems.
- (vi) There are no clusters in the core above the secondary air feed ports.
- (vii) The primary zone is in the developing flow region near the bottom of the riser, and the assumptions on the behavior of the particles, listed above, do not apply in this region; therefore, only the bulk density was predicted in the primary zone.
- (viii) For simplicity, the height of the top of the developing flow region is also the secondary air feed port height. In reality, the top of the developing flow region is usually 0.5 m to 1.5 m above the secondary air.

The region above the secondary air is in fully-developed flow. The developing flow region is the region near the bottom of the reactor, where there is a steep decline in the density profile and large core to wall flux of solids. In the fully developed region, there is less interchange of solids between the core and the annulus. The interface between these two regions are described in more detail in Senior's thesis.

- (ix) In the developing flow region, an exponential decaying profile is assumed for the bulk suspension density.

- (x) The average streamer velocity in the annulus is assumed to be -1.1 m/s. The average velocity of the falling streamer usually ranges from -0.5 m/s to -1.8 m/s, and this velocity is dependent on the suspension density. This range of streamer velocity was found experimentally using high speed cinematography by Wu [Wu et al., 1990], and is the same order of magnitude as suggested by other researchers such as Glicksman [1988].

Another observation that was included in Senior's model is the non-homogeneous nature of the annulus. Some wall sections contain streamers and others are exposed to the dilute upwards flow of particle suspension in the core. Both of these conditions were modeled in the annulus, by computing the thickness of the streamer and the fraction of the wall coverage by the streamers as a function of riser height.

Some limitations in Senior's model include the assumptions made in the developing flow region or the primary zone, and the assigned reflection coefficient, which is presently modeled as not a function of solids recirculation rate, superficial gas velocity, gas viscosity, gas density, particle density, particle size distribution and exit geometry. The reflection coefficient is defined as the fraction of solids traveling upwards at the exit height that are returned down the walls of the riser. Figure 2.3 shows the gas and solids flow patterns at a sharp riser exit [Brereton, 1987] and Figure 2.4 shows the effects of riser exit smoothness on a suspension density profile [Senior, 1992]

Figure 2.3 Observed Gas and Solid Flow Patterns in a Sharp CFB Riser Exit
[Brereton, 1987]

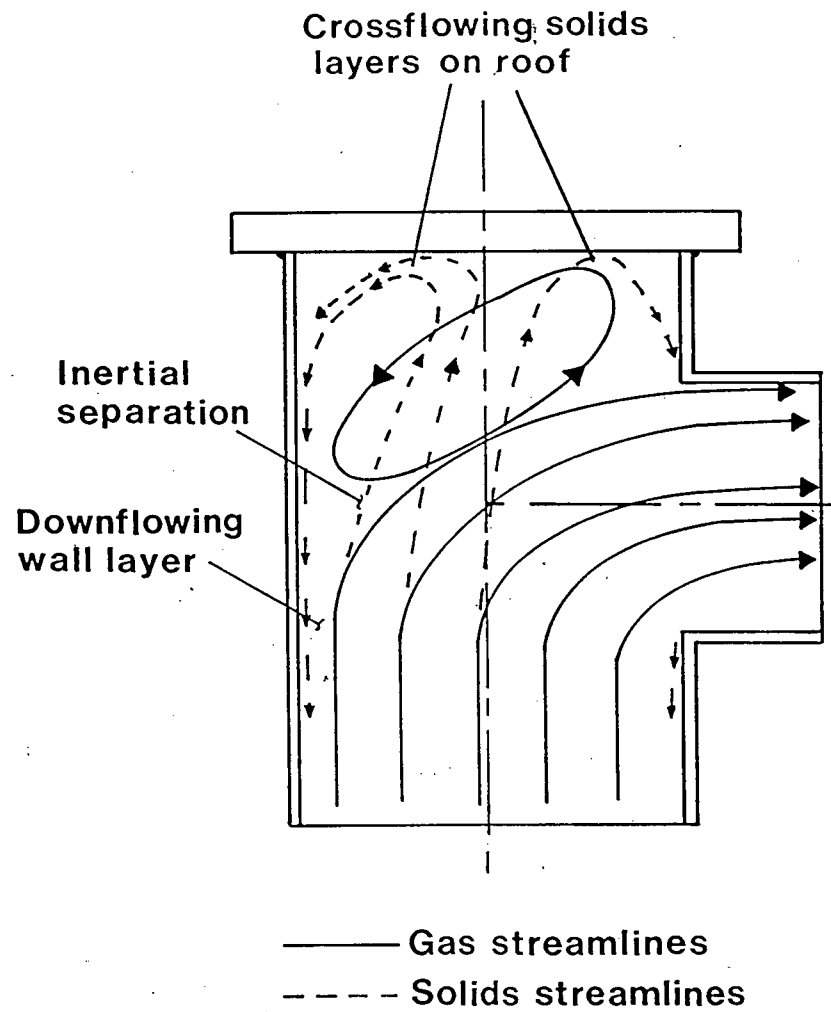
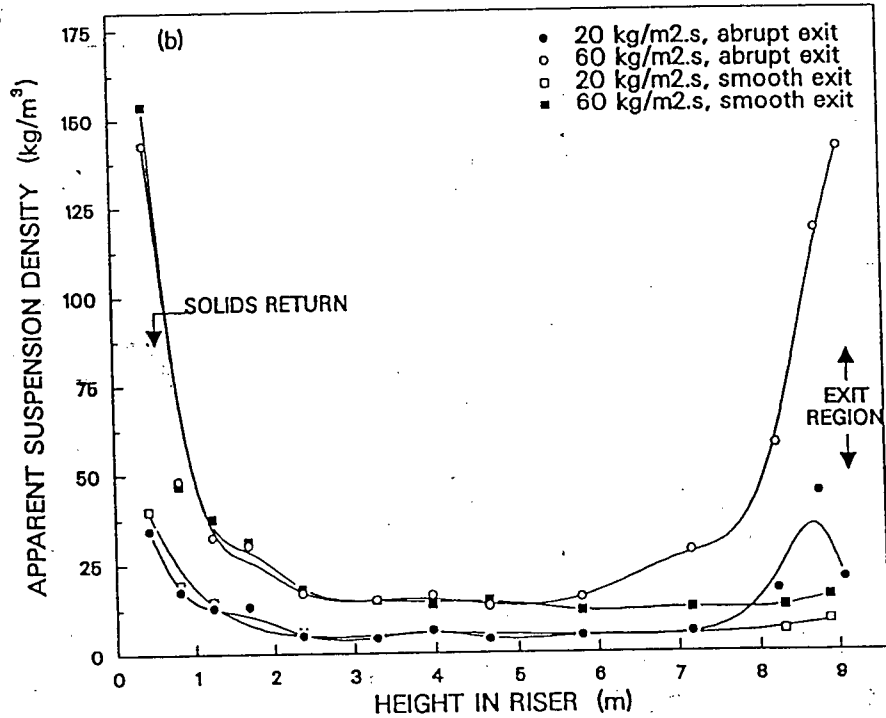
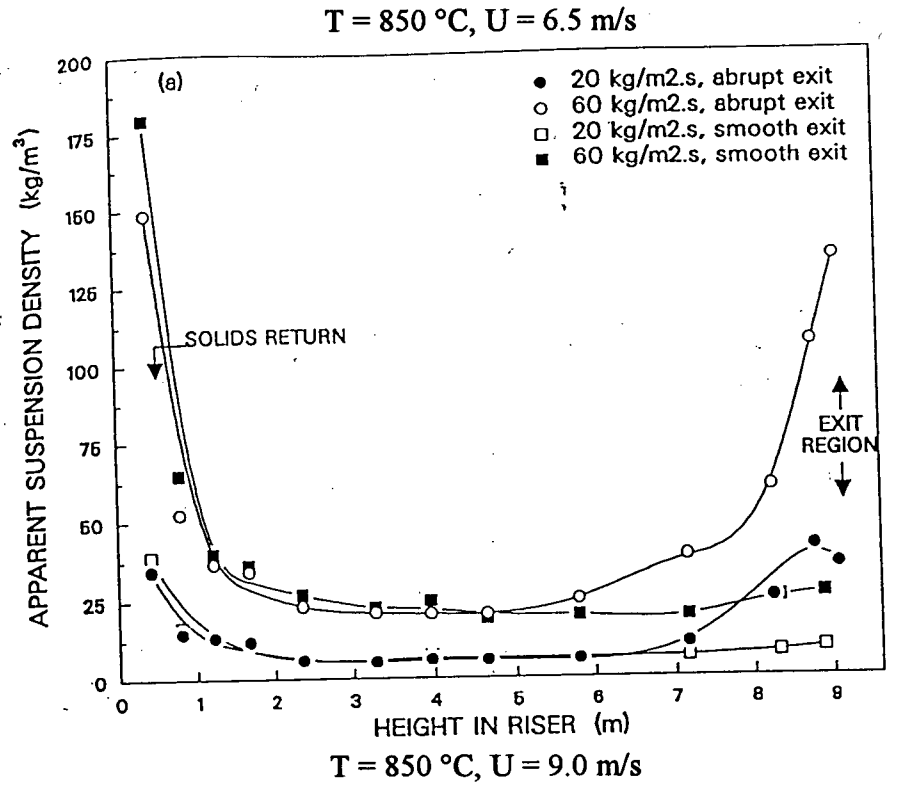


Figure 2.4 Apparent Suspension Density Profile as a Function of Riser Exit Geometries [Senior, 1992]



2.4 HEAT TRANSFER

Presently, there is a lack of experimental data from commercial operating CFBs that is not considered proprietary; however, a few researchers have made their data available [Werdermann et al., 1993], [Couturier et al., 1991] and [Leckner et al., 1992]. The majority of other CFB data that are available are for CFBs with either small heat transfer surfaces, small diameter CFBs or for CFBs operating at room temperatures, for example [Bi et al., 1990] and [Furchi et al., 1988]. In addition, most experimental data do not include radiative heat transfer and when compared with each other are often scattered.

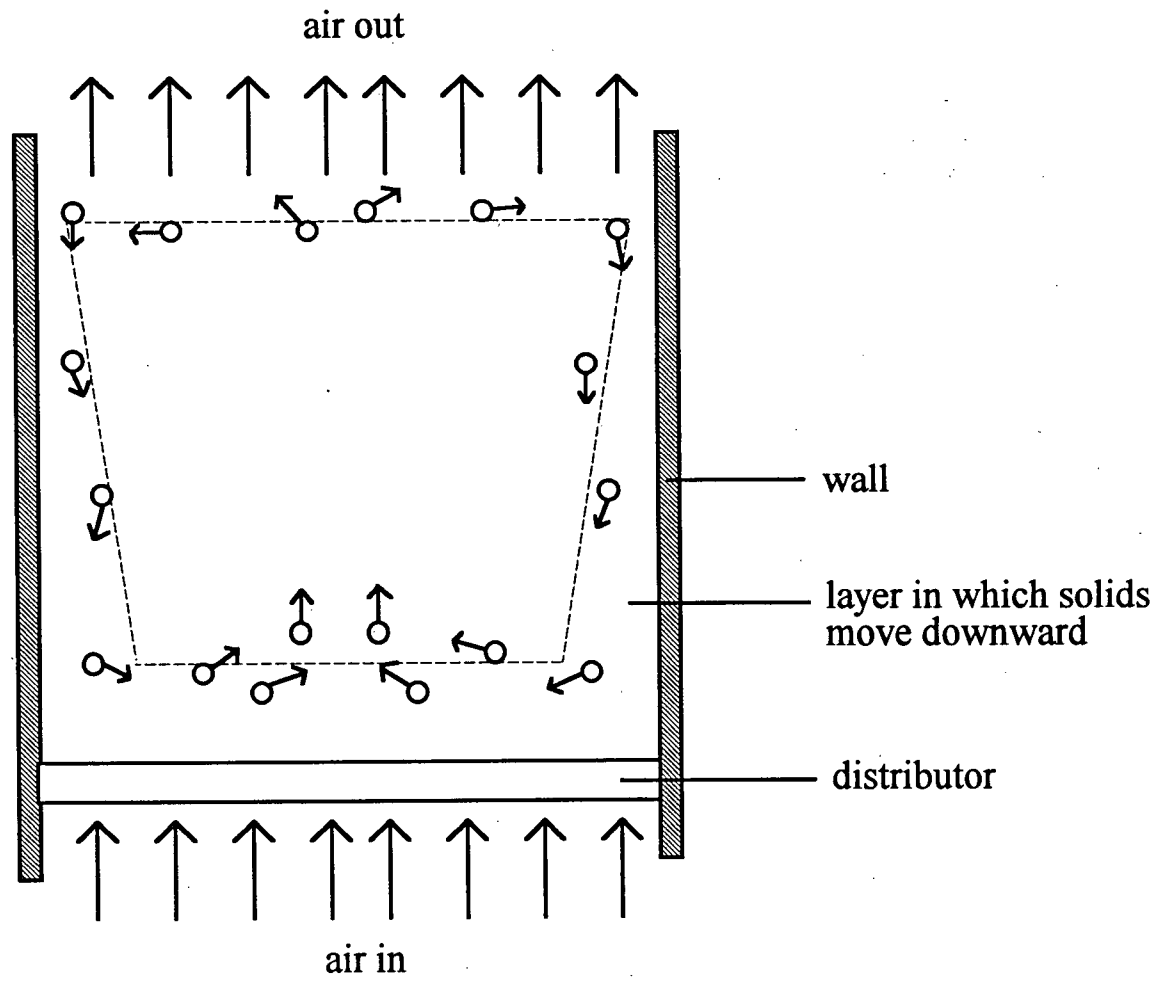
Generally speaking, heat transfer models fall into three categories depending on how they treat the solid suspension near the riser wall. These categories are as follows:

- (1) Film theory
- (2) Penetration theory
- (3) Gas film-emulsion packet theory

2.4.1 Film Theory

The film theory was first proposed by Dow and Jacob [Dow et al., 1951]. They conducted experiments with various particle sizes and column diameters to study the heat transfer mechanism between a fluidized bed and a heat transfer surface. In their model there is an air film between the downward moving solids and the wall of the riser. Adjacent to this air film, the solid suspension is treated as discrete particles that move down the film, and discrete hot particles move up through the center of the bed. See Figure 2.5. The particle to surface contact is assumed to be negligible and heat is transferred through this film, which may be as thin as 0.01 mm thick. As expected, there is a temperature gradient across the film, and there is also a temperature gradient near the distributor as the cold primary air mixes with the hot particles in the bed; however, the rest of the bed is at a uniform temperature. In reality, this film layer is not continuous, but it is scoured by particles at irregular intervals.

Figure 2.5 Film Theory



Leva [1952] used the same model as Dow and Jacob, but assumed that the air film thickness is strongly dependent on the gas viscosity. In addition, as the particles scour the air film, the film's resistance decreases; therefore, the particle's velocity should also be included in the heat transfer equation. Leva, derived an equation that contains the thermal conductivity and the viscosity of the gas as well as the mass and velocity of the particles, and a new dimensionless variable called the "fluidization efficiency" was defined. The fluidization efficiency value was determined by fitting a derived bed to wall heat transfer coefficient with experimental data.

Levenspiel and Walton [Levenspiel et al., 1954] also used the film theory, but did not assume that the air film was continuous along the wall. They assumed that a fresh film starts at every point on the heat transfer wall where a solid particle touches the surface; thereby, producing several films and predicting a smaller total resistance to heat transfer. The total resistance is expressed as an "equivalent film thickness".

2.4.2 General Comments on the Film Theory

The film theory emphasizes the role of thermal conductivity of the gas and neglects thermal capacity of the solid particles. Also, the air film is scoured by solids which decreases the thickness of the film. The results of this theory may appear reasonable; however, the assumption that the role of the solid particles in heat transfer are insignificant is not seen experimentally.

This model wrongly suggests that at minimum fluidization the heat transfer is zero, because an anomaly in the derived equation at minimum fluidization gives zero equivalent film thickness, which leads to zero heat transfer. Therefore, the heat transfer value at minimum fluidization must be extrapolated from a higher value. In addition, extrapolation of heat transfer values for higher fluidization ranges must also be done.

Most models using the film theory predicts that radiation heat transfer is insignificant at temperatures less than 1000 °C. Radiation heat transfer was shown, by

subsequent researchers [Szekely et al., 1969], [Botterill et al., 1970], [Baskakov, 1985] and [Han et al., 1992], to be significant at much lower operating temperatures.

2.4.3 Penetration Theory

Mickley and Trilling [Mickley et al., 1949] were first to develop the penetration theory for fluid bed heat transfer. Emphasis was placed on the transport of heat by the solid particles, which suggests that because the heat transport by the solids is fast, the temperature gradient is present only in a thin layer near the heat transfer surface. In addition, the effective thickness of this layer is reduced by the motion of the particles and heat flows by conduction and convection.

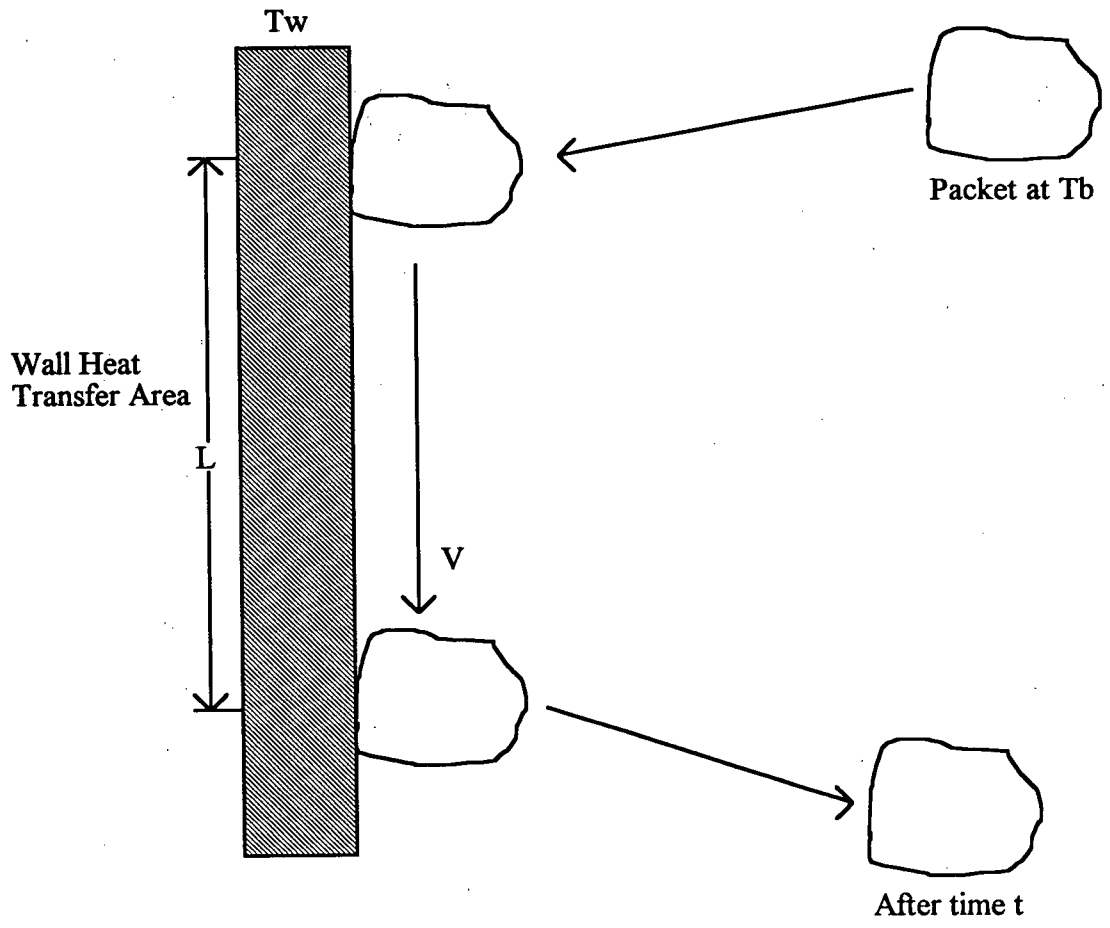
Mickley and Fairbanks [Mickley et al., 1955] were the first to represent the solid suspension as a packet. They recognized the heat transfer mechanism to be unsteady conduction and they researched the role of heat capacity of solid particles. The packet resides within a thin layer near the wall and the physical properties of the packet are the same as that of the bed. The packet has a finite life span before it is re-entrained into the core of the riser, and is replaced by a fresh packet. A continuous flow of such packets is the chief mechanism of heat exchange. See Figure 2.6.

The boundary conditions are such that the packet instantaneously attains the temperature of the wall when it comes into contact with it, i.e., there is zero resistance or an infinite heat transfer coefficient between the packet and the wall.

Mickley and Fairbanks considered two models for bed dynamics.

- (i) Slug model - all the packets move down the wall at a uniform velocity. They all have the same residence time and behave alike.
- (ii) Side mixing model - there is a radial exchange of packets between the surface and the bed.

Figure 2.6 Penetration Theory



From their experiments, they showed that the heat transfer coefficient was proportional to the square root of the thermal conductivity of the packet, assuming constant packet density and heat capacity. Their model also explained how heat transfer increases due to a decrease in the particle size, because smaller particles circulate at surfaces more rapidly than larger particles.

The disadvantage of this model is that it predicts infinite heat transfer coefficients as the contact time approaches zero. The model also assumes that the bed is homogenous, which is not the case, since there are porosity changes.

Baskakov [1964] used the packet model of Mickley and Fairbanks, but he included additional thermal resistance between the wall and the packet to account for changes in porosity. His model is essentially a combination of the film theory and the penetration theory. Changes in porosity are significant near walls where gas layer thicknesses are approximately one particle radius.

Baskakov's model gives finite values of the heat transfer coefficient as the contact time approaches zero, as compared to Mickley and Fairbanks model. In addition, this additional thermal resistance seems to suggest a gap between the fluidized bed and the membrane wall.

Gorelik [1967] used a model similar to Baskakov's except the packet that reaches the wall is divided into a higher and a lower porosity zone. The higher porosity zone is close to the wall, and the lower one is equal to the bed porosity. However, the heat transfer problem becomes the unsteady heating of two zones, each having different thermal properties due to different porosities. Two zones with different thermal conductivities causes a temperature gradient at their interface. The difficulty then is to determine the thermal properties of the two zones.

2.4.4 Gas Film - Emulsion Packet Theory

The gas film-emulsion packet theory, also called the "alternate-slab model", proposed by Gabor [1970], assumes that the solid suspension near the riser wall is made up of alternate slabs of gas and solid. See Figure 2.7. Many investigators [Vedamurthy et al., 1974], [Bhattacharya et al., 1977] and [Kolar et al., 1979], using this theory assume that radiation only occurs between adjacent plates along with conduction through the gas film between the plates. The bed and heat transfer surface are considered grey and the gas is assumed to be transparent [Kolar, 1979]. The properties are evaluated at an average temperature equal to the mean of the temperature of the two bounding slab surfaces.

The radiation incident on each slab is assumed to undergo reflection, radiation, and scattering. The limiting values of these parameters as the number of slabs approaches infinity are considered to be the effective bed values.

The predictions from this model over predicts the heat transfer coefficient values at high temperatures; however, the maximum prediction error using this model is less than $\pm 35\%$, which is remarkably good considering its simplifying assumptions.

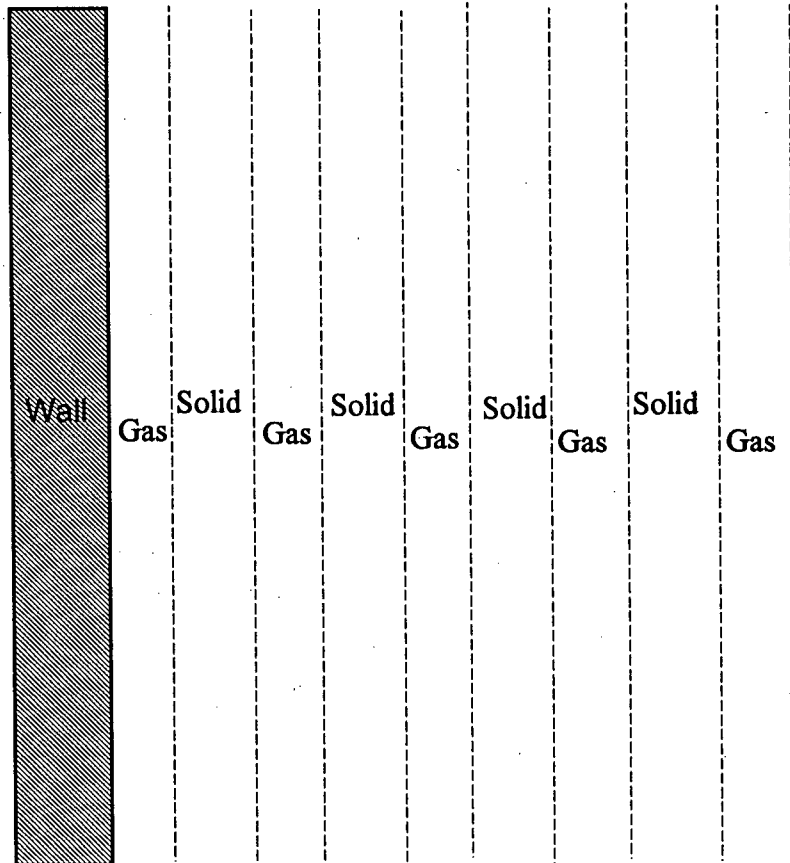
All of the above models were initially developed for bubbling beds. Many have subsequently been adapted for CFBs.

2.4.5 Radiative Heat Transfer

Most studies on heat transfer in CFBs only deal with particle convective heat transfer or overall heat transfer. Although an investigation by Jolley [1949] showed that radiative heat transfer term is significant at operating temperature of 1000°C , experimental measurements of the radiative heat transfer contribution is difficult.

There are many views as to the contribution of radiation to the overall heat transfer in a CFB. One point of agreement is that it is insignificant at low temperatures; however, there is no agreement as to what temperatures are considered "low" and what are

Figure 2.7 Gas Film - Emulsion Packet Theory



considered "high" temperatures. According to Han's experimental measurements [Han et al., 1992], the contribution of radiative heat transfer to the total heat flux can range from 5% to 50% for suspension temperatures from 200 °C to 600 °C. In addition, there is uncertainty as to how other variables, such as particle diameter, particle surface temperature, fluidizing velocity, and effective bed and surface emissivities, affect the radiative heat transfer term. It is therefore necessary for a model of heat transfer in CFB to predict the radiative contribution in high temperature beds as a function of various parameters and operating conditions.

The additional heat transfer in the packet due to radiation using the penetration theory was studied by several researchers, such as work done in model 3. Another more complex model, by Chen [1988], involves developing a model of the heat transfer process by a non-linear differential formulation of the simultaneous radiative-conductive flux in the packet. In Chen's model, the radiative flux is split into an absorption and a scattering flux in both the forward and backward directions.

The general limitation of the penetration theory is that a number of the mean packet properties must be known, such as effective packet thermal conductivity, packet residence time and bubble fraction. In addition, for Chen's model, the packet's absorption and scattering cross-sections must also be known, which are difficult to evaluate. One assumption in the penetration theory is the packet's surface adjacent to the wall is assumed to immediately attain the wall temperature; in other words, there is zero resistance. Other assumptions include the packet leaves the wall before the thermal wave penetrates the packet, and the packet and the bed are assumed to have the same thermal properties.

The penetration theory gives predictions that are only accurate for long contact times. As time approaches zero, the heat transfer coefficient predicted approaches infinity.

2.4.5.1 Chen's Model

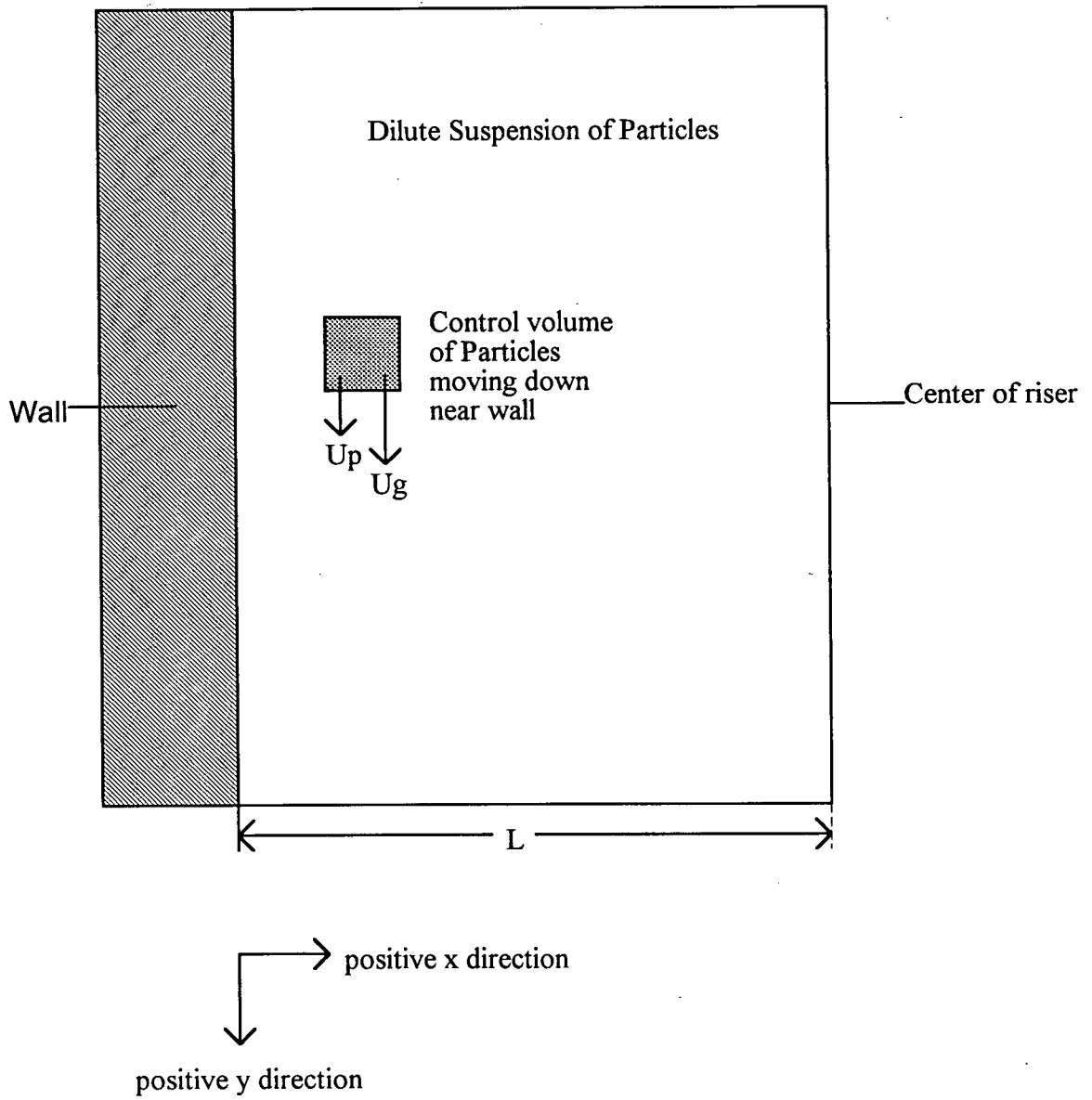
Chen developed a model that represents the interactive convective and radiative heat transfer process in a CFB. In the past, radiative heat transfer models usually treat the two-phase suspension as an opaque grey body with an effective suspension emissivity. The radiative heat transfer coefficient is then added to the convective heat transfer coefficient to obtain the overall heat transfer coefficient. In reality, radiative and convective heat transfer occur simultaneously throughout the suspension and are non-linear. The resulting equation is non-linear and has not been solved analytically. Numerical methods were used to solve the general case.

Chen's model considers an axial segment of the riser from the wall to the center of the riser. See Figure 2.8. Solid suspension is characterized by local parameters such as volume fraction of solid particles, temperature, heat generation rate, effective thermal conductivity, absorption cross-section, back-scattering cross-section, axial particle velocity and axial gas velocity.

For steady-state conditions, an energy balance can be made for the control volume. The general formulation is given in Equation 2.1.

$$\frac{\partial}{\partial x} \left(k_{\text{eff}} \frac{\partial T}{\partial x} \right) - [(\alpha_p \rho_p c_p u_p) + (1 - \alpha_p) \rho_g c_g u_g] \frac{\partial T}{\partial y} - \frac{\partial}{\partial x} (I - J) = -G_v \quad \dots\dots\dots(2.1)$$

Figure 2.8 Radiative Heat Transfer Model [Chen, 1988]



where, y	distance in the axial direction (m)
x	distance in the transverse direction (m)
k_{eff}	effective thermal conductivity (W/m·K)
T	absolute temperature (K)
α_p	volume fraction of the particle
ρ_p	density of the particle (kg/m ³)
c_p	specific heat of the particle (J/kg·K)
u_p	velocity of the particle (m/s)
ρ_g	density of the gas (kg/m ³)
c_g	specific heat of the gas (J/kg·K)
u_g	velocity of the gas (m/s)
I	radiative flux in the positive y direction (W/m ²)
J	radiative flux in the negative y direction (W/m ²)
G_v	heat source intensity per unit volume (W/m ³)

From the energy balance equation, Chen's model ignores the axial conductive and axial radiative fluxes as well as radial convection of the particles and gas.

The photon transport equations for the radiant energy passing through the solid suspension by absorption and back-scattering are given below.

$$\frac{\partial I}{\partial x} = -(A_r + S_r)I + S_r J + A_r \sigma T^4 \quad \dots\dots\dots(2.2)$$

$$\frac{\partial J}{\partial x} = (A_r + S_r)J - S_r I - A_r \sigma T^4 \quad \dots\dots\dots(2.3)$$

where, A_r radiation absorption cross-section / unit volume
 S_r back-scattering cross-section / unit volume
 σ Stefan-Boltzman constant (W/m²K⁴)

and A_r and S_r are calculated by:

$$A_r = CL \frac{3\alpha_p \epsilon_p}{d_p} \quad \dots\dots\dots(2.4)$$

$$S_r = CL \frac{3b\alpha_p(1 - \epsilon_p)}{d_p} \quad \dots\dots\dots(2.5)$$

where, CL dimensionless proportionality factor
 ϵ_p emissivity of the particles
 d_p diameter of the particles (m)
b back-scattering coefficient

The boundary conditions used are:

$$T(0,y) = T_w$$

$$\frac{\partial T}{\partial x}(L,y) = 0$$

$$T(x,0) = T_i$$

$$I_w(0,y) = \epsilon_w \sigma T_w^4 + (1 - \epsilon_w) J_w$$

$$J_L(L,y) = I_L$$

where the subscripts representation are,

w wall condition
i initial condition
L condition at the center of the reactor column

2.4.5.2 Radiative Contribution in Heat Transfer Model

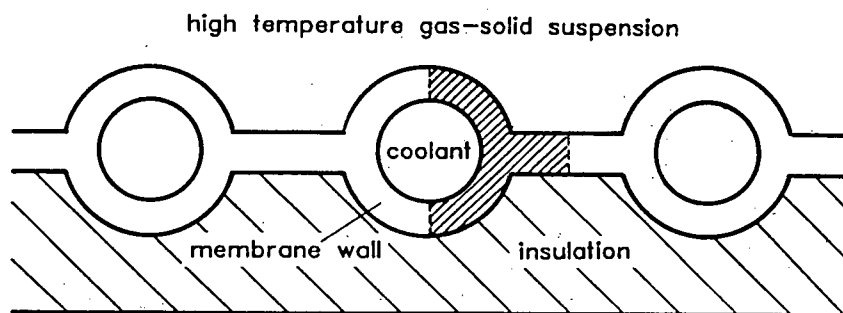
The convective and radiative heat transfer process in a CFB in reality is interactive. The equations are highly non-linear and difficult to solve numerically. Initially, Chen's equations were used in the heat transfer model developed in this work. The riser was divided into 20 axial cells and 2 radial cells. The annulus cell and the core cell were separated as individual control volumes, and the finite difference method was used to solve Equation 2.1. Temperature convergence was difficult to achieve; therefore, a less sophisticated non-interactive convective and radiative heat transfer equation was used to solve for the temperature profile in this thesis work. Due to the modular nature of the program developed, the heat transfer subroutine can be replaced with a more sophisticated heat transfer equation at a later date.

2.4.6 Heat Transfer in Overall Model

There are various models developed to describe high temperature heat transfer processes in CFBs and all of them use the penetration theory. Models 2, 3, 5, 6, 7, 8 and 10, listed previously include a heat transfer model. Model 2 uses a heat transfer model according to Nag [Nag et al., 1991], which includes particle and gas convection to all of the neighboring cells. Model 3 uses a more complex heat transfer model that includes conduction, convection and radiative heat transfer. The overall heat transfer in this model is determined by a mass and energy balance on all solid and gas phases. Model 5 uses an enthalpy balance on each chemical species and a constant wall heat transfer coefficient to determine the heat transfer in the CFB. Models 6 and 8 are similar to model 5's treatment of heat transfer; however, the wall heat transfer rates are determined by energy balances at the furnace wall. Model 7 calculates the amount of chemical heat generated using the Delft SURE Model [Lin et al., 1989]; however, this model does not include bed to wall heat transfer to be implemented into an overall model. Finally, model 10 determines the amount of chemical heat generated by solving a mass balance for each gas species and assuming a constant wall temperature, a heat balance is done according to a model by Martin [1980].

None of the overall models look at heat transfer to a membrane waterwall surface, which consists of tubes connected by longitudinal fins [Bowen et al., 1991], see Figure 2.9.

Figure 2.9 Schematic Cross-Section of a Membrane Waterwall Surface
[Bowen et al, 1991]



CHAPTER 3

MODELLING OF HEAT RELEASE, OXYGEN PROFILES AND

TEMPERATURE PROFILES OF CFBs

In this chapter, a detailed description of the model, developed in this thesis work, to predict heat release, oxygen and temperature distributions in CFB combustors will be discussed. The equations used are simple exponential equations for devolatilization and char combustion. The oxygen partial pressure profile is determined by a mass balance for each cell, given the initial oxygen pressure, and the temperature is determined by solving a nonlinear partial differential equation with the temperature term to the 4th power.

The program code is modular, so that each subroutine can be easily replaced by other equations. The heat release and heat transfer subroutines are coupled, which is required to solve for the temperature distribution.

3.1 MODEL ASSUMPTIONS

The assumptions used in the heat release and heat transfer subroutines are as follows.

- (i) The heat capacity of the gas is assumed to be constant and equal to the heat capacity of the gas at a temperature of 850 °C.

The heat capacity of the gas is recognized to be a function of temperature. However, this assumption was made to simplify the heat transfer equation to show, at this initial stage, that the program gives reasonable predictions. The program can be easily modified to include more sophisticated energy balances, including a heat capacity term that is a function of temperature.

- (ii) The heat capacity of the particle is assumed to be constant.
- (iii) The density of the particle is assumed to be constant.
- (iv) The density of the gas is assumed to be constant.

- (v) Velocity changes of the gas due to combustion are neglected.

Realistically, the variables in assumptions (iv) and (v) are both a function of temperature and gas velocity does change as more combustion gas is produced. However, this assumption is consistent with the hydrodynamics model used. In Senior's model, the mass flux of the gas is assumed to be constant. Since the mass flux of the gas is the product of gas density and gas velocity, both of these values were taken as constants. In the absence of a hydrodynamic model that is a function of temperature, these assumptions were made.

- (vi) Fragmentation and attrition of coal particles were assumed to be insignificant. In practice, the reaction of coal in CFBs, namely devolatilization and char combustion where heat is released, may be complicated by fragmentation that typically occurs near the end of devolatilization and by attrition, which occurs throughout char burning.
- (vii) The mass transfer rates of oxygen to the char particle and carbon dioxide away from the particle are assumed to be rapid [Howard, 1983]. Therefore, the limiting step is the kinetic rate of char combustion.

This assumption is valid for high gas velocities or good gas-solid mixing, which is a characteristic of CFBs [Basu and Yan, 1993].

- (viii) The char is assumed to be completely burned to form carbon dioxide, i.e., no carbon monoxide present.
- (ix) No heat release occurs in the standpipe, since there is very little oxygen present to support combustion.
- (x) The gas and particles in each cell are well mixed and at the same temperature.
- (xi) The higher heating value of the fuel was used for both the volatile and the char combustion.

This neglects some of the complexities at the local heat balance, and more detailed balances are needed for further development of the work.

- (xii) The model first calculates the enthalpy needed to dry all the moisture from the fuel before the coal undergoes combustion. The amount of moisture in each cell is calculated based on the fractional heat released within the cell.
- (xiii) The particle heat up rate is assumed to be infinite. In other words, the volatiles immediately start being released from the coal particles upon entering the primary zone.
- (xiv) There is 100% combustion of the coal particles. This is easily modified.

3.2 DESCRIPTION OF MODEL APPROACH AND SUBROUTINE EQUATIONS

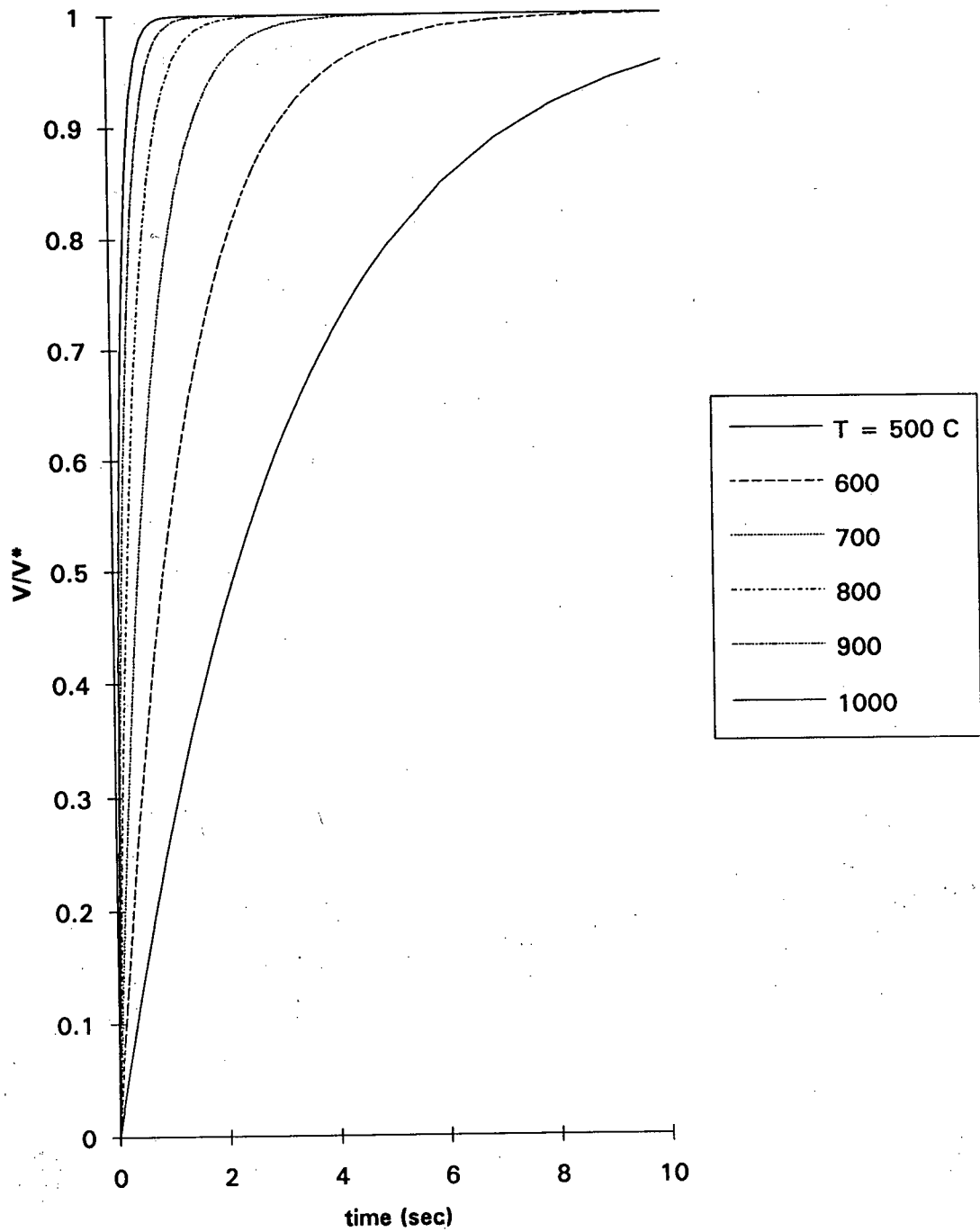
3.2.1 Devolatilization

Several devolatilization expressions were considered. These expressions were developed by Jia [Jia et al., 1993], Anthony [Anthony et al., 1975], and a combined devolatilization expression by Agarwal [1986] and Davidson [Davidson et al., 1985].

The devolatilization expression by Anthony, shown in Equation 3.1, was determined by heating up to 950 °C, in a helium environment, monolayer samples of lignite and bituminous coal supported on wire mesh. Devolatilization was found to be a function of time and temperature and not a function of particle diameter. For bituminous coal, the correlation was found to have a standard deviation of approximately 3 wt%. Figure 3.1 shows how the correlation predicts the time to devolatilize as a function of temperature.

$$V = V^* \left(1 - \exp \left[-k_0 t \exp \left\{ \frac{-E_0}{RT} \right\} \right] \right) \quad \dots\dots\dots(3.1)$$

Figure 3.1 Devolatilization Time as a Function of Temperature Predicted by Equation 3.1



where,	V	fraction of volatiles released at time t
	V*	initial fraction of volatiles in coal (from proximate analysis)
	t	time (s)
	T	temperature (K)
	k _o	= 706 s
	E _o	= 11.8 kcal/mol
	R	= 1.978x10 ⁻³ kcal/mol.K

The devolatilization expression by Jia, shown in Equation 3.2, is a function of particle diameter; however, it is not a function of time.

$$t_d = 5.10 \times 10^{10} T_b^{-1.95} d_p^{1.6} P_o^{-0.086} \quad \dots\dots\dots(3.2)$$

where,	t _d	devolatilization time (s)
	T _b	bed temperature (K)
	d _p	particle diameter (m)
	P _o	partial pressure of oxygen (atm.)
		must be within the range 0.01 atm. to 0.14 atm.

Very recently, a third devolatilization expression, which is a combination of the expressions by Agarwal and Davidson, was used. This devolatilization expression is both a function of particle diameter and time. The equations and results are listed and compared in the following chapter.

Although for all of the test cases, the devolatilization expression by Anthony was used, due to the modular nature of the program, Equation 3.1 can be easily replaced by another equation which may incorporate pressure, heating rate and particle size.

3.2.2 Plume Model

Experimentally, in both large and small CFBs, volatile plumes are found. These plumes are caused by poor radial mixing of gas, and the effect of the plume is that volatiles are not necessarily burned at the location where they are released. Clearly, as shown in Figure 3.2, this is a 2 or 3 dimensional mixing problem; however, the core/annulus model is only 1 dimensional. In order to superimpose the 2 dimensional phenomenon upon the 1 dimensional model, it is necessary to perform separate computations and then transfer the results into the 1 dimensional case.

In this model, the volatiles are assumed to burn at their point of release; therefore, the plume phenomena was handled by looking at the volatiles release as a function of height, and then transferring some fraction of the volatiles to the cell above. This transfer simulates the poor mixing, which prevents volatiles from releasing their heat of combustion at their point of evolution.

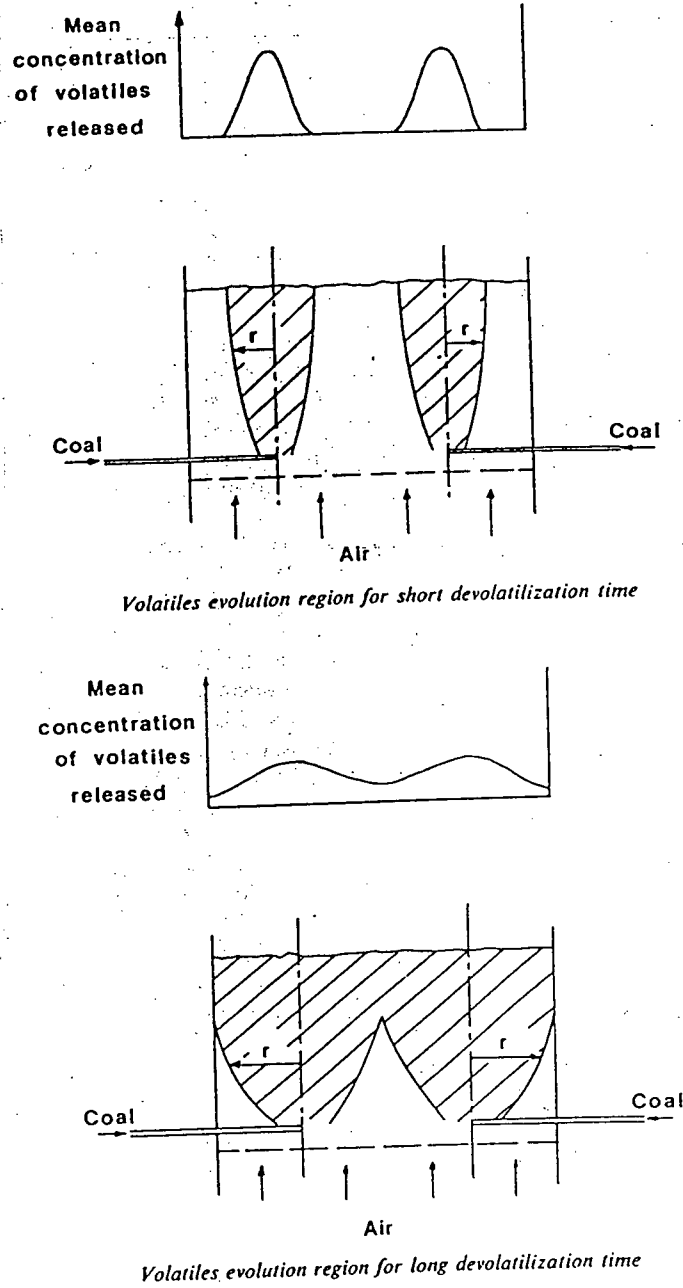
Devolatilization is rapid and generally takes place 3 to 20 seconds after the coal is fed into a CFB. Since the volatile matter will disperse from the fuel feed point rapidly in the axial direction, but only slowly in the radial direction, the volatiles evolution region forms an axial symmetric region centered on the fuel feed point [Stubington, 1980] and [Park et al., 1981]. If the fuel feed point is located at the wall, then the evolution region's axis of symmetry will be centered at the wall.

The volatiles must mix with oxygen for combustion to occur. Therefore, oxygen availability can be the limiting factor in volatile combustion, if the oxygen concentration is less than stoichiometric in the region near the fuel feed. This is more prevalent in large CFBs, where the volatiles burn higher up the riser.

As the volatiles travel up the height of the bed, they also diffuse a significant radial distance, which is given by Einstein's diffusion equation [Stubington, 1980].

$$x^2 = 2D_r t \quad \dots\dots\dots(3.3)$$

Figure 3.2 Plume Model of Volatiles Dispersion
[Stubington, 1980]



where, x^2 average displacement squared
 D_{rv} radial volatile diffusion coefficient
 $= 0.01 \text{ m}^2/\text{s}$
 t time (s)

To correct for the volatile dispersion, the above equation was solved for t , then knowing the velocity of the gas in the axial direction, the height h above the coal feed point where we observe fully radial mixing of volatiles is calculated. Fully radial mixing is achieved when the volatile evolution region spans the full cross-sectional area of the riser. For any cells below this height h , the amount of volatiles released is corrected for by transferring a fraction of the total volatiles to the cell above. This fraction is called the volatiles transfer fraction and is set at 0.3, which seemed to produce reasonable results.

The current volatiles release rate, calculated from Equation 3.1, is very fast and mainly occurs in the primary zone. The effects of using the plume model is not clearly seen, including the effect of various volatile transfer fraction values.

3.2.3 Char Combustion

After devolatilization, the char particle that remains may take several minutes to burn out, depending on the size of the particle. Since the mass transfer rate of oxygen to the coal particle was assumed to be rapid and the limiting step is char combustion, the Arrhenius equation was used to express char combustion. Assuming a first-order reaction, the following equation was used [Howard, 1983].

$$k_R = A_C \exp\left[-\frac{E_A}{RT_S}\right] \dots\dots\dots(3.4)$$

where,	k_R	reaction rate (kg/m ² ·s·atm)
	T_S	surface temperature (K)
	E_A	= 150,000 kJ/kg
	A_C	= 7260 kg/m ² ·s·atm
	R	= 8.314 kJ/kg·K

The char combustion equation was also included in a separate subroutine within the program; thereby, making replacement expressions of the char combustion rate an easy task. The time for burnout of a particle is given by:

$$\tau = \frac{\rho_c d_c}{24k_R P_o} \quad \text{.....(3.5)}$$

where,	d_c	diameter of the char particle (m)
	k_R	reaction rate (kg/m ² ·s·atm)
	P_o	partial pressure of oxygen (atm)
	ρ_c	density of the char particle (kg/m ³)
	τ	burn-out time (s)

From Table 3.1, we can compare the predicted burnout times and riser residence times for various particle diameters. It should be noted that the devolatilization time, calculated from Equation 3.1 [Anthony et al., 1975], is not a function of particle diameter. Also, the average particle residence times, given in Table 3.1, are determined based on a single pass.

Table 3.1 Comparison of Predicted Burnout Times with Particle Diameters

Studsvik CFB Bed Temperature = 850 °C Particle Surface Temperature = 900 °C Partial Pressure of O ₂ = 0.05 atm Particle Density = 1400 kg/m ³ Superficial Gas Velocity = 7 m/s				
Time (s)	dp = 100 μm	dp = 1 mm	dp = 3 mm	dp = 1 cm
Devolatilization [Anthony et al., 1975]]	4			
Devolatilization [Jia et al., 1993]	1.8x10 ⁻⁵	1.1	6.5	44.9
Devolatilization [Agarwal, 1986]	0.047	1.5	7.8	47.4
Char burnout	0.784	784	2352	7840
Average single pass particle residence in the riser above the secondary air	30			
Average single pass particle residence in the primary zone	10			

Comparing the devolatilization time prediction by Anthony with Jia shows that Anthony's formulation over predicts the devolatilization time for small particle diameters and under predicts the time for large particles. Therefore, there is a limited range of particle size (approximately 2 mm) where this correlation is valid.

The model assumes that the fuel particle travels through the bed in the same way as the bed particles. Then the single pass residence time for the primary and secondary zone is independent of the particle diameter. This assumption is valid for small diameter particles that are approximately the same size or smaller than the bed particles. For larger diameter particles, this assumption breaks down. However, typical coal particle diameters in CFBs are no more than approximately 4 mm, compared to an average bed particle of 0.5 mm [Senior, 1992].

By comparing the char combustion time with the single pass residence time in the secondary zone, for large diameter particles, we can conclude that the coal particle will pass through the riser many times before it is completely burnt out. The heat release distribution for large particles will then be similar to the density distribution. Therefore, there is a potential for simplification in the heat release model for large particles, by setting the heat release distribution to equal the density distribution.

Finally, by comparing the devolatilization time with the single pass residence time, for small diameter particles, we can conclude that if the devolatilization time is much less than the residence time in the primary zone, then most of the volatiles will be released in this zone. In addition, from Figure 3.1, most of the volatiles are released within the first few seconds from when the fuel enters the riser; therefore, most of the volatiles will be released in the primary zone, according to Anthony's correlation.

3.2.4 Monte Carlo Approach

The Monte Carlo Method is a class of mathematical methods first used by scientists in the 1940s. The essence of this method is the use of random or pseudo random numbers to study some phenomena. Although the problem may be non-probabilistic, an individual event that makes up the problem has the structure of a stochastic process, a sequence of states determined by random events. Therefore, although the answers obtained are statistical in nature and subject to the laws of chance, the average value of the answer isn't. In order to determine how accurate the answer is or to obtain a more accurate answer more experiments can be conducted. In this program approximately 100 particles will give reasonable heat release distributions due to char combustion.

Many people use the Monte Carlo Method and it has become an accepted part of scientific practice in many fields. Some advantages are convenience, ease and directness

of the method. In addition, Monte Carlo Methods are computationally effective, compared with deterministic methods when treating many dimensional problems.

For the Monte Carlo method to be effective, a source of randomness is needed. Unfortunately, the random functions supplied with different computers are pseudo random, which is to say that they are deterministic but mimic the properties of independent uniformly distributed random variables.

3.2.5 Comparison of Monte Carlo Approach with Analytic Technique

An alternative method to the Monte Carlo Approach is to solve the heat release and the heat transfer equations simultaneously by formulating mass and energy balance equations for each particle size within each cell. There are approximately 40 cells and the greater the number of particle sizes considered in the mass and energy balances the more accurate the final result. Assuming that there are 20 particle sieve sizes considered, which is the number in the fuel feed's particle size distribution, there would be over 800 simultaneous non-linear equations that must be solved for each time step. This very large and sparse matrix must then be iterated until a final converged value is reached. Such an approach will be time consuming, and due to the nonlinear nature of the energy balance equation, the solution may be difficult to converge.

The Monte Carlo approach was chosen because it seems to be a simpler method to program than the analytic technique method. In addition, using the Monte Carlo method, CFB systems of hundreds or thousands of particles can be treated quite routinely.

3.2.6 Monte Carlo Approach within the Program

In this program a large number of coal particles are individually traced throughout the bed riser and solids recirculation system. In each cell, the coal particle's probability of being transferred to the wall, from the wall, up the riser or down the riser is simply the ratio of the flow of particles out of the cell in a given direction, to the cell mass. The time

steps were selected such that at any given time step, the probability of the coal particle leaving the cell is set at 10%. See Figure 3.3. This probability value of 10% was chosen after initial experiments, using various probability values, showed that at higher probability values the accuracy of representing particle movement within the riser decreased. At lower probability values, accuracy increased; however, total run time also increased. A probability value of 10% seemed to be the optimum value.

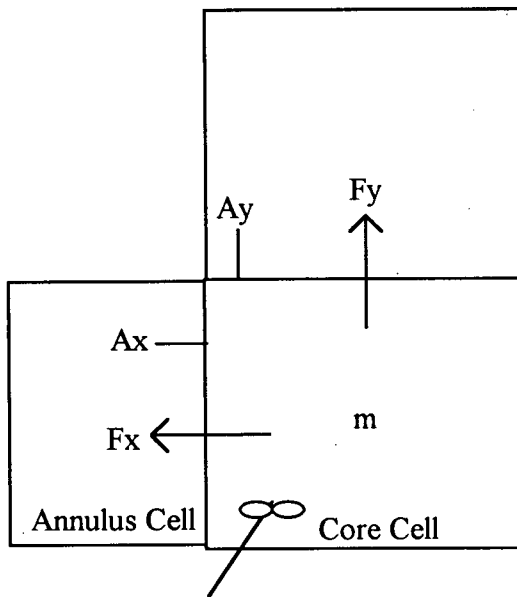
Several hydrodynamic assumptions were made in this program. The particles in the core were assumed to move only up the riser or to the streamer, and the particles in the streamer were assumed to only move down the streamer or to the core. See Figure 3.4. This assumption is the same as in Senior's hydrodynamic model. In addition, the coal particles were assumed to move in the same way as the bulk ash and sand particles.

A fraction of the particles that hit the top of the riser is reflected back into the streamer, based on a given reflection coefficient in the CFB. The rest of the coal particles that leave the top of the riser enter the cyclone, which is treated as a CSTR with a residence time of 0.3 seconds. This cyclone model can be replaced by alternative models. The coal particles less than 50 μm exit with the flue gas while larger particles leaving the cyclone are returned to the CFB's primary zone through the standpipe.

As the coal particle move throughout the riser, it first undergoes devolatilization then char combustion. In addition, to tracking the path of the particle, the Monte Carlo method also follows in which cell and at what time heat is released. Ultimately, this form of "bookkeeping" produces a heat release distribution.

The resultant heat release distribution is a function of temperature and partial pressure of oxygen, which must be initially guessed. However, once the heat release distribution is determined a new partial pressure of oxygen profile can be calculated and then a new temperature profile. The Monte Carlo method is repeated until a converged heat release distribution, partial pressure of oxygen profile and temperature profiles are obtained.

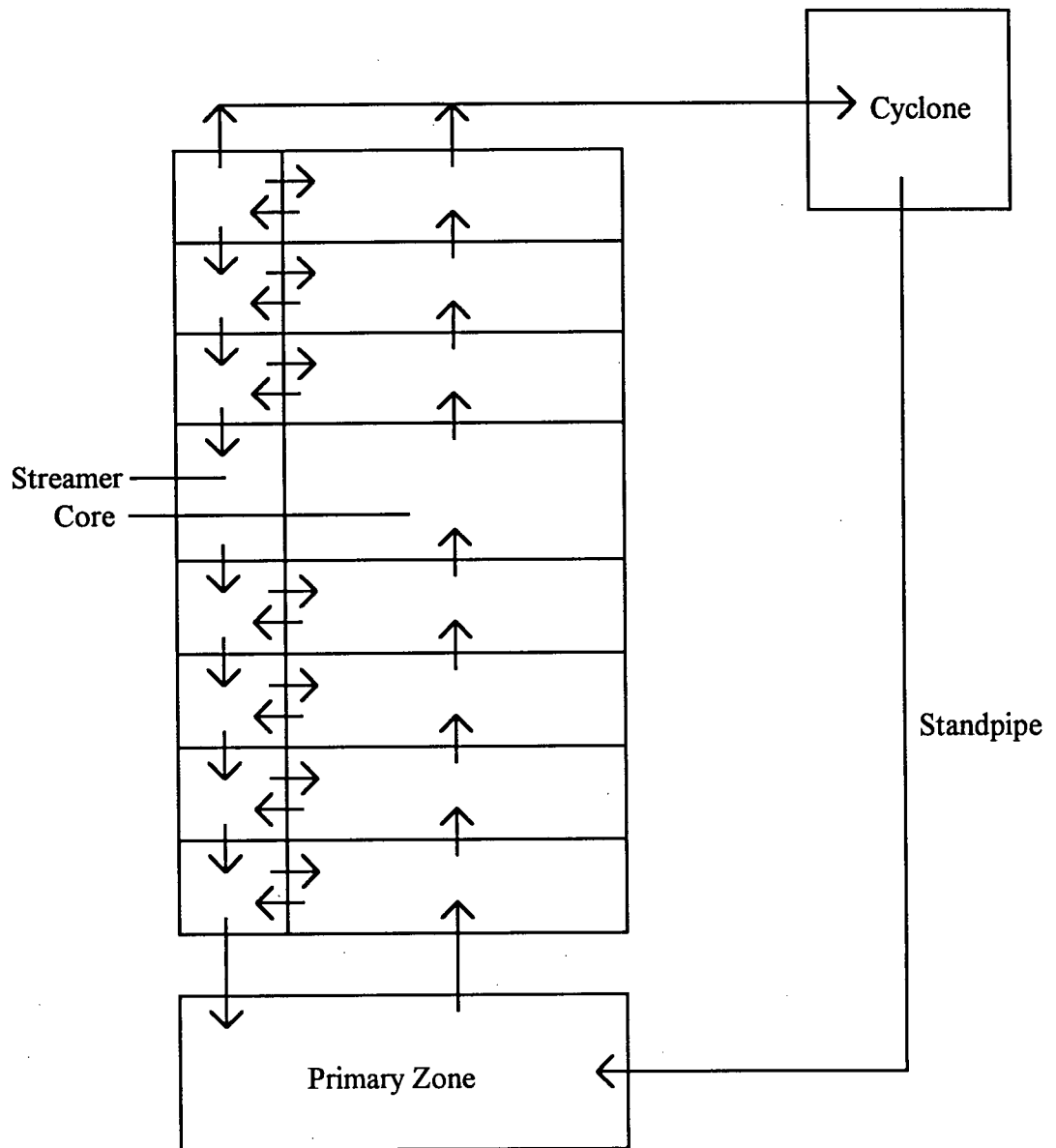
Figure 3.3 Probability of a Particle Leaving a Cell



Variables:

 m mass of particles in cell (kg) F_y flow across A_y (kg/s) F_x flow across A_x (kg/s) t time step (s)Probability of a particle moving vertically: $P_y = F_y \cdot t / m$ Probability of a particle moving horizontally: $P_x = F_x \cdot t / m$ Probability of a particle staying within the cell: $P_m = 1 - P_y - P_x$ 

Figure 3.4 Solid Particle Paths in the Riser



In order to validate the predicted particle paths throughout the riser, based on the Monte Carlo method, a test run was conducted. In this experiment one large "theoretical" particle, with a diameter of 1 m, was introduced into the primary zone and was traced as it underwent devolatilization and char combustion. The large size of the particle ensures that it will move through all of the cells many times before it is finally consumed. If the particles that hit the top of the riser are assumed to all reflect back down the streamer and the riser's temperature and oxygen concentration are constant, then the resultant heat release distribution should equal to the density distribution of the CFB.

The expression for devolatilization time chosen for this test is from Jia [Jia et al, 1993], since the time for volatiles release in this expression is given as a function of bed temperature and particle diameter. However, the devolatilization rate was assumed to be constant. The devolatilization time expression for Highvale coal is shown in Equation 3.2. The char combustion rate used is from Howard [1993] and was shown previously in Equations 3.4 and 3.5.

The results from this test, assuming a constant riser temperature of 850 °C, is that the heat release distribution due to volatiles and char combustion was indeed found to be the same shape as the density distribution.

3.2.7 Heat Transfer Model

Two types of heat transfer were considered in the model; cell to cell heat transfer and cell to wall heat transfer.

3.2.7.1 Cell to Cell Heat transfer

The overall cell to cell heat transfer equation, given below, includes conduction, convection and radiative heat transfer of both particles and gases.

$$\begin{aligned}
& -\frac{kA_W}{(\delta x)_W}(T_P - T_E) - \frac{kA_E}{(\delta x)_E}(T_P - T_E) - \frac{kA_N}{(\delta y)_N}(T_P - T_N) - \frac{kA_S}{(\delta y)_S}(T_P - T_S) \\
& - (F_x c_p + \rho_g c_g v_g) A_W (T_W - T^0) - (F_x c_p + \rho_g c_g v_g) A_E (T_E - T^0) \\
& - (F_y c_p + \rho_g c_g u_g) A_N (T_N - T^0) - (F_y c_p + \rho_g c_g u_g) A_S (T_S - T^0) \\
& - \varepsilon \sigma A_P T_P^4 + \varepsilon \sigma A_W T_W^4 + \varepsilon \sigma A_E T_E^4 + \varepsilon \sigma A_N T_N^4 + \varepsilon \sigma A_S T_S^4 + G = 0
\end{aligned}$$

.....(3.6)

where,	k	thermal conductivity of the cell (W/m·K)
	A	surface area of one side of the cell (m ²)
	T	temperature (K)
	x	distance in the transverse direction (m)
	y	distance in the axial direction (m)
	F _x	mass flux of particles in the transverse direction (kg/m ² ·s)
	F _y	mass flux of particles in the axial direction (kg/m ² ·s)
	c _p	heat capacity of particles (J/kg·K)
	ρ _g	density of gas (kg/m ³)
	c _g	heat capacity of gas (J/kg·K)
	v _g	represents the mass exchange of gas in the transverse direction due to turbulent mixing (m/s)
	u _g	velocity of the gas in the axial direction (m/s)
	ε	emissivity of the cell
	σ	Stefan-Boltzman constant (W/m ² ·K ⁴)
	G	source term in the cell (W/m)
subscripts,	W	west
	E	east
	N	north
	S	south
	P	control volume
superscripts,	0	reference

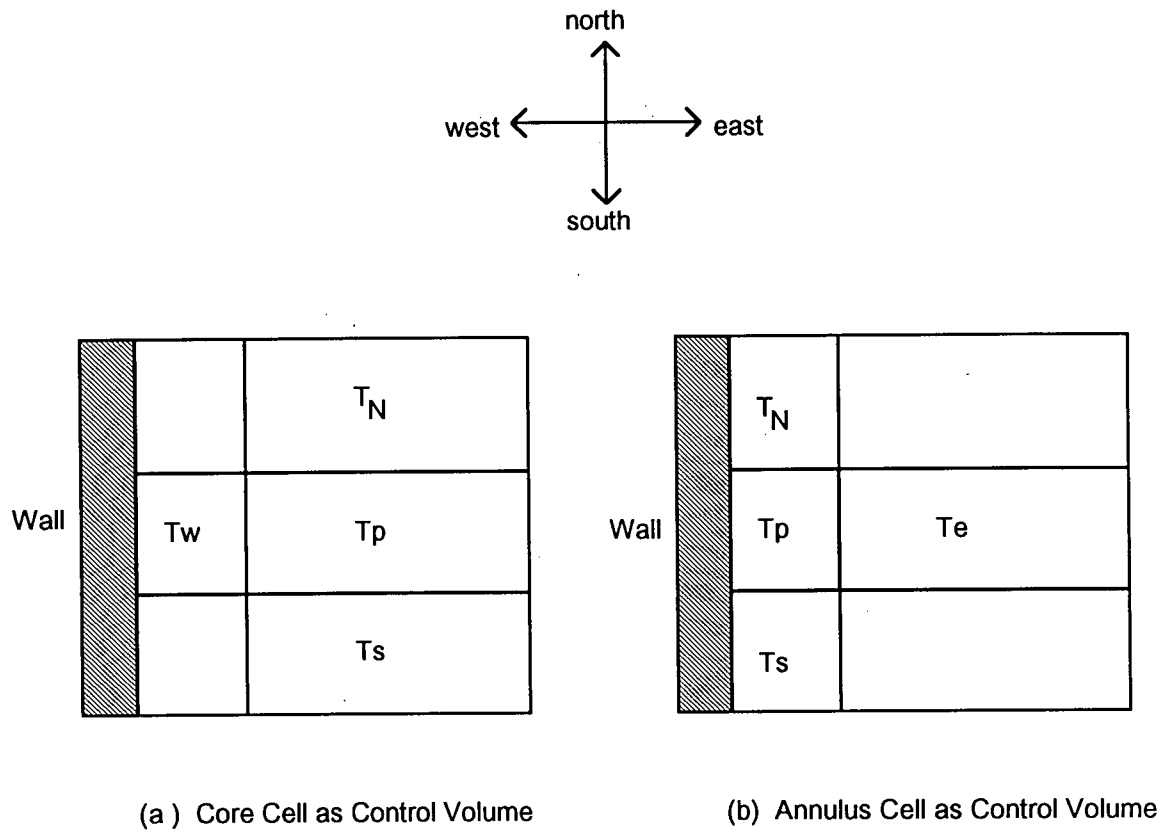
Figure 3.5 shows an enlarged riser cell cross-section, to indicate the direction convention used in the overall cell to cell heat transfer equation.

3.2.7.2 Differences with Chen's Model

The differences between the above heat transfer equation and the one used by Chen, besides the fact that the above equation does not couple the radiative and the conductive heat transfer terms are, the equation above includes heat conduction not only in the radial direction but also in the axial direction. Secondly, in Chen's model only convective heat transfer in the axial direction is considered; whereas, the above equation includes convection in the radial direction.

In Chen's model, the entire riser width is treated as a uniform gas solid suspension. The average suspension properties must be known to solve the steady-state finite differences formulation. However, in this model, the properties of the annulus and the core sections have different properties; therefore, the riser is split into a number of core and annulus cells along the riser height.

Figure 3.5 Direction Convention used in Cell to Cell Heat Transfer Equation



3.2.7.3 Finite Difference Formulation

Since the heat transfer equation is not conducive to analytical solution, numerical methods were used to solve the equation. More specifically, finite differences with the control volume method was used. The width of the riser was divided into four cells: the wall cell, the annulus, the core and the axis of symmetry of the riser. Each cell had different boundary conditions and had to be treated separately. The finite difference formulation of the heat transfer equation for each cell is given below.

For the wall cell, a constant temperature boundary condition was used. The wall temperature was set at 250°C. This assumes that the limiting rate of heat transfer is on the hot gas side, so that the cooling water temperature is equal to the wall temperature.

The annulus cell had the following finite difference formulation.

$$\begin{aligned}
 & -hA_w \left(\frac{T_P A_N + T_E A_{ne}}{at} - T_w \right) - \frac{kA_E}{(\delta x)_E} (T_P - T_E) - \frac{kA_N}{(\delta y)_N} (T_P - T_N) - \frac{kA_S}{(\delta y)_S} (T_P - T_S) \\
 & - (F_x c_p + \rho_g c_g v_g) A_E (T_P - T^0) + (F_{xe} c_p + \rho_g c_g v_g) A_E (T_E - T^0) \\
 & + F_{yn} c_p A_N (T_N - T^0) - \rho_g c_g u_s A_N (T_P - T^0) \\
 & - F_{ys} c_p A_S (T_P - T^0) + \rho_g c_g u_s A_S (T_S - T^0) \\
 & - \varepsilon \sigma A_P T_P^4 + \varepsilon \sigma A_w T_w^4 + \varepsilon \sigma A_E T_E^4 + \varepsilon \sigma A_N T_N^4 + \varepsilon \sigma A_S T_S^4 + G = 0
 \end{aligned}
 \tag{3.7}$$

where,	h	cell to wall heat transfer coefficient (W/m ² ·K)
subscripts,	ne	north face of the cell to the east of the control volume
	xe	transverse direction of the cell to the east of the control volume (m)
	yn	axial direction of the cell to the north of the control volume (m)
	ys	axial direction of the cell to the south of the control volume (m)

For the core cells, the finite difference formulation is as follows.

$$\begin{aligned}
 & -\frac{kA_w}{(\delta x)_w}(T_p - T_w) - \frac{kA_n}{(\delta y)_n}(T_p - T_n) - \frac{kA_s}{(\delta y)_s}(T_p - T_s) \\
 & - (F_x c_p + \rho_g c_g v_g) A_w (T_p - T^0) + (F_{xw} c_p + \rho_g c_g v_g) A_w (T_w - T^0) \\
 & - (F_{yn} c_p + \rho_g c_g u_g) A_n (T_p - T^0) + (F_{ys} c_p + \rho_g c_g u_g) A_s (T_s - T^0) \\
 & - \varepsilon \sigma A_p T_p^4 + \varepsilon \sigma A_w T_w^4 + \varepsilon \sigma A_n T_n^4 + \varepsilon \sigma A_s T_s^4 + G = 0
 \end{aligned}
 \tag{3.8}$$

The finite difference formulation for the core to annulus conduction terms, in Equations 3.7 and 3.8, estimates the temperature gradient as the difference in the core and annulus temperatures divided by their distance apart. This estimation is more valid for small CFB risers, where the distance between the core and annulus is much smaller. In larger CFB units, this estimation assumes that there is a constant gradual temperature gradient between the core and the annulus, when in actuality, the temperature gradient in a CFB is very steep in the annulus and becomes less steep near the core and annulus boundary.

The center of the riser symmetry is handled by setting the temperature gradient across the symmetry point to zero. The temperature of the center symmetry point, within the finite difference formulation, is set to equal to the core temperature at the same riser height. This boundary condition becomes less valid near the top and bottom of the riser, where the solids exit and entry points are not symmetric.

Using the given equation and boundary conditions, a temperature profile of the riser was obtained.

3.2.7.4 Wall to Cell Heat Transfer Equation

The wall heat transfer coefficient term used is from a Studsvik report [Morris, 1988]. This term was obtained by fitting experimental data on the Studsvik CFB unit. A linear relationship between the furnace side heat transfer coefficient and the furnace solids bulk density was observed to be the following.

$$h_f = 1.8\rho_b \quad \dots\dots\dots(3.9)$$

where, h_f furnace side heat transfer coefficient (W/m²·K)
 ρ_b furnace solids bulk density (kg/m³)

3.2.7.5 Cyclone and Standpipe

The cyclone is treated as adiabatic. The total amount of devolatilization and char combustion is recorded and an overall heat balance is calculated. There are two possible selections for the solids return particle temperature. The first selection is assuming that a heat exchanger is placed between the cyclone and the standpipe, the solids return particles are assumed to re-enter the riser at a constant temperature, set by the user. The second selection is to set the temperature of the solids return equal to the operating temperature of the cyclone. The second selection was chosen in the sensitivity analysis cases.

The solids return particles are initially mixed with the combustion air and the fuel feed. The initial temperature of this mixture is used as the boundary condition of the surface temperature of the south face of the primary zone. Since this surface temperature is usually not equal to the temperature of the primary zone, there is heat loss due to conduction and radiative heat transfer through this surface. The magnitude of the heat

loss is less than 0.5% of the total heat transfer through the membrane wall; therefore, this loss does not affect the accuracy of the heat balance equation and the final temperature results. However, better alternative to this boundary condition, is to set the boundary condition as being an adiabatic surface. In this way, there would be no heat loss through this surface.

3.3 DESCRIPTION OF MODEL PROGRAM

3.3.1 Input and Output Files

The model's algorithm is seen in Figure 3.6, a description of the convergence loops and tolerances used are listed in Table 3.2, and the program listing is included in appendix A. Initially, input and output files are assigned. There are 2 input files included in appendix B; one containing the CFB initial conditions and specifications, most of which are output values obtained from Senior's CFB model. The other input file includes the fuel specifications, the relaxation parameters used in the specific case and the number of particles in the Monte Carlo method. The four output files generated by the program are listed below.

- (i) A final output file included in appendix C
- (ii) A file that contains the temperature distributions at every iteration
- (iii) A file that contains information used in the enthalpy balance check
- (iv) A file that contains the temperature of one cell at every iteration, which show whether or not convergence has been achieved.

A description of the input and output variables used in the program are listed in appendix D.

Figure 3.6 Model Algorithm

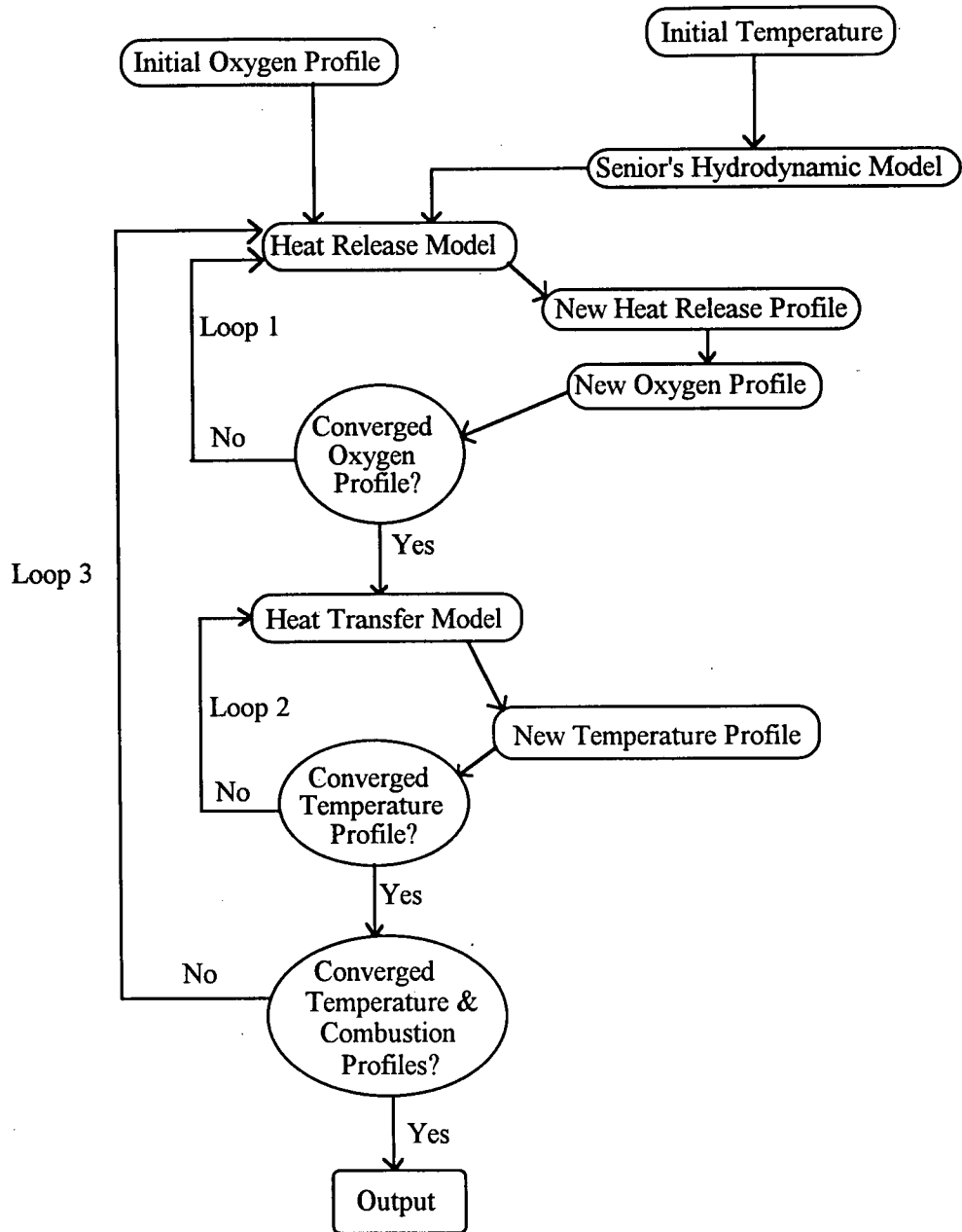


Table 3.2 Description of Convergence Loops and Tolerances used in Program

Convergence Loop	Description	Tolerance	Relaxation
1	Partial pressure of oxygen profile convergence for the core cells only	Absolute 0.001 atm.	0.7
2	Temperature profile convergence	Relative 1%	0.7
3	Heat Transfer Subroutine convergence is met by monitoring the convergence of 1 core cell's temperature at every call to the heat transfer subroutine calculation, or comparing the temperature profile with the previous iteration's profile, until the absolute error is less than the set tolerance.	Absolute approx. 0.01 °C	--

3.3.2 Program Steps

- (i) The program initially reads the input files and creates the output files.
- (ii) The riser is divided into core and annulus cells, and cell dimensions are then determined. For all the test cases, the riser was divided into 20 core cells and 20 annulus cells, which have equal height and corresponds to the cell divisions used in Senior's model. Also there is a cell that represents the primary zone and a cell that represents the cyclone.
- (iii) Given the gas velocities, the combustion efficiency and the excess oxygen value of the gas and the ultimate analysis of the fuel, the air and fuel feedrates are calculated.
- (iv) The transverse and radial mass fluxes for all the cells are converted into mass flowrates.
- (v) The mass flowrate values are used in a mass balance where the axial mass flowrates of particles in the core cells were changed to ensure conservation of mass throughout the riser. Due to the nature of Senior's mass fluxes output

values, the mass balance for each cell in the riser was not entirely balanced. The error in the mass balance varies from + 4% near the bottom of the riser to - 5% at the top of the riser. Although this did not pose problems to Senior's hydrodynamic model, the enthalpy balance is very sensitive to the mass balance. A mass balance was needed to solve the temperature distribution in this model.

- (vi) Next a uniform initial value of 21% partial pressure of oxygen was set for the riser, and a uniform temperature of 850 °C was guessed for the bed. In addition, the user was prompted by the program to specify whether the solids return temperature will be equal to the cyclone temperature or a set temperature, specified by the user.
- (vii) A probability matrix is then set up using the mass flowrate information. This matrix is used to determine how a coal particle will travel within the CFB riser during devolatilization and char combustion.
- (viii) Next the total membrane surface area is determined if a CFB design approach is used. Given an initial operating temperature of the bed, the program will calculate the fractional heat transfer area needed to achieve that temperature. If a rating approach is used, the user can specify the heat transfer area and the program will then calculate the operating temperature. Presently, the program sets the heat transfer surface as evenly distributed on all sides and along the full height of the riser above the secondary zone. The location of the heat transfer surface can be easily set at specific locations, at a later date.
- (ix) The devolatilization subroutine is called.
- (x) This heat release profile due to devolatilization is corrected by using a volatile transfer fraction term, which assumes that the unburnt volatiles travel up the riser in a plume until they reach a cell with more oxygen, or until the volatiles are radially fully mixed with other gases. This phenomena is discussed in more detail in Section 3.2.2.

- (xi) The heat release due to devolatilization is determined, by summing up the total volatiles released in each cell and assuming the volatiles have the same higher heating value as for char.
- (xii) The subroutine to determine the partial pressure of oxygen profile is called. A mass balance is done to determine the oxygen profile. The secondary air is introduced into both the core and the annulus cells just above the primary zone. The split is determined on the core and the annulus cross-sectional area. In this way, the mean gas velocities in the core and annulus will be constant and equal to the gas velocities set in the user input file.
- (xiii) This updated partial pressure profile of oxygen is compared with the previous iteration's profile to determine if convergence has been met. If convergence has not been met, the heat release due to char combustion is recalculated using the updated partial pressure of oxygen profile.
- (xiv) The subroutine to calculate the temperature profile of the CFB riser is called. Finite differences with a control volume formulation was used to conduct an enthalpy balance around each cell to determine the temperature profile.
- (xv) The updated temperature profile is determined.
- (xvi) The temperatures for the core and annulus cells at a height that corresponds to the beginning of the developing zone are altered to smooth the temperature profile. The other cell's temperatures were not altered. This discontinuity in the temperature profile is discussed in the Section 3.3.4.
- (xvii) The updated temperature profile is compared to the previous iteration to ensure convergence is reached. If convergence has not been achieved, the heat release due to devolatilization and char combustion and the partial pressure of oxygen subroutines are recalculated.
- (xviii) A printout of the output is generated.

3.3.3 Model Tuning

The major parameters in the user input file, found in appendix B, that can be varied for convergence reasons are listed below.

(i) Number of particles in the Monte Carlo method.

The greater the number of particles used, the heat release distribution, the oxygen partial pressure profile and the temperature profile will be more smooth. The errors associated with not enough particles become more evident in the oxygen partial pressure profile in the annulus. A coal particle does not travel through many annulus cells, especially near the bottom of the riser; therefore, as the number of particles increases, more particles will travel through any given cell.

Initial tests of the Monte Carlo method showed that approximately 100 particles are needed for reproducible results, in the core cells, which do not significantly change as more particles in the Monte Carlo method are used. More than 400 particles are needed to produce smooth profiles in the annulus cells. However, as more particles are used, the total run time increases linearly.

(ii) Tolerance used in the partial pressure of oxygen profile calculation.

This value is used in convergence loop 1, which is shown in Figure 3.6 and Table 3.2. The tolerance is an absolute tolerance, set at 0.001 atmospheres, which corresponds to a relative tolerance of 1% to 2.5%, and is based on the partial pressure of oxygen in the core. The change in the partial pressure of oxygen in the core was used as the basis, because there is very little oxygen in some parts of the annulus and its' absolute and relative tolerance errors would be too small to be meaningful. Conversely, the absolute and relative variations in the partial pressure of oxygen in the core is not large, and this iterative calculation converges steadily, normally within 10 iterations if an under relaxation factor of 0.7 is used.

(iii) Tolerance used in the temperature profile calculation

This is a relative tolerance, used in convergence loop 2 which is shown in Figure 3.6 and Table 3.2, and is set at 1% of any cell's temperature compared to the cell's temperature in the previous iteration. This calculation is very rapid, using an under relaxation factor of 0.7.

- (iv) Tolerance in the heat transfer subroutine.

This value is used in convergence loop 3, which is shown in Figure 3.6 and Table 3.2. Normally, the temperature for 1 core cell was monitored to determine whether a steady-state temperature had been reached; however, the user may also specify a temperature tolerance to determine whether convergence is achieved.

For the test runs conducted, by monitoring the temperature of 1 core cell until convergence has been achieved, the final absolute temperature tolerance was less than 0.01 °C.

- (v) Relaxation parameter in the partial pressure of oxygen calculation.

This under relaxation factor is set to 0.7.

- (vi) Relaxation parameter in temperature profile calculation.

This under relaxation factor is set at 0.7 and prevents this subroutine from diverging.

The relaxation parameters used in the partial pressure of oxygen and the temperature calculations are used to prevent the profile predictions from diverging. Even if increasing the relaxation parameters does not cause the profile predictions to diverge, this will not significantly decrease the program's computation time, since the limiting calculation is the Monte Carlo method.

- (vii) Residence time of the cyclone.

This value is set at 0.3 seconds, and can be easily replaced with a more sophisticated cyclone model, if necessary.

3.3.4 Discontinuity of Temperature Profile

There is a discontinuity in the temperature profile calculated by this model, which varies for different CFBs and initial conditions. The position and magnitude of the discontinuity coincides with the boundary between the developing and the fully-developed zone. The discontinuity results from the hydrodynamic model, which uses different equations to predict the mass fluxes for the developing and the fully-developed zones.

Figure 3.7, shows a plot of mass flowrate versus height for the UBC CFB, and the discontinuity can be seen clearly. Since the discontinuity does not significantly affect the hydrodynamic code, but affects the temperature profile, and since only 1 cell is affected, namely the boundary cell, a curve smoothing subroutine was used to correct for this one point. From Figure 3.8, it can be seen that the curve smoothing subroutine does not change the results of the other points or affect the temperature prediction in subsequent iterations.

Several other methods to correct for the discontinuity were considered. Initially, subdividing the riser into more cells in the axial direction was tested. The result of this test is shown in Figure 3.7. By increasing the number of axial cells, the bounds of the discontinuity location were constricted and the magnitude of the discontinuity was reduced; however, by increasing the number of cells, the run time increased. Secondly, the tolerance in the hydrodynamics code that controls the convergence of the boundary mass fluxes prediction was decreased. This caused the discontinuity to decrease, but not to an extent that the temperature profile would be continuous. In fact, if the tolerance was decreased too much, the hydrodynamic code would not converge.

Figure 3.7 Net Mass Flowrate From the Core to the Streamer versus Height for the UBC CFB

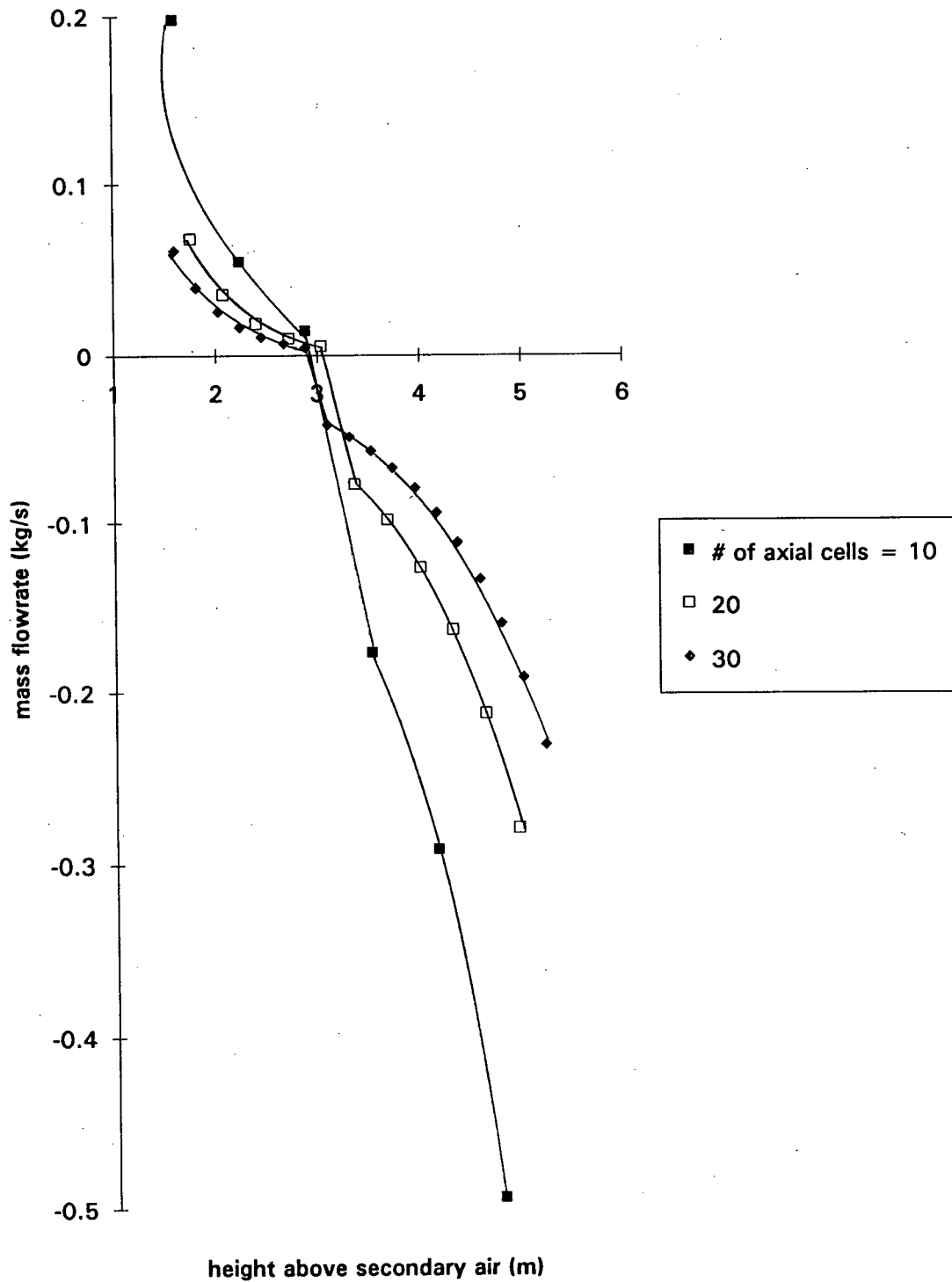
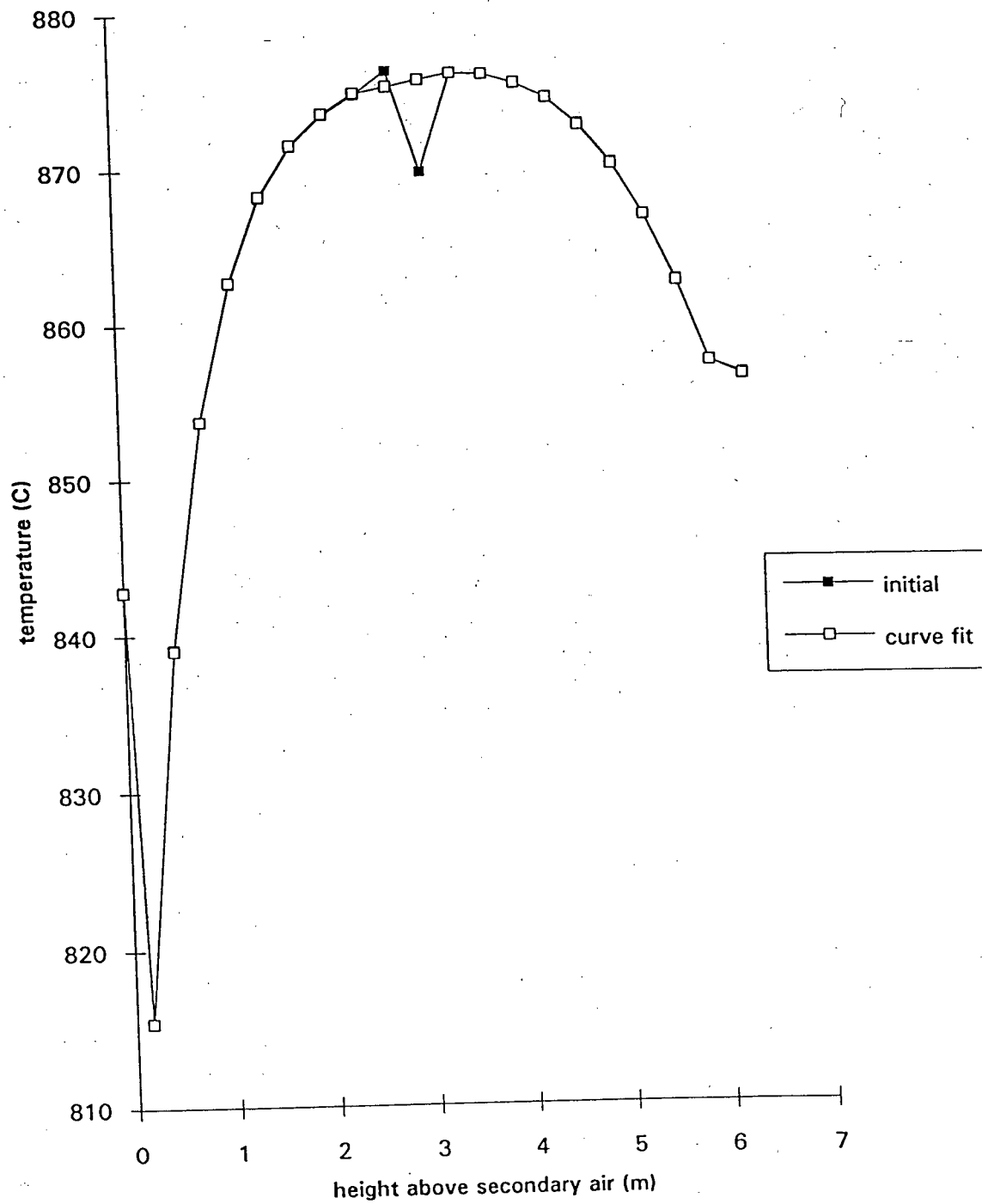


Figure 3.8 Temperature Distribution of Core Cells
(before and after curve smoothing)



Since this discontinuity also affected the heat generation profile slightly, smoothing the heat generation profile was considered. This reduced the magnitude of the discontinuity; however, it was still present.

The best method found to date to deal with the discontinuity is to smooth the temperature profile directly, at every iteration.

3.3.5 Convergence

Due to the non-linear nature of the equations, it takes several hundred iterations until a final converged solution is obtained. In practice, several test runs were first conducted at different initial temperature guesses, to determine the bounds of the final temperature solution. These bounds, within ± 20 °C were then used in the final run. In this way, the initial guess of the temperatures is close to the final solution, so that convergence is achieved in less than 100 iterations. If the test runs were not conducted, it may take more than 600 hundred iterations to obtain the final converged result.

Figure 3.9 shows that there is indeed a final temperature solution, since a higher or a lower initial temperature guess will still converge on the same final value.

Repeatability of the results was also studied by running the same conditions several times, starting with different initial temperature profiles. The results, shown in Figure 3.10, were such that each run produced effectively identical profiles, provided that sufficient time was given for convergence; therefore, the repeatability of the program is good.

3.3.6 Numerical Stability of Partial Pressure of Oxygen Profile

An analysis was done to determine if and when instabilities arose in the partial pressure of oxygen profile iteration and in the temperature profile iteration. For the partial pressure of oxygen profile, it was shown that the greatest relative variation in the amount

Figure 3.9 Temperature Convergence for Various Initial Temp. Guesses
(Studsvik CFB, case sh0)

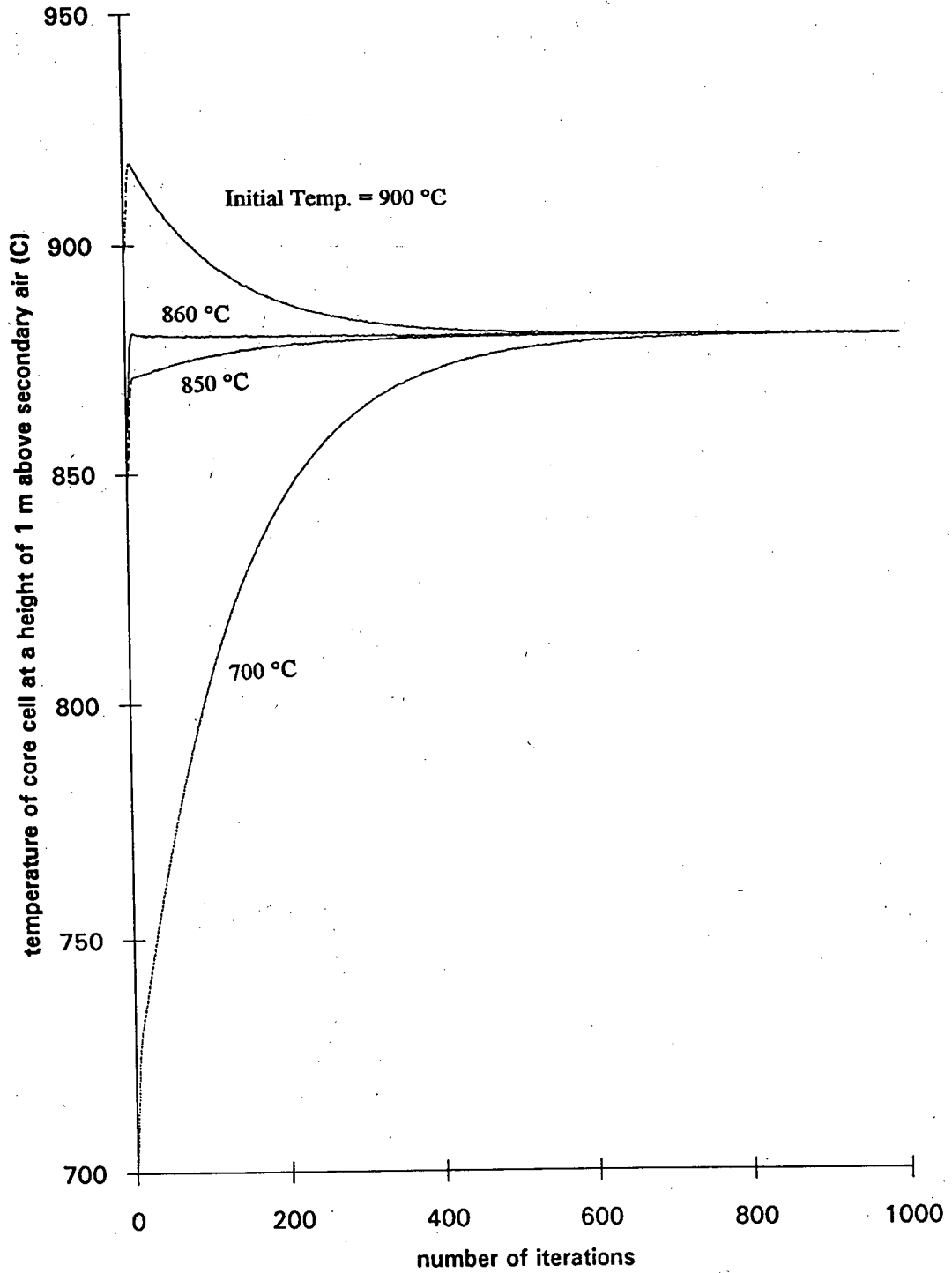
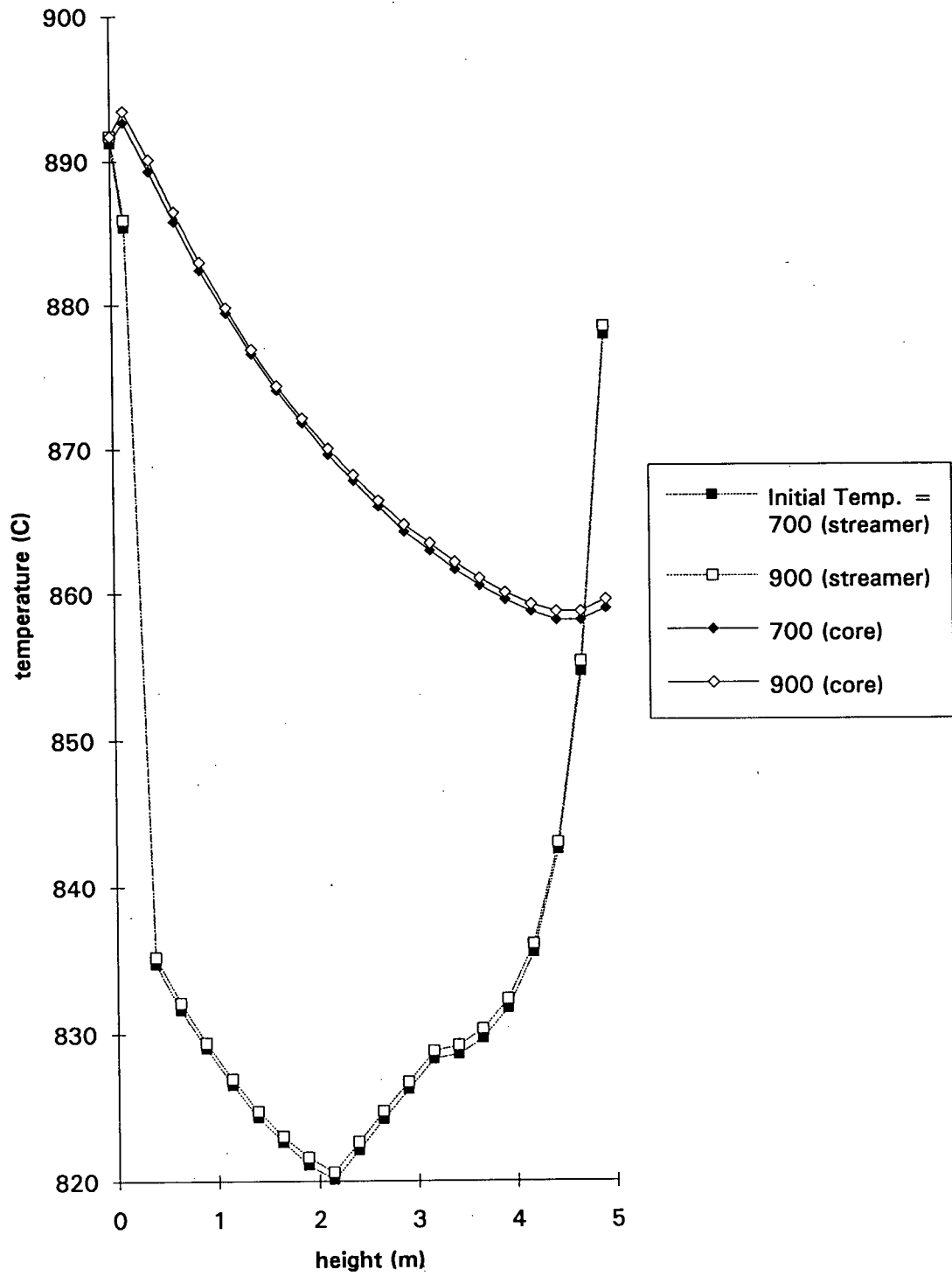


Figure 3.10 Temperature Profiles of Case sh0
(for various initial temperature guesses)



of oxygen was in the annulus cells. This suggests that because only 100 particles were used in the Monte Carlo method, and the volume and residence time in the annulus is small compared to the core cells, if one extra coal particle enters an annulus cell, the oxygen partial pressure profile can be significantly different. A test run was conducted for the Studsvik CFB, in which the number of particles in the Monte Carlo method was increased from 100 particles to 400 particles, see Figure 3.11. From this figure we see that with 400 particles the partial pressure profile in the annulus is more smooth, but clearly more particles are needed to obtain a final converged annulus profile.

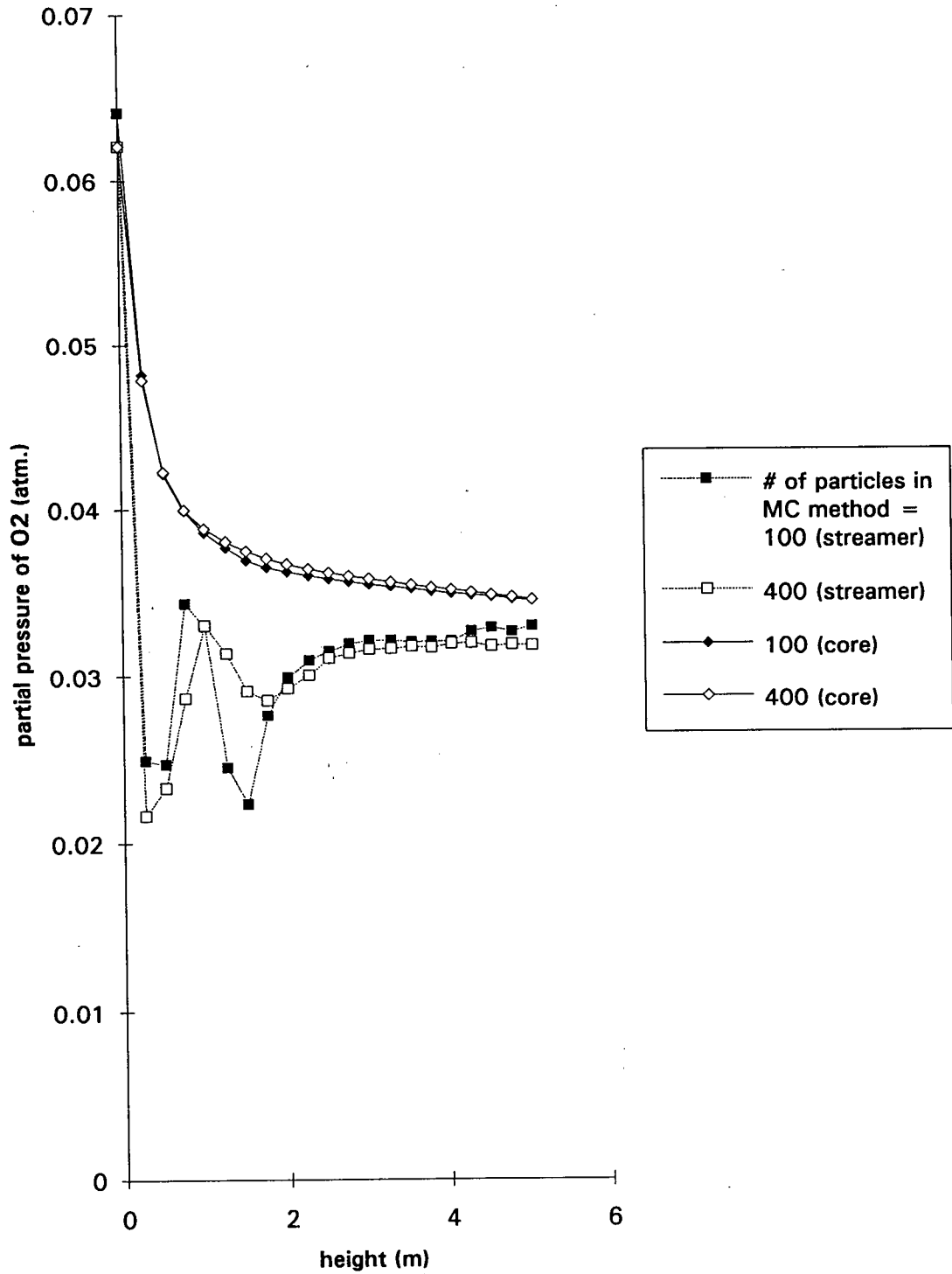
This error in the partial pressure of oxygen in the core cells was small compared to the streamer and seemed to reach a converged value quickly, as will be shown in the next chapter, Figure 4.1.

3.3.7 Run Time

The run time required for convergence could be slightly improved by varying the relaxation parameters and the convergence tolerance values. However, as mentioned previously, the limiting subroutine in the program was generating the heat release distribution using the Monte Carlo method. Decreasing the minimum number of particles needed in the Monte Carlo method, can significantly decrease the overall run time of the program.

For the test cases studied, which are rating problems, initially several quick runs of approximately 10 minutes each were conducted using only 10 particles in the Monte Carlo method and starting each run at a different initial temperature guess, to determine the range of the final converged temperature profile. Then using relaxation parameters of 0.7 for both the partial pressure of oxygen profile and the temperature profile calculations, setting 0.001 atmospheres for the absolute tolerance value of the partial pressure of oxygen and 0.01 °C for the absolute tolerance of the heat transfer subroutine, and using

Figure 3.11 Partial Pressure of O₂ vs Height
 (Studsvik CFB, Combustion of Highvale Coal with $U = 7\text{m/s}$ and $G_s = 15\text{ kg/m}^2\text{s}$)



100 particles in the Monte Carlo method, the program took approximately 2.5 minutes per iteration. With a initial guess of the final temperature of the riser, which is close to the final converged temperature, program convergence can be obtained within 20 iterations; however, with most of the test runs, the program was allowed to run for 200 iterations to ensure that convergence has been met. The total run time for 200 iterations was approximately 8 hours. If more particles are used in the Monte Carlo method, then the total run time of the program would increase linearly in proportion to the number of particles.

For a design problem, where we wish to find the total heat transfer area needed to achieve a given average operating bed temperature, initial quick test runs were also conducted using a different heat transfer area for each test. The design problem was found to take just as long to run as a rating problem.

The program was executed on Sun workstations, which is approximately 3 to 4 times as fast as a 33 MHz 486 PC.

CHAPTER 4

DISCUSSION OF RESULTS AND VALIDATION

4.1 INTRODUCTION

The goal of a Circulating Fluidized Bed Boiler's operation is to generate steam for energy production. In a typical day, the demand for energy varies, with a higher demand early mornings and early evenings. Since the CFB boiler is unable to store any energy, the operation of the CFB will have to be changed to meet the various steam demands throughout the day.

The basic strategy for meeting varying steam demands is to vary the heat flux from the boiler. The basic heat flux equation is given below.

$$Q = UA\Delta T \quad \dots\dots\dots(4.1)$$

Since the heat transfer area, A , is constant and the temperature difference, ΔT , cannot change significantly, this implies that the heat transfer coefficient, U , must be varied.

Some parameters must be kept within certain operating ranges. One of these parameters is the percentage of air leaving with the flue gas. Ideally, this value is kept at a minimum, usually between 10% and 30% excess air, or just enough air is added for complete combustion; thereby, minimizing heat loss by heating the excess air. Secondly, the average temperature of the bed is kept within the operating range of 750 °C to 900 °C. A temperature greater than this range will cause more NO_x to be generated, decrease sulphur capture and cause other operating problems. Operating temperatures considerably less than 750 °C will hinder coal combustion.

The exact temperature will depend upon fuel reactivity. The above arguments assume that the reactor is approximately isothermal. At low load, the gas velocity may be low and the circulation rate may drop correspondingly. In this case, the primary zone

must be held at the desired operating temperature; therefore, there may be a significant drop in the upper furnace temperatures.

In order to change the heat transfer coefficient to meet the steam demands, the suspension density profile of the CFB must be varied. There are several parameters that can be changed to achieve the desired heat transfer coefficient. The typical parameters include air feedrate, solids recirculation rate and flue gas recycle rate.

To verify that CFB control can be effectively modeled using the program developed here, results were obtained for both the Studsvik CFB and for the UBC CFB using various superficial gas velocities and solids recirculation rate inputs. The model does not consider flue gas recirculation; therefore, the effects of this parameter on a CFB's operations were not studied.

4.1.1 Initial Test Runs

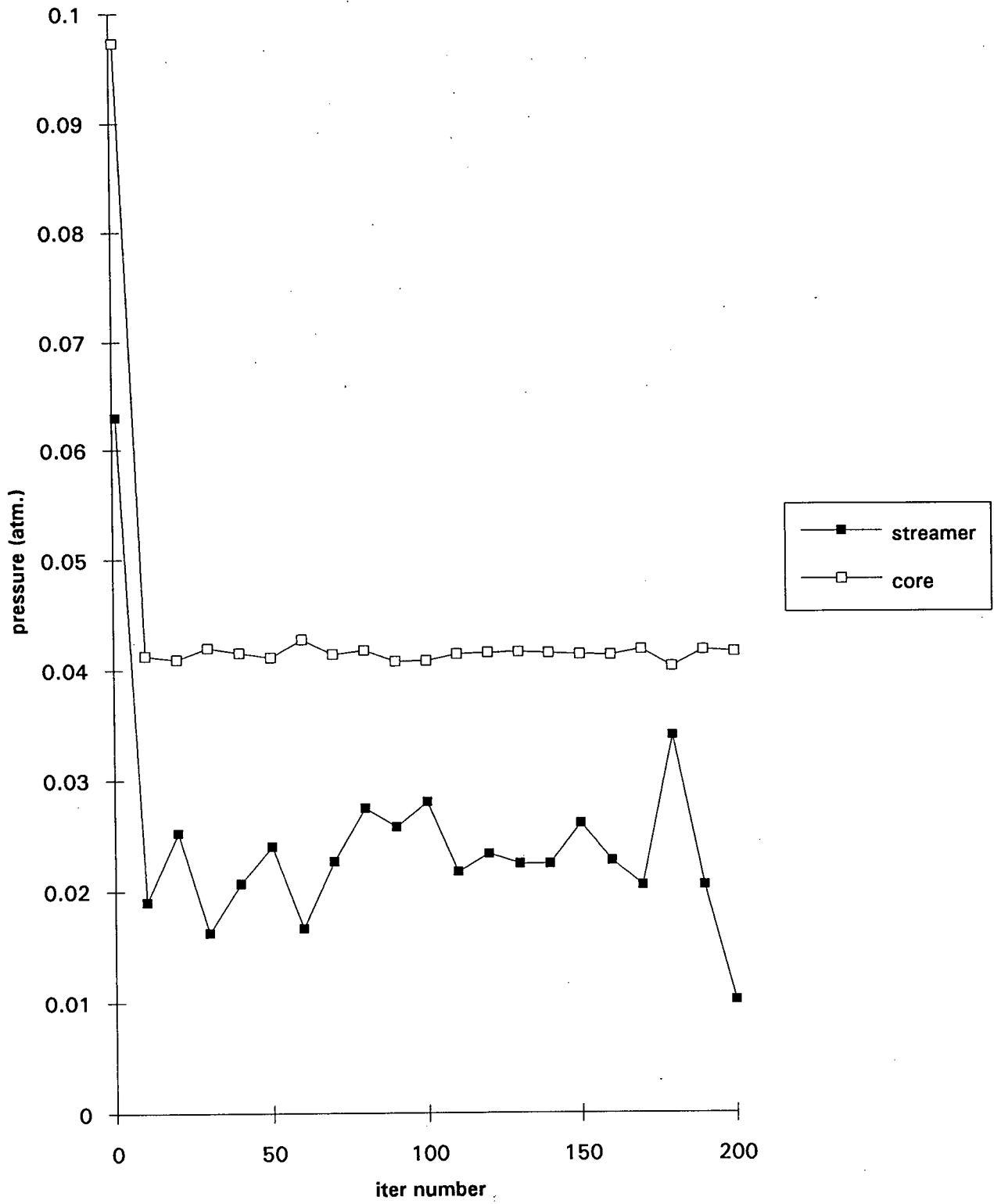
To ensure that a random number was generated with each call to the random number generator, when the program was executed on a 486 PC, a new seed was selected with each call for a random number. The results of several Studsvik CFB runs, sh0, with the same initial inputs were conducted with similar, but not identical results. When this program was executed on the Sun Workstation, it was not possible to generate a random seed with each call to the random number generator; however, the random numbers generated are sufficiently random, such that different initial starting points of the same test case gave the same, but not identical profile predictions.

From previous testing of the model, it is clear that the temperature profile changes affect the pressure profile to a larger extent than the pressure profile causing changes in the temperature profile calculations. The reason for this is that the high solids recirculation rates tend to smooth out the temperature profile, making the temperature more uniform throughout the riser. This effect masks changes in the heat release and partial pressure of oxygen profiles under the conditions studied. Therefore, test runs were

conducted to ensure that the CFB's partial pressure of oxygen profile had indeed converged before the program called the subroutine to predict the temperature profile. On average, the program conducted 10 to 20 iterations of the partial pressure of oxygen profile before the tolerance was met and the temperature profile could then be predicted. There was some concern that the tolerance was not tight enough for the pressure convergence. In one test, the partial pressure of oxygen calculation was allowed to continue for 200 iterations, tracking the pressure of oxygen in a core and streamer cell at a height which shows the greatest pressure variations. The height chosen, based on behaviour in previous runs, was 1 m above the secondary air. Figure 4.1 shows that the partial pressure of oxygen in the core cell quickly reached a steady value of approximately 0.04 atm. within the first 10 iterations, while the streamer cell's partial pressure of oxygen did not converge but varied around an average value of 0.02 atm. The reason, which was previously mentioned, is that the number of Monte Carlo particles used may not be large enough so that if one extra particle enters an annulus cell, its oxygen partial pressure profile can be significantly changed. Therefore, more particles in the Monte Carlo method will be needed. This will cause the total run time to increase.

A third test run was conducted to show that the Monte Carlo Method was simulating the path of the coal particle as it traveled throughout the CFB, based on the CFB's hydrodynamics. For this test, a very large "theoretical" particle with a diameter of 1 m was introduced into the primary zone of the CFB and tracked throughout its devolatilization and combustion. The riser was assumed to be at a constant temperature and partial pressure of oxygen. In addition, the devolatilization expression used was from Jia, which is a function of particle diameter. Since the primary zone is normally much larger and denser than a core or streamer cell, a small coal particle will devolatilize and combust before it has the chance to travel up the riser. A large coal particle should have a long enough combustion time for it to travel through all of the cells many times over. In these circumstances, the percentage of the total heat release in each cell should be the

Figure 4.1 Oxygen Partial Pressure of Cells at a Height of 1m Above Secondary Air
(Studsvik CFB; case sh0)



same as the cell's percentage suspension density. This was indeed found to be the case; thereby, showing that the Monte Carlo Method was working as the program intended.

4.2 STUDSVIK CFB

4.2.1 General Description

The Studsvik 2.5 MW thermal prototype CFB is a boiler that is 6.1 m tall with a square cross-sectional area of 0.65 m by 0.65 m. There are membrane surfaces on all four sides of the riser. The riser has a smooth exit geometry with a riser top reflection coefficient of 0.1 [Senior, 1992]. A schematic of the Studsvik CFB is shown in Figure 4.2.

4.2.2 Sensitivity Analysis

A set of sensitivity analysis was conducted for the Studsvik CFB to study the effects of varying superficial gas velocity and solid recirculation rates, while combusting Highvale coal. An analyses of Highvale coal is given in Table 4.1, and the particles size distribution of the Highvale coal and the bed are given in Table 4.2. The inputs and the operating conditions of the six cases studied in the sensitivity analysis are listed in Table 4.3. The three different solids recirculation rates studied were 15 kg/m²s, 30 kg/m²s and 50 kg/m²s. In addition, two superficial gas velocities cases of approximately 7 m/s and 6m/s were also studied.

In practice, a commercial CFB may have a "turndown", a reduction in the load, as low as 3:1, or a corresponding decrease in the superficial gas velocity from a full load value of 7m/s to as low as 2.5 m/s. It would be useful to model a case where the superficial gas velocity is 2.5 m/s, to observe changes in the temperature distribution. However, it was found that at superficial gas velocities less than approximately 5 m/s, the hydrodynamic model breaks down. Low gas velocities in the hydrodynamic model, coupled with the existing "wall disturbance factor", which is a value fitted to experimental

Figure 4.2 Schematic of the Studsvik CFB
[Kobro, 1984]

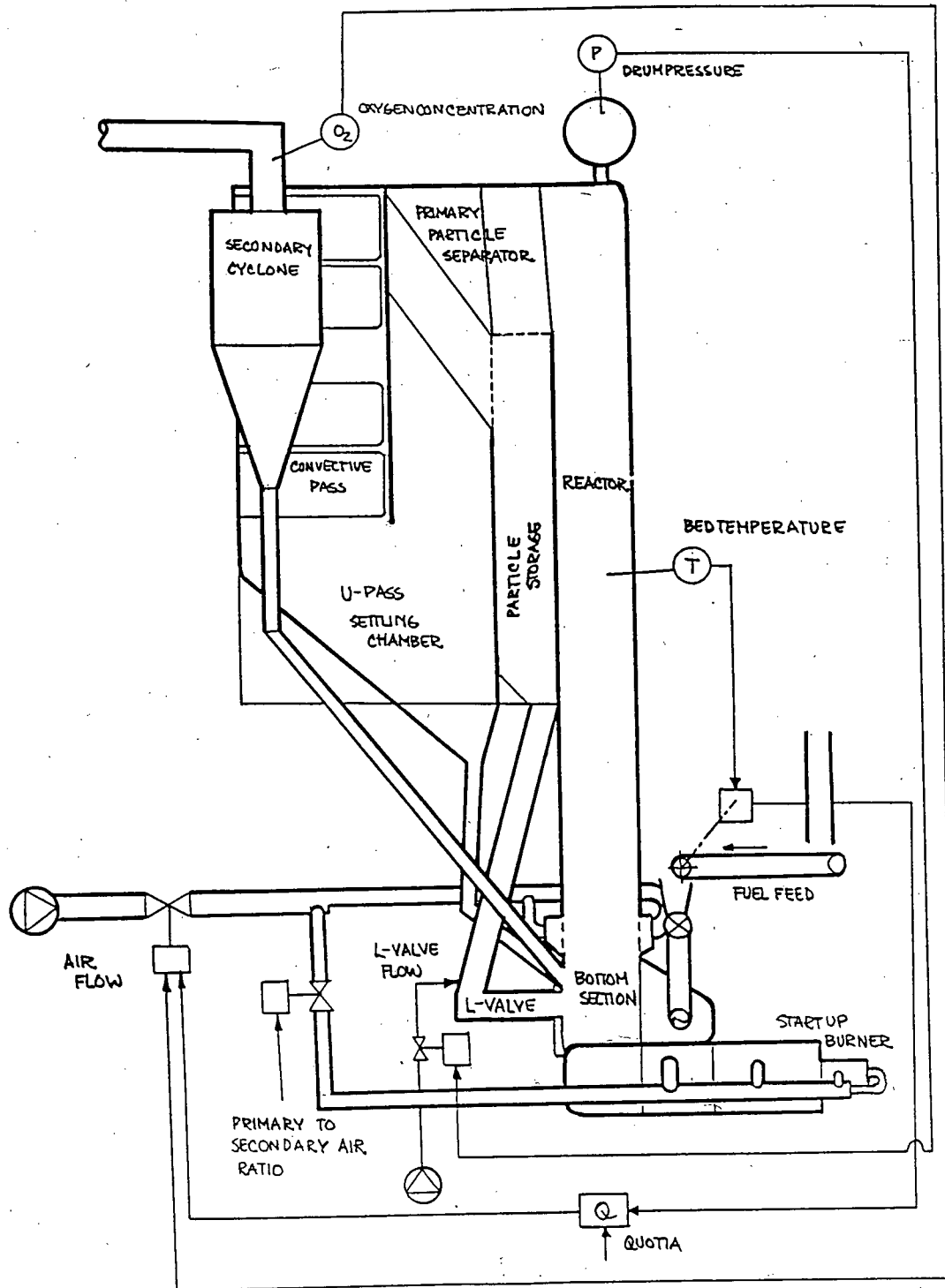


Table 4.1 Characteristics of Highvale Coal [Grace et al, 1989]

Proximate Analysis	(%)
Volatile Matter	30.5
Fixed Carbon	42.1
Ash	12.2
Moisture	15.2
Ultimate Analysis - Dry Basis (%)	
Carbon	62.4
Hydrogen	3.6
Nitrogen	0.8
Sulphur	0.2
Oxygen	18.7
Ash	14.3
Higher Heating Value (MJ/kg)	24

Table 4.2 Particle Size Distribution of Highvale Coal and Bed

Particle Size (mm)	Highvale Coal (%)	Lime (%)	Bed (%)
7.925	9.25	0	0
5.613	10.92	0	0
3.962	13.18	0	0
2.794	12.11	0.34	0
1.981	11.09	0.61	0
1.397	8.73	1.36	2.0
0.991	7.75	0.95	4.44
0.701	5.48	4.33	3.7
0.495	4.75	14.06	3.27
0.351	3.74	13.33	10.78
0.246	3.41	13.19	28.29
0.175	3.99	20.54	23.72
0.124	1.29	19.76	14.33
0.088	0	7.02	5.95
0.053	0	2.91	1.54
0.045	0	1.51	0.66
0.038	0	0	0.57
0	0	0	0.75

Table 4.3 Major Parameters in the Sensitivity Analysis Cases
(Studsvik CFB, base case sh0)

cases:	sh0	sh1	sh2	sh3	sh4	sh5
superficial gas velocity (m/s)	7	7	7	6	6	6
solids recirculation rate (kg/m ² s)	30	50	15	30	50	15
solids return temperature (°C)	859	835	898	812	764	852
fuel feedrate (kg/hr)	396	389	403	341	335	347
air feedrate (kg/hr)	3070	3018	3129	2644	2599	2694
height of developed zone (m)	2.8	2.5	3.3	2.5	2.5	3.0
Highvale coal	yes	yes	yes	yes	yes	yes
Fuel density (kg/m ³)	1400	1400	1400	1400	1400	1400
bed density (kg/m ³)	2800	2800	2800	2800	2800	2800
average particle size (mm)	2.89	2.89	2.89	2.89	2.89	2.89
excess air (%)	20	20	20	20	20	20
number of particles used in the Monte Carlo Method	100	100	100	100	100	100

data over a limited range, produced unreasonable core-wall flux calculations. Therefore, only a 15% reduction in the maximum load has been studied to this point.

In order to study the effects of turndown by decreasing the superficial gas velocity to a value of 3.3 m/s, the wall disturbance factor was increased from 310 to 470. However, there is insufficient experimental hydrodynamic data to validate this modification. The results from this low superficial gas velocity test, sh6, for the Studsvik CFB, is presented at the end of appendix C. Clearly, further work is needed to extend the hydrodynamic model to cover a greater operating range.

Initially, the heat transfer area needed to give an average operating temperature of 850 °C was calculated. The heat transfer area calculated was approximately 70 % of the total wall area. This percentage wall area was used for all the runs in the sensitivity analysis. The actual heat transfer area of the CFB can be modified depending on the type of fuel combusted by installing refractory, but is approximately 50% of the total wall area.

As expected, the heat transfer area calculated using the model was larger than the actual heat transfer area. This is a result of two major reasons.

The model assumes that the membrane surfaces are smooth and not made up of membranes, or parallel tubes connected longitudinally by fins. Therefore, the actual total membrane surface area is greater than the area calculated in the model. The model corrects for this inconsistency by calculating the total heat transfer area based on the steady state bed temperature one would like the model to operate at. In this way, the total heat transfer area would be equivalent to the actual heat transfer area of a membrane surface. Further work on the details of the membrane wall heat transfer would aid in the calculation of the cell to wall heat transfer rate. The performance of the membrane surface should include an effectiveness factor.

Secondly, the model does not include heat loss from the riser. However, based on a rough overall energy balance on the Studsvik CFB, assuming 50% heat transfer area, the surface of the CFB is at 35 °C, the heat transfer coefficient from the CFB surface to the surrounding air is 15 W/m²C, the surrounding air is at 20 °C and a coal feedrate of 400 kg/hr, the heat loss from the riser is less than 10 % of the total heat generated.

4.2.3 Results

The following figures of heat release, oxygen partial pressure and temperature profiles are for conditions above the secondary air. At a height of 0 m, this point indicates the condition in the primary zone.

4.2.3.1 Heat Release Profiles

The results from the sensitivity analysis, Figures 4.3, 4.4 and 4.5, show that the volatiles and char heat release is mainly in the primary zone. This is because the devolatilization expression used releases the volatiles quickly from the coal upon entry into the primary zone. In addition, the density and size of the primary zone is large compared

Figure 4.4 Char Heat Release vs Height
 (Combustion of Highvale Coal with $U = 7$ m/s; Studsvik CFB; cases sh0, sh1 & sh2)

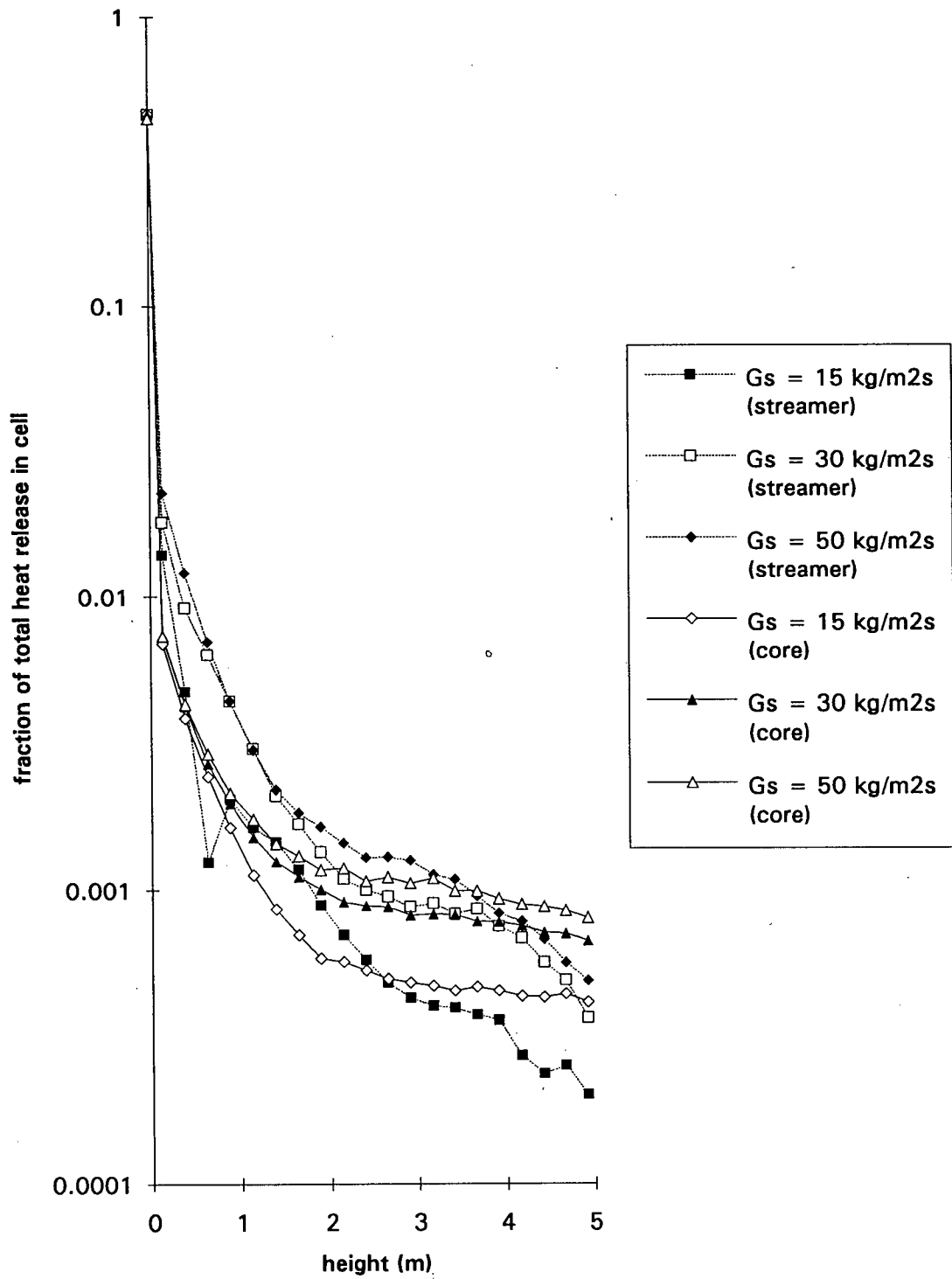
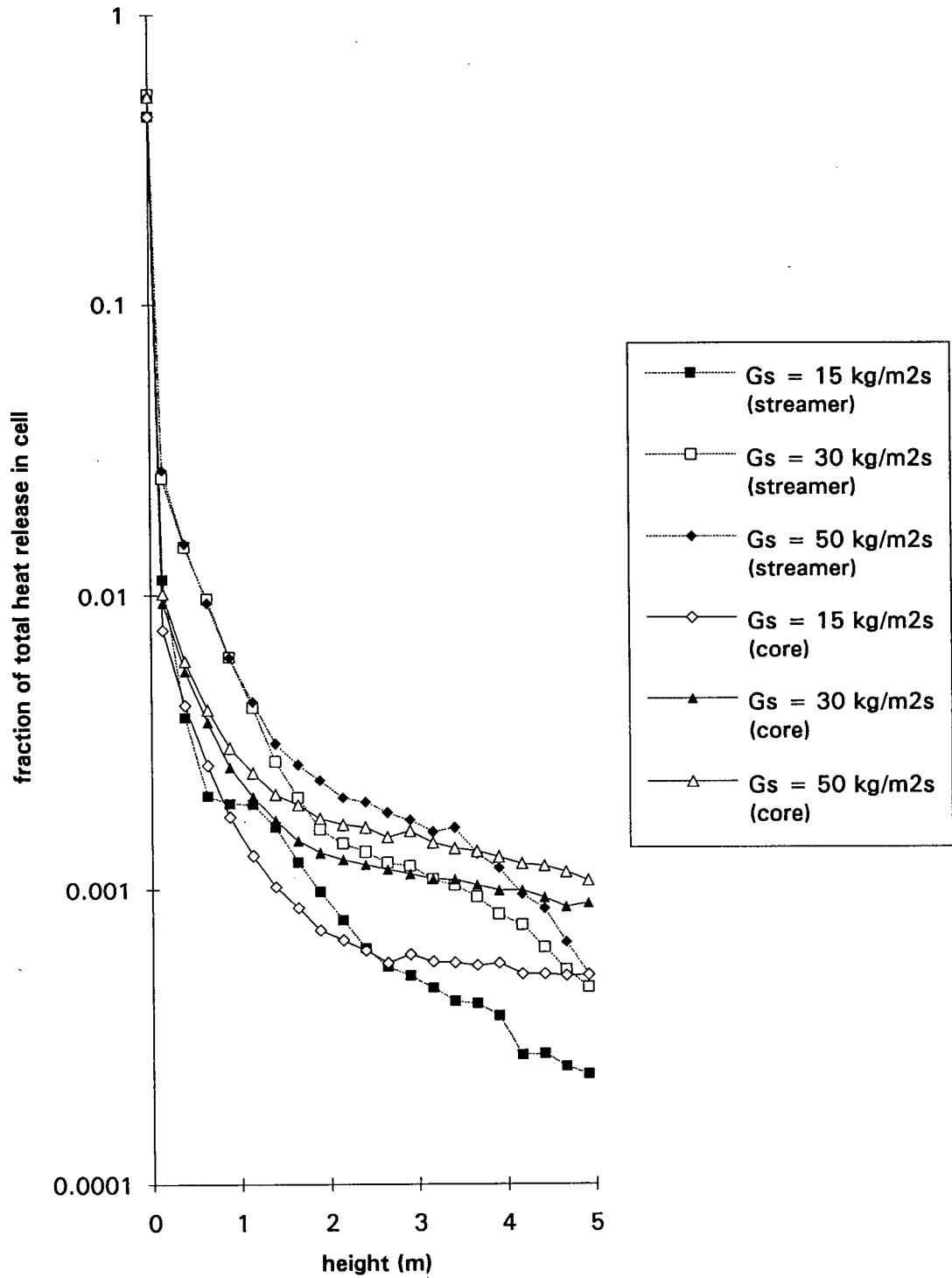


Figure 4.5 Char Heat Release vs Height
 (Combustion of Highvale Coal with $U = 6$ m/s; Studsvik CFB; cases sh3, sh4 & sh5)



to other cells in the riser, and the residence time in the primary zone compared to other cells is considerably larger. The primary zone is approximately 6 to 8 times larger than a core cell and 6 to 50 times as dense.

The second observation from these figures is that the char heat release profiles for various solid recirculation rates are almost the same; however for higher solid recirculation rates, the fraction of heat release in the primary zone is less; thereby, a larger percentage of heat is released in the riser and cyclone. This is because as more solids are being added to the riser, the primary zone begins to become saturated with solids, and the percentage density increase in that zone is not great. The density of the primary zone stays almost constant at approximately 315 kg/m^3 . Instead, the solids are transferred up the riser and the percentage density change of the riser in the secondary zone is significantly increased, causing more heat to be released further up the riser. The density changes can be seen in Figure 4.6.

In addition, the case with a higher superficial gas velocity show a slightly lower fraction of heat release near the bottom the riser. The higher gas velocity seem to contribute to carrying the particles from the primary zone up the riser, consequently releasing the heat in the secondary zone. This can be seen by comparing the heat release results from runs sh0 and sh3, shown in Figure 4.7.

4.2.3.2 Partial Pressure Profiles

From the partial pressure of oxygen profiles, shown in Figures 4.8 and 4.9, a higher partial pressure of oxygen was shown for higher solid recirculation rates and for higher gas velocities. However, the higher oxygen concentration in the core meant fewer oxygen in the streamer cells. The total amount of oxygen in the streamer is very small, approximately 1.5% of the total oxygen in the riser. In addition, the oxygen profile in the streamer varied from iteration to iteration. It is difficult to obtain a converged oxygen profile, as can be seen in Figure 4.1.

Figure 4.6 Changes in Core Density in Secondary Zone for Various Solids
Recirculation Rates - Primary Zone Density = 315 kg/m^3
(Combustion of Highvale Coal with $U = 7 \text{ m/s}$; Studsvik CFB; cases sh0, sh1 & sh2)

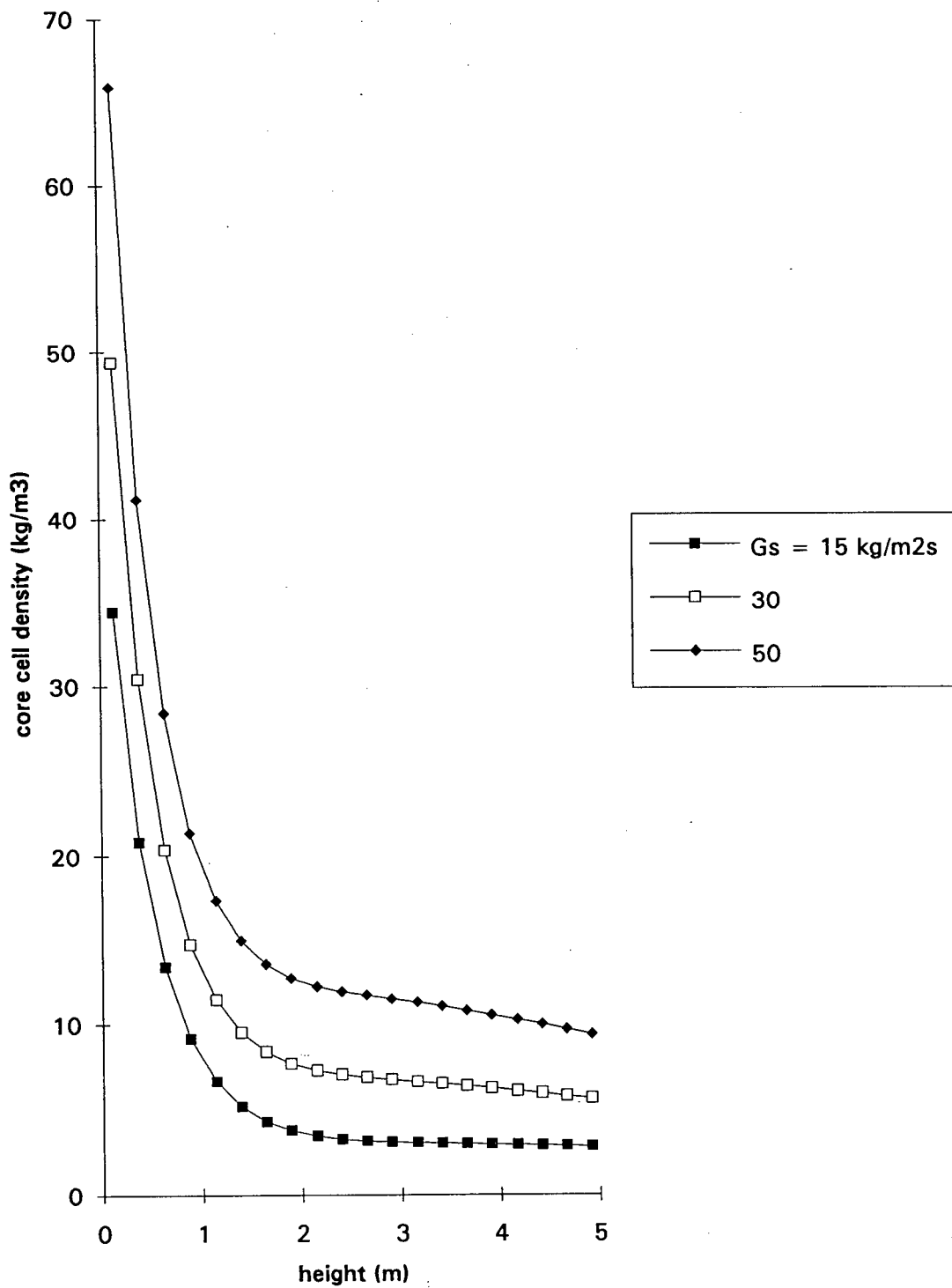


Figure 4.7 Char Heat Release Distribution vs Height
(Combustion of Highvale Coal, Studsvik CFB; cases sh0 and sh3)

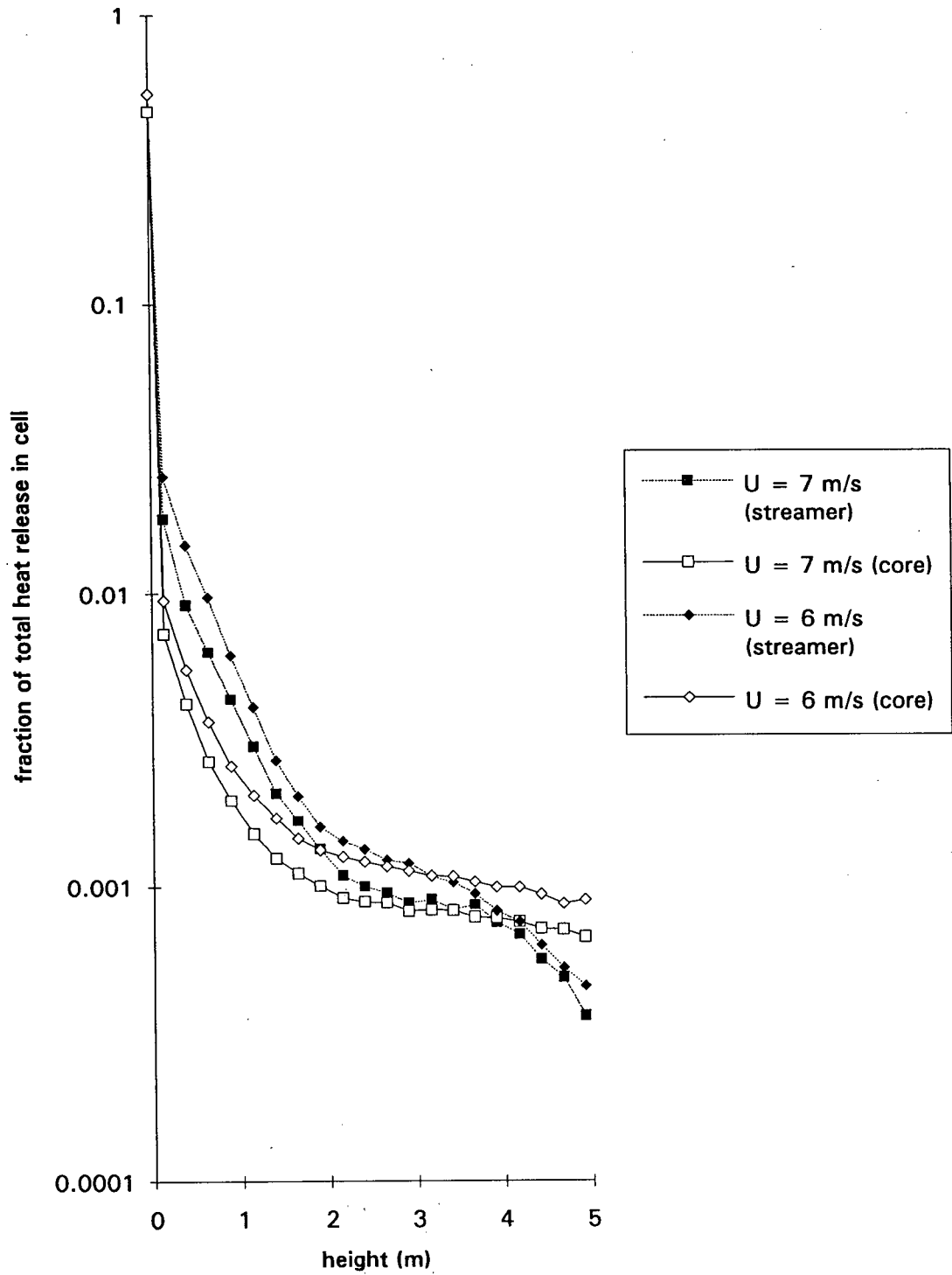


Figure 4.8 Partial Pressure of O₂ vs Height
 (Combustion of Highvale Coal with $U = 7$ m/s; Studsvik CFB; cases sh0, sh1 & sh2)

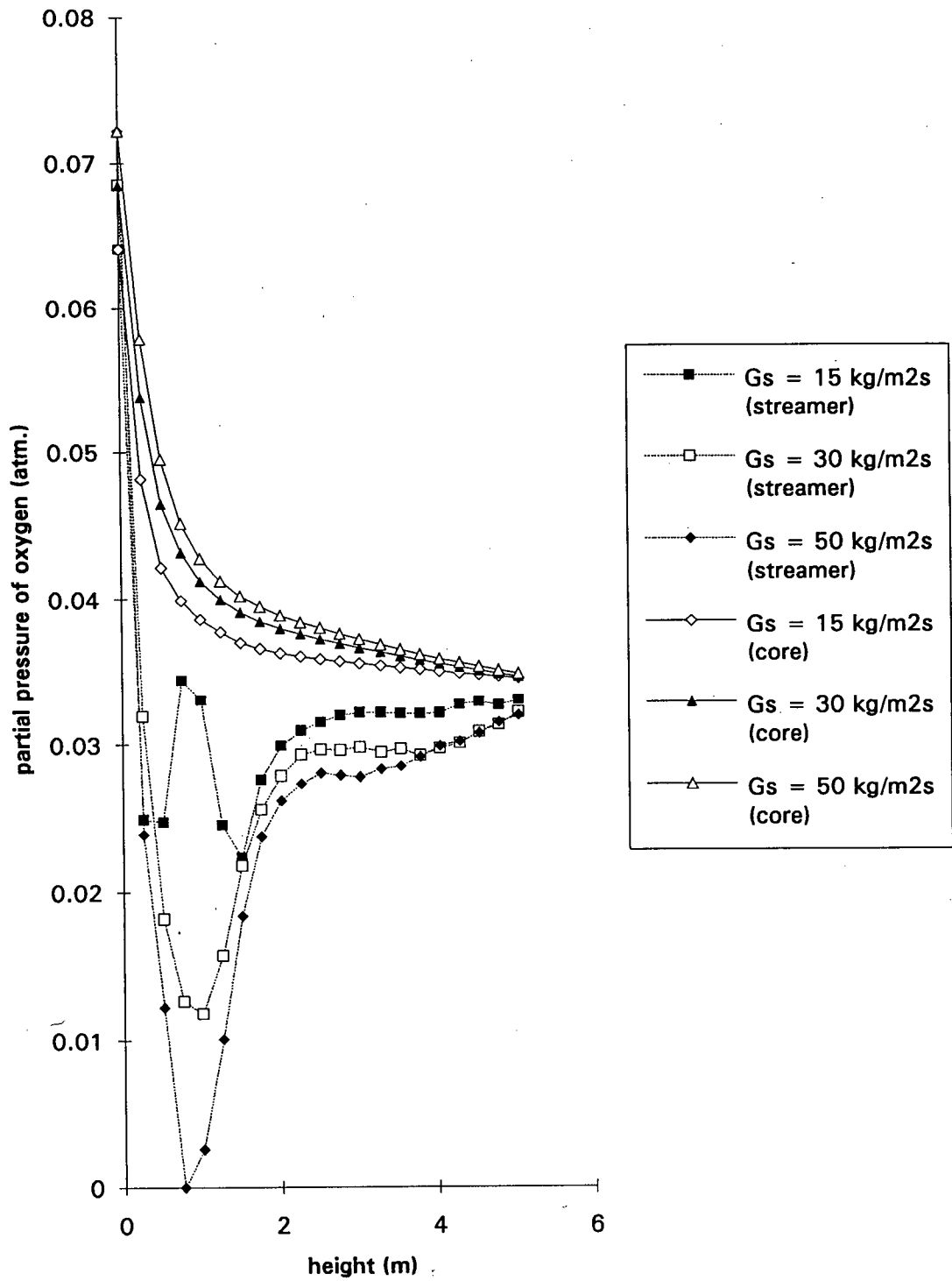
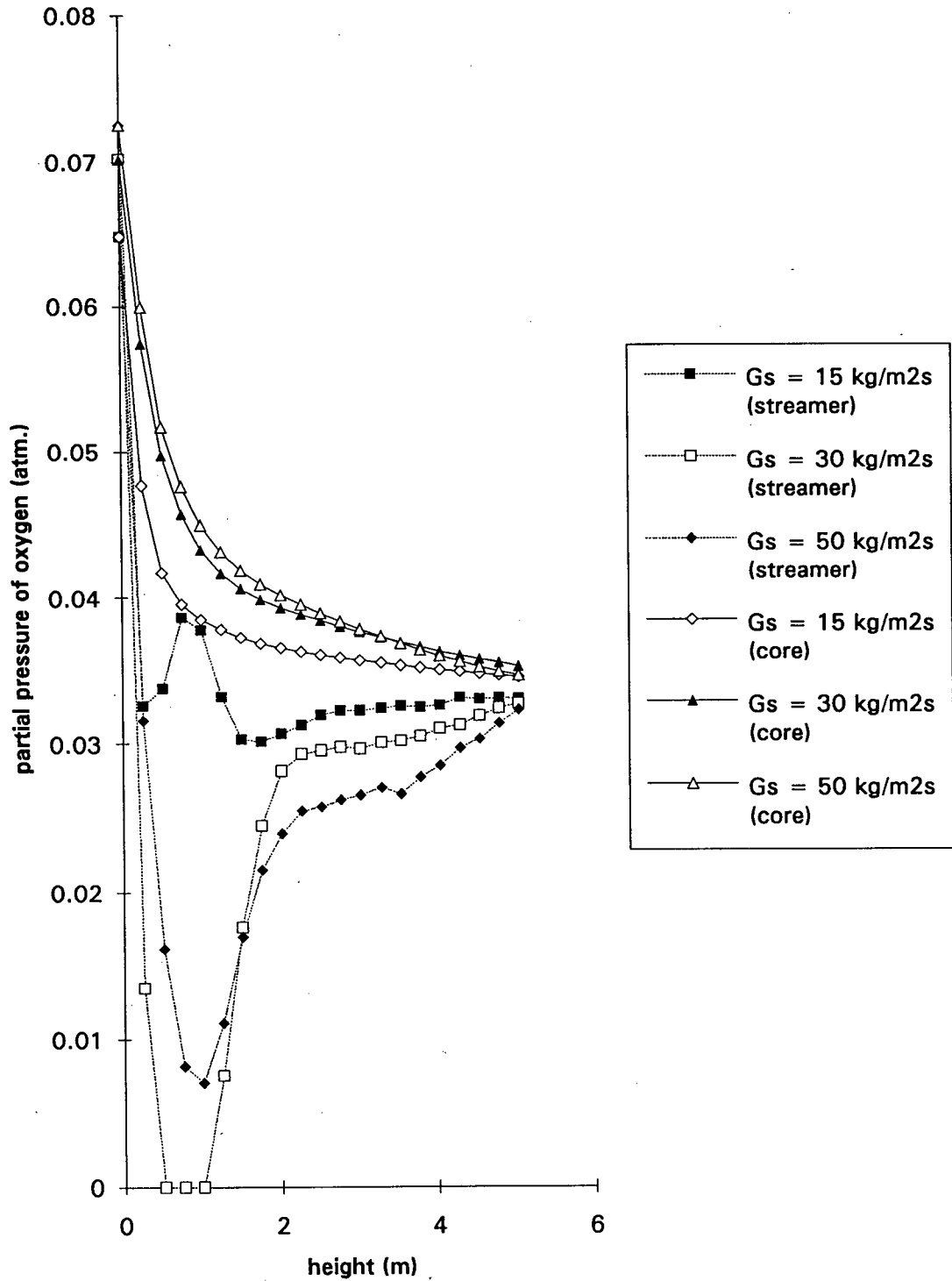


Figure 4.9 Partial Pressure of O₂ vs Height
 (Combustion of Highvale Coal with $U = 6$ m/s; Studsvik CFB; cases sh3, sh4 & sh5)



As the superficial gas velocity decreased, there seems to be even less oxygen in the annulus cells. In fact, there are cells where there is no oxygen, near the bottom of the riser. The partial pressure of oxygen in the core cells, however, seems to change very little.

The variation in the partial pressure of oxygen in the streamer cells is due to the insufficient number of particles used in the Monte Carlo method. From Figure 3.11, when more particles are used, we see less fluctuations in the partial pressure predictions.

4.2.3.3 Temperature Profiles

From the temperature profiles, Figures 4.10 and 4.11, we see that although various solids recirculation rates and superficial gas velocities were used in these test cases, the temperature profiles were similarly shaped and uniform; however, they are displaced by approximately 50 °C. This is due to the significant contribution of the heat release distribution to the overall temperature distribution. However, the high internal circulation rates tends to smooth out huge maldistributions in the heat release distribution. Although approximately 80% of the heat release occurs in the primary zone, there are sufficient recirculating solids that there is still only a 50 °C temperature change throughout the riser. It is then understandable that the heat release distributions are similar, and subsequently the temperature profiles will also be similar although the pressure profiles may not be. Pressure has less of an affect on temperature as the reverse situation.

Another interesting phenomena is that the temperature of the streamer increases near the top of the riser, which is due to the nature of the energy balance. The volume of the streamer at the top of the riser is small; approximately 0.0003 m^3 , or 0.3% of the core volume at the top. Therefore, hot particles from the core and particles that are reflected off the top of the riser cause the streamer cells to heat up to temperatures that are greater than the core temperatures.

Figure 4.10 Temperature vs Height
 (Combustion of Highvale Coal with $U = 7$ m/s; Studsvik CFB; cases sh0, sh1 & sh2)

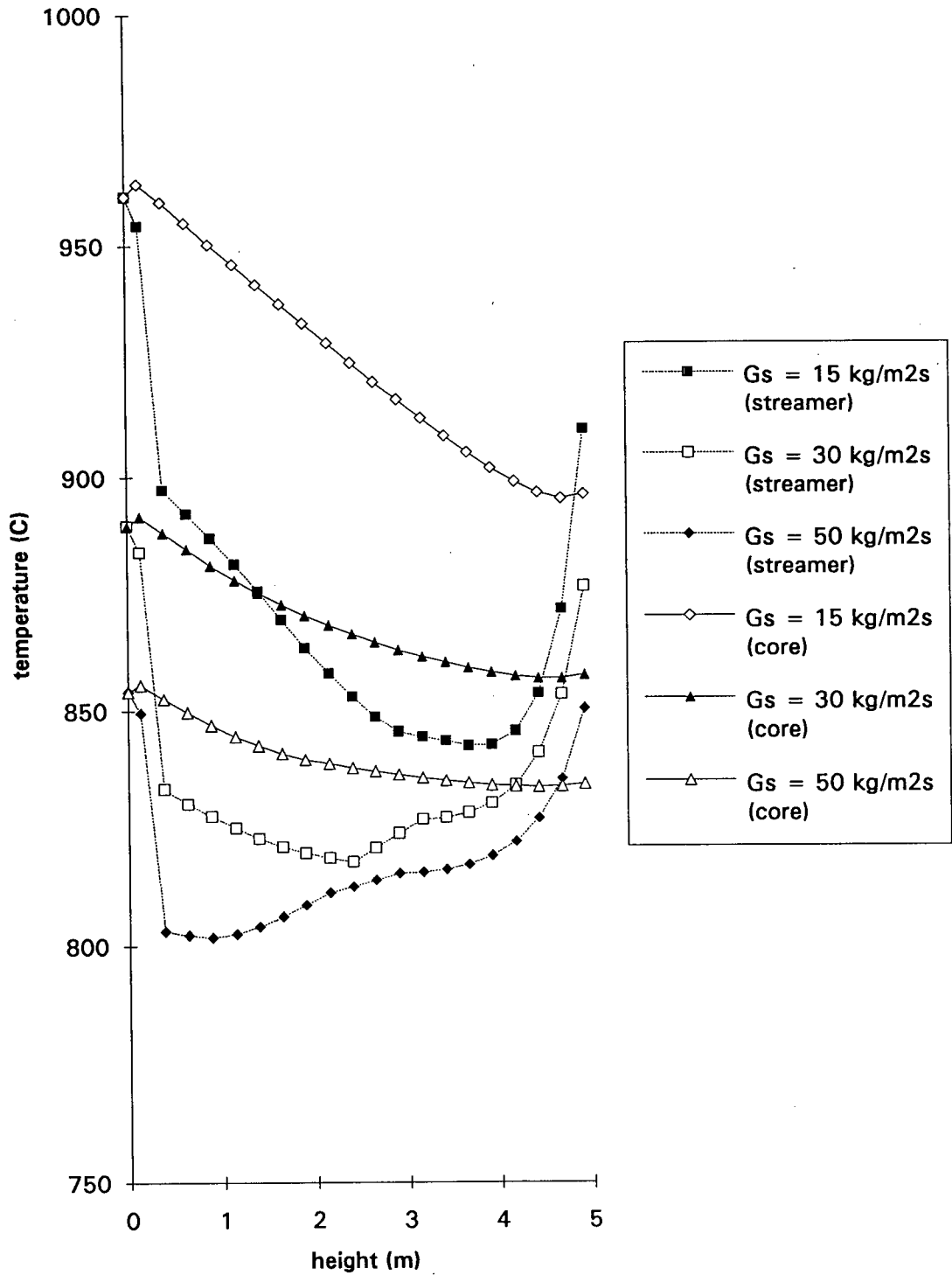
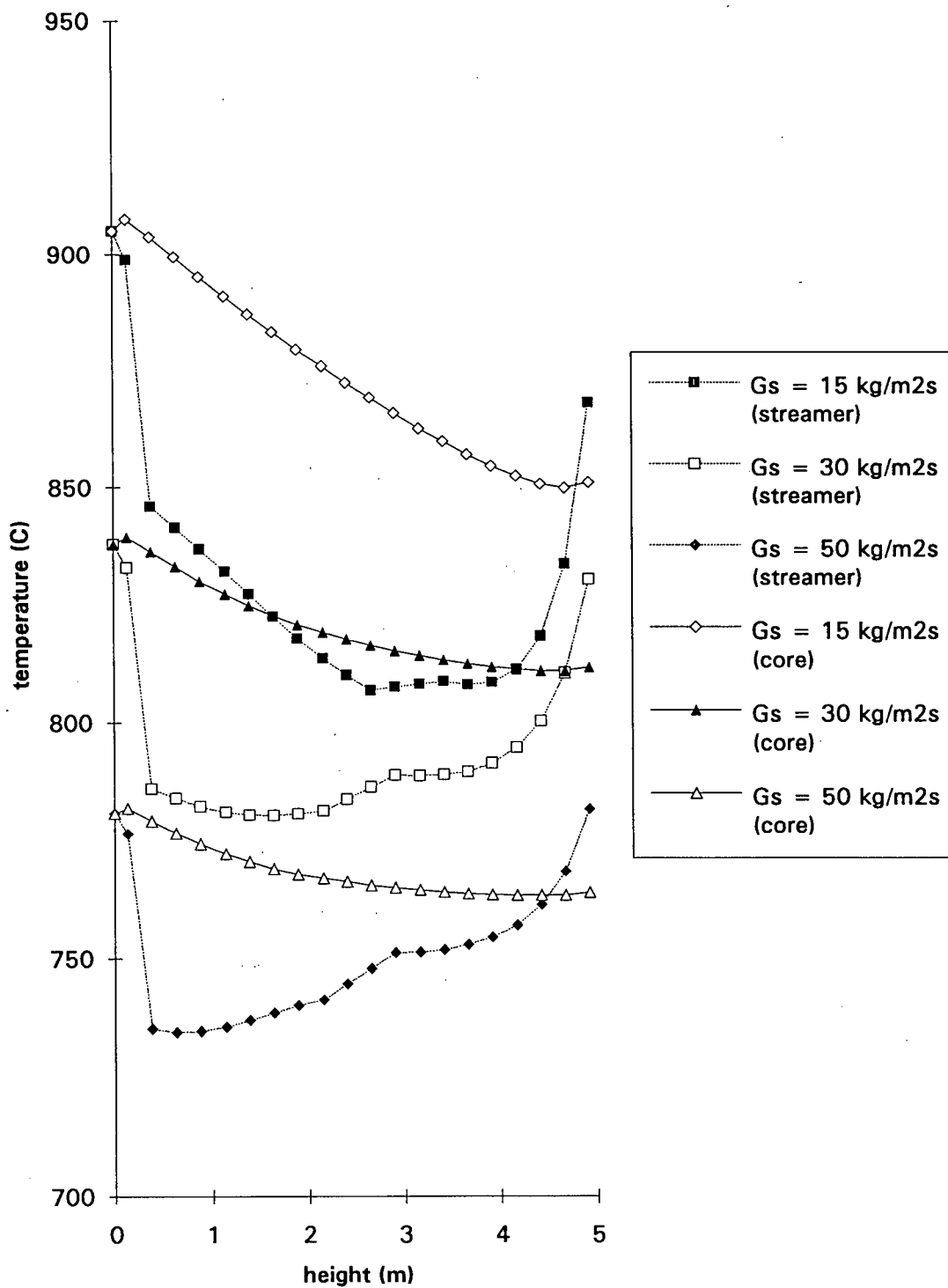


Figure 4.11 Temperature vs Height
 (Combustion of Highvale Coal with $U = 6$ m/s; Studsvik CFB; cases sh3, sh4 & sh5)



The temperature of the core cells is a steady decreasing curve, but the streamer cells have temperatures approximately 50 °C less than the core. This thermal boundary layer near the wall follows the same trends as experimental measurements [Leckner, 1991] and theoretical equations [Brewster, 1984], shown in Figure 4.12.

Although the model's temperature gradient predictions match Leckner's experimental measurements very well, this is not an indication of the sophistication of the heat transfer model, since a number of simplifying assumptions have been made. However, this does indicate that the average temperature predictions of the model can be used as a starting point to predict combustion and heat transfer rates in the streamer and might be extended to predict the production of certain flue gases such as NO_x and SO₂.

4.3 UBC PILOT CFB

4.3.1 Description

The detailed description of the UBC pilot-scale circulating fluidized bed combustion facility can be found in Grace [Grace et al, 1989]. A schematic of the major components can be seen in Figure 4.13.

The reactor column is 7.32 m high and has a cross-section of 152 mm by 152 mm. Primary air flows through the bottom of the CFB, through a distributor plate into a tapered primary zone. The secondary air enters the CFB through 2 opposed air ports located 0.9 m above the distributor plate. The solids and gas leaving the top of the CFB are separated in a refractory lined primary cyclone with 0.31 m ID, and finer particles are captured in a secondary cyclone with a 0.2 m ID. The solids from the primary cyclone are returned through the standpipe located 0.4 m above the distributor.

Figure 4.12 Comparison of Wall Temperature Gradient at a Height of 2.4 m Above Secondary Air with Other Experimental and Theoretical Works

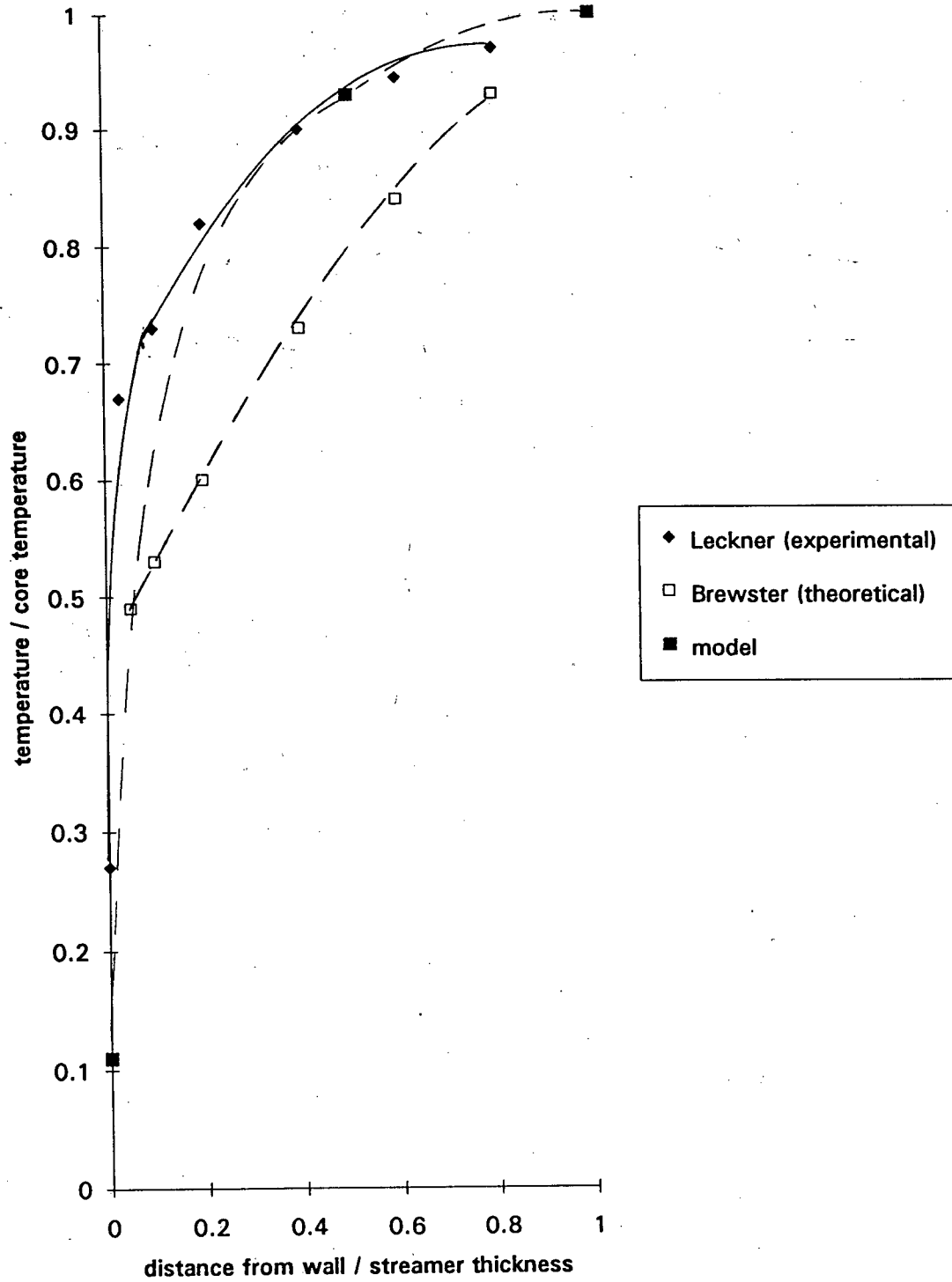
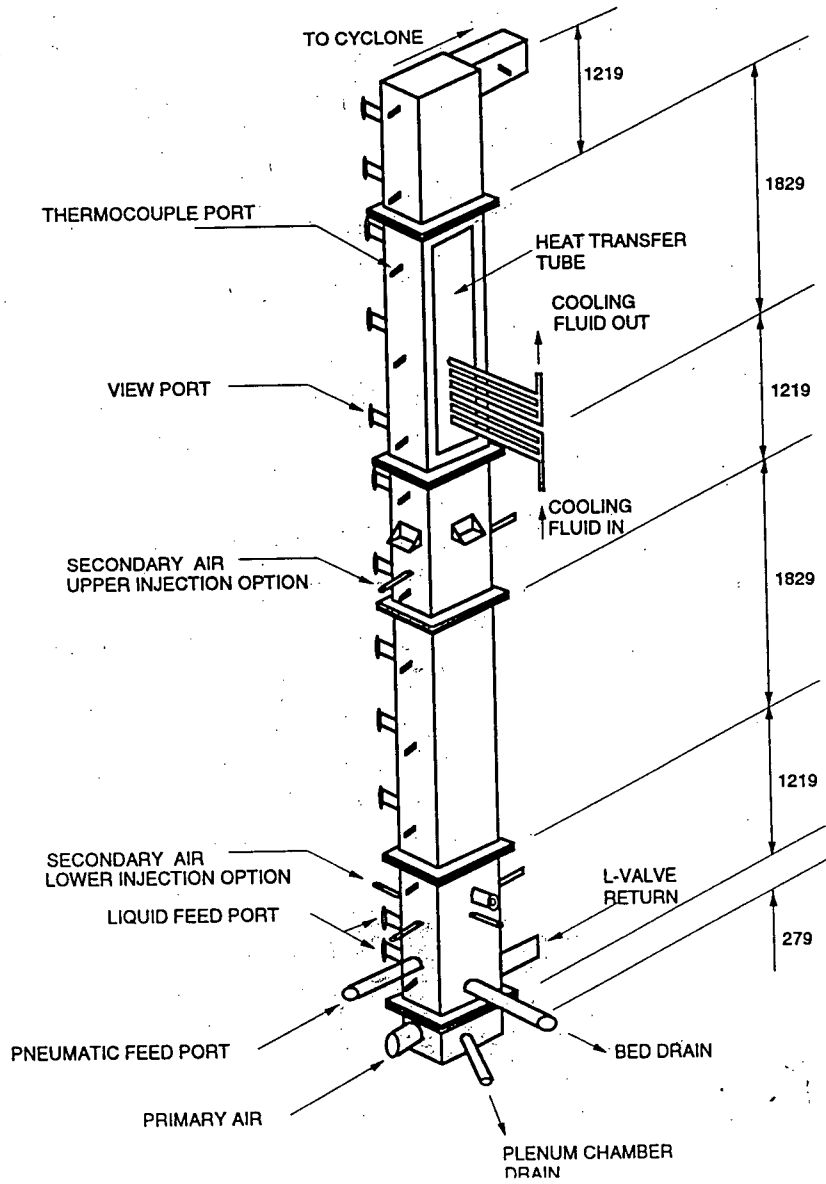


Figure 4.13 Simplified Schematic Diagram of UBC Pilot-Scale CFB



4.3.2 Test Run

A test case, uh0, was conducted using the model of the UBC CFB, to see how well the model predicts operating parameters in a pilot-scale CFB as compared to a commercial CFB. In addition, experimental data are available for the UBC CFB for various load control parameters. These data can be used to qualitatively validate the model.

The baseline conditions for case uh0 are superficial gas velocity of 7.03 m/s and a solids recirculation rate of 30 kg/m²s.

The heat transfer area calculated by the model, which gave a corresponding CFB operating temperature of 850 °C is 35% of the total wall area. The model assumes that the heat transfer area is evenly distributed on all four sides of the CFB riser and no heat transfer or heat loss from the primary cyclone and standpipe.

The UBC CFB's actual heat transfer area is only approximately 5% of the total wall area located in a small section near the top of the riser. However, the UBC CFB has high heat loss from all four sides of the riser and from the primary cyclone and standpipe. The heat loss from the riser is evenly distributed throughout the full height of the riser, and as much as 50% of the heat loss is from the primary cyclone and standpipe. For this CFB, the heat transfer assumptions made in the model, would reasonably represent the actual heat transfer and heat loss from the CFB, except that the high capacitance of the refractory and the axial heat transfer through the refractory would tend to make experimental temperature results more uniform.

4.3.3 Results

The heat release results from run uh0 compared to that from case sh0 of the Studsvik CFB, listed in Table 4.4 of baseline conditions, shows the volatiles completely devolatilizing in the bottom 3 m of the riser in the UBC CFB; whereas, in the Studsvik

CFB, the volatiles are released within the first meter upon entering the riser. The volatiles and char heat release profiles are shown in Figures 4.14 and 4.15.

From Figures 4.14 and 4.15, we can see that the fraction of heat released in the streamer is higher than in the core for UBC's CFB, but in the Studsvik CFB the reverse is seen.

In the Studsvik CFB, the annulus region's average cross-sectional area is approximately 0.9 % of the total cross-sectional area; whereas in the UBC CFB, the average annulus region is approximately 3 % of the total cross-sectional area. While even 3% may not seem significant in terms of total cross-sectional area occupied, the annulus region contains approximately 80% of the total solids in the cross-section. Therefore, the streamer is much more significant in terms of its effect upon combustion and pollutant formation behaviour in small cross-sectional CFB risers.

Table 4.4 Parameters in Baseline Test

cases:	uh0 (UBC)	sh0 (Studsvik)
superficial gas velocity (m/s)	7	7
solids recirculation rate (kg/m ² s)	30	30
solids return temperature (°C)	793	859
fuel feedrate (kg/hr)	23	396
air feedrate (kg/hr)	177	3070
height of developed zone (m)	3.2	2.8
Highvale coal	yes	yes
fuel density (kg/m ³)	880	1400
bed density (kg/m ³)	2650	2700
average particle size (mm)	2.89	2.89
excess air (%)	20	20
number of particles used in the Monte Carlo Method	100	100

Figure 4.14 Volatile Heat Release
(Combustion of Highvale Coal with $U = 7$ m/s and $G_s = 30$ kg/m²s)

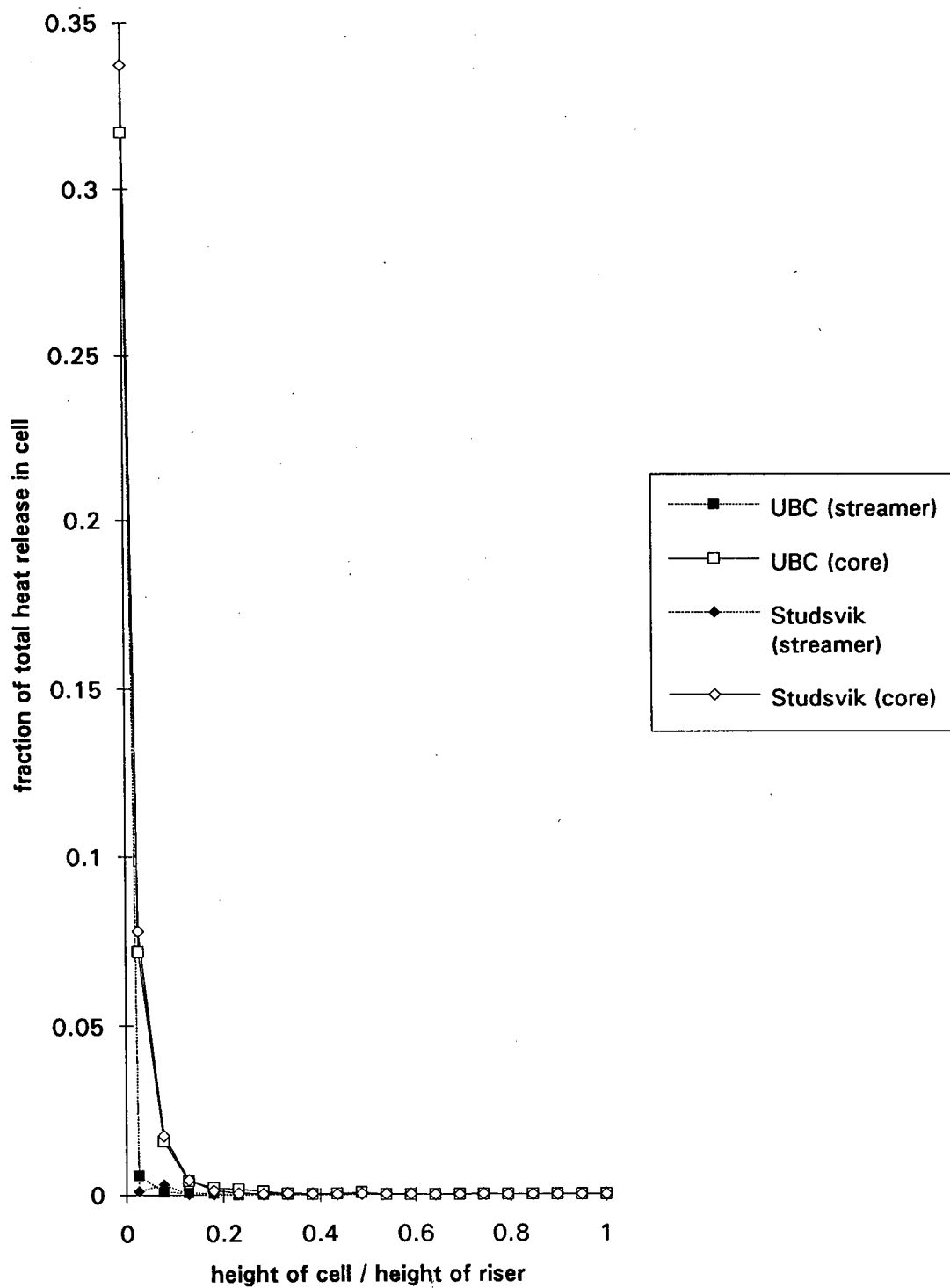
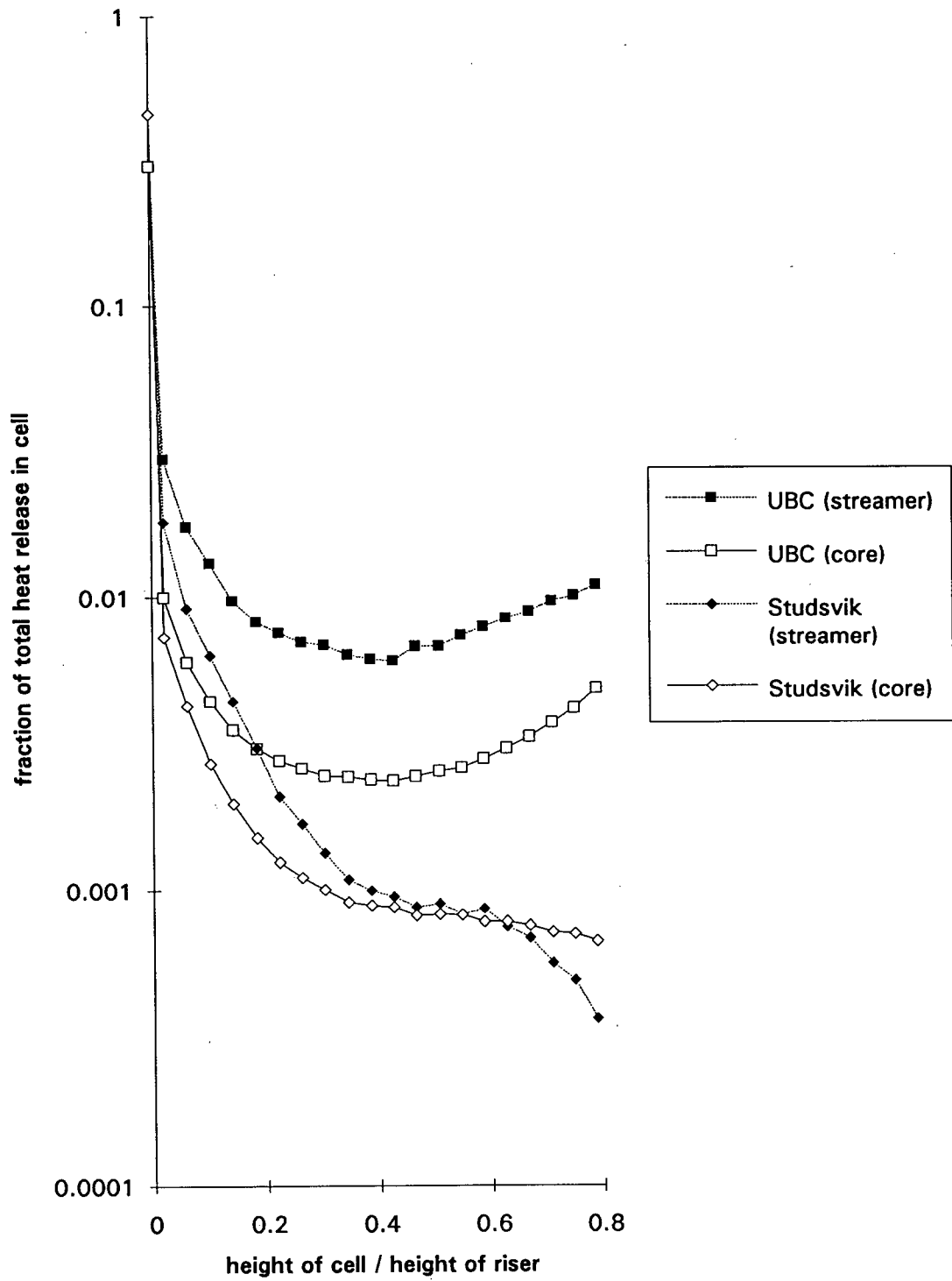


Figure 4.15 Char Heat Release
(Combustion of Highvale Coal with $U = 7$ m/s and $G_s = 30$ kg/m²s)



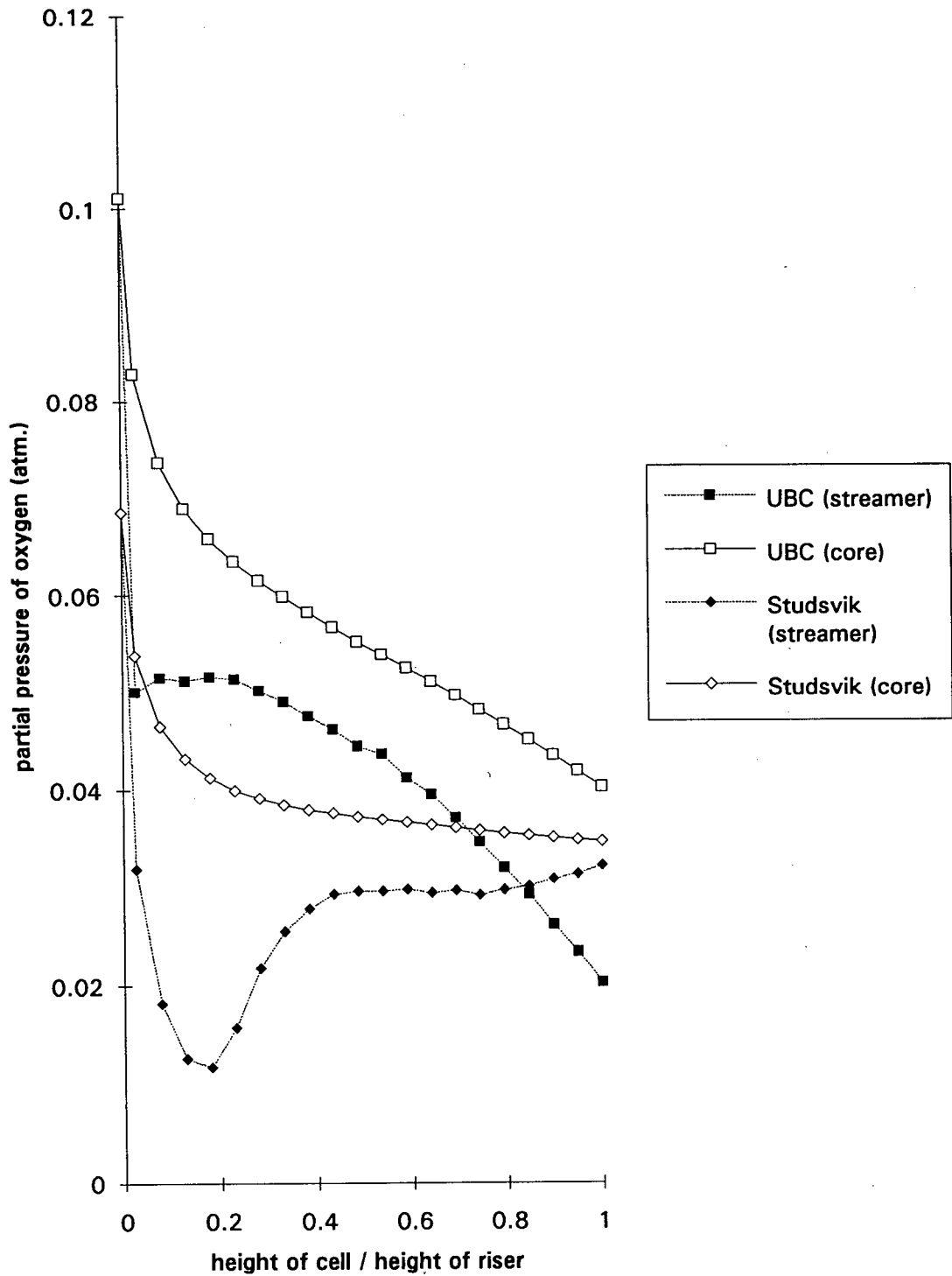
In terms of modelling, because the streamer's influence on combustion and emissions is less for a large cross-sectional CFB riser, a one dimensional combustion/pollutant model that considers the core cells only will be faster to converge, and properly applied, the temperature and pressure profile results may still be valid. A core annulus model for heat transfer is still vital, since heat transfer occurs in the wall layer.

For this test run, most of the volatiles are released in the primary zone, because the primary zone in the UBC CFB is approximately 2.3 times as large as a core cell and 12 to 35 times as dense. Therefore, the residence time in this zone is more than 10 times as long as any other cell in the riser. From Figure 4.14, we see that for the UBC CFB, the fraction of volatiles released near the bottom of the riser is greater than in the Studsvik CFB. This may be due to the smaller riser diameter of the UBC CFB. In the UBC CFB, the volatile plume that forms, quickly spans the full diameter of the riser; therefore, there is enough oxygen present, near the bottom of the riser, for volatiles combustion.

The char heat release profiles with various particle diameters, at a constant temperature profile, can be seen in Figures 4.16. This figure shows that the solids in the UBC CFB is well mixed; therefore causing the char heat release profiles to stay the same regardless of particle diameter. If larger particles are combusted, not only would the devolatilization expression used be invalid, but the assumption that the fuel particle behave in the same way as the bed particles would also be invalid. The heat release profiles would then be different.

Comparing UBC's partial pressure of oxygen profiles with the profile from case sh0, Figure 4.17, shows that for UBC's CFB, the pressure profile in the streamer cells is more smooth and uniform. Again, this is due to the streamer's significance in a smaller cross-sectional CFB. The amount of oxygen present in the annulus is approximately 5% of the total oxygen in the UBC CFB; whereas in the Studsvik CFB, there is only 1.5% oxygen in the annulus. If additional coal particles were to combust in the Studsvik CFB's

Figure 4.17 Partial Pressure of O₂ vs Height
 (Combustion of Highvale Coal with $U = 7$ m/s and $G_s = 30$ kg/m²s)



annulus, the oxygen partial pressure profile results can be quite different. Combustion in the cyclone for both the UBC CFB and the Studsvik CFB are insignificant, less than 0.5% of the total heat release, in this model.

The temperature profile, Figure 4.18, shows the UBC's CFB to give temperature in the streamer and core that are 50 °C apart near the bottom of the riser, but quickly become only 10 °C apart further up the riser. In the Studsvik CFB, the streamer's temperature is much less than the core's temperature. In addition, for UBC's CFB, we do not observe the temperature of the streamer heating up near the top of the riser.

The "kink" in the temperature profile of the streamer is due to the discontinuity in the temperature profile prediction, as discussed in Section 3.5. Although the temperature at the discontinuity point has been smoothed, by just averaging the temperatures in the adjacent cells, at times the streamer temperature profile is not as smooth as is desirable. Finally, similarly to the Studsvik CFB, there is a high solids recirculation rate in the CFB, which causes the temperature profile to become more uniform; however, for the UBC CFB, the dense annulus region, causes the average bed density for a given riser height to be greater than for the Studsvik CFB and therefore, the heat transfer coefficient is also greater. As more heat leaves through the heat transfer surface, the CFB temperature cools considerably. Figure 4.19 shows the magnitude of the particle convective term compared to the conduction and radiative terms.

Figure 4.18 Temperature vs Height
(Combustion of Highvale Coal with $U = 7$ m/s; UBC CFB; case uh0)

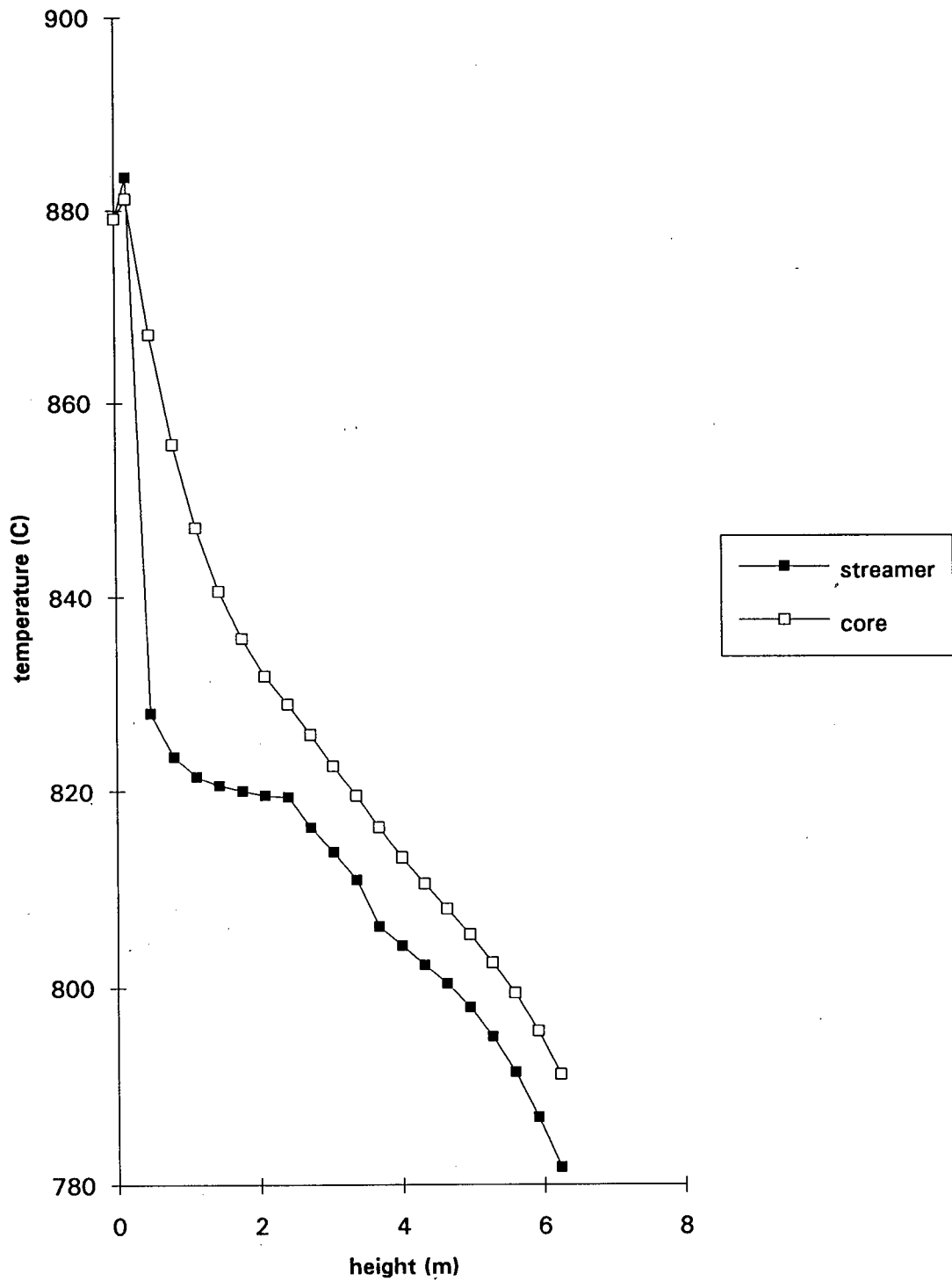
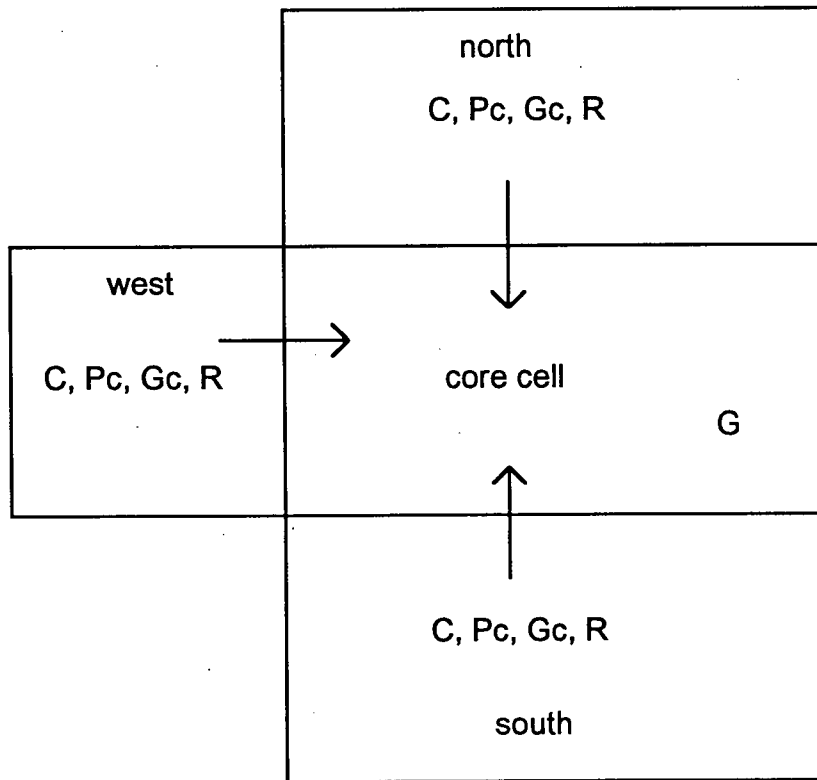


Figure 4.19 Enthalpy Balance for Core Cell at Height = 3.36 m (UBC CFB, case uh0)



Heat Transfer (W)	core cell	west	north	south
Temperature (C)	826			
G : heat generation	447			
C : conduction		-2	0	0
Pc : particle convection		-5681	-1016630	1022077
Gc : gas convection		-37	-46664	46779
R : radiation		-263	-35	8
Total Enthalpy Balance		-1		

4.4 VALIDATION

The oxygen partial pressure profiles for the UBC CFB were computed using two different devolatilization expressions. The first expression of Anthony et. al. was shown in Equation 3.1, and the second expression is a combination of expressions by Agarwal [1986] and Davidson et. al. [1985], which are shown below. The expression by Anthony, is not a function of particle diameter and is valid for small particles with diameters less than 2 mm. This expression is not valid for larger particles; therefore, the second expression by Agarwal and Davidson was also looked at to observed the differences. The results were compared with experimental partial pressure of oxygen values measured by Zhao [1992]. Experimental and predicted profiles are shown in Figure 4.20.

The devolatilization time and rate are given by the following expressions by Agarwal and Davidson, respectively. The equation presented by Davidson is the prediction of a shrinking core model with diffusion control.

$$\tau_d = k_v d_p^n \quad \text{.....(4.2)}$$

where,

τ_d	devolatilization time (s)
d_p	particle diameter (mm)
k_v	constant (s/mm ⁿ)
	= 1.5
n	constant
	= 1.5

$$\frac{t}{\tau_d} = 1 - 3(1-f)^{\frac{2}{3}} + 2(1-f) \quad \text{.....(4.3)}$$

where,

t	time (s)
τ_d	devolatilization time (s)
f	fractional yield of volatiles

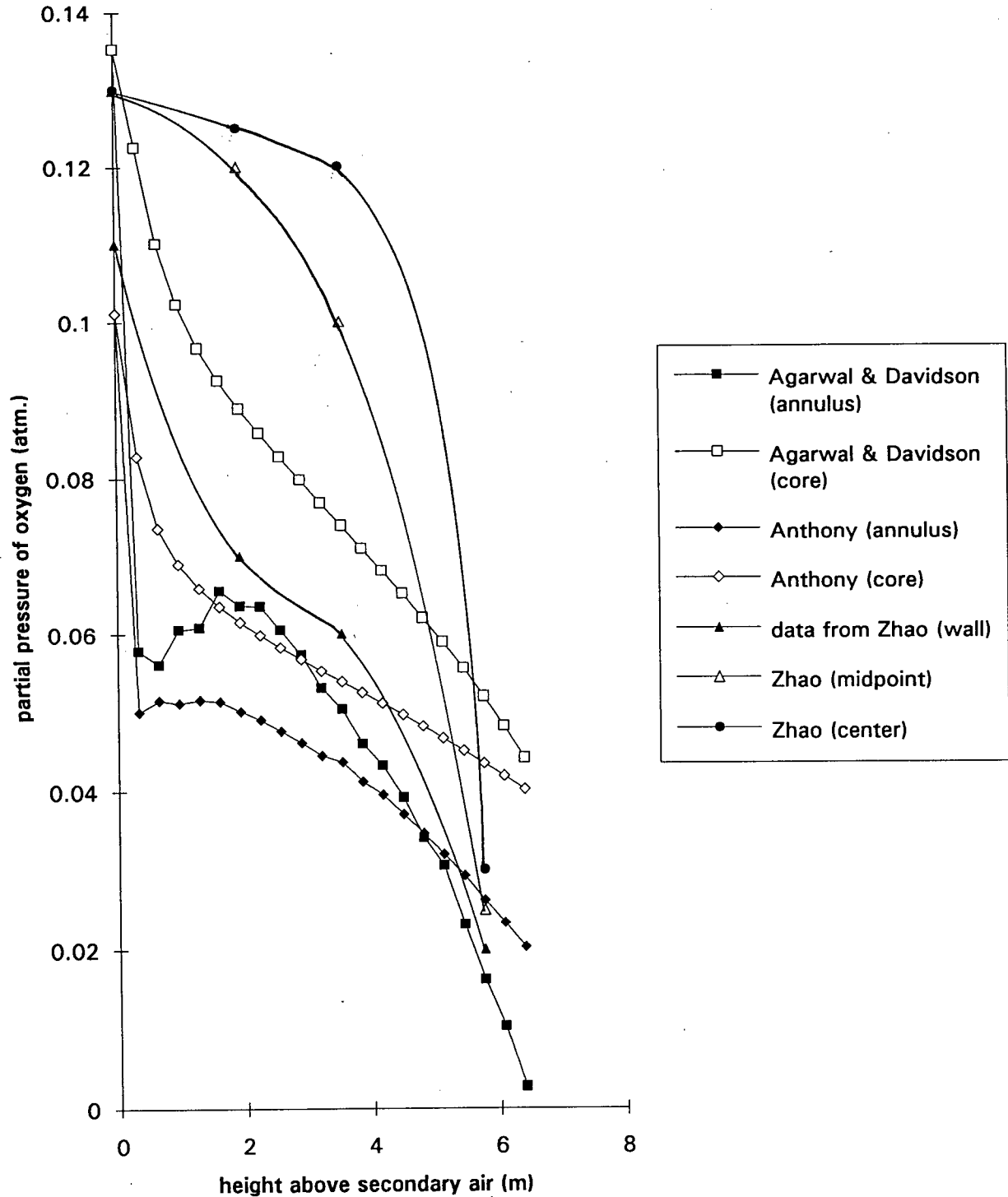
Differences in the predicted partial pressure of oxygen profiles and experimental data may be due to several reasons. The combustion conditions used in the model and by Zhao are not identical. In addition, the devolatilization expression by Anthony is not a

Figure 4.20 Oxygen Concentration Profiles for Highvale Coal

Conditions: Zhao ($T=891\text{ }^{\circ}\text{C}$, $U = 8.26\text{ m/s}$, O_2 in flue gas = 2.9%)

Anthony ($T=830\text{ }^{\circ}\text{C}$, $U = 7\text{ m/s}$, O_2 in flue gas = 3.7%)

Agarwal & Davidson ($T=830\text{ }^{\circ}\text{C}$, $U = 7\text{ m/s}$, O_2 in flue gas = 3.8%)



function of particle diameter. Results using Anthony's expression shows most of the volatiles being released in the primary zone and not further up the riser. This is reflected in less oxygen near the bottom of the riser. The devolatilization expression by Agarwal is a function of particle diameter. This expression shifts the volatiles release further up the riser and also causes the oxygen partial pressure profile to be shifted up. This prediction is closer to the experimentally measured results. The oxygen profile in the annulus is also predicted better in this case.

In addition, accurate experimental oxygen measurements are extremely difficult to obtain, and the experimental measurements show oxygen concentrations at the wall, the center and a point midway between the wall and the center of the riser. These measurements were conducted on a square cross-sectional area riser with entrance/exit effects. In this model, oxygen profiles are calculated for the core and annulus of an equivalent circular cross-sectional riser, without considering entrance/exit effects. Therefore, only a qualitative comparison can be done.

Figure 4.20 does show the effects of a core/annulus structure in a CFB. Secondly, the expression by Agarwal and Davidson predicts approximately the correct combustion in the primary zone. The shape of the partial pressure of oxygen curve in the annulus was also correctly predicted by Agarwal and Davidson. There are some differences in the partial pressure of oxygen curves in the core; however, these differences may be due to the reasons stated above or due to experimental errors.

CHAPTER 5

CONCLUSION AND RECOMMENDATIONS

5.1 CONCLUSION

In this thesis, a computer model was developed to predict heat release partial pressure of oxygen profiles and temperature profiles in a CFB combustor, given the geometry, hydrodynamic properties of the CFB and the physical properties of the fuel. This model can be used for designing purposes to predict the heat transfer area needed to operate at a given temperature or it can be used in a rating problem to predict the temperature profile given the heat transfer area of the CFB. The program structure is modular, with separate subroutines for devolatilization, plume model, char combustion, oxygen profile and temperature calculations.

Several test cases were conducted to observe how the model predictions change with various inputs of superficial gas velocities and solid recirculation rates. In addition, comparisons were made between the UBC CFB, a pilot scale CFB with a cross-sectional area of 0.15 m by 0.15 m, and the Studsvik CFB, a 2.5 MW thermal prototype CFB with a cross-sectional area of 0.65 m by 0.65 m. A qualitative validation was made between the model predictions of the UBC CFB and experimental data. The results from this validation seems to suggest that the model can predict the correct trends, with a more representative devolatilization model.

There are some limitations to the operating cases the model can predict and the accuracy of the predictions. They are listed below.

- (i) The primary zone and the cyclone are both treated as CSTRs (Continuous Stirred Tank Reactors).
- (ii) Superficial gas velocities below 5 m/s were not studied. Due to the limitations in the hydrodynamic code as discussed in Section 4.2.2, hydrodynamic predictions for low velocity cases were not possible.

- (iii) Combustion air was not recycled back into the riser.
- (iv) Incomplete combustion to for CO was not looked at.
- (v) The devolatilization equation used is not a function of particle diameter.
- (vi) A simplified energy equation was used, where the radiative and convective heat transfer terms are not coupled. Due to the highly non-linear nature of the energy balance equation, convergence was extremely difficult to achieve and it took many iterations to arrive at the final output, even with a good initial guess of the temperature. In addition, the particle convective term is orders of magnitude larger than the other terms, see Figure 4.19. Therefore, any changes in heat release, oxygen profile or temperature within a cell will take many iterations for that disturbance to affect the whole riser. An attempt to converge an equation where the convective and radiative heat transfer terms are coupled was unsuccessful.
- (vii) Radiative heat transfer from one cell was assumed to affect its adjacent cells or surface only. This assumption is valid for a annulus cell, where there are dense particles; however, for the dilute core cells, this assumption may not be valid.

5.2 RECOMMENDATIONS FOR FUTURE WORK

Future work can be done on the model to remove the limitations listed in the previous section. Some of the limitations to the devolatilization and char combustion equation can be easily programmed due to the modular nature of the program. In addition, incorporating this model as a subroutine to Senior's hydrodynamic model, and changing the hydrodynamics code so that the temperature profile output from the model can be placed back into the hydrodynamics code and iterated until a final converged solution is achieved. Finally, the addition of a NO_x and SO₂ emissions model would make the overall CFB program complete.

NOMENCLATURE

<u>Variables</u>		Units
y	distance in axial direction	m
x	distance in radial direction	m
k_{eff}	effective thermal conductivity	W/m·K
T	absolute temperature	K
α_p	volume fraction of particles	
ρ_p	density of particle	kg/m ³
c_p	specific heat of particle	J/kg·K
u_p	velocity of particle	m/s
ρ_g	density of gas	kg/m ³
c_g	specific heat of gas	J/kg·K
u_g	velocity of gas in the axial direction	m/s
I	radiative flux in the positive x direction	W/m ²
J	radiative flux in the negative x direction	W/m ²
G_v	heat source intensity per unit volume	W/m ³
A_r	radiative absorption cross-section per unit volume	
S_r	back-scattering cross-section per unit volume	
σ	Stefan-Boltzman constant	W/m ² ·K ⁴
CL	dimensionless proportionality factor	
ϵ_p	emissivity of the particles	
d_p	diameter of the particles	m
b	back-scattering coefficient	
V	fraction of volatiles released at time t	
V*	initial fraction of volatiles in coal (from proximate analysis)	
t	time	s
R	gas constant	kJ/kg·K kcal/mol·K
t_d	devolatilization time	s
T_b	bed temperature	K
P_0	partial pressure of oxygen	atm.
x^2	average displacement squared	
D_{rv}	radial volatile diffusion coefficient	
k_R	reaction rate	kg/m ² ·s·atm
T_s	surface temperature	K
d_c	diameter of char particle	m
ρ_c	density of char particle	kg/m ³
τ	burnout time	s
k	thermal conductivity of the cell	W/m·K
A	surface area of one side of the cell	m ²
F_x	mass flux of particles in the transverse direction	kg/m ² ·s

F_y	mass flux of particles in the axial direction	$\text{kg/m}^2 \cdot \text{s}$
V_g	represents the mass exchange of gas in the transverse direction due to turbulent mixing	m/s
ε	emissivity of the cell	
G	source term in the cell	W/m
h	cell to wall heat transfer coefficient	$\text{W/m}^2 \cdot \text{K}$
h_f	furnace side heat transfer coefficient	$\text{W/m}^2 \cdot \text{K}$
ρ_b	furnace solids bulk density	kg/m^3
U	overall heat transfer coefficient	$\text{W/m} \cdot \text{K}$
Q	heat transfer	W
f	fractional yield of volatiles	

Subscripts

w	wall	
i	initial	
L	condition at the center of the reactor column	
W	west	
E	east	
N	north	
S	south	
P	control volume	
NE	north face of the cell to the east of the control volume	
xE	transverse direction of the cell to the east of the control volume	m
yN	axial direction of the cell to the north of the control volume	m
yS	axial direction of the cell to the south of the control volume	m

Superscripts

0	reference
---	-----------

REFERENCES

- Agarwal, P.K., *"A Single Particle Model for the Evolution and Combustion of Coal Volatiles"*, Fuel, Vol. 65, p. 803-810, June 1986.
- Anthony, D.B., Howard, J.B., Hottel, H.C. and Meissner, H.P., *"Rapid Devolatilization of Pulverized Coal"*, Symp. Int. Combust. Proc., 15, p. 1303-1317, 1975.
- Baskakov, A.P., *"The Mechanism of Heat Transfer Between a Fluidized Bed and a Surface"*, Int. Chem. Eng., 4(2), p. 320-323, 1964.
- Baskakov, A.P., *"Radiative Heat Transfer in Fluidized Beds"*, Fluidization, 2nd ed., Academic Press, London, Ch. 13B, p. 465-472, 1985.
- Basu, P. and Fraser, S.A., Circulating Fluidized Bed Boilers: Design and Operations, Butterworth-Heinemann, 1991.
- Basu, P. and Yan, J., *"Characterization of the Fine Char Particle Combustion in CFBs"*, Fluidized Bed Combustion, Volume 1, ASME 1993.
- Bhattacharya, S.C. and Harrison, D., *"Heat Transfer in High Temperature Fluidized Beds"*, European Congress on Particle Technology, Nuremburg, p. 23, session K2, 1977.
- Bi, H., Jin, Y., Yu, Z. and Bai, D., *"An Investigation on Heat Transfer in CFB"*, Circulating Fluidized Bed Technology III, 1990.
- Botterill, J.S.M. and Sealey, C.J., *"Radiative Heat Transfer Between a Gas-Fluidized Bed and an Exchange Surface"*, British Chem. Eng., Vol. 15, No. 9, p. 1167, 1970.
- Bowen, B.D., Fournier, N. and Grace, J.R., *"Heat Transfer in Membrane Waterwalls"*, Int. J. Heat Mass Transfer, Vol. 34, No. 4/5, p. 1043-1057, 1991.
- Brereton, C. and Stromber, L., *"Some Aspects of the Fluid Dynamic Behavior of Fast Fluidized Beds"*, CFB Technology, Pergamon Press, Toronto, 1986.
- Brereton, C., *"Fluid Mechanics of High Velocity Fluidized Beds"*, Ph.D. Dissertation, Department of Chemical Engineering, U.B.C., 1987.
- Brewster, M.Q., *"Effective Emissivity of Fluidized Bed"*, ASME Heat Transfer Division, Vol. 40, p.7-13, 1984.
- Chen, J.C., Cimini, R.J. and Dou, S., *"A Theoretical Model for Simultaneous Convective and Radiative Heat Transfer in Circulating Fluidized Beds"*, Circulating Fluidized Bed Technology II, p. 255-262, 1988.

Couturier, M.F. and Stevens, D., *"Measurements of Heat Transfer, Temperature, Solids Mass Flux, Gas Concentration and Cyclone Capture Efficiency in the Chatham CFB Unit"*, Energy Conversion Engineering Group, University of New Brunswick, 1991.

Davidson, J.F., Cliff, R. and Harrison, D., *Fluidization*, 2nd ed., Academic Press, 1985, p. 642.

Dow, W.M. and Jakob, M., *"Heat Transfer Between a Vertical Tube and a Fluidized Air-Solid Mixture"*, Chem. Eng. Prog., 47(12), p. 637-648, 1951.

Energy, Mines and Resources Canada, *Energy in Canada : A Background Paper*, November 1987.

Furchi, J.C.L., Golstein Jr., L., Lombardi, G. and Mohseni, M., *"Experimental Local Heat Transfer in a CFB"*, Circulating Fluidized Bed Technology II, 1988.

Gabor, J.D., *"Wall-to-Bed Heat Transfer in Fluidized and Packed Beds"*, Chem. Eng. Progress Sym. Series, 66(105), p. 76-86, 1970.

Glicksman, L.R., *"CFB Heat Transfer"*, *CFB Technology II*, 1988.

Gorelik, A.G., *"Mechanism of Heat Exchange Between Surfaces and a Fluidized Bed"*, J. Eng. Phys., 13(6), p. 495-498, 1967.

Grace, J.R., Brereton, C., Lim, C.J., Legros, R., Zhao, J., Senior, R.C., Wu, R.L., Muir, J.R. and Engman, R., *"Circulating Fluidized Bed Combustion of Western Canadian Fuels"*, Final Report Prepared for Energy, Mines and Resources Canada under contract 52SS.23440-7-9136, 1989.

Han, G.Y., Tuzla, K. and Chen, J.C., *"Radiative Heat Transfer from High Temperature Suspended Flows"*, Institute of Thermo-Fluid Engineering and Science, 1992.

Howard, J.R., *Fluidized Beds*, London: Applied Science, p. 62, 1983.

Jia, L., Becker, H.A. and Code, R.K., *"Devolatilization and Char Burning of Coal Particles in a Fluidized Bed Combustor"*, The Canadian Journal of Chemical Engineering, Vol. 71, Feb. 1993.

Jolley, L.J., *"Heat Transfer in Beds of Fluidized Solids"*, Fuel Research 28(5), p. 114-115, 1949.

Kobro, H. *"Description of Studsvik's Fast Fluidized Bed Prototype"*, Studsvik Report, Studsvik/EM-84/3, 1984.

- Kolar, A.K., Grewal, N.S. and Saxena, S.C., "*Investigation of Radiative Contribution in a High Temperature Fluidized-Bed Using the Alternate-Slab Model*", Int. J. Heat Mass Transfer, Vol. 22, p. 1695-1703, 1979.
- Leckner, B., "*Heat Transfer in Circulating Fluidized Bed Boilers*", Circulating Fluidized Bed Technology III, p. 27-37, 1991.
- Leckner, B. and Andersson, B.A. "*Characteristic Features of Heat Transfer in CFB Boilers*", Powder Technology, 70, p. 303-314, 1992.
- Leva, M., and Grummer, M., "*A Correlation of Solids Turnover in Fluidized Systems - Its Relation to Heat Transfer*", Chem. Eng. Prog. 48(6), p.307-313, 1952.
- Levenspiel, O., and Walton, J.S., "*Bed-Wall Heat Transfer in Fluidized Systems*", Chem. Eng. Prog. Symp. Ser. 50(9), p. 1-13, 1954.
- Lin, W., and Van den Bleek, C.M., "*The SO_x/NO_x Emissions in CFB Combustion of Coal*", Proc. of the 3rd Int. Conf. on CFB, p. 545-550, 1989.
- Martin, H., "*Wärme-und Stoffübertragung in der Wirbelschicht*", Chem-Ing-Tech, 52, nr 3, s.199/209, 1980.
- Mickley, H.S. and Fairbanks, D.F., "*Mechanism of Heat Transfer to Fluidized Beds*", A.I.Ch.E. Journal, 1(3), p. 374-384, 1955.
- Mickley, H.S. and Trilling, C.A., "*Heat Transfer Characteristics of Fluidized Beds*", Ind. Eng. Chem. 41(6), p. 1135-1147, 1949.
- Morris, M., "*Furnace-Side Heat Transfer Coefficient Within Circulating Fluidized Beds*", Studsvik Report, p. 110, 1988.
- Nag, P.K. and Moran, M.N., "*Prediction of Heat Transfer in Circulating Fluidized Beds*", Proc. of the 3rd Int. Conf. on CFB, 1991.
- Park, D., Levenspiel, O. and Fitzgerald, T.J., "*A Model for Large Scale Atmospheric Fluidized Bed Combustors*", The American Institute of Chemical Engineers Symp. Series, 77(205), p. 116-126, 1981.
- Sanderson, W.E., "*A Review of Overall Models of Circulating Fluidized Bed Combustors - A Literature Study*", Technische Universiteit Delft, September 1993.
- Saxena, S.C. and Gabor, J.D., "*Mechanisms of Heat Transfer Between a Surface and a Gas-Fluidized Bed for Combustion Application*", Prog. Energy Combust. Sci., Vol. 7, p. 73-102, 1981.

Senior, R., "*Circulating Fluidized Bed Fluid and Particle Mechanics: Modeling and Experimental Studies with Application to Combustion*", Ph.D Dissertation, Department of Chemical Engineering, U.B.C., 1992.

Stubington, J.F., "*The Role of Coal Volatiles in Fluidized Bed Combustion*", Journal of the Institute of Energy, p. 191-195, 1980.

Szekely, J. and Fisher, R.J., "*Bed to Wall Radiative Heat Transfer in a Gas-Solid Fluidized Bed*", Chemical Engineering Science, Vol. 24, p. 833-849, 1969.

Vedamurthy, V.N. and Sastri, V.M.K., "*An Analysis of the Conductive and Radiative Heat Transfer to the Walls of Fluidized Bed Combustors*", Int. J. Heat Mass Transfer, 17, p.1-9, 1974.

Werdermann, C.C. and Werther, J., "*Heat Transfer in Large-Scale CFB Combustors of Different Sizes*", Technical University Hamburg, 1993.

Wu, R.L., "*Heat Transfer in Circulating Fluidized Beds*", Ph.D. Dissertation, Department of Chemical Engineering, U.B.C., August 1989.

Wu, R.L., Grace, J.R., and Lim, C.J., "*A Model for Heat Transfer in Circulating Fluidized Beds*", Chemical Engineering Science, Vol. 45, No. 12, p. 3389-3398, 1990.

Yang, W., "*The Hydrodynamics of CFBs*", Encyclopedia of Fluid Mechanics Supplements, Gulf Publishing, 1992.

Yang, Y., Jin, Y., Yu, Z., Wang, Z. and Bai, D., "*The Radial Distribution of Local Particle Velocity in a Dilute Circulating Fluidized Bed*", CFB Technology III, Pergamon Press, Oxford, 1991.

Yerushalmi, J., Cankurt, N.T., Geldart, D. and Liss, B., "*Flow Regimes in Vertical Gas-Solid Contact Systems*", A.I.Ch.E. Symp., Series No. 176, Vol. 74, 1, 1978.

Zhao, J., "*Nitrogen Oxide Emissions from Circulating Fluidized Bed Combustion*", Ph.D. Dissertation, Department of Chemical Engineering, U.B.C., 1992.

APPENDIX A

PROGRAM LISTING

```

1      C      ***** HEAT.F *****
2      C      *
3      C      *          HEAT GENERATION and          *
4      C      *          HEAT TRANSFER PROBLEM          *
5      C      *
6      C      *          rev. 8.1, 1995 Feb. 8          *
7      C      *          by: D.W. Ju                    *
8      C      *
9      C      *****
10     C
11     C This program uses the Monte Carlo Method to compute the heat
12     C release, oxygen and temperature profile in a CFB riser. Initially,
13     C the y-dir flux of the core cells had to be recalculated to force a
14     C mass balance. The devolatilization rate is calculated as a function of
15     C bed temperature. The program also incorporates char combustion assuming
16     C only kinetic rates and a first order reaction. It calculates the partial
17     C pressure of oxygen along the streamer and core by assuming air enters at
18     C 21% O2. Dispersion of air in the radial direction has been corrected
19     C for using the plume model. Some of the particles that leave the top of
20     C the riser is returned to the CFB after passing through a cyclone with a
21     C residence time of RT sec. The streamer cross-sectional area varies along the
22     C CFB riser. The heat transfer subroutine uses a simplified radiation heat
23     C transfer term. The temperature profile was smoothed for 1 point at every
24     C iteration. The control-volume method was also used.
25     C
26     C *****
27
28     implicit real*8(a-h,o-z)
29     real*8 mcyc,k
30     character*65 title1,title2,cyclon
31     common/blka/acell(300),o2feed,x,fuel,uc,us
32     common/blkb/cycv,npart,dt(300),pmatt(300),pmat1(300),rc,
33     1 volf,valh,rt,distv(300),siv(20),pdist(20)
34     common/blkc/heatc(300),dpcut,pressc(300),press(300),denp,coeff
35     common/blkd/heat(300),total,dycell,cross,press2(300),press2(300),con0,
36     1 oxyclc,mcyc,pair
37     common/blke/vtf,nfeed
38     common/blkf/to(5,300),k,at,twall,tair,vg,tref,cp,cg,afeed,fin
39     common/blkg/flux(300,5),dx(5,300),dy(5,300),f,emiss,denb(300)
40     common/blkh/acinit,asinit,acfin,asfin

```

```

41      common/blki/areaw(5,300),areae(5,300),arean(5,300),
42      1  areas(5,300),areat(5,300),effh(300),deng,sbc,const1,effc(300),effr(300),v2,
43      2  v5,v6,cyc,gcyc
44      dimension fluxc(300,5),heatv(300),ult(7)
45      dimension pmat2(300),tempo(300),temp(300)

```

c Unit 1 and 2 are input files, and 3,7,8,9 are output files.

```

48
49      open(unit=1,file='sh0.dat')
50      open(unit=2,file='h14.inp')
51      open(unit=3,file='sh0.plt')
52      open(unit=7,file='sh0.xls')
53      open(unit=8,file='sh0.out')
54      open(unit=9,file='sh0.txt',form='print')
55
56      data nx,dpcut/2,5.d-5/
57      data po2,cp,cg/0.21d0,800.d0,1172.d0/
58      data deng,sbc/0.3d0,5.67d-8/
59
60      pi=4.d0*datan(1.d0)

```

c Error handler during generation of the executable file.

```

63
64      ieee=ieee_handler('set', 'common', SIGFPE_DEFAULT)
65      if (ieee.ne.0) print *, 'could not establish fp signal handler'
66

```

c Read input file 1.

```

67
68
69      read(1,900) title1,title2
70      900  format(1x,a65,/1x,a65,/)
71      read(1,910) ny,at,rc,per,primev,dbavg,devh,pair,tb,twall
72      910  format(1x,i3,/1x,8(f10.6,/1x),f10.6)
73
74      tinit=855.d0
75
76      read(1,*)
77      read(1,*)
78      read(1,*)
79
80      primeh=primev/at
81      ncell=ny*nx+1
82
83      do i=1,ncell
84          read(1,920) (flux(i,j),j=1,4)
85      920  format(8x,f6.2,3f11.4)

```

```

86         enddo
87
88         read(1,*)
89         read(1,*)
90         read(1,*)
91         read(1,930) asinit
92         acinit=at-asinit
93         do i=1,ny
94             read(1,930) acell(ny+i)
95     930         format(14x,f10.6)
96         enddo
97         read (1,930) asfin
98         acfin=at-asfin
99         do i=1,ny
100            acell(i)=at-acell(ny+i)
101         enddo
102         acell(ncell)=at
103
104         read(1,*)
105         read(1,*)
106         read(1,*)
107         do i=1,7
108             read(1,940) ult(i)
109     940         format(1x,f10.3)
110         enddo
111         read(1,*)
112         read(1,941) volf,denp
113     941         format(1x,f10.3,/1x,f10.3)
114         volf=volf/100.d0
115         read(1,*)
116         read(1,941) uc,us
117         read(1,942) sug,fluxr,k,emiss
118     942         format(1x,f10.5,3(/1x,f10.5),///)
119         do i=1,18
120             read(1,943) siv(i),pdist(i)
121     943         format(1x,f10.3,5x,f10.3)
122         enddo
123         close(1)
124
125         recirc=fluxr*at
126
127     c Calculate the furnace solids bulk density as a function of height.
128
129         do i=1,ny+2
130             denb(i+2)=(flux(i,4)*acell(i)+flux(i+ny,4)*acell(i+ny))/at

```

```

131         enddo
132         denb(2)=flux(ncell,4)
133
134
135     c Read input file 2.
136
137         read(2,945) c1,c2,valh
138     945   format(//1x,f8.2,5x,f8.2,/1x,f8.1)
139         read(2,946) npart,perc,nfeed,eps,eps2,eps3,rf2,rf,cross,vtf,rt,exair,ceff,tsp,
140         1 tair,tref,const1
141     946   format(/1x,i10,/1x,f10.6,/1x,i10,14(/1x,f10.6))
142         close(2)
143
144         vg=cross
145
146     c Set dx and dy values for each cell.
147
148         dycell=flux(2,1)-flux(1,1)
149         r=dsqrt(at/pi)
150         do j=1,ny+3
151             dx(1,j)=0.d0
152             dx(4,j)=0.d0
153         enddo
154         do j=3,ny+2
155             rcore=dsqrt(acell(j-2)/pi)
156             ra=r-rcore
157             dx(2,j)=ra
158             dx(3,j)=rcore
159         enddo
160         rcore=dsqrt(acinit/pi)
161         ra=r-rcore
162         do i=1,2
163             dx(2,i)=ra
164             dx(3,i)=rc
165         enddo
166         rcore=dsqrt(acfin/pi)
167         ra=r-rcore
168         dx(2,ny+3)=ra
169         dx(3,ny+3)=rc
170
171         do i=1,4
172             dy(i,1)=0.d0
173             dy(i,2)=primeh
174         do j=3,ny+2
175             dy(i,j)=dycell

```

```

176         enddo
177         dy(i,ny+3)=0.d0
178     enddo
179
180     c Call subroutine to determine air and fuel feedrates.
181
182         call feed(tb,po2,ceff,exair,ult)
183
184     c Multiply the mass flux matrix (FLUX) by the dimensions of the riser and store
185     c in the mass flowrate matrix (FLUXC).
186
187         do i=1,ny-1
188             fluxc(i,1)=flux(i,1)
189             fluxc(i,2)=flux(i,2)*dycell*per
190             fluxc(i,4)=flux(i,4)*dycell*acell(i)
191         enddo
192         fluxc(ny,1)=flux(ny,1)
193         fluxc(ny,2)=flux(ny,2)*dycell*per
194         fluxc(ny,4)=flux(ny,4)*dycell*acell(ny)
195         fluxc(ny+1,1)=flux(ny+1,1)
196         fluxc(ny+1,2)=flux(ny+1,2)*dycell*per
197         fluxc(ny+1,3)=flux(ny+1,3)*asinit
198         fluxc(ny+1,4)=flux(ny+1,4)*dycell*acell(ny+1)
199         do i=ny+2,ncell-1
200             fluxc(i,1)=flux(i,1)
201             fluxc(i,2)=flux(i,2)*dycell*per
202             fluxc(i,3)=flux(i,3)*(acell(i)+acell(i-1))/2.d0
203             fluxc(i,4)=flux(i,4)*dycell*acell(i)
204         enddo
205         fluxc(ncell,1)=flux(ncell,1)
206         fluxc(ncell,2)=0.d0
207         fluxc(ncell,4)=flux(ncell,4)*primeh*at
208
209     c calculate axial flux of the core cells to ensure a mass balance.
210
211         fluxc(ncell,3)=recirc+fluxc(ny+1,3)
212         fluxc(1,3)=fluxc(ncell,3)-fluxc(1,2)+fluxc(ny+1,2)
213         do i=2,ny
214             fluxc(i,3)=fluxc(i-1,3)-fluxc(i,2)+fluxc(ny+i,2)
215         enddo
216
217         flux(ncell,3)=fluxc(ncell,3)/acinit
218         do i=1,ny-1
219             flux(i,3)=fluxc(i,3)/((acell(i)+acell(i+1))/2.d0)
220         enddo

```

```

221      flux(ny,3)=fluxc(ny,3)/acfin
222      afeed=o2feed/32.d0/.21d0*29.d0
223
224      c Set initial guess of pressure and temperature.
225
226          do i=1,ny+2
227              press(i)=0.21d0
228              presc(i)=0.21d0
229          enddo
230
231          do i=1,ncell
232              temp(i)=tinit
233              tempo(i)=temp(i)
234          enddo
235          do j=2,ny+3
236              to(1,j)=twall
237              do i=2,4
238                  to(i,j)=tinit
239              enddo
240          enddo
241
242      c Input solids return temperature. It can be set to equal the cyclone
243      c temperature, calculated by the program, or set at a bed temp. set
244      c by the user (normally 850C).
245
246          2  print*, 'Select solids return temperature. (C=cyclone,
247          1  B=temperature selected by user)'
248          read(*,950) cyclon
249          950  format(a3)
250
251          if(cyclon.ne.'C'.and. cyclon.ne.'B') goto 2
252
253          if(cyclon.eq.'B') then
254              print*, 'Enter temperature of inlet particles (C)'
255              read(*,*) tp
256          endif
257          tcyc=tp
258          fin=fuel/at
259
260      c Determine the time step and the probabilities of how the particle
261      c will move, depending on the location of the particle.
262
263          do i=1,ncell
264              pmat1(i)=fluxc(i,2)/fluxc(i,4)
265              pmat2(i)=fluxc(i,3)/fluxc(i,4)

```

```

266         pmatt(i)=pmat1(i)+pmat2(i)
267         dt(i)=perc/pmatt(i)
268
269         pmat1(i)=pmat1(i)*dt(i)
270         pmat2(i)=pmat2(i)*dt(i)
271         pmatt(i)=pmat1(i)+pmat2(i)
272     enddo
273
274     c Calculate the fraction of the wall covered by membrane tubes (f), or
275     c set it at a specified wall area.
276
277     c  htarea=(fuel*valh*1000.d0/2.5d0)/(const1*dbavg*(tinit-twall)
278     c  2+emiss*sbc*((tinit+273.15d0)**4-(twall+273.15d0)**4))
279     c  rarea=per*(primeh+flux(ny,1)+dycell/2.d0)
280     c  if(htarea.le.0.d0) htarea=0.d0
281     c  f=htarea/rarea
282
283         f=0.7d0
284
285     c Initialize heat distribution terms
286
287         iter2=0
288     5   iter2=iter2+1
289
290     c Determine the areas.
291
292         do j=1,ny+3
293             do i=1,4
294                 areaw(i,j)=0.d0
295                 areae(i,j)=0.d0
296                 arean(i,j)=0.d0
297                 areas(i,j)=0.d0
298                 areat(i,j)=0.d0
299             enddo
300         enddo
301
302         areaw(1,2)=primeh*per*f
303         areae(1,2)=primeh*per*f
304         areaw(2,2)=primeh*per*f
305         areae(2,2)=primeh*per
306         do i=3,4
307             areaw(i,2)=primeh*per
308             areae(i,2)=primeh*per
309         enddo
310         do j=3,ny+2

```

```

311         areaw(1,j)=dycell*per*f
312         areae(1,j)=dycell*per*f
313         areaw(2,j)=dycell*per*f
314         areae(2,j)=dycell*per
315         do i=3,4
316             areaw(i,j)=dycell*per
317             areae(i,j)=dycell*per
318         enddo
319     enddo
320     do j=3,ny+1
321         arean(3,j)=(acell(j-2)+acell(j-1))/2.d0
322         arean(2,j)=(acell(j-2+ny)+acell(j-1+ny))/2.d0
323         areas(3,j+1)=arean(3,j)
324         areas(2,j+1)=arean(2,j)
325     enddo
326     arean(3,ny+2)=acfin
327     arean(2,ny+2)=asfin
328     arean(3,ny+3)=acfin
329     arean(2,ny+3)=asfin
330     arean(3,1)=acinit
331     arean(2,1)=asinit
332     arean(3,2)=acinit
333     arean(2,2)=asinit
334     areas(3,3)=acinit
335     areas(2,3)=asinit
336     areas(3,2)=acinit
337     areas(2,2)=asinit
338     areas(3,1)=acinit
339     areas(2,1)=asinit
340     areas(3,ny+3)=acfin
341     areas(2,ny+3)=asfin
342     do j=2,ny+2
343         areat(1,j)=areaw(1,j)
344         areat(2,j)=areae(2,j)+areaw(2,j)+arean(2,j)+areas(2,j)
345         areat(3,j)=areaw(3,j)+arean(3,j)+areas(3,j)
346     enddo
347     areat(2,1)=areas(2,1)
348     areat(3,1)=areas(3,1)
349     areat(2,ny+3)=arean(2,ny+3)
350     areat(3,ny+3)=arean(3,ny+3)
351
352     cycv=0.d0
353
354     c Call subroutine to calculate volatilization heat distribution
355

```

```

356         call volat(ny,heatv,tdvol,totv,ncell,c1,c2,temp,pi)
357
358         coeff=7.26d3*exp(-1.5d5/(8.314d0*(tsp+273)))
359
360     c Call subroutine to correct for volatile dispersion
361
362         call vdisp(heatv,ncell,ny,pi,flux)
363
364     c Count the number of iterations and call subroutine to calculate
365     c the char heat distribution
366
367         iter=0
368     10    iter=iter+1
369
370         call char(ny,cyc,pi,ncell,ult)
371
372         cycc=cyc-cycv
373
374     c Calculate fraction of the total heat generated in each cell.
375
376         do i=1,nmax
377             heat(i)=0.d0
378         enddo
379
380         total=0.d0
381         do i=1,ncell
382             heat(i)=heatv(i)+heatc(i)
383             total=total+heat(i)
384         enddo
385         total=total+cyc
386
387         do i=1,ncell
388             heat(i)=heat(i)/total
389         enddo
390
391     c Call subroutine to calculate the O2 partial pressure profile
392
393         call pres(ny,cyc,pi,po2,ncell)
394
395     c Check that the errors in the pressure of the core cells are less than EPS.
396
397         ermax=0.d0
398         do i=1,ny+2
399             errorc=abs(presc(i)-presc2(i))
400             if(errorc.gt.ermax) then

```

```

401             ermax=errorc
402             ic=i
403             endif
404         enddo
405
406     c Print the error and the iteration number.
407
408         print*, 'iter,error',iter,ermax
409
410     c Update the pressures.
411
412         do i=1,ny+2
413             press(i)=press(i)+rf*(press2(i)-press(i))
414             presc(i)=presc(i)+rf*(presc2(i)-presc(i))
415         enddo
416
417     c Decide whether convergence has been met. If not, go back
418     c to statement number 10.
419
420         if(ermax.gt.eps) goto 10
421         er1=ermax
422
423     c Set the temperature of the solids return.
424
425         if(cyclon.eq.'C') then
426             trec=tcyc
427         else
428             trec=tp
429         endif
430
431         tin=(afeed*cg*tair+fuel*cp*tref+recirc*cp*trec)/(afeed*cg+fuel*cp+
432     1   recirc*cp)
433         do i=1,4
434             to(i,1)=tin
435         enddo
436
437     c Call subroutine heat to determine temperature profile.
438
439         call htrans(ncell,ny,eps3,per,rfl,recirc,ult)
440
441         print*, 'No. of iterations in htrans=', iter2
442         write(8,*) 'No. of iterations in htrans=', iter2
443
444     c New temperatures
445

```

```

446         do j=ny+2,3,-1
447             temp(j-2+ny)=to(2,j)
448             temp(j-2)=to(3,j)
449         enddo
450         temp(ncell)=to(3,2)*acinit/at+to(2,2)*asinit/at
451
452     c Smooth temperature profile for 1 point (at the boundary between
453     c developing and fully developed region).
454
455         do i=1,ny
456             if(devh.le.flux(i,1)) then
457                 i=i-1
458                 ratio=(temp(i+1)-temp(i-2))/(flux(i+1,1)-flux(i-2,1))
459                 temp(i)=ratio*(flux(i,1)-flux(i-2,1))+temp(i-2)
460                 temp(i-1)=ratio*(flux(i-1,1)-flux(i-2,1))+temp(i-2)
461                 i=i+1+ny
462                 ratio=(temp(i+1)-temp(i-3))/(flux(i+1,1)-flux(i-3,1))
463                 temp(i)=ratio*(flux(i,1)-flux(i-3,1))+temp(i-3)
464                 temp(i-1)=ratio*(flux(i-1,1)-flux(i-3,1))+temp(i-3)
465                 temp(i-2)=ratio*(flux(i-2,1)-flux(i-3,1))+temp(i-3)
466                 goto 20
467             endif
468         enddo
469
470     c Write the temperature to output file.
471
472     20     write(8,960) (to(i,ny+3),i=1,3)
473     960     format(3(1x,f10.2))
474         do j=ny+2,3,-1
475             write(8,965) twall,temp(j+ny-2),temp(j-2),effh(j)
476     965     format(4(1x,f10.2))
477             if(j.eq.7) then
478                 write(3,*) temp(j-2)
479             endif
480         enddo
481         write(8,965) (to(i,2),i=1,3),effh(2)
482         write(8,960) (to(i,1),i=1,3)
483         call flush(3)
484         call flush(7)
485         call flush(8)
486
487     c Calculate the temperature of the cyclone.
488
489         tcycn=temp(ny)+gcyc/(afeed*cg+recirc*cp)
490

```

491 c Set the number of iterations in the temperature profile subroutine to
 492 c ensure that a converged solution is obtained.

493
 494 if(iter2.ge.200) goto 50

495
 496 c Check the convergence of the temperature.

497
 498 error=0.d0
 499 ermax=0.d0
 500 ierr=0
 501 do i=1,ncell
 502 error=dabs(temp(i)-tempo(i))
 503 if(error.gt.ermax) then
 504 ermax=error
 505 ierr=i
 506 endif
 507 enddo
 508 error=dabs(tcycn-tcyc)
 509 if(error.gt.ermax) then
 510 ermax=error
 511 ierr=ncell+1
 512 endif
 513
 514 print*,'eps2,ermax,cell',eps2,ermax,ierr
 515 write(8,*) 'eps2,ermax,cell',eps2,ermax,ierr
 516 if(ierr.eq.(ncell+1)) then
 517 print*,'tempo,temp',tcyc,tcycn
 518 write(8,*) 'tempo,temp',tcyc,tcycn
 519 else
 520 print*,'tempo,temp',tempo(ierr),temp(ierr)
 521 write(8,*) 'tempo,temp',tempo(ierr),temp(ierr)
 522 endif
 523 write(8,*)

524
 525 c Update temperature and check that convergence has been met.

526 c If not, go back to statement number 5.

527
 528 if(ermax.gt.eps2) then
 529 rf3=1.d0
 530 do i=1,ncell
 531 tempo(i)=tempo(i)-rf3*(tempo(i)-temp(i))
 532 tcyc=tcyc-rf3*(tcyc-tcycn)
 533 enddo
 534 goto 5
 535 endif

```

536
537 c Calculate average partial pressure of O2 leaving riser and cyclone (atm).
538
539 50 pout=presc(ny+2)*acfin/at+press(ny+2)*asfin/at
540 pccyc=(oxyclc-mccyc*x)/(uc*acfin+us*asfin)*po2/con0
541
542 c Print output results to unit 9.
543
544 write(9,800) title1,title2
545 800 format(45x,'page 1 of 6',/////15x,
546 1 'CFB HEAT RELEASE AND HEAT TRANSFER MODEL',/15x,
547 2 '-----',/15x,
548 3 'RUN RESULTS FROM HEAT TRANSFER ROUTINE HEAT.F,
549 4 VERSION 1.1',/15x,
550 5 'WRITTEN BY: DALE W.C. JU',///15x,a65,/15x,a65,///15x,
551 6 'FUEL PHYSICAL PROPERTIES AND COMPOSITION',/15x,
552 7 '-----',/15x,
553 8 'PROXIMATE ANALYSIS',/15x,'Weight %')
554 write(9,802) (ult(i),i=1,7)
555 802 format(15x,f8.3,5x,'Ash',/15x,f8.3,5x,'Moisture',/15x,f8.3,5x,
556 1 'Sulphur',/15x,f8.3,5x,'Hydrogen',/15x,f8.3,5x,'Carbon',/15x,
557 2 f8.3,5x,'Nitrogen',/15x,f8.3,5x,'Oxygen',/15x,
558 3 'PARTICLE SIZE DISTRIBUTION',/15x,5x,'mm',13x,'wt %')
559 do i=1,18
560 write(9,804) siv(i),pdist(i)
561 804 format(15x,f10.3,5x,f10.3)
562 enddo
563
564 write(9,806) npart,f*100.d0
565 806 format(("1"),45x,'page 2 of 6',/////15x,
566 1 'COMBUSTION CONDITIONS',/15x,'-----',/15x,
567 2 '# of particles in Monte Carlo Method',4x,i10,/15x,
568 3 '% of total wall area with membranes',5x,f10.1,'%')
569
570 if(cyclon.eq.'C') then
571 write(9,808) trec
572 808 format(15x,'Solids return temp. equals cyclone temp.',f10.1,' C')
573 else
574 write(9,810) trec
575 810 format(15x,'Solids return temp. set at',14x,f10.1,' C')
576 endif
577
578 write(9,812) recirc,fluxr,cross,ceff*100.d0,exair*100.d0,vtf,
579 1 nfeed,fuel*3600.d0,afeed*3600.d0,pair*100.d0,rt,rc,devh
580 812 format(15x,'Solids recirculation rate',16x,f10.3,' kg/s',/15x,

```

```

581      1 'Solids recirculation flux',15x,f10.3,' kg/m2s',/15x,
582      2 'Gas cross-flow coefficient',14x,f10.3,' m/s',/15x,
583      3 'Combustion efficiency',19x,f10.1,' %',/15x,'Excess air',30x,f10.3,' %',/15x,
584      4 'Volatile transfer fraction',14x,f10.3,/15x,'Number of fuel feed points',
585      5 14x,i10,/15x,'Fuel feedrate',27x,f10.3,' kg/hr',/15x,'Air feedrate',28x,
586      6 f10.3,' kg/hr',/15x,'% of total air that is primary',10x,f10.1,' %',/15x
587      7 'Residence time of particles in cyclone',2x,f10.3,' sec.',/15x,
588      8 'Reflection coefficient',18x,f10.3,/15x,
589      9 'Height at which developed zone begins',3x,f10.3,' m')
590
591      write(9,814) uc,us,sug,tb
592      814 format(//15x,'GAS VELOCITIES',/15x,'-----',/15x,
593      1 'Core interstitial gas velocity',9x,f10.3,' m/s',/15x,
594      2 'Streamer interstitial gas velocity',6x,f10.3,' m/s',/15x,
595      3 'Superficial gas velocity',16x,f10.3,' m/s',/15x,
596      4 'Bed temperature used in calculating',/17x,
597      5 'heat transfer area and gas velocities',3x,f10.1,' C')
598
599      write(9,816)
600      816 format(("1"),45x,'page 3 of 6',/////15x,
601      1 'HEAT RELEASE DISTRIBUTION',/15x,
602      2 '-----',/15x,'Height',8x,
603      3 'Fraction of Total Heat Release',/34x,'Volatiles',16x,
604      4 'Char',/17x,'(m)',9x,'Streamer',4x,'Core',6x,'Streamer',4x,'Core',/)
605
606      write(9,818) fluxc(ncell,1),heatv(ncell)/total,heatc(ncell)/total
607      818 format(15x,f5.2,12x,f10.6,12x,f10.6)
608      do i=1,ny
609          write(9,820) fluxc(i,1),heatv(i+ny)/total,heatv(i)/total,heatc(i+ny)/total,
610      1      heatc(i)/total
611      820      format(15x,f5.2,6x,3(1x,f10.6),2x,f10.6)
612      enddo
613      write(9,822) cycv/total,cycc/total,totv/total,(total-totv)/total
614      822 format(15x,'Cyclone',10x,f10.6,12x,f10.6,/15x,'TOTAL',12x,f10.6,12x,
615      1 f10.6)
616
617      write(9,824) fluxc(ncell,1),press(2)
618      824 format(("1"),45x,'page 4 of 6',/////15x,
619      1 'OXYGEN PARTIAL PRESSURE DISTRIBUTION',
620      2 /15x,'-----',/15x,'Height',8x,
621      3 'Partial Pressure of Oxygen (atm.)',/17x,'(m)',9x,
622      4 'Streamer',4x,'Core',/15x,f5.2,12x,f10.6)
623      do i=1,ny
624          write(9,826) fluxc(i,1)+dycell/2.d0,press2(i+2),presc2(i+2)
625      826      format(15x,f5.2,6x,2(1x,f10.6))

```

```

626         enddo
627         write(9,828) er1,po2,pout,pcyc
628     828   format(//15x,'Pressure convergence tolerance',10x,f10.4,' atm.',
629           1   /15x,'Partial pressure of oxygen entering',5x,f10.6,' atm.',/15x,
630           2   'Partial pressure of oxygen leaving riser',f10.3,' atm.',/15x,
631           3   'Partial pressure of oxygen leaving cyclone',f8.3,' atm.')
```

```

632
633         write(9,830) fluxc(ncell,1),temp(ncell)
634     830   format(("1"),45x,'page 5 of 6',/////15x,
635           1   'TEMPERATURE DISTRIBUTION',/15x,
636           2   '-----',/15x,'Height',8x,'Temperature (C)',
637           3   /17x,'(m)',9x,'Streamer',4x,'Core',/15x,f5.2,11x,f10.1)
638         do i=1,ny
639             write(9,832) fluxc(i,1),temp(i+ny),temp(i)
640     832   format(15x,f5.2,4x,2(1x,f10.1))
641         enddo
642         write(9,834) trec,ermax,tcyc,twall
643     834   format(//15x,'Solids return temperature',15x,f10.1,' C',/15x,
644           1   'Temperature convergence tolerance',7x,f10.3,' C',/15x,
645           2   'Cyclone temperature',21x,f10.1,' C',/15x,'Wall temperature',24x,f10.1,' C')
```

```

646
647         write(9,836)
648     836   format(("1"),45x,'page 6 of 6',/////15x,
649           1   'HEAT TRANSFER COEFFICIENTS',/15x,
650           2   '-----',/15x,'Height',2x,'Density',
651           3   2x,'Core Temp.',2x,'Heat Transfer Coefficient (W/m2C)',
652           4   /17x,'(m)',3x,'(kg/m3)',5x,'(C)',6x,'Radiative',2x,'Convective',3x,'Overall',/)
653         write(9,838) fluxc(ncell,1),flux(ncell,4),temp(ncell),effr(2),effc(2),effh(2)
654         do i=1,ny
655             denav=(flux(i,4)*acell(i)+flux(i+ny,4)*acell(i+ny))/at
656             write(9,838) fluxc(i,1),denav,temp(i),effr(i+2),effc(i+2),effh(i+2)
657     838   format(15x,f5.2,2x,f8.3,2x,f7.1,3(2x,f10.1))
658         enddo
659
660     100   close(9)
661         close(3)
662         close(7)
663         close(8)
664         stop
665         end
```

```

666
667     c***** subroutine feed *****
668         subroutine feed(tb,po2,ceff,exair,ult)
669     c Subroutine to calculate the coal feedrate (fuel), given
670     c the ultimate analysis of the coal and the gas velocity in the
```

```

671 c streamer and the core (us and uc).
672 c
673 c Variables are:
674 c
675 c fuel      coal feedrate (kg/s)
676 c o2feed oxygen feedrate (kg/s)
677 c o2need oxygen feedrate needed for every 1 kg/s of coal feed
678 c          (kg/s)
679 c ult      ultimate analysis of coal
680 c uc      gas velocity in the core (m/s)
681 c us      gas velocity in the streamer (m/s)
682 c*****
683
684 c          implicit real*8(a-h,o-z)
685 c          common/blka/acell(300),o2feed,x,fuel,uc,us
686 c          common/blkh/acinit,asinit,acfin,asfin
687 c          dimension ult(7)
688
689 c Calculate the O2 feedrate (kg/s)
690
691 c          o2feed=101.325d0*(uc*acinit+us*asinit)/8.314d0/(273.15d0+tb)*
692 c          1 po2*32.d0
693
694 c Calculate the O2 feedrate needed for 1 kg/s fuel (kg/s)
695
696 c          x=(ceff*(ult(3)/32.d0+ult(4)/4.d0+ult(5)/12.d0)*32.d0-ult(7))/100.d0
697 c          o2need=exair*x+x
698
699 c Calculate the fuel feedrate (kg/s)
700
701 c          fuel=o2feed/o2need
702 c          return
703 c          end
704
705 c***** subroutine volat *****
706 c          subroutine volat(ny,heatv,tdvol,totv,ncell,c1,c2,temp,pi)
707 c Subroutine to determine the heat release distribution due to
708 c devolatilization (heatv).
709 c*****
710
711 c          implicit real*8(a-h,o-z)
712 c          common/blkb/cycv,npart,dt(300),pmatt(300),
713 c          1 pmat1(300),rc,volf,valh,rt,distv(300),siv(20),pdist(20)
714 c          common/blkc/heatc(300),dpcut,presc(300),press(300),denp,coeff
715 c          dimension heatv(300),temp(300)

```

```

716
717   c Intialize heatv.
718
719       voli=0.d0
720       do i=1,ncell
721           heatv(i)=0.d0
722       enddo
723
724   c Main loop over the number of particles.
725
726       do 30 ii=1,npart
727
728   c Determine the initial size of the particle based on the particle
729   c size distribution.
730
731           rval=d_lcran()
732           totwt=0.d0
733           do i=1,18
734               totwt=totwt+pdist(i)/100.d0
735               if(rval.le.totwt) then
736                   dpinit=siv(i)/1000.d0
737                   goto 5
738               endif
739           enddo
740
741   5       volp=pi*dpinit**3/6.d0
742           pmas=denp*volp
743
744           vol=voli
745           voldif=1.d0
746           time=0.d0
747           icell=ncell
748           icello=icell
749
750   c Generate a random real number between [0,1] to determine the position
751   c of the particle.
752
753   10       time=time+dt(icell)
754
755           if(voldif.le.1.d-6) then
756               tdvol=time-dt(icell)
757               goto 30
758           endif
759
760           rval=d_lcran()

```

```

761
762         if(icell.eq.ncell) then
763             if(rval.le.pmat1(icell)) icell=1
764             goto 20
765         endif
766
767         if(rval.le.pmat1(icell)) then
768             if(icell.le.ny) then
769                 icell=icell+ny
770             else
771                 icell=icell-ny
772             endif
773         elseif(rval.le.pmat1(icell)) then
774             if(icell.eq.ny) then
775
776                 c If the particle exits the top of the riser, another random number
777                 c is generated to determine whether the particle is transferred to
778                 c the streamer or is removed to the cyclone.
779
780                 rval=d_lcran()
781                 if(rval.le.rc) then
782                     icell=ncell-1
783                     goto 20
784                 else
785                     voldif=volf*(1.d0-dexp(-c1*time*dexp(-c2/
786             1         (1.987d-3*(273.15d0+temp(icello))))))-vol
787                     vol=vol+voldif
788                     heatv(icello)=heatv(icello)+valh*voldif*pmas
789                     time=time+rt
790                     voldif=volf*(1.d0-dexp(-c1*time*dexp(-c2/
791             1         (1.987d-3*(273.15d0+temp(icello))))))-vol
792                     vol=vol+voldif
793                     cycv=cycv+valh*voldif*pmas
794                     icell=ncell
795                     icello=icell
796                     goto 10
797                 endif
798             elseif(icell.lt.ny) then
799                 icell=icell+1
800             elseif(icell.eq.ny+1) then
801                 icell=ncell
802             else
803                 icell=icell-1
804             endif
805         endif

```

```

806
807 c Add the heat generation due to volatiles to each cell.
808
809 20      voldif=vol*(1.d0-dexp(-c1*time*dexp(-c2/
810      1      (1.987d-3*(273.15d0+temp(icello))))))-vol
811      vol=vol+voldif
812      heatv(icello)=heatv(icello)+valh*voldif*pmas
813      icello=icell
814      goto 10
815 30      continue
816
817 c Calculate the heat distribution.
818
819      totv=0.d0
820      do 40 i=1,ncell
821      totv=totv+heatv(i)
822 40      continue
823      distv(1)=heatv(1)/totv
824      do 50 i=2,ncell
825      sum=0.d0
826      do j=1,i
827      sum=sum+heatv(j)
828      enddo
829      distv(i)=sum/totv
830 50      continue
831      return
832      end
833
834 c***** subroutine vdisp *****
835      subroutine vdisp(heatv,ncell,ny,pi,flux)
836 c Subroutine which uses the plume model to correct for volatile
837 c dispersion
838 c.
839 c Variables are:
840 c
841 c nfeed Number of feed points.
842 c height Height above the feed where there is full radial mixing
843 c sdisp Average displacement in the radial direction (m)
844 c tdisp Time (sec.)
845 c r Radius (m)
846 c*****
847
848      implicit real*8(a-h,o-z)
849      common/blka/acell(300),o2feed,x,fuel,uc,us
850      common/blkb/cycv,npart,dt(300),pmatt(300),

```

```

851      1  pmat1(300),rc,volf,valh,rt,distv(300),siv(20),pdist(20)
852          common/blke/vtf,nfeed
853          dimension r(300),heatv(300),flux(300,5)
854          data drp/0.015d0/
855
856          r(ncell)=dsqrt(ace11(ncell)/pi)
857          ndiv=1
858          if(nfeed.ne.1) ndiv=(nfeed-2)*2+2
859
860          sdisp=r(ncell)/ndiv
861          tdisp=sdisp**2/(2.d0*drp)
862
863      c Calculate the height where the volatiles are fully mixed in the
864      c radial direction.
865
866          height=uc*tdisp
867
868      c Transfer a fraction (vtf) of the volatiles to the cell above where
869      c the volatiles are released.
870
871          heatv(ncell)=heatv(ncell)-vtf*heatv(ncell)
872          if(flux(1,1).ge.height) return
873          heatv(1)=heatv(1)+vtf*heatv(ncell)
874          heatv(1)=heatv(1)-vtf*heatv(1)
875          do i=2,ny-1
876              if(flux(i,1).ge.height) return
877              heatv(i)=heatv(i)+vtf*heatv(i-1)
878              heatv(i)=heatv(i)-vtf*heatv(i)
879          enddo
880
881          if(flux(ny,1).ge.height) return
882          heatv(ny)=heatv(ny)+vtf*heatv(ny-1)
883          heatv(ny)=heatv(ny)-vtf*heatv(ny)
884          cycv=cycv+vtf*heatv(ny)
885          return
886          end
887
888      c***** subroutine char *****
889          subroutine char(ny,cyc,pi,ncell,ult)
890      c Subroutine to determine the char heat release distribution.
891      c
892      c Variables are:
893      c
894      c cmass Mass of char particle
895      c cyc Total heat released in the cyclone

```

```

896      c dp   Particle diameter (m)
897      c icell Position of the particle at a given time
898      c volmas Mass of volatiles
899      c*****
900
901      implicit real*8(a-h,o-z)
902      common/blkbc/cycv,npart,dt(300),pmatt(300),
903      1  pmat1(300),rc,volf,valh,rt,distv(300),siv(20),pdist(20)
904      common/blkc/heatc(300),dpcut,presc(300),press(300),denp,coeff
905      dimension ult(7)
906
907      c Intialize the heat due to char combustion vector to zero, and the
908      c heat released in the cyclone to equal the heat released due to
909      c devolatilization.
910
911      do i=1,ncell
912          heatc(i)=0.d0
913      enddo
914      cyc=cycv
915
916      c Main loop over the number the particles.
917
918      do 30 ii=1,npart
919
920      c Determine the initial size of the particle based on the particle
921      c size distribution.
922
923          rval=d_lcran()
924          totwt=0.d0
925          do i=1,18
926              totwt=totwt+pdist(i)/100.d0
927              if(rval.le.totwt) then
928                  dpinit=siv(i)/1000.d0
929                  goto 5
930              endif
931          enddo
932
933      5      volp=pi*dpinit**3/6.d0
934          pmas=denp*volp
935          volmas=pmas*volf
936          ashmas=pmas*ult(1)/100.d0
937          cmas=pmas-volmas-ashmas
938
939      c Determine diameter of a particle of fixed carbon only.
940

```

```

941         dp=(6.d0*cmas/(denp*pi)**(1.d0/3.d0)
942
943     c Generate a random real number between [0,1] to determine the initial
944     c position of the char particle based on the devolatilization heat
945     c released distribution.
946
947         rval=d_lcran()
948         icell=1
949         do i=1,ncell-1
950             if(rval.ge.distv(i)) icell=i+1
951         enddo
952         icello=icell
953
954         time=0.d0
955     10     time=time+dt(icell)
956
957         rval=d_lcran()
958         if(icell.eq.ncell) then
959             if(rval.lt.p matt(icell)) icell=1
960             goto 20
961         endif
962
963         if(rval.le.p mat1(icell)) then
964             if(icell.le.ny) then
965                 icell=icell+ny
966             else
967                 icell=icell-ny
968             endif
969         elseif(rval.le.p matt(icell)) then
970             if(icell.eq.ny) then
971
972     c If the particle exits the top of the riser, another random number
973     c is generated to determine whether the particle is transferred to
974     c the streamer or is removed to the cyclone.
975
976         rval=d_lcran()
977         if(rval.lt.rc) then
978             icell=ncell-1
979         else
980             if(dp.gt.dp cut) then
981                 fi=coeff*pi*(dp**2)*presc(icello+2)*dt(icello)*12.d0
982                 cmas2=cmas-fi
983                 if(cmas2.le.0.d0) then
984                     heatc(icello)=heatc(icello)+cmas2*valh
985                     goto 30

```

```

986         endif
987         heatc(icello)=heatc(icello)+fi*valh
988         cmas=cmas-fi
989
990         time=time+rt
991         fi=coeff*pi*(dp**2)*presc(ny)*rt*12.d0
992         cmas2=cmas-fi
993         if(cmas2.le.0.d0) then
994             cyc=cyc+cmas2*valh
995             goto 30
996         endif
997         cyc=cyc+fi*valh
998         cmas=cmas-fi
999         dp=(6.d0*cmas/(denp*pi))**(1.d0/3.d0)
1000        icell=ncell
1001        icello=icell
1002        goto 10
1003    else
1004        goto 30
1005    endif
1006    endif
1007
1008    elseif(icell.lt.ny) then
1009        icell=icell+1
1010    elseif(icell.eq.ny+1) then
1011        icell=ncell
1012    else
1013        icell=icell-1
1014    endif
1015    endif
1016
1017    c Calculate the heat generation due to char combustion, assuming first
1018    c order reaction. From: Howard, J.R.
1019
1020    20    if(icello.le.ny) then
1021        fi=coeff*pi*(dp**2)*presc(icello+2)*dt(icello)*12.d0
1022    elseif(icello.eq.ncell) then
1023        fi=coeff*pi*(dp**2)*presc(2)*dt(icello)*12.d0
1024    else
1025        fi=coeff*pi*(dp**2)*press(icello-ny+2)*dt(icello)*12.d0
1026    endif
1027    heatc(icello)=heatc(icello)+fi*valh
1028    icello=icell
1029
1030    c Mass balance to determine the new particle diameter, DP.

```

```

1031
1032         cmas=cmas-fi
1033         if(cmas.lt.0.d0) goto 30
1034         dp=(6.d0*cmas/(denp*pi))**(1.d0/3.d0)
1035         goto 10
1036     30    continue
1037         return
1038         end
1039
1040     c***** subroutine pres *****
1041         subroutine pres(ny,cyc,pi,po2,ncell)
1042     c Subroutine to determine the partial pressure of oxygen profile.
1043     c Secondary in injected into the core and the streamer cells to
1044     c keep the gas velocities in the streamer and core at a constant
1045     c value.
1046     c
1047     c Variables are:
1048     c
1049     c cc      Concentration of oxygen in the core
1050     c cs      Concentration of oxygen in the streamer
1051     c mcyc    Mass of fuel in the cyclone (kg)
1052     c mfuel   Mass of fuel in each cell (kg)
1053     c o2prim  Oxygen feed in the primary air
1054     c rcore   Radius of the core
1055     c*****
1056
1057         implicit real*8(a-h,o-z)
1058         real*8 mfuel,mcyc
1059         common/blk_a/acell(300),o2feed,x,fuel,uc,us
1060         common/blk_d/heat(300),total,dycell,cross,preSc2(300),
1061     1    press2(300),con0,oxyc,mcyc,pa,r
1062         common/blk_h/acinit,asinit,acfin,asfin
1063         dimension mfuel(300),conc(300)
1064
1065     c Assume time duration is 1 sec.
1066     c Calculate the mass of fuel in each cell (kg) based on the fraction
1067     c of heat released.
1068
1069         do i=1,ncell
1070             mfuel(i)=heat(i)*fuel
1071         enddo
1072         mcyc=cyc/total*fuel
1073
1074     c Calculate the concentration of O2 in each cell (kg/m3)
1075

```

```

1076      con0=o2feed/(uc*acinit+us*asinit)
1077      cprim=o2feed*pair-mfuel(ncell)*x
1078
1079      c Addition of secondary air, in both the streamer and core,
1080      c after the primary zone.
1081
1082      if(cprim.le.0.d0) then
1083          conin=(o2feed*(1.d0-pair))/(uc*acinit+us*asinit)
1084      else
1085          conin=(o2feed-mfuel(ncell)*x)/(uc*acinit+us*asinit)
1086      endif
1087
1088      conc(ncell)=conin
1089      oxyc=conin*uc*(acell(1)+acell(2))/2.d0
1090      oxys=conin*us*(acell(ny+1)+acell(ny+2))/2.d0
1091
1092      do i=1,ny-1
1093          rcore=dsqrt(acell(i)/pi)
1094          frac=cross*2.d0*pi*rcore*dycell
1095          cc=(acell(i)+acell(i+1))/2.d0*uc
1096          cs=(acell(ny+i)+acell(ny+i+1))/2.d0*us
1097
1098          oxys=(oxys-mfuel(ny+i)*x+frac*(oxyc-mfuel(i)*x)/
1099      1 (cc+frac))/(1.d0+frac/cs-frac**2/cs/(cc+frac))
1100          oxyc=(oxyc-mfuel(i)*x+frac*oxys/cs)/(1.d0+frac/cc)
1101          if(oxys.lt.0.d0) oxys=0.d0
1102          if(oxyc.lt.0.d0) oxyc=0.d0
1103          conc(i)=oxyc/cc
1104          conc(ny+i)=oxys/cs
1105      enddo
1106          rcore=dsqrt(acell(ny)/pi)
1107          frac=cross*2.d0*pi*rcore*dycell
1108          cc=acfin*uc
1109          cs=asfin*us
1110
1111          oxys=(oxys-mfuel(ny+ny)*x+frac*(oxyc-mfuel(ny)*x)/
1112      1 (cc+frac))/(1.d0+frac/cs-frac**2/cs/(cc+frac))
1113          oxyc=(oxyc-mfuel(ny)*x+frac*oxys/cs)/(1.d0+frac/cc)
1114          if(oxys.lt.0.d0) oxys=0.d0
1115          if(oxyc.lt.0.d0) oxyc=0.d0
1116          oxyclc=oxys+oxyc
1117          conc(ny)=oxyc/cc
1118          conc(2*ny)=oxys/cs
1119
1120      c Calculate the partial pressure of O2 in each cell

```

```

1121
1122     press2(1)=po2
1123     presc2(1)=po2
1124     press2(2)=conc(ncell)*po2/con0
1125     presc2(2)=press2(2)
1126
1127     do i=3,ny+2
1128         presc2(i)=conc(i-2)*po2/con0
1129         press2(i)=conc(ny+i-2)*po2/con0
1130     enddo
1131
1132     return
1133     end
1134
1135 c***** subroutine htrans *****
1136     subroutine htrans(ncell,nycell,eps,per,rf2,recirc,ult)
1137 c Subroutine to calculate the temperature profile given the partial
1138 c pressure of oxygen profile and heat release distribution.
1139 c To aid convergence, the particle convective term entering the riser
1140 c is set to equal the term leaving the riser.
1141 c
1142 c Variables are:
1143 c
1144 c a,b,c,r  Entries in the tridiagonal matrix
1145 c cg      Heat capacity of the gas (J/kgK)
1146 c cp      Heat capacity of the particles (J/kgK)
1147 c deng    Density of the gas (kg/m3)
1148 c emiss   Emissivity
1149 c f        Fraction of the wall covered by membrane
1150 c fx      Matrix of mass flux in the radial direction (kg/m2s)
1151 c fyn     Matrix of mass flux in the north direction (kg/m2s)
1152 c fys     Matrix of mass flux in the south direction (kg/m2s)
1153 c g        Matrix of source term for each cell (W)
1154 c heatev  Heat of evaporation of water at 25 C (J/kg)
1155 c sbc     Stefan-Boltzmann constant (W/m2K4)
1156 c t        Temperature matrix for present iteration
1157 c to      Temperature matrix for previous iteration
1158 c u        Solution vector from subroutine tridag
1159 c*****
1160     implicit real*8(a-h,o-z)
1161     real*8 k
1162     common/blka/acell(300),o2feed,x,fuel,uc,us
1163     common/blkb/cycv,npart,dt(300),pmatt(300),
1164     1 pmat1(300),rc,volf,valh,rt,distv(300),siv(20),pdist(20)
1165     common/blkd/heat(300),total,dycell,cross,presc2(300),

```

```

1166      1 press2(300),con0,oxyclc,mcyc,pair
1167      common/blkf/to(5,300),k,at,twall,tair,vg,tref,cp,cg,afeed,fin
1168      common/blkg/flux(300,5),dx(5,300),dy(5,300),f,emiss,denb(300)
1169      common/blkh/acinit,asinit,acfin,asfin
1170      common/blki/areaw(5,300),areae(5,300),arean(5,300),
1171      1 areas(5,300),areat(5,300),effh(300),deng,sbc,const1,
1172      2 effc(300),effr(300),v2,v5,v6,cyc,gcyc
1173      dimension t(5,300),fyn(5,300),fys(5,300),fx(5,300)
1174      dimension a(300),b(300),c(300),r(300),u(300),heat(300)
1175      dimension g(5,300),ult(7)
1176      data heatev/2.44d6/
1177
1178      ny=nycell+3
1179      nx=4
1180
1181      c Convert temperatures from C to K
1182
1183      do i=1,nx
1184          do j=1,ny
1185              to(i,j)=to(i,j)+273.15d0
1186              t(i,j)=to(i,j)
1187          enddo
1188      enddo
1189
1190      c Determine fx, fyn and fys values.
1191
1192      do j=1,ny
1193          do i=1,nx
1194              fx(i,j)=0.d0
1195              fyn(i,j)=0.d0
1196              fys(i,j)=0.d0
1197          enddo
1198      enddo
1199
1200      do j=3,ny-1
1201          fx(3,j)=flux(j-2,2)
1202          fx(2,j)=flux(j-2+nycell,2)
1203      enddo
1204      fx(2,2)=flux(nycell+1,3)*asinit/(dy(2,2)*per)
1205      fx(3,2)=0.d0
1206      do j=4,ny-2
1207          fyn(3,j)=flux(j-2,3)
1208          fys(3,j)=flux(j-3,3)
1209          fys(2,j)=flux(j-2+nycell,3)
1210          fyn(2,j)=flux(j-1+nycell,3)

```

```

1211         enddo
1212         fys(2,3)=flux(nycell+1,3)
1213         fyn(2,3)=flux(nycell+2,3)
1214         fyn(2,2)=flux(nycell+1,3)
1215         fyn(3,3)=flux(1,3)
1216         fys(3,3)=flux(ncell,3)
1217         fyn(3,2)=flux(ncell,3)
1218         fys(3,2)=(recirc+fuel)/acinit
1219         fyn(3,ny-1)=flux(nycell,3)
1220         fys(3,ny-1)=flux(nycell-1,3)
1221         fys(2,ny-1)=flux(ncell-1,3)
1222         fyn(2,ny-1)=flux(nycell,3)*acfin*rc/asfin
1223
1224     c Calculate heat generation term (W), subtracting the heat loss due
1225     c to the evaporation of water at (25 C).
1226
1227         g(2,2)=heat(ncell)*(fuel*valh*1000.d0-
1228     1   (fuel*ult(2)+fuel*ult(4)/2.d0*18.d0)/100.d0*heatev)*asinit/at
1229         g(3,2)=heat(ncell)*(fuel*valh*1000.d0-
1230     1   (fuel*ult(2)+fuel*ult(4)/2.d0*18.d0)/100.d0*heatev)*acinit/at
1231         do j=3,ny-1
1232             g(2,j)=heat(j-2+nycell)*(fuel*valh*1000.d0-
1233     1   (fuel*ult(2)+fuel*ult(4)/2.d0*18.d0)/100.d0*heatev)
1234             g(3,j)=heat(j-2)*(fuel*valh*1000.d0-
1235     1   (fuel*ult(2)+fuel*ult(4)/2.d0*18.d0)/100.d0*heatev)
1236         enddo
1237         gcyc=cyc/total*fuel*valh*1000.d0
1238
1239     c Start N-S sweep
1240
1241         iter=0
1242     10   iter=iter+1
1243
1244         do 100 j=2,ny
1245
1246     C Calculate A,B,C and R.
1247
1248         a(1)=0.d0
1249         b(1)=1.d0
1250         c(1)=0.d0
1251         r(1)=twall+273.15d0
1252
1253         if(j.eq.ny) then
1254             do i=2,4
1255                 a(i)=0.d0

```

```

1256             b(i)=1.d0
1257             c(i)=0.d0
1258             r(i)=t(3,j-1)
1259             enddo
1260             goto 50
1261         endif
1262
1263     c Set an upper limit of the heat transfer coefficient to 100.
1264
1265             h=cons1*denb(j)
1266
1267             if(h.ge.100.d0) h=100.d0
1268
1269             i=2
1270             t1=(fx(2,j)*cp+deng*cg*vg)*areae(i,j)
1271             t2=(fx(3,j)*cp+deng*cg*vg)*areae(i,j)
1272             t3=fyn(i,j)*cp*arean(i,j)
1273             t4=deng*cg*us*arean(i,j)
1274             t5=fys(i,j)*cp*areas(i,j)
1275             t6=deng*cg*us*areas(i,j)
1276
1277             ae=-k*areae(i,j)/((dx(i,j)+dx(i+1,j))/2.d0)
1278             an=-k*arean(i,j)/((dy(i,j)+dy(i,j+1))/2.d0)
1279             as=-k*areas(i,j)/((dy(i,j)+dy(i,j-1))/2.d0)
1280             s=-g(i,j)
1281             ap=ae+an+as
1282             a(i)=h*areaw(i,j)+emiss*sbc*areaw(i,j)*to(i-1,j)**3
1283             b(i)=ap-h*areaw(i,j)*arean(i,j)/at-emiss*sbc*areat(i,j)*to(i,j)**3-
1284             1 t1-t4-t5
1285             c(i)=-ae-h*areaw(i,j)*arean(i+1,j)/at+emiss*sbc*areae(i,j)*to(i+1,j)
1286             1 **3+t2
1287             r(i)=an*to(i,j+1)+as*to(i,j-1)+s-emiss*sbc*arean(i,j)*
1288             1 to(i,j+1)**4-emiss*sbc*areas(i,j)*to(i,j-1)**4+
1289             2 (-t1+t2-t4-t5)*(tref+273.15d0)-t3*(to(i,j+1)-(tref+273.15d0))
1290             3 -t6*(to(i,j-1)-(tref+273.15d0))
1291
1292             i=3
1293             t1=(fx(3,j)*cp+deng*cg*vg)*areaw(i,j)
1294             t2=(fx(2,j)*cp+deng*cg*vg)*areaw(i,j)
1295             t3=(fyn(i,j)*cp+deng*cg*uc)*arean(i,j)
1296             t4=(fys(i,j)*cp+deng*cg*uc)*areas(i,j)
1297
1298             aw=-k*areaw(i,j)/((dx(i,j)+dx(i-1,j))/2.d0)
1299             an=-k*arean(i,j)/((dy(i,j)+dy(i,j+1))/2.d0)
1300             as=-k*areas(i,j)/((dy(i,j)+dy(i,j-1))/2.d0)

```

```

1301      s=-g(i,j)
1302      ap=aw+an+as
1303      a(i)=-aw+emiss*sbc*areaw(i,j)*to(i-1,j)**3+t2
1304      b(i)=ap-emiss*sbc*areat(i,j)*to(i,j)**3-t1-t3
1305      c(i)=0.d0
1306      r(i)=an*to(i,j+1)+as*to(i,j-1)+s-emiss*sbc*arean(i,j)*
1307      1      to(i,j+1)**4-emiss*sbc*areas(i,j)*to(i,j-1)**4+
1308      1      (-t1+t2-t3)*(tref+273.15d0)-t4*(to(i,j-1)-(tref+273.15d0))
1309
1310      if(j.eq.2) r(i)=r(i)+gcyc
1311
1312      i=4
1313      aw=1.d0
1314      ap=aw
1315      a(i)=-aw
1316      b(i)=ap
1317      c(i)=0.d0
1318      r(i)=0.d0
1319
1320      50      call tridag(a,b,c,r,u,nx)
1321
1322      do i=1,nx
1323          t(i,j)=u(i)
1324      enddo
1325
1326      c Update temperature solution.
1327
1328      90      do i=1,4
1329          to(i,j)=to(i,j)-rf2*(to(i,j)-t(i,j))
1330      enddo
1331
1332      100     continue
1333
1334      c Calculate the temperature of the cyclone.
1335
1336      tcyc=to(3,ny)+gcyc/(afeed*cg+recirc*cp)
1337
1338      error=0.d0
1339      ermax=0.d0
1340      itab=0
1341      jtab=0
1342      do j=2,ny
1343          do i=1,nx
1344              error=dabs(t(i,j)-to(i,j))/t(i,j)
1345              if(error.gt.erman) then

```

```

1346             ermax=error
1347             itab=i
1348             jtab=j
1349         endif
1350     enddo
1351 enddo
1352 print*, 'i,j,iter,error',itab,jtab,iter,ermax
1353
1354 c Calculate the new mixing temperature.
1355
1356     tmix=(afeed*cg*(tair+273.15d0)+fuel*cp*(tref+273.15d0)+
1357 1     recirc*cp*tcyc)/(afeed*cg+fuel*cp+recirc*cp)
1358     do i=1,4
1359         to(i,1)=tmix
1360     enddo
1361
1362     if(ermax.gt.eps) goto 10
1363
1364 c-----
1365 c Check the energy balance (for debugging purposes).
1366
1367     v1=0.d0
1368     v2=0.d0
1369     v3=0.d0
1370     v4=0.d0
1371
1372     do j=ny-1,2,-1
1373         do i=2,3
1374             gen=g(i,j)
1375             v1=v1+gen
1376             write(7,900) i,j,t(i,j),gen
1377 900         format(i15,2x,i15,2x,f15.4,2x,f15.4)
1378
1379 c Set upper limit of the heat transfer coefficient.
1380
1381             h=const1*denb(j)
1382
1383             if(h.ge.100.d0) h=100.d0
1384
1385             if(i.eq.2) then
1386                 condw=-h*areaw(i,j)*((t(i,j)*arean(i,j)+t(i+1,j)*
1387 1                 arean(i+1,j))/at-t(i-1,j))
1388                 conde=-k*areae(i,j)/((dx(i,j)+dx(i+1,j))/2.d0)*(t(i,j)-t(i+1,j))
1389                 v2=v2+condw
1390             else

```

```

1391          condw=-k*areaw(i,j)/((dx(i,j)+dx(i-1,j))/2.d0)*
1392          (t(i,j)-t(i-1,j))
1393          conde=0.d0
1394      endif
1395      condn=-k*arean(i,j)/((dy(i,j)+dy(i,j+1))/2.d0)*(t(i,j)-to(i,j+1))
1396      conds=-k*areas(i,j)/((dy(i,j)+dy(i,j-1))/2.d0)*(t(i,j)-to(i,j-1))
1397      if(j.eq.ny-1) v3=v3+condn
1398      if(j.eq.2) v4=v4+conds
1399      write(7,910) condw,conde,condn,conds
1400      910      format(4(f15.4,2x))
1401
1402      if(i.eq.2) then
1403          convwp=0.d0
1404          convwg=0.d0
1405          convep=-fx(2,j)*cp*areae(i,j)*(t(i,j)-298.15d0)+
1406          1      fx(3,j)*cp*areae(i,j)*(t(i+1,j)-298.15d0)
1407          conveg=-deng*cg*vg*areae(i,j)*
1408          1      (t(i,j)-298.15d0)+deng*cg*vg*areae(i,j)*(t(i+1,j)-298.15d0)
1409          convnp=fyn(i,j)*cp*arean(i,j)*(to(i,j+1)-298.15d0)
1410          convng=-deng*cg*us*arean(i,j)*(t(i,j)-298.15d0)
1411          convsp=-fys(i,j)*cp*areas(i,j)*(t(i,j)-298.15d0)
1412          convsg=deng*cg*us*areas(i,j)*(to(i,j-1)-298.15d0)
1413          if(j.eq.ny-1) htop=convng+convnp
1414          if(j.eq.2) then
1415              convsg=0.d0
1416              convsp=0.d0
1417          endif
1418      else
1419          convwp=-fx(3,j)*cp*areaw(i,j)*(t(i,j)-298.15d0)+
1420          1      fx(2,j)*cp*areaw(i,j)*(t(i-1,j)-298.15d0)
1421          convwg=-deng*cg*vg*areaw(i,j)*
1422          1      (t(i,j)-298.15d0)+deng*cg*vg*areaw(i,j)*
1423          2      (t(i-1,j)-298.15d0)
1424          convep=0.d0
1425          conveg=0.d0
1426          convnp=-fyn(i,j)*cp*arean(i,j)*(t(i,j)-298.15d0)
1427          convng=-deng*cg*uc*arean(i,j)*(t(i,j)-298.15d0)
1428          convsp=fys(i,j)*cp*areas(i,j)*(to(i,j-1)-298.15d0)
1429          convsg=deng*cg*uc*areas(i,j)*(to(i,j-1)-298.15d0)
1430          if(j.eq.ny-1) htop=htop+convng+convnp
1431          if(j.eq.2) then
1432              convsg=0.d0
1433              convsp=-htop-(v1+v2)+gcyc
1434          endif
1435      endif

```

```

1436      if(j.eq.ny-1) v3=v3+convnp+convng
1437      if(j.eq.2) v4=v4+convsp+convsg
1438      write(7,910) convwp,convvp,convnp,convsp
1439      write(7,910) convwg,conveg,convng,convsg
1440
1441      radw=-emiss*sbc*areaw(i,j)*(to(i,j)**3*t(i,j)-to(i-1,j)**3*t(i-1,j))
1442      radn=-emiss*sbc*arean(i,j)*(to(i,j)**3*t(i,j)-to(i,j+1)**4)
1443      rads=-emiss*sbc*areas(i,j)*(to(i,j)**3*t(i,j)-to(i,j-1)**4)
1444      if(i.eq.2) then
1445          rade=-emiss*sbc*areae(i,j)*(to(i,j)**3*t(i,j)-
1446              to(i+1,j)**3*t(i+1,j))
1447          v2=v2+radw
1448      else
1449          rade=0.d0
1450      endif
1451      if(j.eq.ny-1) v2=v2+radn
1452      if(j.eq.2) v2=v2+rads
1453      write(7,910) radw,rade,radn,rads
1454
1455      if(i.eq.2) then
1456          effc(j)=-condw/areaw(i,j)/(to(i,j)-to(i-1,j))
1457          effr(j)=-radw/areaw(i,j)/(to(i,j)-to(i-1,j))
1458          effh(j)=effc(j)+effr(j)
1459      endif
1460      enddo
1461  enddo
1462
1463      v5=v1+v2+v3+v4
1464      v6=v5/v1*100.d0
1465      print*, v1,v2,v3,v4,v5
1466      write(8,*) 'v1 - v5',v1,v2,v3,v4,v5
1467
1468      print*, 'heat balance % diff. of heat gen. = ',v6
1469      write(8,*) 'heat balance % diff. of heat gen. = ',v6
1470      z1=v1
1471      z2=v2
1472      z3=v3
1473
1474      c-----
1475
1476      c Convert the temperatures back from K to C.
1477
1478      do j=1,ny
1479          do i=1,nx
1480              to(i,j)=to(i,j)-273.15d0

```

```

1481         enddo
1482     enddo
1483     return
1484     end
1485
1486     c***** subroutine tridag*****
1487         subroutine tridag(a,b,c,r,u,n)
1488     c Subroutine to solve a nxn tridiagonal matrix.
1489     c*****
1490
1491         implicit real*8(a-h,o-z)
1492         dimension gam(300),a(300),b(300),c(300),r(300),u(300)
1493         bet=b(1)
1494         u(1)=r(1)/bet
1495
1496     c Decomposition and forward substitution.
1497
1498         do j=2,n
1499             gam(j)=c(j-1)/bet
1500             bet=b(j)-a(j)*gam(j)
1501             u(j)=(r(j)-a(j)*u(j-1))/bet
1502         enddo
1503
1504     c Backsubstitution.
1505
1506         do j=n-1,1,-1
1507             u(j)=u(j)-gam(j+1)*u(j+1)
1508         enddo
1509         return
1510         end
1511
1512     c***** IEEE error handling routine *****
1513         integer function common_handler (sig, sip, uap)
1514         integer sig
1515
1516     c define the structure siginfo, as in < sys/siginfo.h>
1517
1518         structure /fault/
1519             integer address
1520         end structure
1521         structure /siginfo/
1522             integer si_signo
1523             integer si_code
1524             integer si_erno
1525             record /fault/ fault

```

```
1526         end structure
1527         record /siginfo/ sip
1528
1529     c for error codes see p 89 numerical computation guide
1530
1531         write (0,10) sip.si_code, sip.fault.address
1532     10     format('ieee exception ', i1,' occurred at address ', z8 )
1533         end
1534
```

APPENDIX B

SAMPLE INPUT FILES**B.1 HYDRODYNAMIC INPUT FILE LISTING**

COMBUSTOR: Studsvik Prototype
CASE: sh0

20 ---- no. of cells in y-dir
425000 ---- x-sectional area (m2)
0.100000 ---- reflection coeff.
2.607681 ---- perimeter of riser (m)
0.680000 ---- primary zone volume (m3)
107.334949 ---- average bed density (kg/m3)
2.777500 ---- height of start of dev. zone (m)
0.719603 ---- frac. of total air that is primary
849.850000 ---- bed temperature (C)
106.850000 ---- wall temperature (C)

cell#	height(m)	flux out X-dir.	flux out Y-dir.	densities
1	.13	76.6772	238.1944	49.3334
2	.38	46.5892	151.6668	30.4128
3	.63	28.5548	104.8062	20.3644
4	.88	17.6849	78.2123	14.7241
5	1.14	11.0329	62.7280	11.4609
6	1.39	6.9686	53.5793	9.5401
7	1.64	4.5322	48.1274	8.3980
8	1.89	3.0692	44.8620	7.7148
9	2.15	2.1894	42.9003	7.3047
10	2.40	1.6597	41.7035	7.0580
11	2.65	1.3395	40.8774	6.9041
12	2.90	1.3410	40.1386	6.7814
13	3.16	1.3169	39.3816	6.6567
14	3.41	1.2920	38.6006	6.5280
15	3.66	1.2663	37.7956	6.3953
16	3.91	1.2398	36.9665	6.2585
17	4.17	1.2126	36.1136	6.1177
18	4.42	1.1847	35.2373	5.9729
19	4.67	1.1560	34.3383	5.8243
20	4.92	1.1266	33.4162	5.6720
21	.13	12.1690	1247.4000	1134.0000

22	.38	7.6581	1247.4000	1134.0000
23	.63	5.0597	1247.4000	1134.0000
24	.88	3.5054	1247.4000	1134.0000
25	1.14	2.4755	1247.4000	1134.0000
26	1.39	1.8042	1247.4000	1134.0000
27	1.64	1.4154	1247.4000	1134.0000
28	1.89	1.1882	1247.4000	1134.0000
29	2.15	1.0542	1247.4000	1134.0000
30	2.40	.9746	1247.4000	1134.0000
31	2.65	.9262	1247.4000	1134.0000
32	2.90	.8862	1247.4000	1134.0000
33	3.16	.8467	1247.4000	1134.0000
34	3.41	.8063	1247.4000	1134.0000
35	3.66	.7650	1247.4000	1134.0000
36	3.91	.7229	1247.4000	1134.0000
37	4.17	.6801	1247.4000	1134.0000
38	4.42	.6367	1247.4000	1134.0000
39	4.67	.5929	1247.4000	1134.0000
40	4.92	.5489	1247.4000	1134.0000
41	.00	.0000	369.1127	316.9441

height (m)	Aa (m2)
.00	.089157
.13	.072131
.38	.044831
.63	.028355
.88	.018412
1.14	.012411
1.39	.008790
1.64	.006604
1.89	.005285
2.15	.004489
2.40	.004009
2.65	.003708
2.90	.003469
3.16	.003225
3.41	.002972
3.66	.002712
3.91	.002444
4.17	.002167
4.42	.001882
4.67	.001589
4.92	.001288

5.05 .001136

Particle Physical Properties and Composition

Fuel	Weight %
12.200	ash
15.200	moisture
.170	sulphur
3.050	hydrogen
52.900	carbon
.680	nitrogen
15.800	oxygen
40.000	% volatiles yield
1400.000	particle density (kg/m ³)
7.122	mean core gas velocity (m/s)
3.567	mean streamer gas velocity (m/s)
6.95850	superficial gas velocity (m/s)
30.00000	solids recirc. flux (kg/m ² s)
.07921	thermal conductivity of gas
.85000	particle radiation emissivity

Particle Sieve Sizing

mm	wt%
7.925	9.250
5.613	10.920
3.962	13.180
2.794	12.110
1.981	11.090
1.397	8.730
.991	7.750
.701	5.480
.495	4.750
.351	3.740
.246	3.410
.175	3.990
.124	1.290
.088	.000
.053	.000
.045	.000
.038	.000
.000	.000

B.2 USER INPUT FILE LISTING**INPUT FILE FOR HEAT.F****Constants Used With the Devolatilization Rate Equation**

11.8	706.0	bituminous coal
24000.0		higher heating value (kJ/kg)
100		number of particles in the Monte Carlo method
0.1		frac. of particles that exit a cell within dt
1		number of feed points
0.001		tolerance for partial pressure of O ₂ (atm)
1.0		tolerance for bed temperature (C)
0.01		convergence tolerance in subroutine heat
0.7		relaxation factor in subroutine heat
0.7		relaxation factor for partial pressure of O ₂
0.1		mass transfer crossflow coefficient
0.3		volatile transfer fraction
0.3		residence time in the cyclone (sec.)
0.2		excess air
1.0		combustion efficiency
900.0		particle surface temperature (C)
25.0		temperature of inlet air (C)
25.0		reference temperature (C)
1.0		const. in wall convective heat transfer coeff. term

APPENDIX C
OUTPUT FILES

CFB HEAT RELEASE AND HEAT TRANSFER MODEL

RUN RESULTS FROM HEAT TRANSFER ROUTINE HEAT.F, VERSION 8.1
 WRITTEN BY: DALE W.C. JU

COMBUSTOR: Studsvik Prototype

CASE: Sardinian Coal

Case : sh0 (base case)

Superficial gas velocity = 6.96 m/s

Solids recirculation rate = 30 kg/m²s

Highvale coal(mean dp = 2.89 mm)

FUEL PHYSICAL PROPERTIES AND COMPOSITION**PROXIMATE ANALYSIS**

Weight %

12.200	Ash
15.200	Moisture
0.170	Sulphur
3.050	Hydrogen
52.900	Carbon
0.680	Nitrogen
15.800	Oxygen

PARTICLE SIZE DISTRIBUTION

mm	wt %
7.925	9.250
5.613	10.920
3.962	13.180
2.794	12.110
1.981	11.090
1.397	8.730
0.991	7.750
0.701	5.480
0.495	4.750
0.351	3.740
0.246	3.410
0.175	3.990
0.124	1.290
0.088	0.000
0.053	0.000
0.045	0.000
0.038	0.000
0.000	0.000

COMBUSTION CONDITIONS

# of particles in Monte Carlo Method	100
% of total wall area with membranes	70.0 %
Solids return temp. equals cyclone temp.	858.6 C
Solids recirculation rate	12.750 kg/s
Solids recirculation flux	30.000 kg/m ² s
Gas cross-flow coefficient	0.100 m/s
Combustion efficiency	100.0 %
Excess air	20.000 %
Volatile transfer fraction	0.300
Number of fuel feed points	1
Fuel feedrate	395.687 kg/hr
Air feedrate	3070.295 kg/hr
% of total air that is primary	72.0 %
Residence time of particles in cyclone	0.300 sec.
Reflection coefficient	0.100
Height at which developed zone begins	2.777 m

GAS VELOCITIES

Core interstitial gas velocity	7.122 m/s
Streamer interstitial gas velocity	3.567 m/s
Superficial gas velocity	6.958 m/s
Bed temperature used in calculating heat transfer area and gas velocities	849.9 C

HEAT RELEASE DISTRIBUTION

Height (m)	Fraction of Total Heat Release			
	Volatiles		Char	
	Streamer	Core	Streamer	Core
0.00		0.337328	0.464242	
0.13	0.001086	0.077952	0.017981	0.007278
0.38	0.003157	0.017585	0.009128	0.004215
0.63	0.000082	0.004516	0.006292	0.002686
0.88	0.000003	0.001274	0.004353	0.001962
1.14	0.000000	0.000414	0.003025	0.001509
1.39	0.000004	0.000233	0.002080	0.001248
1.64	0.000001	0.000448	0.001675	0.001108
1.89	0.000007	0.000271	0.001341	0.001003
2.15	0.000001	0.000200	0.001087	0.000910
2.40	0.000000	0.000257	0.000996	0.000883
2.65	0.000000	0.000123	0.000947	0.000874
2.90	0.000000	0.000076	0.000874	0.000818
3.16	0.000000	0.000039	0.000898	0.000825
3.41	0.000000	0.000063	0.000825	0.000822
3.66	0.000000	0.000079	0.000860	0.000781
3.91	0.000000	0.000027	0.000751	0.000779
4.17	0.000000	0.000017	0.000686	0.000754
4.42	0.000000	0.000007	0.000564	0.000716
4.67	0.000000	0.000007	0.000491	0.000709
4.92	0.000000	0.000051	0.000364	0.000670
Cyclone		0.000037	0.004644	
TOTAL		0.502019	0.497981	

OXYGEN PARTIAL PRESSURE DISTRIBUTION

Height (m)	Partial Pressure of Oxygen (atm.)	
	Streamer	Core
0.00	0.068524	
0.26	0.031904	0.053800
0.51	0.018193	0.046472
0.76	0.012646	0.043154
1.00	0.011824	0.041219
1.26	0.015730	0.039964
1.51	0.021778	0.039116
1.76	0.025567	0.038457
2.01	0.027828	0.037964
2.27	0.029310	0.037572
2.52	0.029630	0.037212
2.77	0.029585	0.036890
3.02	0.029795	0.036598
3.29	0.029436	0.036308
3.54	0.029658	0.036025
3.79	0.029217	0.035742
4.04	0.029720	0.035482
4.29	0.030067	0.035238
4.54	0.030834	0.035020
4.79	0.031302	0.034815
5.04	0.032164	0.034630

Pressure convergence tolerance	0.0040 atm.
Partial pressure of oxygen entering	0.210000 atm.
Partial pressure of oxygen leaving riser	0.035 atm.
Partial pressure of oxygen leaving cyclone	0.034 atm.

TEMPERATURE DISTRIBUTION

Height (m)	Temperature (C)	
	Streamer	Core
0.00	889.4	
0.13	883.8	891.4
0.38	833.4	888.0
0.63	830.3	884.5
0.88	827.6	881.0
1.14	825.1	877.8
1.39	822.9	875.0
1.64	821.1	872.5
1.89	819.8	870.2
2.15	818.7	868.1
2.40	817.9	866.3
2.65	820.9	864.5
2.90	823.9	862.8
3.16	826.9	861.4
3.41	827.3	860.2
3.66	828.4	859.0
3.91	830.4	858.0
4.17	834.2	857.2
4.42	841.1	856.7
4.67	853.3	856.7
4.92	876.3	857.4

Solids return temperature	858.6 C
Temperature convergence tolerance	0.004 C
Cyclone temperature	858.6 C
Wall temperature	106.8 C

HEAT TRANSFER COEFFICIENTS

Height (m)	Density (kg/m ³)	Core Temp. (C)	Heat Transfer Coefficient (W/m ² C)		
			Radiative	Convective	Overall
0.00	316.944	889.4	110.3	100.5	210.8
0.13	233.423	891.4	109.9	100.8	210.7
0.38	146.824	888.0	98.1	106.9	205.0
0.63	94.664	884.5	97.4	101.4	198.7
0.88	63.214	881.0	96.8	67.7	164.5
1.14	44.242	877.8	96.2	47.4	143.6
1.39	32.797	875.0	95.7	35.1	130.9
1.64	25.889	872.5	95.3	27.7	123.1
1.89	21.720	870.2	95.0	23.2	118.3
2.15	19.205	868.1	94.8	20.5	115.3
2.40	17.688	866.3	94.6	18.9	113.5
2.65	16.738	864.5	94.8	17.8	112.6
2.90	15.982	862.8	96.6	16.8	113.4
3.16	15.211	861.4	96.6	15.9	112.6
3.41	14.412	860.2	96.7	15.1	111.8
3.66	13.591	859.0	97.0	14.2	111.1
3.91	12.744	858.0	97.4	13.2	110.6
4.17	11.869	857.2	98.3	12.2	110.5
4.42	10.968	856.7	99.8	11.2	111.0
4.67	10.042	856.7	102.6	10.1	112.7
4.92	9.091	857.4	108.0	8.9	116.9

CFB HEAT RELEASE AND HEAT TRANSFER MODEL

RUN RESULTS FROM HEAT TRANSFER ROUTINE HEAT.F, VERSION 8.1
 WRITTEN BY: DALE W.C. JU

COMBUSTOR: Studsvik Prototype

CASE: Sardinian Coal

Case : sh1

Superficial gas velocity = 6.96 m/s

Solids recirculation rate = 50 kg/m²s

Highvale coal(mean dp = 2.89 mm)

FUEL PHYSICAL PROPERTIES AND COMPOSITION**PROXIMATE ANALYSIS**

Weight %

12.200	Ash
15.200	Moisture
0.170	Sulphur
3.050	Hydrogen
52.900	Carbon
0.680	Nitrogen
15.800	Oxygen

PARTICLE SIZE DISTRIBUTION

mm	wt %
7.925	9.250
5.613	10.920
3.962	13.180
2.794	12.110
1.981	11.090
1.397	8.730
0.991	7.750
0.701	5.480
0.495	4.750
0.351	3.740
0.246	3.410
0.175	3.990
0.124	1.290
0.088	0.000
0.053	0.000
0.045	0.000
0.038	0.000
0.000	0.000

COMBUSTION CONDITIONS

# of particles in Monte Carlo Method	100
% of total wall area with membranes	70.0 %
Solids return temp. equals cyclone temp.	835.1 C
Solids recirculation rate	21.250 kg/s
Solids recirculation flux	50.000 kg/m ² s
Gas cross-flow coefficient	0.100 m/s
Combustion efficiency	100.0 %
Excess air	20.000 %
Volatile transfer fraction	0.300
Number of fuel feed points	1
Fuel feedrate	388.886 kg/hr
Air feedrate	3017.519 kg/hr
% of total air that is primary	72.0 %
Residence time of particles in cyclone	0.300 sec.
Reflection coefficient	0.100
Height at which developed zone begins	2.525 m

GAS VELOCITIES

Core interstitial gas velocity	7.187 m/s
Streamer interstitial gas velocity	3.600 m/s
Superficial gas velocity	6.958 m/s
Bed temperature used in calculating heat transfer area and gas velocities	849.9 C

HEAT RELEASE DISTRIBUTION

Height (m)	Fraction of Total Heat Release			
	Volatiles		Char	
	Streamer	Core	Streamer	Core
0.00		0.330548		0.451193
0.13	0.008532	0.072786	0.022746	0.007294
0.38	0.001237	0.016510	0.012063	0.004265
0.63	0.004695	0.005423	0.006954	0.002901
0.88	0.000078	0.001387	0.004356	0.002131
1.14	0.000033	0.000365	0.002992	0.001742
1.39	0.000000	0.000267	0.002187	0.001434
1.64	0.000010	0.000123	0.001822	0.001301
1.89	0.000000	0.000287	0.001637	0.001168
2.15	0.000000	0.000080	0.001444	0.001182
2.40	0.000000	0.000029	0.001286	0.001070
2.65	0.000000	0.000027	0.001289	0.001105
2.90	0.000000	0.000054	0.001260	0.001052
3.16	0.000000	0.000017	0.001123	0.001092
3.41	0.000000	0.000013	0.001082	0.000990
3.66	0.000000	0.000005	0.000949	0.000990
3.91	0.000000	0.000036	0.000831	0.000929
4.17	0.000000	0.000022	0.000781	0.000890
4.42	0.000000	0.000006	0.000678	0.000875
4.67	0.000000	0.000005	0.000565	0.000847
4.92	0.000000	0.000006	0.000489	0.000803
Cyclone		0.000012		0.005618
TOTAL		0.497612		0.502388

OXYGEN PARTIAL PRESSURE DISTRIBUTION

Height (m)	Partial Pressure of Oxygen (atm.)	
	Streamer	Core
0.00	0.072215	
0.26	0.023893	0.057783
0.51	0.012219	0.049493
0.76	0.000000	0.045156
1.00	0.002534	0.042749
1.26	0.010056	0.041216
1.51	0.018399	0.040186
1.76	0.023755	0.039461
2.01	0.026177	0.038872
2.27	0.027334	0.038395
2.52	0.028038	0.037992
2.77	0.027895	0.037594
3.02	0.027771	0.037204
3.29	0.028304	0.036830
3.54	0.028480	0.036482
3.79	0.029135	0.036152
4.04	0.029855	0.035846
4.29	0.030160	0.035557
4.54	0.030736	0.035289
4.79	0.031467	0.035042
5.04	0.031969	0.034815

Pressure convergence tolerance	0.0039 atm.
Partial pressure of oxygen entering	0.210000 atm.
Partial pressure of oxygen leaving riser	0.035 atm.
Partial pressure of oxygen leaving cyclone	0.034 atm.

TEMPERATURE DISTRIBUTION

Height (m)	Temperature (C)	
	Streamer	Core
0.00	854.0	
0.13	849.5	855.4
0.38	803.1	852.4
0.63	802.2	849.6
0.88	801.8	846.9
1.14	802.5	844.5
1.39	804.0	842.6
1.64	806.1	841.0
1.89	808.6	839.7
2.15	811.2	838.8
2.40	812.6	837.9
2.65	814.0	837.1
2.90	815.4	836.4
3.16	815.6	835.7
3.41	816.2	835.1
3.66	817.3	834.6
3.91	819.2	834.2
4.17	822.2	833.9
4.42	827.2	833.8
4.67	835.5	833.9
4.92	850.3	834.4

Solids return temperature	835.1 C
Temperature convergence tolerance	0.004 C
Cyclone temperature	835.1 C
Wall temperature	106.8 C

HEAT TRANSFER COEFFICIENTS

Height (m)	Density (kg/m ³)	Core Temp. (C)	Heat Transfer Coefficient (W/m ² C)		
			Radiative	Convective	Overall
0.00	383.621	854.0	102.3	100.3	202.6
0.13	288.739	855.4	101.7	100.6	202.4
0.38	185.084	852.4	91.4	106.3	197.7
0.63	122.702	849.6	91.2	106.3	197.6
0.88	85.097	846.9	91.2	90.3	181.5
1.14	62.419	844.5	91.3	66.1	157.4
1.39	48.736	842.6	91.6	51.4	143.0
1.64	40.479	841.0	92.1	42.5	134.5
1.89	35.495	839.7	92.6	37.0	129.7
2.15	32.488	838.8	93.2	33.7	126.9
2.40	30.757	837.9	93.4	31.8	125.3
2.65	29.504	837.1	94.2	30.4	124.6
2.90	28.167	836.4	94.1	29.0	123.1
3.16	26.773	835.7	94.1	27.5	121.7
3.41	25.316	835.1	94.3	26.0	120.2
3.66	23.795	834.6	94.5	24.4	118.9
3.91	22.212	834.2	94.9	22.7	117.6
4.17	20.559	833.9	95.6	20.9	116.5
4.42	18.840	833.8	96.7	19.0	115.7
4.67	17.052	833.9	98.5	17.0	115.6
4.92	15.196	834.4	101.9	14.9	116.8

CFB HEAT RELEASE AND HEAT TRANSFER MODEL

RUN RESULTS FROM HEAT TRANSFER ROUTINE HEAT.F, VERSION 8.1
 WRITTEN BY: DALE W.C. JU

COMBUSTOR: Studsvik Prototype

CASE: Sardinian Coal

Case : sh2

Superficial gas velocity = 6.96 m/s

Solids recirculation rate = 15 kg/m²s

Highvale coal(mean dp = 2.89 mm)

FUEL PHYSICAL PROPERTIES AND COMPOSITION**PROXIMATE ANALYSIS**

Weight %

12.200	Ash
15.200	Moisture
0.170	Sulphur
3.050	Hydrogen
52.900	Carbon
0.680	Nitrogen
15.800	Oxygen

PARTICLE SIZE DISTRIBUTION

mm	wt %
7.925	9.250
5.613	10.920
3.962	13.180
2.794	12.110
1.981	11.090
1.397	8.730
0.991	7.750
0.701	5.480
0.495	4.750
0.351	3.740
0.246	3.410
0.175	3.990
0.124	1.290
0.088	0.000
0.053	0.000
0.045	0.000
0.038	0.000
0.000	0.000

COMBUSTION CONDITIONS

# of particles in Monte Carlo Method	100
% of total wall area with membranes	70.0 %
Solids return temp. equals cyclone temp.	897.8 C
Solids recirculation rate	6.375 kg/s
Solids recirculation flux	15.000 kg/m ² s
Gas cross-flow coefficient	0.100 m/s
Combustion efficiency	100.0 %
Excess air	20.000 %
Volatile transfer fraction	0.300
Number of fuel feed points	1
Fuel feedrate	403.300 kg/hr
Air feedrate	3129.367 kg/hr
% of total air that is primary	72.0 %
Residence time of particles in cyclone	0.300 sec.
Reflection coefficient	0.100
Height at which developed zone begins	3.283 m

GAS VELOCITIES

Core interstitial gas velocity	7.064 m/s
Streamer interstitial gas velocity	3.536 m/s
Superficial gas velocity	6.958 m/s
Bed temperature used in calculating heat transfer area and gas velocities	849.9 C

HEAT RELEASE DISTRIBUTION

Height (m)	Fraction of Total Heat Release			
	Volatiles		Char	
	Streamer	Core	Streamer	Core
0.00		0.368394	0.466610	
0.13	0.001269	0.078107	0.013888	0.006876
0.38	0.000458	0.017016	0.004697	0.003829
0.63	0.000093	0.004032	0.001244	0.002424
0.88	0.000300	0.001880	0.002026	0.001628
1.14	0.001258	0.000603	0.001626	0.001121
1.39	0.000767	0.000655	0.001453	0.000861
1.64	0.000000	0.000138	0.001174	0.000704
1.89	0.000000	0.000029	0.000887	0.000586
2.15	0.000000	0.000006	0.000704	0.000569
2.40	0.000000	0.000001	0.000578	0.000531
2.65	0.000000	0.000000	0.000482	0.000497
2.90	0.000000	0.000000	0.000427	0.000482
3.16	0.000000	0.000000	0.000402	0.000471
3.41	0.000000	0.000000	0.000394	0.000451
3.66	0.000000	0.000000	0.000375	0.000466
3.91	0.000000	0.000000	0.000358	0.000451
4.17	0.000000	0.000000	0.000272	0.000433
4.42	0.000000	0.000000	0.000236	0.000428
4.67	0.000000	0.000000	0.000252	0.000440
4.92	0.000000	0.000000	0.000199	0.000413
Cyclone		0.000000	0.003048	
TOTAL		0.535547	0.464453	

OXYGEN PARTIAL PRESSURE DISTRIBUTION

Height (m)	Partial Pressure of Oxygen (atm.)	
	Streamer	Core
0.00	0.064113	
0.26	0.024916	0.048143
0.51	0.024727	0.042146
0.76	0.034367	0.039890
1.00	0.033023	0.038603
1.26	0.024529	0.037719
1.51	0.022326	0.036985
1.76	0.027596	0.036556
2.01	0.029910	0.036262
2.27	0.030934	0.036028
2.52	0.031514	0.035833
2.77	0.031949	0.035666
3.02	0.032133	0.035514
3.29	0.032136	0.035370
3.54	0.032060	0.035230
3.79	0.032083	0.035092
4.04	0.032094	0.034959
4.29	0.032669	0.034841
4.54	0.032881	0.034731
4.79	0.032650	0.034617
5.04	0.032975	0.034515

Pressure convergence tolerance	0.0020 atm.
Partial pressure of oxygen entering	0.210000 atm.
Partial pressure of oxygen leaving riser	0.035 atm.
Partial pressure of oxygen leaving cyclone	0.034 atm.

TEMPERATURE DISTRIBUTION

Height (m)	Temperature (C)	
	Streamer	Core
0.00	960.6	
0.13	954.2	963.3
0.38	897.2	959.3
0.63	892.0	954.8
0.88	886.8	950.2
1.14	881.2	945.9
1.39	875.4	941.6
1.64	869.3	937.4
1.89	863.3	933.2
2.15	857.8	929.0
2.40	852.8	924.7
2.65	848.5	920.5
2.90	845.4	916.7
3.16	844.4	912.7
3.41	843.5	908.8
3.66	842.5	905.2
3.91	842.7	901.9
4.17	845.6	898.9
4.42	853.5	896.5
4.67	871.4	895.2
4.92	910.2	896.2

Solids return temperature	897.8 C
Temperature convergence tolerance	0.002 C
Cyclone temperature	897.8 C
Wall temperature	106.8 C

HEAT TRANSFER COEFFICIENTS

Height (m)	Density (kg/m ³)	Core Temp. (C)	Heat Transfer Coefficient (W/m ² C)		
			Radiative	Convective	Overall
0.00	244.887	960.6	127.9	100.7	228.7
0.13	176.105	963.3	127.9	101.0	228.8
0.38	108.381	959.3	113.1	107.4	220.5
0.63	67.562	954.8	111.8	72.8	184.6
0.88	42.946	950.2	110.6	46.4	156.9
1.14	28.095	945.9	109.2	30.4	139.6
1.39	19.131	941.6	107.8	20.8	128.6
1.64	13.725	937.4	106.4	14.9	121.3
1.89	10.462	933.2	104.9	11.4	116.4
2.15	8.491	929.0	103.6	9.3	112.9
2.40	7.304	924.7	102.5	8.0	110.5
2.65	6.586	920.5	101.5	7.2	108.7
2.90	6.153	916.7	100.8	6.7	107.5
3.16	5.899	912.7	100.2	6.5	106.6
3.41	5.709	908.8	100.7	6.2	106.9
3.66	5.503	905.2	100.1	6.0	106.1
3.91	5.295	901.9	100.2	5.7	105.9
4.17	5.083	898.9	100.8	5.4	106.3
4.42	4.871	896.5	102.6	5.2	107.8
4.67	4.656	895.2	106.9	4.8	111.7
4.92	4.440	896.2	116.4	4.4	120.7

CFB HEAT RELEASE AND HEAT TRANSFER MODEL

RUN RESULTS FROM HEAT TRANSFER ROUTINE HEAT.F, VERSION 8.1
 WRITTEN BY: DALE W.C. JU

COMBUSTOR: Studsvik Prototype

CASE: Sardinian Coal

Case : sh3

Superficial gas velocity = 5.99 m/s

Solids recirculation rate = 30 kg/m²s

Highvale coal(mean dp = 2.89 mm)

FUEL PHYSICAL PROPERTIES AND COMPOSITION**PROXIMATE ANALYSIS**

Weight %

12.200	Ash
15.200	Moisture
0.170	Sulphur
3.050	Hydrogen
52.900	Carbon
0.680	Nitrogen
15.800	Oxygen

PARTICLE SIZE DISTRIBUTION

mm	wt %
7.925	9.250
5.613	10.920
3.962	13.180
2.794	12.110
1.981	11.090
1.397	8.730
0.991	7.750
0.701	5.480
0.495	4.750
0.351	3.740
0.246	3.410
0.175	3.990
0.124	1.290
0.088	0.000
0.053	0.000
0.045	0.000
0.038	0.000
0.000	0.000

COMBUSTION CONDITIONS

# of particles in Monte Carlo Method	100
% of total wall area with membranes	70.0 %
Solids return temp. equals cyclone temp.	812.3 C
Solids recirculation rate	12.750 kg/s
Solids recirculation flux	30.000 kg/m ² s
Gas cross-flow coefficient	0.100 m/s
Combustion efficiency	100.0 %
Excess air	20.000 %
Volatile transfer fraction	0.300
Number of fuel feed points	1
Fuel feedrate	340.730 kg/hr
Air feedrate	2643.858 kg/hr
% of total air that is primary	72.0 %
Residence time of particles in cyclone	0.300 sec.
Reflection coefficient	0.100
Height at which developed zone begins	2.525 m

GAS VELOCITIES

Core interstitial gas velocity	6.147 m/s
Streamer interstitial gas velocity	3.077 m/s
Superficial gas velocity	5.992 m/s
Bed temperature used in calculating heat transfer area and gas velocities	849.9 C

HEAT RELEASE DISTRIBUTION

Height (m)	Fraction of Total Heat Release			
	Volatiles		Char	
	Streamer	Core	Streamer	Core
0.00		0.258625	0.534937	
0.13	0.006435	0.060164	0.025247	0.009468
0.38	0.000144	0.012962	0.014644	0.005495
0.63	0.000058	0.002760	0.009723	0.003660
0.88	0.000027	0.000635	0.006133	0.002588
1.14	0.000002	0.000137	0.004100	0.002051
1.39	0.000000	0.000031	0.002707	0.001709
1.64	0.000001	0.000013	0.002032	0.001462
1.89	0.000000	0.000003	0.001593	0.001332
2.15	0.000000	0.000001	0.001429	0.001263
2.40	0.000000	0.000000	0.001335	0.001217
2.65	0.000000	0.000000	0.001232	0.001170
2.90	0.000000	0.000000	0.001201	0.001126
3.16	0.000000	0.000000	0.001078	0.001083
3.41	0.000000	0.000000	0.001027	0.001080
3.66	0.000000	0.000000	0.000939	0.001031
3.91	0.000000	0.000000	0.000818	0.000989
4.17	0.000000	0.000000	0.000755	0.000988
4.42	0.000000	0.000000	0.000629	0.000936
4.67	0.000000	0.000000	0.000528	0.000868
4.92	0.000000	0.000000	0.000459	0.000893
Cyclone		0.000000	0.005050	
TOTAL		0.385113	0.614887	

OXYGEN PARTIAL PRESSURE DISTRIBUTION

Height (m)	Partial Pressure of Oxygen (atm.)	
	Streamer	Core
0.00	0.070199	
0.26	0.013500	0.057427
0.51	0.000000	0.049735
0.76	0.000000	0.045732
1.00	0.000000	0.043320
1.26	0.007485	0.041694
1.51	0.017631	0.040611
1.76	0.024464	0.039862
2.01	0.028172	0.039301
2.27	0.029309	0.038829
2.52	0.029512	0.038400
2.77	0.029735	0.038000
3.02	0.029642	0.037614
3.29	0.030066	0.037253
3.54	0.030170	0.036901
3.79	0.030455	0.036571
4.04	0.031002	0.036266
4.29	0.031235	0.035972
4.54	0.031846	0.035706
4.79	0.032373	0.035467
5.04	0.032682	0.035236

Pressure convergence tolerance	0.0054 atm.
Partial pressure of oxygen entering	0.210000 atm.
Partial pressure of oxygen leaving riser	0.035 atm.
Partial pressure of oxygen leaving cyclone	0.034 atm.

TEMPERATURE DISTRIBUTION

Height (m)	Temperature (C)	
	Streamer	Core
0.00	837.8	
0.13	832.7	839.3
0.38	786.1	836.2
0.63	784.0	833.0
0.88	782.3	829.8
1.14	781.1	827.0
1.39	780.5	824.5
1.64	780.4	822.4
1.89	780.7	820.5
2.15	781.3	819.0
2.40	783.8	817.6
2.65	786.4	816.2
2.90	788.9	815.1
3.16	788.8	814.1
3.41	789.0	813.2
3.66	789.7	812.3
3.91	791.4	811.6
4.17	794.6	811.1
4.42	800.2	810.8
4.67	810.3	810.8
4.92	830.1	811.5

Solids return temperature	812.3 C
Temperature convergence tolerance	0.005 C
Cyclone temperature	812.3 C
Wall temperature	106.8 C

HEAT TRANSFER COEFFICIENTS

Height (m)	Density (kg/m ³)	Core Temp. (C)	Heat Transfer Coefficient (W/m ² C)		
			Radiative	Convective	Overall
0.00	331.166	837.8	98.3	100.4	198.7
0.13	246.560	839.3	97.9	100.8	198.7
0.38	156.579	836.2	87.9	106.7	194.6
0.63	102.403	833.0	87.4	106.8	194.2
0.88	69.743	829.8	87.1	74.5	161.5
1.14	50.044	827.0	86.8	53.4	140.2
1.39	38.157	824.5	86.7	40.6	127.3
1.64	30.984	822.4	86.7	32.9	119.6
1.89	26.657	820.5	86.7	28.2	114.9
2.15	24.045	819.0	86.8	25.4	112.2
2.40	22.460	817.6	87.0	23.6	110.6
2.65	21.317	816.2	88.2	22.2	110.4
2.90	20.224	815.1	88.4	21.0	109.4
3.16	19.101	814.1	88.4	19.8	108.2
3.41	17.948	813.2	88.4	18.6	107.0
3.66	16.760	812.3	88.6	17.3	105.9
3.91	15.542	811.6	89.0	16.0	105.0
4.17	14.292	811.1	89.6	14.6	104.3
4.42	13.013	810.8	90.8	13.2	104.0
4.67	11.707	810.8	93.0	11.7	104.7
4.92	10.373	811.5	97.3	10.1	107.4

CFB HEAT RELEASE AND HEAT TRANSFER MODEL

RUN RESULTS FROM HEAT TRANSFER ROUTINE HEAT.F, VERSION 8.1
 WRITTEN BY: DALE W.C. JU

COMBUSTOR: Studsvik Prototype

CASE: Sardinian Coal

Case : sh4

Superficial gas velocity = 5.99 m/s

Solids recirculation rate = 50 kg/m²s

Highvale coal(mean dp = 2.89 mm)

FUEL PHYSICAL PROPERTIES AND COMPOSITION**PROXIMATE ANALYSIS**

Weight %

12.200	Ash
15.200	Moisture
0.170	Sulphur
3.050	Hydrogen
52.900	Carbon
0.680	Nitrogen
15.800	Oxygen

PARTICLE SIZE DISTRIBUTION

mm	wt %
7.925	9.250
5.613	10.920
3.962	13.180
2.794	12.110
1.981	11.090
1.397	8.730
0.991	7.750
0.701	5.480
0.495	4.750
0.351	3.740
0.246	3.410
0.175	3.990
0.124	1.290
0.088	0.000
0.053	0.000
0.045	0.000
0.038	0.000
0.000	0.000

COMBUSTION CONDITIONS

# of particles in Monte Carlo Method	100
% of total wall area with membranes	70.0 %
Solids return temp. equals cyclone temp.	764.4 C
Solids recirculation rate	21.250 kg/s
Solids recirculation flux	50.000 kg/m ² s
Gas cross-flow coefficient	0.100 m/s
Combustion efficiency	100.0 %
Excess air	20.000 %
Volatile transfer fraction	0.300
Number of fuel feed points	1
Fuel feedrate	334.951 kg/hr
Air feedrate	2599.018 kg/hr
% of total air that is primary	72.0 %
Residence time of particles in cyclone	0.300 sec.
Reflection coefficient	0.100
Height at which developed zone begins	2.525 m

GAS VELOCITIES

Core interstitial gas velocity	6.212 m/s
Streamer interstitial gas velocity	3.107 m/s
Superficial gas velocity	5.992 m/s
Bed temperature used in calculating heat transfer area and gas velocities	849.9 C

HEAT RELEASE DISTRIBUTION

Height (m)	Fraction of Total Heat Release Volatiles		Char	
	Streamer	Core	Streamer	Core
0.00		0.257134		0.527291
0.13	0.000530	0.055538	0.026825	0.010168
0.38	0.001910	0.012797	0.015019	0.005935
0.63	0.000014	0.002853	0.009405	0.004031
0.88	0.000013	0.001002	0.006096	0.003002
1.14	0.000003	0.000353	0.004286	0.002480
1.39	0.000113	0.000254	0.003105	0.002090
1.64	0.000001	0.000081	0.002637	0.001927
1.89	0.000000	0.000065	0.002335	0.001734
2.15	0.000004	0.000021	0.002037	0.001652
2.40	0.000004	0.000031	0.001967	0.001618
2.65	0.000003	0.000014	0.001808	0.001501
2.90	0.000004	0.000008	0.001710	0.001572
3.16	0.000006	0.000007	0.001558	0.001435
3.41	0.000004	0.000018	0.001604	0.001371
3.66	0.000000	0.000005	0.001320	0.001343
3.91	0.000001	0.000002	0.001180	0.001287
4.17	0.000000	0.000001	0.000960	0.001219
4.42	0.000000	0.000000	0.000857	0.001197
4.67	0.000000	0.000000	0.000659	0.001142
4.92	0.000000	0.000000	0.000511	0.001071
Cyclone		0.000001		0.006260
TOTAL		0.375245		0.624755

OXYGEN PARTIAL PRESSURE DISTRIBUTION

Height (m)	Partial Pressure of Oxygen (atm.)	
	Streamer	Core
0.00	0.072593	
0.26	0.031569	0.059943
0.51	0.016184	0.051720
0.76	0.008136	0.047600
1.00	0.006963	0.044969
1.26	0.011088	0.043167
1.51	0.016966	0.041880
1.76	0.021508	0.040922
2.01	0.023921	0.040157
2.27	0.025435	0.039510
2.52	0.025717	0.038910
2.77	0.026202	0.038355
3.02	0.026501	0.037807
3.29	0.027027	0.037303
3.54	0.026612	0.036807
3.79	0.027727	0.036352
4.04	0.028494	0.035931
4.29	0.029672	0.035555
4.54	0.030273	0.035201
4.79	0.031363	0.034886
5.04	0.032257	0.034608

Pressure convergence tolerance	0.0042 atm.
Partial pressure of oxygen entering	0.210000 atm.
Partial pressure of oxygen leaving riser	0.035 atm.
Partial pressure of oxygen leaving cyclone	0.034 atm.

TEMPERATURE DISTRIBUTION

Height (m)	Temperature (C)	
	Streamer	Core
0.00	780.8	
0.13	776.5	781.9
0.38	735.2	779.2
0.63	734.5	776.6
0.88	734.7	774.3
1.14	735.6	772.2
1.39	737.0	770.5
1.64	738.6	769.0
1.89	740.1	767.8
2.15	741.3	767.0
2.40	744.6	766.2
2.65	747.8	765.4
2.90	751.1	764.9
3.16	751.3	764.4
3.41	751.8	764.0
3.66	752.8	763.6
3.91	754.3	763.4
4.17	756.9	763.2
4.42	761.2	763.2
4.67	768.4	763.3
4.92	781.7	763.8

Solids return temperature	764.4 C
Temperature convergence tolerance	0.004 C
Cyclone temperature	764.4 C
Wall temperature	106.8 C

HEAT TRANSFER COEFFICIENTS

Height (m)	Density (kg/m ³)	Core Temp. (C)	Heat Transfer Coefficient (W/m ² C)		
			Radiative	Convective	Overall
0.00	401.087	780.8	86.4	100.3	186.6
0.13	306.273	781.9	85.9	100.7	186.5
0.38	198.719	779.2	77.7	106.2	183.9
0.63	134.022	776.6	77.6	106.2	183.8
0.88	95.034	774.3	77.6	100.7	178.3
1.14	71.518	772.2	77.8	75.5	153.3
1.39	57.334	770.5	78.0	60.3	138.3
1.64	48.776	769.0	78.4	51.1	129.4
1.89	43.612	767.8	78.6	45.5	124.1
2.15	40.494	767.0	78.9	42.1	121.0
2.40	38.535	766.2	79.2	39.9	119.1
2.65	36.836	765.4	81.0	37.6	118.6
2.90	34.966	764.9	80.8	35.7	116.5
3.16	33.027	764.4	80.8	33.7	114.5
3.41	31.010	764.0	80.9	31.6	112.5
3.66	28.918	763.6	81.1	29.4	110.5
3.91	26.748	763.4	81.4	27.1	108.5
4.17	24.498	763.2	81.9	24.7	106.7
4.42	22.173	763.2	82.8	22.2	105.0
4.67	19.766	763.3	84.2	19.6	103.8
4.92	17.282	763.8	86.9	16.8	103.8

CFB HEAT RELEASE AND HEAT TRANSFER MODEL

RUN RESULTS FROM HEAT TRANSFER ROUTINE HEAT.F, VERSION 8.1
 WRITTEN BY: DALE W.C. JU

COMBUSTOR: Studsvik Prototype

CASE: Sardinian Coal

Case : sh5

Superficial gas velocity = 5.99 m/s

Solids recirculation rate = 15 kg/m²s

Highvale coal(mean dp = 2.89 mm)

FUEL PHYSICAL PROPERTIES AND COMPOSITION**PROXIMATE ANALYSIS****Weight %**

12.200	Ash
15.200	Moisture
0.170	Sulphur
3.050	Hydrogen
52.900	Carbon
0.680	Nitrogen
15.800	Oxygen

PARTICLE SIZE DISTRIBUTION

mm	wt %
7.925	9.250
5.613	10.920
3.962	13.180
2.794	12.110
1.981	11.090
1.397	8.730
0.991	7.750
0.701	5.480
0.495	4.750
0.351	3.740
0.246	3.410
0.175	3.990
0.124	1.290
0.088	0.000
0.053	0.000
0.045	0.000
0.038	0.000
0.000	0.000

COMBUSTION CONDITIONS

# of particles in Monte Carlo Method	100
% of total wall area with membranes	70.0 %
Solids return temp. equals cyclone temp.	852.1 C
Solids recirculation rate	6.375 kg/s
Solids recirculation flux	15.000 kg/m ² s
Gas cross-flow coefficient	0.100 m/s
Combustion efficiency	100.0 %
Excess air	20.000 %
Volatile transfer fraction	0.300
Number of fuel feed points	1
Fuel feedrate	347.226 kg/hr
Air feedrate	2694.266 kg/hr
% of total air that is primary	72.0 %
Residence time of particles in cyclone	0.300 sec.
Reflection coefficient	0.100
Height at which developed zone begins	3.030 m

GAS VELOCITIES

Core interstitial gas velocity	6.090 m/s
Streamer interstitial gas velocity	3.049 m/s
Superficial gas velocity	5.992 m/s
Bed temperature used in calculating heat transfer area and gas velocities	849.9 C

HEAT RELEASE DISTRIBUTION

Height (m)	Fraction of Total Heat Release			
	Volatiles		Char	
	Streamer	Core	Streamer	Core
0.00		0.384113		0.449719
0.13	0.000993	0.081644	0.011341	0.007597
0.38	0.001149	0.017436	0.003789	0.004170
0.63	0.000019	0.003700	0.002066	0.002620
0.88	0.000010	0.000954	0.001942	0.001758
1.14	0.000000	0.000240	0.001930	0.001303
1.39	0.000001	0.000103	0.001620	0.001022
1.64	0.000001	0.000047	0.001235	0.000863
1.89	0.000001	0.000034	0.000981	0.000724
2.15	0.000016	0.000018	0.000784	0.000671
2.40	0.000001	0.000027	0.000627	0.000617
2.65	0.000000	0.000006	0.000540	0.000561
2.90	0.000000	0.000001	0.000505	0.000598
3.16	0.000000	0.000000	0.000458	0.000566
3.41	0.000000	0.000000	0.000413	0.000559
3.66	0.000000	0.000000	0.000406	0.000549
3.91	0.000000	0.000000	0.000368	0.000557
4.17	0.000000	0.000000	0.000271	0.000510
4.42	0.000000	0.000000	0.000273	0.000511
4.67	0.000000	0.000000	0.000247	0.000504
4.92	0.000000	0.000000	0.000232	0.000507
Cyclone		0.000000		0.002974
TOTAL		0.553297		0.446703

OXYGEN PARTIAL PRESSURE DISTRIBUTION

Height (m)	Partial Pressure of Oxygen (atm.)	
	Streamer	Core
0.00	0.064817	
0.26	0.032562	0.047682
0.51	0.033750	0.041712
0.76	0.038638	0.039566
1.00	0.037759	0.038501
1.26	0.033150	0.037794
1.51	0.030272	0.037249
1.76	0.030134	0.036829
2.01	0.030661	0.036503
2.27	0.031216	0.036236
2.52	0.031911	0.036014
2.77	0.032211	0.035826
3.02	0.032213	0.035642
3.29	0.032355	0.035472
3.54	0.032526	0.035309
3.79	0.032435	0.035150
4.04	0.032545	0.034995
4.29	0.033092	0.034863
4.54	0.032986	0.034731
4.79	0.033042	0.034605
5.04	0.033026	0.034481

Pressure convergence tolerance	0.0031 atm.
Partial pressure of oxygen entering	0.210000 atm.
Partial pressure of oxygen leaving riser	0.035 atm.
Partial pressure of oxygen leaving cyclone	0.034 atm.

TEMPERATURE DISTRIBUTION

Height (m)	Temperature (C)	
	Streamer	Core
0.00	905.0	
0.13	898.8	907.5
0.38	845.8	903.7
0.63	841.3	899.4
0.88	836.7	895.1
1.14	831.9	891.0
1.39	827.0	887.1
1.64	822.2	883.3
1.89	817.7	879.6
2.15	813.5	876.0
2.40	809.9	872.4
2.65	806.7	869.2
2.90	807.4	865.9
3.16	808.0	862.6
3.41	808.7	859.8
3.66	807.9	857.0
3.91	808.4	854.5
4.17	811.2	852.3
4.42	818.2	850.6
4.67	833.5	849.8
4.92	868.0	850.9

Solids return temperature	852.1 C
Temperature convergence tolerance	0.003 C
Cyclone temperature	852.1 C
Wall temperature	106.8 C

HEAT TRANSFER COEFFICIENTS

Height (m)	Density (kg/m ³)	Core Temp. (C)	Heat Transfer Coefficient (W/m ² C)		
			Radiative	Convective	Overall
0.00	255.628	905.0	113.6	100.7	214.4
0.13	185.093	907.5	113.5	101.0	214.5
0.38	114.618	903.7	100.9	107.3	208.2
0.63	72.151	899.4	99.9	77.6	177.5
0.88	46.542	895.1	98.8	50.2	149.0
1.14	31.091	891.0	97.7	33.6	131.3
1.39	21.771	887.1	96.6	23.6	120.2
1.64	16.146	883.3	95.6	17.5	113.1
1.89	12.750	879.6	94.6	13.9	108.4
2.15	10.701	876.0	93.7	11.6	105.3
2.40	9.465	872.4	92.9	10.3	103.2
2.65	8.721	869.2	92.2	9.5	101.7
2.90	8.264	865.9	91.8	9.0	100.8
3.16	7.896	862.6	93.2	8.5	101.7
3.41	7.504	859.8	92.6	8.0	100.7
3.66	7.106	857.0	92.5	7.6	100.1
3.91	6.708	854.5	92.6	7.1	99.7
4.17	6.304	852.3	93.2	6.7	99.8
4.42	5.902	850.6	94.7	6.2	100.9
4.67	5.495	849.8	98.1	5.6	103.7
4.92	5.090	850.9	106.0	5.0	111.0

CFB HEAT RELEASE AND HEAT TRANSFER MODEL

RUN RESULTS FROM HEAT TRANSFER ROUTINE HEAT.F, VERSION 8.1
 WRITTEN BY: DALE W.C. JU

COMBUSTOR: Studsvik Prototype

CASE: Sardinian Coal

Case : sh2b

Superficial gas velocity = 6.96 m/s

Solids recirculation rate = 15 kg/m²s

Highvale coal (mean dp = 2.89 mm)

of particles in MC method = 400

FUEL PHYSICAL PROPERTIES AND COMPOSITION**PROXIMATE ANALYSIS****Weight %**

12.200	Ash
15.200	Moisture
0.170	Sulphur
3.050	Hydrogen
52.900	Carbon
0.680	Nitrogen
15.800	Oxygen

PARTICLE SIZE DISTRIBUTION

mm	wt %
7.925	9.250
5.613	10.920
3.962	13.180
2.794	12.110
1.981	11.090
1.397	8.730
0.991	7.750
0.701	5.480
0.495	4.750
0.351	3.740
0.246	3.410
0.175	3.990
0.124	1.290
0.088	0.000
0.053	0.000
0.045	0.000
0.038	0.000
0.000	0.000

COMBUSTION CONDITIONS

# of particles in Monte Carlo Method	400
% of total wall area with membranes	70.0 %
Solids return temp. equals cyclone temp.	898.9 C
Solids recirculation rate	6.375 kg/s
Solids recirculation flux	15.000 kg/m ² s
Gas cross-flow coefficient	0.100 m/s
Combustion efficiency	100.0 %
Excess air	20.000 %
Volatile transfer fraction	0.300
Number of fuel feed points	1
Fuel feedrate	403.300 kg/hr
Air feedrate	3129.367 kg/hr
% of total air that is primary	72.0 %
Residence time of particles in cyclone	0.300 sec.
Reflection coefficient	0.100
Height at which developed zone begins	3.283 m

GAS VELOCITIES

Core interstitial gas velocity	7.064 m/s
Streamer interstitial gas velocity	3.536 m/s
Superficial gas velocity	6.958 m/s
Bed temperature used in calculating heat transfer area and gas velocities	849.9 C

HEAT RELEASE DISTRIBUTION

Height (m)	Fraction of Total Heat Release			
	Volatiles		Char	
	Streamer	Core	Streamer	Core
0.00		0.296334		0.554419
0.13	0.000769	0.062872	0.014896	0.008152
0.38	0.000290	0.013703	0.004266	0.004592
0.63	0.000306	0.003105	0.002118	0.002852
0.88	0.000135	0.000735	0.001509	0.001890
1.14	0.000084	0.000309	0.001702	0.001367
1.39	0.000002	0.000141	0.001592	0.001048
1.64	0.000001	0.000063	0.001323	0.000854
1.89	0.000000	0.000032	0.001051	0.000751
2.15	0.000000	0.000020	0.000860	0.000674
2.40	0.000000	0.000012	0.000671	0.000635
2.65	0.000000	0.000006	0.000591	0.000620
2.90	0.000000	0.000002	0.000526	0.000599
3.16	0.000000	0.000003	0.000493	0.000588
3.41	0.000000	0.000001	0.000455	0.000580
3.66	0.000000	0.000001	0.000445	0.000571
3.91	0.000000	0.000000	0.000395	0.000555
4.17	0.000000	0.000000	0.000378	0.000557
4.42	0.000000	0.000000	0.000384	0.000554
4.67	0.000000	0.000000	0.000351	0.000538
4.92	0.000000	0.000000	0.000342	0.000537
Cyclone		0.000001		0.003794
TOTAL		0.427439		0.572561

OXYGEN PARTIAL PRESSURE DISTRIBUTION

Height (m)	Partial Pressure of Oxygen (atm.)	
	Streamer	Core
0.00	0.062086	
0.26	0.021621	0.047834
0.51	0.023283	0.042258
0.76	0.028653	0.039970
1.00	0.033086	0.038825
1.26	0.031379	0.038072
1.51	0.029099	0.037510
1.76	0.028511	0.037075
2.01	0.029260	0.036731
2.27	0.030054	0.036453
2.52	0.031068	0.036223
2.77	0.031391	0.036017
3.02	0.031620	0.035830
3.29	0.031655	0.035652
3.54	0.031780	0.035481
3.79	0.031715	0.035314
4.04	0.031962	0.035158
4.29	0.031970	0.035004
4.54	0.031778	0.034850
4.79	0.031890	0.034703
5.04	0.031827	0.034558

Pressure convergence tolerance	0.0032 atm.
Partial pressure of oxygen entering	0.210000 atm.
Partial pressure of oxygen leaving riser	0.035 atm.
Partial pressure of oxygen leaving cyclone	0.034 atm.

TEMPERATURE DISTRIBUTION

Height (m)	Temperature (C)	
	Streamer	Core
0.00	962.0	
0.13	955.2	964.3
0.38	898.1	960.2
0.63	893.0	955.7
0.88	887.6	951.1
1.14	882.0	946.7
1.39	876.2	942.4
1.64	870.3	938.3
1.89	864.3	934.1
2.15	858.8	929.9
2.40	853.8	925.7
2.65	849.5	921.6
2.90	848.1	917.7
3.16	846.5	913.7
3.41	845.0	909.9
3.66	843.6	906.3
3.91	843.6	903.0
4.17	846.7	900.0
4.42	854.7	897.6
4.67	872.5	896.4
4.92	911.5	897.4

Solids return temperature	898.9 C
Temperature convergence tolerance	0.003 C
Cyclone temperature	898.9 C
Wall temperature	106.8 C

HEAT TRANSFER COEFFICIENTS

Height (m)	Density (kg/m ³)	Core Temp. (C)	Heat Transfer Coefficient (W/m ² C)		
			Radiative	Convective	Overall
0.00	244.887	962.0	128.2	100.8	229.0
0.13	176.105	964.3	128.1	101.0	229.1
0.38	108.381	960.2	113.3	107.4	220.7
0.63	67.562	955.7	112.1	72.7	184.8
0.88	42.946	951.1	110.8	46.3	157.1
1.14	28.095	946.7	109.4	30.4	139.8
1.39	19.131	942.4	108.0	20.8	128.8
1.64	13.725	938.3	106.6	14.9	121.5
1.89	10.462	934.1	105.2	11.4	116.6
2.15	8.491	929.9	103.9	9.3	113.2
2.40	7.304	925.7	102.7	8.0	110.7
2.65	6.586	921.6	101.7	7.2	109.0
2.90	6.153	917.7	101.1	6.7	107.8
3.16	5.899	913.7	100.4	6.5	106.9
3.41	5.709	909.9	100.9	6.2	107.1
3.66	5.503	906.3	100.4	6.0	106.3
3.91	5.295	903.0	100.4	5.7	106.1
4.17	5.083	900.0	101.1	5.4	106.5
4.42	4.871	897.6	102.9	5.2	108.1
4.67	4.656	896.4	107.1	4.8	111.9
4.92	4.440	897.4	116.7	4.4	121.1

CFB HEAT RELEASE AND HEAT TRANSFER MODEL

RUN RESULTS FROM HEAT TRANSFER ROUTINE HEAT.F, VERSION 8.1
 WRITTEN BY: DALE W.C. JU

COMBUSTOR: Studsvik Prototype

CASE: Sardinian Coal

Case : sh700

Superficial gas velocity = 6.96 m/s

Solids recirculation rate = 30 kg/m²s

Highvale coal(mean dp = 2.89 mm)

FUEL PHYSICAL PROPERTIES AND COMPOSITION**PROXIMATE ANALYSIS**

Weight %

12.200	Ash
15.200	Moisture
0.170	Sulphur
3.050	Hydrogen
52.900	Carbon
0.680	Nitrogen
15.800	Oxygen

PARTICLE SIZE DISTRIBUTION

mm	wt %
7.925	9.250
5.613	10.920
3.962	13.180
2.794	12.110
1.981	11.090
1.397	8.730
0.991	7.750
0.701	5.480
0.495	4.750
0.351	3.740
0.246	3.410
0.175	3.990
0.124	1.290
0.088	0.000
0.053	0.000
0.045	0.000
0.038	0.000
0.000	0.000

COMBUSTION CONDITIONS

# of particles in Monte Carlo Method	100
% of total wall area with membranes	70.0 %
Solids return temp. equals cyclone temp.	859.9 C
Solids recirculation rate	12.750 kg/s
Solids recirculation flux	30.000 kg/m ² s
Gas cross-flow coefficient	0.100 m/s
Combustion efficiency	100.0 %
Excess air	20.000 %
Volatile transfer fraction	0.300
Number of fuel feed points	1
Fuel feedrate	395.687 kg/hr
Air feedrate	3070.295 kg/hr
% of total air that is primary	72.0 %
Residence time of particles in cyclone	0.300 sec.
Reflection coefficient	0.100
Height at which developed zone begins	2.777 m

GAS VELOCITIES

Core interstitial gas velocity	7.122 m/s
Streamer interstitial gas velocity	3.567 m/s
Superficial gas velocity	6.958 m/s
Bed temperature used in calculating heat transfer area and gas velocities	849.9 C

HEAT RELEASE DISTRIBUTION

Height (m)	Fraction of Total Heat Release			
	Volatiles		Char	
	Streamer	Core	Streamer	Core
0.00	0.258362		0.566111	
0.13	0.000590	0.055214	0.020026	0.008767
0.38	0.001039	0.013448	0.007124	0.005038
0.63	0.000117	0.003640	0.004689	0.003222
0.88	0.000399	0.001683	0.003693	0.002311
1.14	0.000008	0.001767	0.003065	0.001771
1.39	0.000002	0.000499	0.002469	0.001498
1.64	0.000000	0.000221	0.002033	0.001218
1.89	0.000000	0.000084	0.001562	0.001138
2.15	0.000000	0.000145	0.001418	0.001078
2.40	0.000000	0.000053	0.001351	0.001023
2.65	0.000000	0.000051	0.001158	0.000974
2.90	0.000000	0.000017	0.001013	0.000953
3.16	0.000000	0.000123	0.000976	0.000931
3.41	0.000000	0.000044	0.000852	0.000892
3.66	0.000000	0.000016	0.000808	0.000893
3.91	0.000000	0.000005	0.000753	0.000877
4.17	0.000000	0.000011	0.000636	0.000840
4.42	0.000000	0.000003	0.000645	0.000834
4.67	0.000000	0.000011	0.000479	0.000784
4.92	0.000000	0.000003	0.000433	0.000759
Cyclone	0.000011		0.005340	
TOTAL	0.380679		0.619321	

OXYGEN PARTIAL PRESSURE DISTRIBUTION

Height (m)	Partial Pressure of Oxygen (atm.)	
	Streamer	Core
0.00	0.066418	
0.26	0.025838	0.053535
0.51	0.022029	0.046858
0.76	0.021824	0.043752
1.00	0.020122	0.041830
1.26	0.020567	0.040394
1.51	0.021998	0.039458
1.76	0.023719	0.038775
2.01	0.026167	0.038252
2.27	0.026929	0.037792
2.52	0.026905	0.037386
2.77	0.027740	0.037022
3.02	0.028582	0.036693
3.29	0.028730	0.036359
3.54	0.029381	0.036061
3.79	0.029570	0.035776
4.04	0.029772	0.035505
4.29	0.030455	0.035255
4.54	0.030271	0.035009
4.79	0.031314	0.034793
5.04	0.031600	0.034591

Pressure convergence tolerance	0.0023 atm.
Partial pressure of oxygen entering	0.210000 atm.
Partial pressure of oxygen leaving riser	0.035 atm.
Partial pressure of oxygen leaving cyclone	0.034 atm.

TEMPERATURE DISTRIBUTION

Height (m)	Temperature (C)	
	Streamer	Core
0.00	891.2	
0.13	885.4	892.7
0.38	834.7	889.3
0.63	831.6	885.8
0.88	829.0	882.4
1.14	826.5	879.4
1.39	824.3	876.6
1.64	822.6	874.1
1.89	821.1	871.8
2.15	820.1	869.6
2.40	822.1	867.8
2.65	824.2	866.0
2.90	826.2	864.2
3.16	828.3	862.9
3.41	828.6	861.6
3.66	829.7	860.5
3.91	831.7	859.5
4.17	835.5	858.7
4.42	842.5	858.1
4.67	854.6	858.1
4.92	877.8	858.9

Solids return temperature	859.9 C
Temperature convergence tolerance	0.002 C
Cyclone temperature	859.9 C
Wall temperature	106.8 C

HEAT TRANSFER COEFFICIENTS

Height (m)	Density (kg/m ³)	Core Temp. (C)	Heat Transfer Coefficient (W/m ² C)		
			Radiative	Convective	Overall
0.00	316.944	891.2	110.7	100.5	211.2
0.13	233.423	892.7	110.2	100.8	211.0
0.38	146.824	889.3	98.4	106.8	205.2
0.63	94.664	885.8	97.7	101.3	199.0
0.88	63.214	882.4	97.1	67.7	164.8
1.14	44.242	879.4	96.5	47.4	143.9
1.39	32.797	876.6	96.1	35.1	131.2
1.64	25.889	874.1	95.7	27.7	123.4
1.89	21.720	871.8	95.3	23.2	118.6
2.15	19.205	869.6	95.1	20.5	115.6
2.40	17.688	867.8	95.0	18.9	113.8
2.65	16.738	866.0	95.1	17.8	112.9
2.90	15.982	864.2	96.9	16.8	113.7
3.16	15.211	862.9	96.9	15.9	112.9
3.41	14.412	861.6	97.0	15.1	112.1
3.66	13.591	860.5	97.2	14.2	111.4
3.91	12.744	859.5	97.7	13.2	110.9
4.17	11.869	858.7	98.5	12.2	110.8
4.42	10.968	858.1	100.1	11.2	111.3
4.67	10.042	858.1	102.9	10.1	113.0
4.92	9.091	858.9	108.4	8.9	117.3

CFB HEAT RELEASE AND HEAT TRANSFER MODEL

RUN RESULTS FROM HEAT TRANSFER ROUTINE HEAT.F, VERSION 8.1
 WRITTEN BY: DALE W.C. JU

COMBUSTOR: Studsvik Prototype

CASE: Sardinian Coal

Case : sh900

Superficial gas velocity = 6.96 m/s

Solids recirculation rate = 30 kg/m²s

Highvale coal(mean dp = 2.89 mm)

FUEL PHYSICAL PROPERTIES AND COMPOSITION**PROXIMATE ANALYSIS**

Weight %

12.200	Ash
15.200	Moisture
0.170	Sulphur
3.050	Hydrogen
52.900	Carbon
0.680	Nitrogen
15.800	Oxygen

PARTICLE SIZE DISTRIBUTION

mm	wt %
7.925	9.250
5.613	10.920
3.962	13.180
2.794	12.110
1.981	11.090
1.397	8.730
0.991	7.750
0.701	5.480
0.495	4.750
0.351	3.740
0.246	3.410
0.175	3.990
0.124	1.290
0.088	0.000
0.053	0.000
0.045	0.000
0.038	0.000
0.000	0.000

COMBUSTION CONDITIONS

# of particles in Monte Carlo Method	100
% of total wall area with membranes	70.0 %
Solids return temp. equals cyclone temp.	860.5 C
Solids recirculation rate	12.750 kg/s
Solids recirculation flux	30.000 kg/m ² s
Gas cross-flow coefficient	0.100 m/s
Combustion efficiency	100.0 %
Excess air	20.000 %
Volatile transfer fraction	0.300
Number of fuel feed points	1
Fuel feedrate	395.687 kg/hr
Air feedrate	3070.295 kg/hr
% of total air that is primary	72.0 %
Residence time of particles in cyclone	0.300 sec.
Reflection coefficient	0.100
Height at which developed zone begins	2.777 m

GAS VELOCITIES

Core interstitial gas velocity	7.122 m/s
Streamer interstitial gas velocity	3.567 m/s
Superficial gas velocity	6.958 m/s
Bed temperature used in calculating heat transfer area and gas velocities	849.9 C

HEAT RELEASE DISTRIBUTION

Height (m)	Fraction of Total Heat Release			
	Volatiles		Char	
	Streamer	Core	Streamer	Core
0.00	0.342553		0.477220	
0.13	0.004300	0.074679	0.013539	0.007436
0.38	0.000576	0.017038	0.004955	0.004236
0.63	0.000289	0.003826	0.003514	0.002766
0.88	0.000511	0.001003	0.003038	0.001992
1.14	0.000150	0.000253	0.002745	0.001493
1.39	0.000036	0.000126	0.002074	0.001223
1.64	0.000030	0.000031	0.001647	0.001082
1.89	0.000000	0.000007	0.001382	0.000982
2.15	0.000000	0.000002	0.001109	0.000928
2.40	0.000000	0.000000	0.001106	0.000922
2.65	0.000000	0.000002	0.000942	0.000848
2.90	0.000000	0.000000	0.000905	0.000853
3.16	0.000000	0.000001	0.000822	0.000836
3.41	0.000000	0.000000	0.000741	0.000802
3.66	0.000000	0.000000	0.000717	0.000775
3.91	0.000000	0.000000	0.000651	0.000743
4.17	0.000000	0.000000	0.000567	0.000729
4.42	0.000000	0.000000	0.000512	0.000737
4.67	0.000000	0.000000	0.000466	0.000692
4.92	0.000000	0.000000	0.000398	0.000691
Cyclone	0.000000		0.004768	
TOTAL	0.501927		0.498073	

OXYGEN PARTIAL PRESSURE DISTRIBUTION

Height (m)	Partial Pressure of Oxygen (atm.)	
	Streamer	Core
0.00	0.066846	
0.26	0.031068	0.051215
0.51	0.033960	0.044474
0.76	0.035640	0.041798
1.00	0.032011	0.040337
1.26	0.027738	0.039364
1.51	0.026677	0.038644
1.76	0.027007	0.038093
2.01	0.027774	0.037651
2.27	0.028930	0.037286
2.52	0.028606	0.036946
2.77	0.029225	0.036646
3.02	0.029315	0.036355
3.29	0.029683	0.036079
3.54	0.030116	0.035821
3.79	0.030156	0.035573
4.04	0.030445	0.035339
4.29	0.030921	0.035121
4.54	0.031221	0.034910
4.79	0.031434	0.034714
5.04	0.031819	0.034529

Pressure convergence tolerance	0.0010 atm.
Partial pressure of oxygen entering	0.210000 atm.
Partial pressure of oxygen leaving riser	0.035 atm.
Partial pressure of oxygen leaving cyclone	0.034 atm.

TEMPERATURE DISTRIBUTION

Height (m)	Temperature (C)	
	Streamer	Core
0.00	891.7	
0.13	885.9	893.5
0.38	835.2	890.1
0.63	832.1	886.5
0.88	829.4	883.0
1.14	826.9	879.8
1.39	824.7	876.9
1.64	823.0	874.4
1.89	821.6	872.1
2.15	820.6	870.0
2.40	822.6	868.2
2.65	824.7	866.4
2.90	826.7	864.7
3.16	828.8	863.4
3.41	829.2	862.1
3.66	830.3	861.0
3.91	832.3	860.0
4.17	836.1	859.2
4.42	843.0	858.7
4.67	855.3	858.7
4.92	878.4	859.5

Solids return temperature	860.5 C
Temperature convergence tolerance	0.001 C
Cyclone temperature	860.5 C
Wall temperature	106.8 C

HEAT TRANSFER COEFFICIENTS

Height (m)	Density (kg/m ³)	Core Temp. (C)	Heat Transfer Coefficient (W/m ² C)		
			Radiative	Convective	Overall
0.00	316.944	891.7	110.8	100.5	211.3
0.13	233.423	893.5	110.4	100.8	211.2
0.38	146.824	890.1	98.5	106.9	205.4
0.63	94.664	886.5	97.8	101.4	199.1
0.88	63.214	883.0	97.2	67.7	164.9
1.14	44.242	879.8	96.6	47.4	144.0
1.39	32.797	876.9	96.1	35.1	131.3
1.64	25.889	874.4	95.7	27.7	123.5
1.89	21.720	872.1	95.5	23.2	118.7
2.15	19.205	870.0	95.2	20.5	115.7
2.40	17.688	868.2	95.1	18.9	113.9
2.65	16.738	866.4	95.2	17.8	113.0
2.90	15.982	864.7	97.0	16.8	113.8
3.16	15.211	863.4	97.0	15.9	113.0
3.41	14.412	862.1	97.1	15.1	112.2
3.66	13.591	861.0	97.4	14.2	111.5
3.91	12.744	860.0	97.8	13.2	111.0
4.17	11.869	859.2	98.7	12.2	110.9
4.42	10.968	858.7	100.2	11.2	111.4
4.67	10.042	858.7	103.1	10.1	113.2
4.92	9.091	859.5	108.5	8.9	117.4

CFB HEAT RELEASE AND HEAT TRANSFER MODEL

RUN RESULTS FROM HEAT TRANSFER ROUTINE HEAT.F, VERSION 8.1
 WRITTEN BY: DALE W.C. JU

COMBUSTOR: UBC COMBUSTOR

CASE: RUN NO. 21, APRIL 21 1988

Case : uh0

Superficial gas velocity = 7.03 m/s

Solids recirculation rate = 30 kg/m²s

Highvale coal(mean dp = 2.89 mm)

FUEL PHYSICAL PROPERTIES AND COMPOSITION**PROXIMATE ANALYSIS**

Weight %

12.200	Ash
15.200	Moisture
0.170	Sulphur
3.050	Hydrogen
52.900	Carbon
0.680	Nitrogen
15.800	Oxygen

PARTICLE SIZE DISTRIBUTION

mm	wt %
7.925	9.250
5.613	10.920
3.962	13.180
2.794	12.110
1.981	11.090
1.397	8.730
0.991	7.750
0.701	5.480
0.495	4.750
0.351	3.740
0.246	3.410
0.175	3.990
0.124	1.290
0.088	0.000
0.053	0.000
0.045	0.000
0.038	0.000
0.000	0.000

COMBUSTION CONDITIONS

# of particles in Monte Carlo Method	100
% of total wall area with membranes	35.0 %
Solids return temp. equals cyclone temp.	792.5 C
Solids recirculation rate	0.696 kg/s
Solids recirculation flux	30.000 kg/m ² s
Gas cross-flow coefficient	0.100 m/s
Combustion efficiency	100.0 %
Excess air	20.000 %
Volatile transfer fraction	0.300
Number of fuel feed points	1
Fuel feedrate	22.863 kg/hr
Air feedrate	177.399 kg/hr
% of total air that is primary	50.4 %
Residence time of particles in cyclone	0.300 sec.
Reflection coefficient	0.860
Height at which developed zone begins	3.200 m

GAS VELOCITIES

Core interstitial gas velocity	7.384 m/s
Streamer interstitial gas velocity	3.647 m/s
Superficial gas velocity	7.030 m/s
Bed temperature used in calculating heat transfer area and gas velocities	857.9 C

HEAT RELEASE DISTRIBUTION

Height (m)	Fraction of Total Heat Release			
	Volatiles		Char	
	Streamer	Core	Streamer	Core
0.00		0.317052	0.305613	
0.16	0.005887	0.071983	0.029671	0.009973
0.48	0.000893	0.015944	0.017396	0.005973
0.80	0.000692	0.004155	0.013057	0.004362
1.12	0.000459	0.002142	0.009720	0.003486
1.44	0.000052	0.001592	0.008220	0.003020
1.76	0.000021	0.000909	0.007529	0.002748
2.08	0.000002	0.000222	0.006999	0.002584
2.40	0.000012	0.000200	0.006848	0.002449
2.72	0.000383	0.000344	0.006309	0.002425
3.04	0.000548	0.000692	0.006106	0.002373
3.36	0.000000	0.000007	0.006034	0.002349
3.68	0.000000	0.000001	0.006743	0.002428
4.00	0.000000	0.000000	0.006760	0.002529
4.32	0.000000	0.000000	0.007350	0.002600
4.64	0.000000	0.000000	0.007849	0.002783
4.96	0.000000	0.000000	0.008391	0.003011
5.28	0.000000	0.000000	0.008868	0.003295
5.60	0.000000	0.000000	0.009645	0.003666
5.92	0.000000	0.000000	0.010064	0.004114
6.24	0.000000	0.000000	0.010948	0.004818
Cyclone		0.000000	0.004705	
TOTAL		0.477665	0.522335	

OXYGEN PARTIAL PRESSURE DISTRIBUTION

Height (m)	Partial Pressure of Oxygen (atm.)	
	Streamer	Core
0.00	0.101073	
0.32	0.050014	0.082836
0.64	0.051504	0.073647
0.96	0.051164	0.068944
1.28	0.051587	0.065837
1.60	0.051353	0.063474
1.92	0.050136	0.061521
2.24	0.049017	0.059852
2.56	0.047547	0.058266
2.88	0.046136	0.056704
3.20	0.044455	0.055137
3.52	0.043668	0.053828
3.84	0.041194	0.052458
4.16	0.039494	0.051084
4.48	0.037074	0.049655
4.80	0.034576	0.048167
5.12	0.031930	0.046627
5.44	0.029271	0.045058
5.76	0.026194	0.043449
6.08	0.023381	0.041871
6.40	0.020259	0.040204

Pressure convergence tolerance	0.0016 atm.
Partial pressure of oxygen entering	0.210000 atm.
Partial pressure of oxygen leaving riser	0.037 atm.
Partial pressure of oxygen leaving cyclone	0.037 atm.

TEMPERATURE DISTRIBUTION

Height (m)	Temperature (C)	
	Streamer	Core
0.00	879.1	
0.16	883.4	881.2
0.48	828.0	867.1
0.80	823.6	855.7
1.12	821.5	847.1
1.44	820.6	840.6
1.76	820.0	835.7
2.08	819.4	831.8
2.40	819.6	828.9
2.72	820.6	825.8
3.04	815.8	822.6
3.36	811.0	819.5
3.68	806.2	816.3
4.00	804.3	813.3
4.32	802.3	810.6
4.64	800.4	808.0
4.96	798.0	805.4
5.28	795.0	802.5
5.60	791.4	799.4
5.92	786.9	795.6
6.24	781.8	791.2

Solids return temperature	792.5 C
Temperature convergence tolerance	0.002 C
Cyclone temperature	792.5 C
Wall temperature	106.8 C

HEAT TRANSFER COEFFICIENTS

Height (m)	Density (kg/m ³)	Core Temp. (C)	Heat Transfer Coefficient (W/m ² C)		
			Radiative	Convective	Overall
0.00	394.263	879.1	109.9	99.4	209.2
0.16	171.130	881.2	109.7	99.8	209.5
0.48	111.608	867.1	96.9	105.0	201.9
0.80	80.285	855.7	95.9	83.7	179.6
1.12	63.788	847.1	95.4	66.0	161.4
1.44	55.069	840.6	95.2	56.6	151.8
1.76	50.507	835.7	95.1	51.6	146.7
2.08	48.088	831.8	95.0	48.9	143.9
2.40	46.797	828.9	95.0	47.4	142.4
2.72	46.122	825.8	95.2	46.5	141.7
3.04	46.005	822.6	95.2	46.3	141.5
3.36	47.861	819.5	90.9	49.1	140.0
3.68	51.859	816.3	92.1	52.6	144.7
4.00	57.031	813.3	91.7	57.7	149.4
4.32	63.672	810.6	91.3	64.4	155.7
4.64	72.284	808.0	90.8	73.0	163.9
4.96	83.593	805.4	90.3	84.4	174.8
5.28	98.506	802.5	89.7	99.5	189.2
5.60	118.322	799.4	88.9	101.1	190.0
5.92	144.943	795.6	88.0	101.1	189.1
6.24	180.706	791.2	87.0	101.2	188.1

CFB HEAT RELEASE AND HEAT TRANSFER MODEL

RUN RESULTS FROM HEAT TRANSFER ROUTINE HEAT.F, VERSION 8.1
 WRITTEN BY: DALE W.C. JU

COMBUSTOR: Studsvik Prototype

CASE: Sardinian Coal

Case : low load test case, sh6

Wall disturbance factor changed from 310 to 470

Superficial gas velocity = 3.30 m/s

Solids recirculation rate = 30 kg/m²s

Highvale coal(mean dp = 2.89 mm)

FUEL PHYSICAL PROPERTIES AND COMPOSITION**PROXIMATE ANALYSIS**

Weight %

12.200	Ash
15.200	Moisture
0.170	Sulphur
3.050	Hydrogen
52.900	Carbon
0.680	Nitrogen
15.800	Oxygen

PARTICLE SIZE DISTRIBUTION

mm	wt %
7.925	9.250
5.613	10.920
3.962	13.180
2.794	12.110
1.981	11.090
1.397	8.730
0.991	7.750
0.701	5.480
0.495	4.750
0.351	3.740
0.246	3.410
0.175	3.990
0.124	1.290
0.088	0.000
0.053	0.000
0.045	0.000
0.038	0.000
0.000	0.000

COMBUSTION CONDITIONS

# of particles in Monte Carlo Method	100
% of total wall area with membranes	70.0 %
Solids return temp. equals cyclone temp.	604.5 C
Solids recirculation rate	12.750 kg/s
Solids recirculation flux	30.000 kg/m ² s
Gas cross-flow coefficient	0.100 m/s
Combustion efficiency	100.0 %
Excess air	20.000 %
Volatile transfer fraction	0.300
Number of fuel feed points	1
Fuel feedrate	185.551 kg/hr
Air feedrate	1439.763 kg/hr
% of total air that is primary	67.8 %
Residence time of particles in cyclone	0.300 sec.
Reflection coefficient	0.100
Height at which developed zone begins	2.020 m

GAS VELOCITIES

Core interstitial gas velocity	3.489 m/s
Streamer interstitial gas velocity	1.743 m/s
Superficial gas velocity	3.300 m/s
Bed temperature used in calculating heat transfer area and gas velocities	854.9 C

HEAT RELEASE DISTRIBUTION

Height (m)	Fraction of Total Heat Release			
	Volatiles		Char	
	Streamer	Core	Streamer	Core
0.00	0.376003		0.382288	
0.13	0.002162	0.082293	0.019153	0.013069
0.38	0.000125	0.017668	0.011832	0.007722
0.63	0.000042	0.003817	0.007813	0.005338
0.88	0.000002	0.000833	0.005403	0.004024
1.14	0.000001	0.000188	0.004050	0.003246
1.39	0.000000	0.000045	0.003218	0.002861
1.64	0.000000	0.000014	0.003026	0.002561
1.89	0.000000	0.000004	0.002623	0.002407
2.15	0.000000	0.000002	0.002475	0.002234
2.40	0.000000	0.000001	0.002254	0.002118
2.65	0.000000	0.000000	0.002127	0.001936
2.90	0.000000	0.000000	0.001974	0.001744
3.16	0.000000	0.000000	0.001693	0.001697
3.41	0.000000	0.000000	0.001582	0.001542
3.66	0.000000	0.000000	0.001299	0.001354
3.91	0.000000	0.000000	0.001118	0.001241
4.17	0.000000	0.000000	0.000804	0.001071
4.42	0.000000	0.000000	0.000626	0.000980
4.67	0.000000	0.000000	0.000439	0.000843
4.92	0.000000	0.000000	0.000265	0.000757
Cyclone	0.000000		0.001993	
TOTAL	0.545026		0.454974	

OXYGEN PARTIAL PRESSURE DISTRIBUTION

Height (m)	Partial Pressure of Oxygen (atm.)	
	Streamer	Core
0.00	0.077348	
0.26	0.048006	0.059016
0.51	0.045328	0.050294
0.76	0.041629	0.046541
1.00	0.038226	0.044397
1.26	0.035594	0.042924
1.51	0.033920	0.041784
1.76	0.032109	0.040819
2.01	0.031386	0.039957
2.27	0.030958	0.039141
2.52	0.030936	0.038368
2.77	0.030799	0.037649
3.02	0.030732	0.036987
3.29	0.031092	0.036373
3.54	0.031123	0.035810
3.79	0.031625	0.035319
4.04	0.031970	0.034881
4.29	0.032764	0.034519
4.54	0.033223	0.034208
4.79	0.033683	0.033951
5.04	0.034138	0.033739

Pressure convergence tolerance	0.0011 atm.
Partial pressure of oxygen entering	0.210000 atm.
Partial pressure of oxygen leaving riser	0.034 atm.
Partial pressure of oxygen leaving cyclone	0.033 atm.

TEMPERATURE DISTRIBUTION

Height (m)	Temperature (C)	
	Streamer	Core
0.00	618.3	
0.13	615.6	619.0
0.38	587.4	615.3
0.63	587.4	612.4
0.88	588.8	610.2
1.14	591.1	608.6
1.39	593.7	607.4
1.64	595.3	606.9
1.89	596.8	606.4
2.15	598.4	605.8
2.40	599.9	605.4
2.65	599.8	605.1
2.90	599.7	604.8
3.16	599.6	604.5
3.41	599.7	604.3
3.66	599.9	604.1
3.91	600.4	604.0
4.17	601.5	603.9
4.42	603.4	603.9
4.67	607.2	604.0
4.92	615.9	604.2

Solids return temperature	604.5 C
Temperature convergence tolerance	0.001 C
Cyclone temperature	604.5 C
Wall temperature	106.8 C

HEAT TRANSFER COEFFICIENTS

Height (m)	Density (kg/m ³)	Core Temp. (C)	Heat Transfer Coefficient (W/m ² C)		
			Radiative	Convective	Overall
0.00	490.237	618.3	57.3	100.3	157.6
0.13	400.288	619.0	57.1	100.5	157.7
0.38	273.636	615.3	52.9	105.0	158.0
0.63	197.644	612.4	52.9	104.7	157.6
0.88	151.900	610.2	53.1	104.1	157.2
1.14	124.329	608.6	53.5	103.4	156.8
1.39	107.699	607.4	53.8	102.7	156.5
1.64	97.668	606.9	54.2	99.7	153.8
1.89	91.803	606.4	54.4	93.3	147.7
2.15	86.734	605.8	55.2	87.2	142.4
2.40	80.762	605.4	54.7	81.6	136.4
2.65	74.758	605.1	54.7	75.5	130.3
2.90	68.662	604.8	54.7	69.3	124.1
3.16	62.458	604.5	54.7	63.1	117.8
3.41	56.192	604.3	54.7	56.7	111.4
3.66	49.906	604.1	54.8	50.3	105.1
3.91	43.656	604.0	54.8	44.0	98.8
4.17	37.489	603.9	55.0	37.7	92.7
4.42	31.461	603.9	55.3	31.5	86.8
4.67	25.619	604.0	55.8	25.5	81.3
4.92	20.007	604.2	57.2	19.6	76.7

APPENDIX D

LIST OF VARIABLES**D.1 INPUT FILE FROM HYDRODYNAMIC MODEL**

<u>Variable</u>	<u>Description</u>	<u>Variable Name in Senior's Model</u>
acell(i)	cross-sectional area of core cells (m ²)	
acell(ncell)	primary zone cross-sectional area (m ²)	
acell(ny+i)	cross-sectional area of annulus cells (m ²)	
acfin	cross-sectional area of core at the top of the riser (m ²)	
acinit	core cross-sectional area at height = 0 m (m ²)	
asfin	cross-sectional area of annulus at the top of the riser (m ²)	
asinit	annulus cross-sectional area at height = 0 m (m ²)	
at	riser cross-sectional area (m ²)	bed(4)
dbavg	average density of the bed (kg/m ³)	dbav(3)
denp	particle density (kg/m ³)	pp(1,1)
devh	height of developing zone (m)	
emiss	particle radiation emissivity	pp(4,4)
flux(i,j)	i = cell number j = 1 height of cell (m) = 2 radial flux out of the cell (kg/m ² s) = 3 axial flux out of the cell (kg/m ² s) = 4 cell density (kg/m ³)	
fluxr	solids recirculation rate (kg/m ² s)	hydg(1)
k	thermal conductivity of gas	tcg
ny	number of cells along the riser, not including the primary zone	nzb
pair	fraction of the total combustion air that is primary air	
pdist(i)	weight percentage of particles at sieve size siv(i) (%)	
per	perimeter of riser (m)	peri
primev	volume of primary zone (m ³)	bed(1)
rc	reflection coefficient	hydz(5)
siv(i)	particle sieve sizing (mm)	
sug	superficial gas velocity (m/s)	ug(5)
tb	temperature of the bed (°C)	t
twall	temperature of the heat transfer surface (°C)	
uc	mean core gas velocity (m/s)	ug(1)

ult(i)	ultimate analysis of fuel (%)	
	i = 1 ash	pp(1,2)
	i = 2 moisture	pp(1,10)
	i = 3 sulphur	pp(1,6)
	i = 4 hydrogen	pp(1,4)
	i = 5 carbon	pp(1,3)
	i = 6 nitrogen	pp(1,9)
	i = 7 oxygen	pp(1,5)
us	mean annulus gas velocity (m/s)	ug(2)
volf	fractional volatiles yield	pp(1,7)

D.2 USER INPUT FILE

<u>Variable</u>	<u>Description</u>
c1, c2	constants used in the devolatilization equation
ceff	combustion efficiency
const1	constant in wall convective heat transfer coefficient calculation
cross	gas mass transfer crossflow coefficient
eps	tolerance of oxygen partial pressure calculation
eps2	tolerance of bed temperature calculation
eps3	tolerance of bed temperature within the energy balance subroutine "htrans"
exair	fractional excess air
nfeed	number of equally spaced feed points at the bottom of the primary zone
npart	number of particles used in the Monte Carlo method
perc	fraction of particles that will leave a cell during time step
rf	relaxation factor in oxygen partial pressure calculation
rf2	relaxation factor in temperature calculation
rt	residence time of the cyclone (s)
tair	combustion air inlet temperature (°C)
tref	reference temperature (°C)
tsp	particle surface temperature (°C)
vtf	volatile transfer fraction

D.3 PROGRAM VARIABLES

<u>Variable</u>	<u>Description</u>
afeed	air feedrate (kg/s)
areaw(i,j), areae(i,j), arean(i,j), areas(i,j)	cell area on west, east, north and south face
areat(i,j)	total surface area of cell (m ²)

cg	gas heat capacity
cp	particle heat capacity
denb(2)	primary zone bed density(kg/m ²)
denb(i+2)	bed density at a given height (kg/m ²)
deng	gas density (kg/m ³)
distv(i)	volatiles heat release distribution
dpcut	cut-off particle diameter in the cyclone (m)
dt	time step
dx(i,j), dy(i,j)	dimensions of the cell (m)
f	fraction of total wall area that is a heat transfer surface
fluxc(i,j)	i = cell number j = 1 height of cell (m) = 2 radial flowrate out of the cell (kg/s) = 3 axial flowrate out of the cell (kg/s) = 4 cell mass (kg)
fuel	fuel feedrate (kg/s)
heat (i)	heat release in cell
heatv(i)	heat release due to devolatilization
htarea	heat transfer area (m ²)
ncell	number of cells
nx	number of cells in the radial direction
o2feed	oxygen feedrate (kg/s)
o2need	oxygen feedrate needed per kg/s of fuel feedrate (kg/s)
pcyc	oxygen partial pressure in cyclone (atm)
pmat1(i), pmat2(i), pmatt(i)	probability of how a particle will move in a cell
po2	partial pressure of oxygen in the airfeed (atm)
presc(i)	core cell partial pressure of oxygen (atm)
press(i)	annulus cell partial pressure of oxygen (atm)
primeh	height of primary zone (m)
rarea	total wall area (m ²)
recirc	solids recirculation flowrate(kg/s)
sbc	Stefan-Boltzmann constant (W/m ² k ⁴)
tcyc	cyclone temperature (°C)
temp(i)	cell temperature (°C)
tempo(i)	cell temperature in previous iteration (°C)
tin	mixing temperature of fuel feed and combustion air (°C)
tinit	initial guess of bed temperature (°C)
volp	particle volume (m ³)

APPENDIX E

ENTHALPY BALANCE SPREADSHEETS

case: sh0

I	streamer		g (W)	(W)				core		g (W)	(W)				
	temp (K and C)			west	east	north	south	temp (K and C)			west	east	north	south	
22	1149	876	918	cond	-3114	-5	0	0	1131	1820	cond	5	0	0	0
				p-conv	0	245405	1017428	-1222067	857		p-conv	-245405	0	-10174472	10415631
				g-conv	0	-433	-1213	1494			g-conv	433	0	-883560	882102
				rad	-37637	-3517	-8	-9			rad	3517	0	-1	-89
21	1127	853	1239	cond	-3436	1	0	0	1130	1809	cond	-1	0	0	0
				p-conv	0	245280	1222069	-1434618	857		p-conv	-245280	0	-10416956	10880502
				g-conv	0	78	-1494	178			g-conv	-78	0	-882121	881536
				rad	-34956	804	9	-8			rad	-804	0	88	5
20	1114	841	1424	cond	-3753	4	0	0	1130	1825	cond	-4	0	0	0
				p-conv	0	242908	1434562	-1848749	857		p-conv	-242908	0	-10680754	10904893
				g-conv	0	359	-1776	2055			g-conv	-359	0	-881567	881482
				rad	-33441	2777	6	-4			rad	-2777	0	-8	60
19	1107	834	1731	cond	-4084	6	0	0	1130	1847	cond	-6	0	0	0
				p-conv	0	239288	1848718	-1861808	857		p-conv	-239288	0	-10905293	11148936
				g-conv	0	527	-2055	2329			g-conv	-527	0	-881508	881752
				rad	-32617	4049	4	-2			rad	-4049	0	-82	95
18	1104	830	1895	cond	-4388	8	0	0	1131	2033	cond	-8	0	0	0
				p-conv	0	234997	1861821	-2072113	858		p-conv	-234997	0	-11147254	11385213
				g-conv	0	833	-2329	2598			g-conv	-833	0	-881777	882245
				rad	-32182	4848	2	-1			rad	-4848	0	-98	118
17	1102	828	2170	cond	-4664	9	0	0	1132	2170	cond	-9	0	0	0
				p-conv	0	230278	2072030	-2278708	859		p-conv	-230278	0	-11385535	11619078
				g-conv	0	702	-2598	2960			g-conv	-702	0	-882270	882895
				rad	-31828	5363	1	-1			rad	-5363	0	-119	134
16	1100	827	2082	cond	-4953	9	0	0	1133	2233	cond	-9	0	0	0
				p-conv	0	225408	2278571	-2480731	860		p-conv	-225408	0	-11618385	11848308
				g-conv	0	754	-2880	3118			g-conv	-754	0	-882918	883677
				rad	-31793	5763	1	0			rad	-5763	0	-135	147
15	1100	827	2268	cond	-5238	10	0	0	1135	2180	cond	-10	0	0	0
				p-conv	0	220350	2480708	-2678609	861		p-conv	-220350	0	-11848632	12072782
				g-conv	0	790	-3118	3368			g-conv	-790	0	-883701	884573
				rad	-31754	6047	0	0			rad	-6047	0	-149	159
14	1100	827	2205	cond	-5511	10	0	0	1136	2258	cond	-10	0	0	0
				p-conv	0	215332	2878539	-2871501	863		p-conv	-215332	0	-12073137	12262363
				g-conv	0	824	-3368	3571			g-conv	-824	0	-884800	885571
				rad	-31744	6309	0	-8			rad	-6309	0	-180	189
13	1092	819	2391	cond	-5782	13	0	0	1137	2515	cond	-13	0	0	0
				p-conv	0	202881	2871512	-3055414	864		p-conv	-202881	0	-12262831	12500888
				g-conv	0	1048	-3571	3837			g-conv	-1048	0	-885605	886964
				rad	-30777	7954	8	-1			rad	-7954	0	-171	222
12	1091	818	2514	cond	-6125	14	0	0	1139	2877	cond	-14	0	0	0
				p-conv	0	325019	3055369	-3362060	866		p-conv	-325019	0	-12501389	12831774
				g-conv	0	1104	-3837	4229			g-conv	-1104	0	-887000	888244
				rad	-30707	8398	1	1			rad	-8398	0	-224	239
11	1082	818	2744	cond	-6687	14	0	0	1141	2801	cond	-14	0	0	0
				p-conv	0	528315	3362024	-3870828	868		p-conv	-528315	0	-12832252	13384880
				g-conv	0	1133	-4229	4871			g-conv	-1133	0	-888277	889143
				rad	-30796	8644	-1	1			rad	-8644	0	-241	257
10	1083	820	3400	cond	-7581	14	0	0	1143	3216	cond	-14	0	0	0
				p-conv	0	880443	3870825	-4714643	870		p-conv	-880443	0	-13365184	14232288
				g-conv	0	1157	-4871	5835			g-conv	-1157	0	-889178	889310
				rad	-30819	8867	-1	2			rad	-8867	0	-259	277
9	1094	821	4229	cond	-9037	14	0	0	1146	3929	cond	-14	0	0	0
				p-conv	0	1415577	4714575	-8115182	873		p-conv	-1415577	0	-14232838	15655887
				g-conv	0	1177	-5836	7702			g-conv	-1177	0	-889344	889199
				rad	-31077	9074	-2	3			rad	-9074	0	-279	302
8	1096	823	5258	cond	-11482	15	0	0	1148	3738	cond	-15	0	0	0
				p-conv	0	2338458	8114953	-8440286	875		p-conv	-2338458	0	-15858286	18004896
				g-conv	0	1195	-7702	10637			g-conv	-1195	0	-888222	884943
				rad	-31277	9290	-3	6			rad	-9290	0	-304	341
7	1098	825	7835	cond	-15539	15	0	0	1151	4853	cond	-15	0	0	0
				p-conv	0	3874176	8440038	-12305315	878		p-conv	-3874176	0	-18005204	21892189
				g-conv	0	1208	-10637	15512			g-conv	-1208	0	-884968	877935
				rad	-31536	9428	-8	10			rad	-9428	0	-343	384
6	1101	828	10983	cond	-22277	15	0	0	1154	8165	cond	-15	0	0	0
				p-conv	0	8427881	12304883	-18729275	881		p-conv	-8427881	0	-21892908	28337072
				g-conv	0	1224	-15514	23618			g-conv	-1224	0	-877985	884350
				rad	-31829	9823	-10	18			rad	-9823	0	-388	418
5	1103	830	18085	cond	-33485	15	0	0	1156	18178	cond	-15	0	0	0
				p-conv	0	10874755	18727945	-28408147	884		p-conv	-10874755	0	-28338043	39030895
				g-conv	0	1241	-23618	37100			g-conv	-1241	0	-864380	839408
				rad	-32147	9844	-18	30			rad	-9844	0	-417	418
4	1107	833	31001	cond	-35438	15	0	1	1161	55014	cond	-15	0	0	0
				p-conv	0	17741971	28408283	-47180374	888		p-conv	-17741971	0	-39031763	58774287
				g-conv	0	1252	-37102	62992			g-conv	-1252	0	-839431	785190
				rad	-32517	10017	-30	825			rad	-10017	0	-419	373
3	1157	884	48116	cond	-35755	2	-1	0	1165	215079	cond	-2	0	0	0
				p-conv	0	29196541	47177737	-78411429	891		p-conv	-29196541	0	-56773442	85824429
				g-conv	0	173	-82990	98252			g-conv	-173	0	-795178	727798
				rad	-38953	1488	-825	52			rad	-1488	0	-373	-101
2	1159	886	424343	cond	-228524	21	0	-1	1163	1598444	cond	-21	0	0	-4
				p-conv	0	78582656	78413188	0	890		p-conv	78582656	0	-85807821	89035567
				g-conv	0	859	-98247	0			g-conv	-859	0	-727857	0
				rad	-250895	5774	-52	-2501			rad	-5774	0	108	-9887

heat generated in streamer 574839
 heat generated in core 1837081
 total heat generated 2511720
 heat transferred to cooling wall -1371007
 heat leaving top of riser -10041809
 heat entering bottom of riser 8903554
 total 2457
 % diff. of heat gen. 0

case: sh1

I	streamer		g (W)	(W)				core temp (K and C)	g (W)	(W)				
	temp (K and C)			west	east	north	south			west	east	north	south	
22	1123	1212	cond	-5048	-4	0	0	1107	2008	cond	4	0	0	0
	860		p-conv	0	474182	1608953	-2048215	834		p-conv	-474182	0	-18089284	16570060
			g-conv	0	-385	-1977	2552			g-conv	385	0	-865327	863821
21	1109	1401	rad	-34578	-2780	-8	-10	1107	2112	rad	2780	0	0	-52
	838		cond	-5657	0	0	0			cond	0	0	0	0
			p-conv	0	481522	2048232	-2478888	834		p-conv	-481522	0	-16588810	17030137
20	1100	1881	g-conv	0	-38	-2551	3112	1107	2188	g-conv	38	0	-863808	862332
	827		rad	-32770	-281	10	-7			rad	281	0	63	-11
			cond	-8248	2	0	0			cond	-2	0	0	0
19	1085	1936	p-conv	0	447784	2478703	-2898277	834		p-conv	-447784	0	-17028877	17477884
	822		g-conv	0	151	-3112	3853			g-conv	151	0	-862319	861340
			rad	-31783	1112	7	-5	1107	2282	rad	-1112	0	12	15
18	1062	2081	cond	-8820	3	0	0			cond	-3	0	0	0
	819		p-conv	0	433520	2898321	-3306440	834		p-conv	-433520	0	-17477418	17911858
			g-conv	0	289	-3653	4177			g-conv	289	0	-861328	860588
17	1060	2355	rad	-31201	1988	5	-3	1107	2394	rad	-1988	0	-15	33
	817		cond	-7371	4	0	0			cond	-4	0	0	0
			p-conv	0	419131	3305487	-3898311	834		p-conv	-419131	0	-17911388	18331570
16	1088	2683	g-conv	0	345	-4177	4681			g-conv	345	0	-860563	859862
	816		rad	-30850	2520	3	-2	1108	2487	rad	-2520	0	-33	46
			cond	-7901	5	0	0			cond	-5	0	0	0
15	1089	2788	p-conv	0	404787	3690384	-4079814	835		p-conv	-404787	0	-18331283	18737329
	816		g-conv	0	397	-4681	5188			g-conv	397	0	-859849	858498
			rad	-30840	2890	2	-1	1108	2488	rad	-2890	0	-46	58
14	1089	2788	cond	-8411	5	0	0			cond	-5	0	0	0
	816		p-conv	0	390530	4078871	-4448774	835		p-conv	-390530	0	-18737088	19129035
			g-conv	0	434	-5188	5638			g-conv	434	0	-859485	858152
13	1089	2788	rad	-30513	3158	1	-1	1109	2750	rad	-3158	0	-58	85
	816		cond	-8902	6	0	0			cond	-6	0	0	0
			p-conv	0	378814	4448786	-4800089	836		p-conv	-378814	0	-19128818	19508731
12	1089	3124	g-conv	0	481	-5638	6087			g-conv	481	0	-859142	858005
	816		rad	-30447	3354	1	0	1110	2745	rad	-3354	0	-84	71
			cond	-9373	6	0	0			cond	-6	0	0	0
11	1089	3124	p-conv	0	382938	4800142	-5140377	836		p-conv	-382938	0	-19508518	19878835
	816		g-conv	0	480	-6087	6523			g-conv	480	0	-858895	858751
			rad	-30423	3488	0	1	1110	2808	rad	-3488	0	-70	77
10	1089	3197	cond	-8827	6	0	0			cond	-6	0	0	0
	816		p-conv	0	348370	5140387	-5488825	837		p-conv	-348370	0	-19878882	20221338
			g-conv	0	487	-6523	8904			g-conv	487	0	-858744	858875
9	1085	3188	rad	-30488	3552	-1	-8	1111	2728	rad	-3552	0	-78	80
	812		cond	-10253	7	0	0			cond	-7	0	0	0
			p-conv	0	388984	5488888	-5814485	838		p-conv	-388984	0	-20221234	20592278
8	1084	3582	g-conv	0	584	-8904	7365			g-conv	584	0	-858970	858889
	811		rad	-30078	4238	6	-2	1112	3128	rad	-4238	0	-80	101
			cond	-10843	8	0	0			cond	-8	0	0	0
7	1084	3582	p-conv	0	801198	5814577	-6396519	839		p-conv	-801198	0	-20592358	21198072
	811		g-conv	0	830	-7365	8085			g-conv	830	0	-858973	858818
			rad	-28951	4575	2	-5	1113	3808	rad	-4575	0	-101	115
6	1082	4081	cond	-11882	9	0	0			cond	-9	0	0	0
	809		p-conv	0	887487	6396589	-7384759	840		p-conv	-887487	0	-21188318	22187328
			g-conv	0	714	-8085	8311			g-conv	714	0	-858227	858934
5	1079	4544	rad	-29881	5189	5	-6	1114	3532	rad	-5189	0	-115	139
	806		cond	-13548	10	0	0			cond	-10	0	0	0
			p-conv	0	1827829	7384877	-8978781	841		p-conv	-1827829	0	-22187845	23821202
4	1078	5425	g-conv	0	801	-8311	11355			g-conv	801	0	-858947	854248
	804		rad	-28380	5789	6	-8	1118	4220	rad	-5789	0	-140	173
			cond	-18340	11	0	0			cond	-11	0	0	0
3	1077	5425	p-conv	0	2890647	8978831	-11854582	843		p-conv	-2890647	0	-23821878	28520541
	804		g-conv	0	888	-11355	14755			g-conv	888	0	-854283	849073
			rad	-29145	8399	8	-5	1118	5224	rad	-8399	0	-174	213
2	1078	7504	cond	-20970	12	0	0			cond	-12	0	0	0
	803		p-conv	0	4454832	11854718	-18102020	845		p-conv	-4454832	0	-28521055	30888105
			g-conv	0	883	-14755	20405			g-conv	883	0	-849090	839541
1	1075	10987	rad	-28885	8898	5	-3	1120	8727	rad	-8898	0	-214	256
	802		cond	-28852	13	0	0			cond	-13	0	0	0
			p-conv	0	7384848	18102071	-23487084	847		p-conv	-7384848	0	-30888520	38390284
0	1075	28892	g-conv	0	1033	-20408	28904			g-conv	1033	0	-838552	822401
	802		rad	-28908	7488	3	2	1123	20843	rad	-7488	0	-268	288
			cond	-33738	13	0	0			cond	-13	0	0	0
0	1075	28892	p-conv	0	12255808	23488843	-35788850	850		p-conv	-12255808	0	-38388878	50884348
	802		g-conv	0	1084	-28907	45419			g-conv	1084	0	-822392	792211
			rad	-28948	7907	-3	11	1126	51526	rad	-7907	0	-288	300
0	1078	32988	cond	-33778	14	0	1			cond	-14	0	0	0
	803		p-conv	0	20380894	35782981	-58158955	852		p-conv	-20380894	0	-50880223	71030870
			g-conv	0	1128	-45420	75478			g-conv	1128	0	-792147	740035
0	1123	77573	rad	-29054	8289	-11	880			rad	-8289	0	-288	288
	850		cond	-34109	2	-1	0	1128	188811	cond	-2	0	0	0
			p-conv	0	33489481	58158952	-89727829	855		p-conv	-33489481	0	-71021079	104381085
0	1125	487479	g-conv	0	131	-75478	114148			g-conv	131	0	-739932	882403
	852		rad	-34479	1045	-880	73			rad	-1045	0	-280	-58
			cond	-218174	12	0	-1	1129	1441381	cond	-12	0	0	-2
0			p-conv	0	-8989871	88725047	0	855		p-conv	8989871	0	-104374348	14248628
			g-conv	0	385	-114138	0			g-conv	385	0	-862287	0
			rad	-222816	3088	-73	-1777			rad	-3088	0	85	-5381

heat generated in streamer 698688
 heat generated in core 1767522
 total heat generated 2486190
 heat transferred to cooling wall -1348888
 heat leaving top of riser -16358835
 heat entering bottom of riser 14248628
 total 8215
 % diff. of heat gen. 0

case: sh2

	streamer		g (W)	(W)				core temp (K and C)	g (W)	(W)				
	temp (K and C)			west	east	north	south			west	east	north	south	
22	1183	511	cond	-1800	-4	0	0	1189	1081	cond	4	0	0	0
	910		p-conv	0	56734	561329	-561739	898		p-conv	-56734	0	-5613208	5665983
			g-conv	0	-318	-625	669			g-conv	318	0	-918367	917229
			rad	-42661	-2852	-2	-7			rad	2852	0	0	-127
21	1144	849	cond	-1876	7	0	0	1188	1131	cond	-7	0	0	0
	871		p-conv	0	84027	561789	-564560	895		p-conv	-84027	0	-5665892	5632503
			g-conv	0	548	-889	725			g-conv	-548	0	-917218	918393
			rad	-37278	4642	8	-4			rad	-4642	0	127	183
20	1127	807	cond	-1755	12	0	0	1170	1102	cond	-12	0	0	0
	853		p-conv	0	68242	594808	-637804	898		p-conv	-68242	0	-5632428	5708201
			g-conv	0	987	-725	787			g-conv	-987	0	-918390	920759
			rad	-34978	8182	4	-2			rad	-8182	0	-182	313
19	1119	899	cond	-1837	15	0	0	1172	1115	cond	-15	0	0	0
	846		p-conv	0	70634	637857	-688572	899		p-conv	-70634	0	-5706157	5783786
			g-conv	0	1223	-787	852			g-conv	-1223	0	-920751	923771
			rad	-33990	10071	2	-1			rad	-10071	0	-313	386
18	1116	920	cond	-1821	17	0	0	1175	1180	cond	-17	0	0	0
	843		p-conv	0	71782	688623	-738431	902		p-conv	-71782	0	-5783748	5883489
			g-conv	0	1357	-952	920			g-conv	-1357	0	-923789	927158
			rad	-33634	11189	1	0			rad	-11189	0	-398	447
17	1118	963	cond	-2005	18	0	0	1178	1188	cond	-18	0	0	0
	843		p-conv	0	72502	738448	-791786	905		p-conv	-72502	0	-5883475	5944489
			g-conv	0	1437	-920	989			g-conv	-1437	0	-927155	930770
			rad	-33817	11899	0	1			rad	-11899	0	-448	479
16	1118	1013	cond	-2089	18	0	0	1182	1181	cond	-18	0	0	0
	845		p-conv	0	72802	791757	-845188	909		p-conv	-72802	0	-5944464	6025887
			g-conv	0	1484	-989	1050			g-conv	-1484	0	-930786	934482
			rad	-33910	12218	-1	-1			rad	-12218	0	-478	496
15	1116	1035	cond	-2188	20	0	0	1186	1211	cond	-20	0	0	1
	843		p-conv	0	72302	845215	-900035	912		p-conv	-72302	0	-8025852	8107812
			g-conv	0	1599	-1050	1125			g-conv	-1599	0	-934480	938542
			rad	-33638	13368	1	1			rad	-13368	0	-498	548
14	1119	1099	cond	-2273	20	0	0	1190	1241	cond	-20	0	-1	1
	845		p-conv	0	109181	900048	-991875	918		p-conv	-109181	0	-8107807	8227027
			g-conv	0	1628	-1125	1240			g-conv	-1628	0	-938541	942617
			rad	-33973	13732	-1	1			rad	-13732	0	-548	587
13	1122	1239	cond	-2445	20	0	0	1194	1279	cond	-20	0	-1	1
	848		p-conv	0	170358	991897	-1145083	921		p-conv	-170358	0	-8227031	8407819
			g-conv	0	1853	-1240	1434			g-conv	-1853	0	-942618	948820
			rad	-34348	14088	-1	2			rad	-14088	0	-587	585
12	1128	1485	cond	-2725	20	0	0	1198	1389	cond	-20	0	-1	1
	853		p-conv	0	271785	1145117	-1399772	925		p-conv	-271785	0	-8407845	8690382
			g-conv	0	1848	-1434	1764			g-conv	-1848	0	-948824	950382
			rad	-34888	14198	-2	2			rad	-14198	0	-585	595
11	1131	1811	cond	-3184	20	0	0	1202	1480	cond	-20	0	-1	1
	858		p-conv	0	440484	1399757	-1822878	929		p-conv	-440484	0	-8890419	7141951
			g-conv	0	1832	-1764	2286			g-conv	-1832	0	-950390	953899
			rad	-35517	14215	-2	3			rad	-14215	0	-595	601
10	1136	2281	cond	-3944	20	0	0	1206	1582	cond	-20	0	-1	1
	863		p-conv	0	721381	1822882	-2528867	933		p-conv	-721381	0	-7142032	7874984
			g-conv	0	1802	-2286	3171			g-conv	-1802	0	-953710	956270
			rad	-38229	14125	-3	5			rad	-14125	0	-802	807
9	1143	3019	cond	-5188	19	0	0	1211	2188	cond	-19	0	-1	1
	889		p-conv	0	1189115	2528870	-3688891	937		p-conv	-1189115	0	-7875194	9078357
			g-conv	0	1581	-3171	4842			g-conv	-1581	0	-958298	957588
			rad	-37014	13944	-5	8			rad	-13944	0	-609	611
8	1149	5708	cond	-7282	19	0	0	1215	3901	cond	-19	0	-1	1
	878		p-conv	0	1988228	3888948	-5852727	942		p-conv	-1988228	0	-9078705	11057135
			g-conv	0	1516	-4842	7090			g-conv	-1516	0	-957825	958803
			rad	-37822	13739	-8	11			rad	-13739	0	-813	812
7	1154	7418	cond	-10744	18	0	0	1219	4438	cond	-18	0	-1	1
	881		p-conv	0	3286186	5852097	-8904789	946		p-conv	-3286186	0	-11057221	14338111
			g-conv	0	1481	-7090	11188			g-conv	-1481	0	-958910	952720
			rad	-38598	13584	-11	17			rad	-13584	0	-813	839
6	1180	5983	cond	-18499	18	0	0	1223	9023	cond	-18	0	-1	1
	897		p-conv	0	5429528	8904595	-14322079	950		p-conv	-5429528	0	-14338240	19783456
			g-conv	0	1455	-11188	17951			g-conv	-1455	0	-952728	942882
			rad	-39355	13508	-17	28			rad	-13508	0	-639	655
5	1185	3440	cond	-28087	18	0	0	1228	18805	cond	-18	0	-1	1
	892		p-conv	0	9028303	14321812	-23340089	955		p-conv	-9028303	0	-19783471	28830479
			g-conv	0	1442	-17948	28257			g-conv	-1442	0	-942983	923827
			rad	-40071	13530	-28	43			rad	-13530	0	-855	849
4	1170	13258	cond	-38725	17	0	1	1233	53814	cond	-17	0	-1	0
	897		p-conv	0	15017203	23343402	-38378208	959		p-conv	-15017203	0	-28832454	43847089
			g-conv	0	1425	-28257	50935			g-conv	-1425	0	-923890	887883
			rad	-40805	13548	-43	835			rad	-13548	0	-851	548
3	1227	38988	cond	-39044	3	-1	0	1237	218584	cond	-3	0	0	0
	954		p-conv	0	24725804	38377731	-63120889	963		p-conv	-24725804	0	-43852021	68419387
			g-conv	0	211	-50935	78857			g-conv	-211	0	-867783	830503
			rad	-49443	2152	-835	5			rad	-2152	0	-553	-193
2	1228	344008	cond	-249371	38	0	-1	1235	1803896	cond	-38	0	0	-8
	954		p-conv	0	-83135147	63119952	0	962		p-conv	83135147	0	-88422821	4809790
			g-conv	0	1101	-78857	0			g-conv	-1101	0	-830548	0
			rad	-318864	11210	-5	-3888			rad	-11210	0	188	-21785

heat generated in streamer 438133
 heat generated in core 2128113
 total heat generated 2664248
 heat transferred to cooling wall -1508717
 heat leaving top of riser -5880891
 heat entering bottom of riser 4809782
 total -13570
 % diff. of heat gen. -1

case: sh3

I	streamer		g (W)	(W)				core		g (W)	(W)				
	temp (K and C)			west	east	north	south	temp (K and C)			west	east	north	south	
22	1103	898	cond	-3338	-6	0	0	1086	1939	cond	5	0	0	0	
	830		p-conv	0	318813	981448	-1243728	812		p-conv	-318813	0	-981448	9827332	
			g-conv	0	-425	-989	1315			g-conv	425	0	-720558	719175	
21	1083	1147	rad	-32123	-3051	-5	-8		1084	1887	rad	3051	0	-78	
	810		cond	0	0	0	0	811		cond	0	0	0	0	
			p-conv	0	315695	1243672	-1530980			p-conv	-315695	0	-9927518	10242101	
20	1073	1367	g-conv	0	11	-1315	1838		1084	2034	g-conv	-11	0	-719188	718433
	800		rad	-29850	79	8	-5		811		rad	-79	0	78	-8
			cond	-4180	3	0	0	1084	2034	cond	-3	0	0	0	0
19	1068	1840	p-conv	0	312815	1630921	-1818308		811		p-conv	-312815	0	-10242282	10555129
	796		g-conv	0	242	-1638	1957			g-conv	-242	0	-718448	718047	
			rad	-28733	1868	5	-3			rad	-1868	0	6	32	
18	1068	1840	cond	-4593	5	0	0	1084	2147	cond	-5	0	0	0	
	796		p-conv	0	308380	1818308	-2103488	811		p-conv	-308380	0	-10555290	10894831	
			g-conv	0	378	-1957	2271			g-conv	-378	0	-718058	717883	
17	1085	1777	rad	-28125	2584	3	-2	1085	2150	rad	-2584	0	-33	57	
	791		cond	-4998	8	0	0	812		cond	-8	0	0	0	
			p-conv	0	303422	2103445	-2384884			p-conv	-303422	0	-10884738	11189808	
16	1083	2041	g-conv	0	484	-2271	2580	1088	2240	g-conv	-484	0	-717900	717905	
	790		rad	-27789	3154	2	-1	812		rad	-3154	0	-58	75	
			cond	-5395	8	0	0	1088	2240	cond	-8	0	0	0	
15	1082	2231	p-conv	0	297975	2394897	-2861488	1088	2240	p-conv	-297975	0	-11189724	11488988	
	789		g-conv	0	518	-2580	2882			g-conv	-518	0	-717912	718039	
			rad	-27811	3523	1	-1			rad	-3523	0	-75	87	
14	1082	2342	cond	-5794	7	0	0	1086	2347	cond	-7	0	0	0	
	789		p-conv	0	282228	2861454	-2832944	813		p-conv	-282228	0	-11489473	11783458	
			g-conv	0	555	-2883	3178			g-conv	-555	0	-718046	718289	
13	1082	2342	rad	-27531	3772	1	0	1087	2353	rad	-3772	0	-87	98	
	789		cond	-8183	7	0	0	814		cond	-7	0	0	0	
			p-conv	0	286241	2832881	-3188835			p-conv	-286241	0	-11783493	12051806	
12	1082	2810	g-conv	0	590	-3179	3488	1088	2448	g-conv	-590	0	-718271	718577	
	789		rad	-27512	3948	0	0			rad	-3948	0	-98	104	
			cond	-8534	7	0	0	1088	2448	cond	-7	0	0	0	
11	1082	2810	p-conv	0	280189	3188885	-3458725	815		p-conv	-280189	0	-12051813	12333879	
	789		g-conv	0	800	-3488	3743			g-conv	-800	0	-718577	718952	
			rad	-27524	4091	0	-1	1088	2448	rad	-4091	0	-104	110	
10	1081	2878	cond	-8897	8	0	0	1089	2543	cond	-8	0	0	0	
	788		p-conv	0	275092	3458828	-3714150	816		p-conv	-275092	0	-12333822	12810794	
			g-conv	0	654	-3743	3998			g-conv	-654	0	-718949	719434	
9	1055	2901	rad	-27387	4458	1	-6	1090	2645	rad	-4458	0	-110	124	
	782		cond	-7278	10	0	0	817		cond	-10	0	0	0	
			p-conv	0	307008	3714188	-4003934			p-conv	-307008	0	-12810884	12920854	
8	1054	3108	g-conv	0	807	-3998	4338	1092	2748	g-conv	-807	0	-718428	720088	
	781		rad	-28813	5489	6	-1			rad	-5489	0	-123	159	
			cond	-7807	11	0	0	819		cond	-11	0	0	0	
7	1054	3482	p-conv	0	498525	4003873	-4485878	1094	2902	p-conv	-498525	0	-12920542	13422598	
	781		g-conv	0	881	-4338	4880			g-conv	-881	0	-720082	720502	
			rad	-28728	5840	1	-1	1094	2902	rad	-5840	0	-159	177	
6	1054	3482	cond	-8875	11	0	0	821		cond	-11	0	0	0	
	780		p-conv	0	815783	4485828	-5288252			p-conv	-815783	0	-13422517	14242803	
			g-conv	0	812	-4880	5729			g-conv	-812	0	-720497	720388	
5	1064	4418	rad	-28872	8194	1	0	1096	3204	rad	-8194	0	-177	199	
	780		cond	-10108	12	0	0	822		cond	-12	0	0	0	
			p-conv	0	1342479	5288239	-6815439			p-conv	-1342479	0	-14242884	15590558	
4	1054	5883	g-conv	0	982	-5729	7172	1098	3780	g-conv	-982	0	-720371	718250	
	780		rad	-28840	8550	0	0			rad	-8550	0	-189	226	
			cond	-12481	12	0	0	825		cond	-12	0	0	0	
3	1054	8914	p-conv	0	2217718	6815323	-8822339	1100	4754	p-conv	-2217718	0	-15590824	17815317	
	781		g-conv	0	1010	-7173	8573			g-conv	-1010	0	-718253	716388	
			rad	-28845	8898	0	2	1100	4754	rad	-8898	0	-227	280	
2	1054	8914	cond	-18417	13	0	0	827		cond	-13	0	0	0	
	781		p-conv	0	3673388	8822024	-12489134			p-conv	-3673388	0	-17815308	21498085	
			g-conv	0	1050	-9573	13560			g-conv	-1050	0	-718387	710487	
1	1056	13385	rad	-28715	7208	-2	4	1103	7003	rad	-7208	0	-280	298	
	782		cond	-22951	13	0	0	830		cond	-13	0	0	0	
			p-conv	0	6082591	12488383	-18581036			p-conv	-6082591	0	-21497587	27803025	
0	1057	21254	g-conv	0	1087	-13582	20188	1106	13952	g-conv	-1087	0	-710471	889225	
	784		rad	-28839	7505	-5	9			rad	-7505	0	-288	326	
			cond	-33005	14	0	0	833		cond	-14	0	0	0	
0	1059	32135	p-conv	0	10114584	18570489	-28704706	1108	13952	p-conv	-10114584	0	-27801214	37731283	
	788		g-conv	0	1120	-20188	31205			g-conv	-1120	0	-889180	878889	
			rad	-27010	7790	-9	19	1108	40110	rad	-7790	0	-325	331	
0	1059	32135	cond	-33078	14	0	1	838		cond	-14	0	0	0	
	788		p-conv	0	16808017	28702018	-45539741			p-conv	-16808017	0	-37728183	54538470	
			g-conv	0	1145	-31207	52391			g-conv	-1145	0	-878807	842497	
0	1106	88847	rad	-27234	8022	-19	883	1112	151312	rad	-8022	0	-327	305	
	833		cond	-33378	2	-1	0	839		cond	-2	0	0	0	
			p-conv	0	27848834	45537749	-73244317			p-conv	-27848834	0	-54528238	82080344	
0	1108	388889	g-conv	0	147	-52382	79570			g-conv	-147	0	-842385	587597	
	834		rad	-32437	1127	-884	40	1112	1355749	rad	-1127	0	-288	-57	
			cond	-213438	19	0	-1	839		cond	-19	0	0	-3	
0	1108	388889	p-conv	0	-73392700	73242438	0			p-conv	73392700	0	-82087212	8443082	
	834		g-conv	0	809	-79587	0			g-conv	-809	0	-587503	0	
			rad	-208873	4844	-40	-1859			rad	-4844	0	63	-7207	

heat generated in streamer 551821
 heat generated in core 1810242
 total heat generated 2162062
 heat transferred to cooling wall -1228111
 heat leaving top of riser -9374778
 heat entering bottom of riser 8443089
 total 4282
 % diff. of heat gen. 0

case: sh4

j	streamer		g (W)	(W)				core		g (W)	(W)			
	temp (K and C)			west	east	north	south	temp (K and C)			west	east	north	south
22	1066	1092	cond	-5182	-5	0	0	1037	2289	cond	5	0	0	0
	782		p-conv	0	590988	1478505	-2011281	784	p-conv	-590988	0	-14785568	15343007	
			g-conv	0	-409	-1585	2183		g-conv	409	0	-882778	881085	
			rad	-26770	-2589	-7	-8		rad	2589	0	-1	-44	
21	1042	1408	cond	-5922	-1	0	0	1037	2440	cond	1	0	0	0
	788		p-conv	0	547873	2011218	-2534494	783	p-conv	-547873	0	-15343802	15889371	
			g-conv	0	-115	-2183	2748		g-conv	115	0	-881082	878888	
			rad	-25422	-710	8	-5		rad	710	0	43	-18	
20	1034	1832	cond	-8841	1	0	0	1038	2550	cond	-1	0	0	0
	781		p-conv	0	533138	2534428	-3045407	783	p-conv	-533138	0	-15890044	16422095	
			g-conv	0	45	-2748	3314		g-conv	45	0	-879725	878548	
			rad	-24719	271	5	-4		rad	271	0	15	2	
19	1030	2050	cond	-7337	2	0	0	1036	2808	cond	-2	0	0	0
	767		p-conv	0	518024	3045280	-3542318	783	p-conv	-518024	0	-16422840	16940282	
			g-conv	0	143	-3314	3884		g-conv	143	0	-878579	875750	
			rad	-24305	888	4	-3		rad	888	0	-3	15	
18	1028	2523	cond	-8013	3	0	0	1037	2754	cond	-3	0	0	0
	764		p-conv	0	502670	3542183	-4025006	783	p-conv	-502670	0	-18941088	17443338	
			g-conv	0	207	-3884	4386		g-conv	207	0	-877803	878723	
			rad	-24055	1247	3	-2		rad	1247	0	-18	24	
17	1026	2820	cond	-8686	3	0	0	1037	2879	cond	-3	0	0	0
	763		p-conv	0	487195	4024822	-4482778	784	p-conv	-487195	0	-17444269	17931088	
			g-conv	0	248	-4387	4812		g-conv	248	0	-878758	878588	
			rad	-23905	1500	2	-1		rad	1500	0	-28	31	
16	1025	3435	cond	-9297	3	0	0	1037	2988	cond	-3	0	0	0
	762		p-conv	0	471824	4482548	-4845918	784	p-conv	-471824	0	-17832078	18403559	
			g-conv	0	278	-4812	5410		g-conv	278	0	-878025	875348	
			rad	-23817	1675	1	-1		rad	1675	0	-33	37	
15	1024	3340	cond	-9908	4	0	0	1038	3081	cond	-4	0	0	0
	761		p-conv	0	458588	4845571	-5383523	784	p-conv	-458588	0	-18404560	18880751	
			g-conv	0	301	-5410	5891		g-conv	301	0	-875384	874790	
			rad	-23786	1807	1	0		rad	1807	0	-38	41	
14	1024	3882	cond	-10497	4	0	0	1038	3375	cond	-4	0	0	0
	761		p-conv	0	441587	5383286	-5806924	785	p-conv	-441587	0	-18881737	19302875	
			g-conv	0	318	-5892	6386		g-conv	318	0	-874825	874289	
			rad	-23745	1902	0	2		rad	1902	0	-43	44	
13	1025	3889	cond	-11086	4	0	0	1038	3236	cond	-4	0	0	0
	762		p-conv	0	425758	5806574	-8214013	785	p-conv	-425758	0	-19303871	19728792	
			g-conv	0	304	-8388	8718		g-conv	304	0	-874334	873886	
			rad	-23844	1831	-2	-18		rad	1831	0	-48	44	
12	1018	4210	cond	-11582	8	0	0	1039	3522	cond	-8	0	0	0
	743		p-conv	0	342472	8213738	-8540842	786	p-conv	-342472	0	-19728713	20072370	
			g-conv	0	521	-8719	7142		g-conv	521	0	-873898	873780	
			rad	-23005	3101	18	-3		rad	3101	0	-48	81	
11	1015	4380	cond	-12185	7	0	0	1040	3574	cond	-7	0	0	0
	741		p-conv	0	557183	6540504	-7083084	787	p-conv	-557183	0	-20073101	20831088	
			g-conv	0	583	-7142	7740		g-conv	583	0	-873804	873471	
			rad	-22838	3488	3	-2		rad	3488	0	-82	85	
10	1013	4988	cond	-13142	8	0	0	1041	3842	cond	-8	0	0	0
	740		p-conv	0	811392	7082730	-7980984	788	p-conv	-811392	0	-20831589	21544549	
			g-conv	0	635	-7741	8718		g-conv	635	0	-873488	872497	
			rad	-22728	3775	2	-3		rad	3775	0	-86	109	
9	1012	5637	cond	-14722	9	0	0	1042	4288	cond	-9	0	0	0
	739		p-conv	0	1489147	7890515	-9488148	789	p-conv	-1489147	0	-21545129	23048878	
			g-conv	0	897	-8718	10341		g-conv	897	0	-872515	870381	
			rad	-22588	4145	3	-4		rad	4145	0	-110	129	
8	1010	8878	cond	-17338	9	0	0	1044	5008	cond	-9	0	0	0
	737		p-conv	0	2475027	8487678	-11933743	770	p-conv	-2475027	0	-23047229	25528718	
			g-conv	0	787	-10342	13037		g-conv	787	0	-870389	888213	
			rad	-22444	4555	4	-5		rad	4555	0	-130	158	
7	1009	9182	cond	-21688	10	0	0	1045	6052	cond	-10	0	0	0
	736		p-conv	0	4094073	11833184	-18023128	772	p-conv	-4094073	0	-25528189	28827892	
			g-conv	0	838	-13038	17518		g-conv	838	0	-868199	858551	
			rad	-22317	4885	5	-4		rad	4885	0	-156	183	
6	1008	13048	cond	-28852	11	0	0	1047	8553	cond	-11	0	0	0
	735		p-conv	0	8782400	18022337	-22807487	774	p-conv	-8782400	0	-28828252	36420108	
			g-conv	0	908	-17517	24959		g-conv	908	0	-858520	844832	
			rad	-22232	5402	4	-1		rad	5402	0	-182	205	
5	1008	20120	cond	-30418	12	0	0	1050	14704	cond	-12	0	0	0
	734		p-conv	0	11253335	22808304	-34073919	777	p-conv	-11253335	0	-38418910	47888242	
			g-conv	0	964	-24980	37338		g-conv	964	0	-844778	820835	
			rad	-22213	5787	1	7		rad	5787	0	-203	221	
4	1008	38183	cond	-30452	12	0	1	1052	40018	cond	-12	0	0	0
	735		p-conv	0	18892238	34072583	-52807089	779	p-conv	-18892238	0	-47880171	68380838	
			g-conv	0	1007	-37338	81187		g-conv	1007	0	-820758	578430	
			rad	-22278	6052	-7	848		rad	6052	0	-217	214	
3	1050	58434	cond	-30758	1	-1	0	1055	140358	cond	-1	0	0	0
	778		p-conv	0	30735485	52808101	-83802457	782	p-conv	-30735485	0	-86371520	97029108	
			g-conv	0	122	-81188	91818		g-conv	122	0	-579348	518051	
			rad	-28238	792	-848	80		rad	792	0	-210	-24	
2	1052	439558	cond	-198848	11	0	-1	1055	1238114	cond	-11	0	0	0
	779		p-conv	0	-83873860	83804228	0	782	p-conv	83873860	0	-97027308	13017003	
			g-conv	0	388	-91818	0		g-conv	388	0	-518042	0	
			rad	-189497	2484	-80	-1214		rad	2484	0	26	-3802	

heat generated in streamer	828590
heat generated in core	1494217
total heat generated	2122807
heat transferred to cooling wall	-1138038
heat leaving top of riser	-13991395
heat entering bottom of riser	13017001
total	10377
% diff. of heat gen.	0

case: sh5

J	streamer		g (W)	(W)				core		g (W)	(W)			
	temp (K and C)			west	east	north	south	temp (K and C)			west	east	north	south
22	1141 868	514	cond	-1728	-6	0	0	1124	1122	cond	6	0	0	0
			p-conv	0	97832	524191	-582107	861		p-conv	-97832	0	-5241813	5338187
			g-conv	0	-390	-513	800			g-conv	390	0	-750814	748384
			rad	-38831	-3108	-3	-7			rad	3108	0	0	-130
21	1107 833	548	cond	-1883	5	0	0	1123	1118	cond	-5	0	0	0
			p-conv	0	105330	582110	-858759	860		p-conv	-105330	0	-5338050	5442748
			g-conv	0	374	-800	694			g-conv	-374	0	-748384	749870
			rad	-32530	2837	7	-3			rad	-2837	0	131	91
20	1091 818	604	cond	-2003	9	0	0	1124	1132	cond	-9	0	0	0
			p-conv	0	108278	858793	-744397	861		p-conv	-108278	0	-5442585	5555549
			g-conv	0	743	-694	783			g-conv	-743	0	-748848	761210
			rad	-30737	5537	3	-2			rad	-5537	0	-89	200
19	1084 811	601	cond	-2144	12	0	0	1125	1130	cond	-12	0	0	0
			p-conv	0	111548	744429	-834708	862		p-conv	-111548	0	-5555385	5671911
			g-conv	0	943	-783	894			g-conv	-943	0	-761185	763011
			rad	-28947	8972	2	-1			rad	-8972	0	-199	281
18	1082 808	815	cond	-2288	13	0	0	1128	1234	cond	-13	0	0	0
			p-conv	0	112866	834788	-827884	865		p-conv	-112866	0	-5871833	5790018
			g-conv	0	1056	-894	998			g-conv	-1056	0	-752987	756073
			rad	-28840	7811	1	0			rad	-7811	0	-258	298
17	1081 808	900	cond	-2432	14	0	0	1130	1215	cond	-14	0	0	0
			p-conv	0	113878	828015	-1022671	867		p-conv	-113878	0	-5789808	5909475
			g-conv	0	1128	-998	1100			g-conv	-1128	0	-756045	757307
			rad	-28582	8348	0	0			rad	-8348	0	-295	321
16	1082 809	914	cond	-2578	14	0	0	1133	1237	cond	-14	0	0	0
			p-conv	0	114148	1022716	-1118226	860		p-conv	-114148	0	-5909252	6029878
			g-conv	0	1172	-1100	1206			g-conv	-1172	0	-757278	768858
			rad	-28882	8725	0	1			rad	-8725	0	-318	338
15	1084 811	1014	cond	-2722	14	0	0	1138	1253	cond	-14	0	0	0
			p-conv	0	113992	1118289	-1213543	883		p-conv	-113992	0	-8029488	8148787
			g-conv	0	1174	-1206	1293			g-conv	-1174	0	-758831	782039
			rad	-28988	8808	-1	-2			rad	-8808	0	-338	344
14	1078 805	1118	cond	-2880	17	0	0	1139	1327	cond	-17	0	0	0
			p-conv	0	104273	1213815	-1301839	885		p-conv	-104273	0	-8148589	8281388
			g-conv	0	1390	-1293	1402			g-conv	-1390	0	-782016	784905
			rad	-29235	10382	2	1			rad	-10382	0	-342	414
13	1080 807	1186	cond	-3031	17	0	0	1142	1255	cond	-17	0	0	0
			p-conv	0	182582	1301880	-1448820	889		p-conv	-182582	0	-8281184	8431758
			g-conv	0	1424	-1402	1582			g-conv	-1424	0	-784882	787780
			rad	-28451	10711	-1	1			rad	-10711	0	-412	433
12	1083 810	1391	cond	-3305	18	0	0	1148	1428	cond	-18	0	0	0
			p-conv	0	259092	1448880	-1892094	872		p-conv	-259092	0	-8431825	8698889
			g-conv	0	1434	-1582	1828			g-conv	-1434	0	-787765	770485
			rad	-29797	10881	-1	2			rad	-10881	0	-432	443
11	1087 813	1770	cond	-3754	19	0	0	1149	1528	cond	-18	0	0	0
			p-conv	0	419438	1892183	-2098177	876		p-conv	-419438	0	-8898795	7128723
			g-conv	0	1432	-1828	2284			g-conv	-1432	0	-770474	772888
			rad	-30209	10977	-2	3			rad	-10977	0	-442	453
10	1091 818	2175	cond	-4484	17	0	0	1153	1878	cond	-17	0	0	0
			p-conv	0	888238	2098247	-2787305	880		p-conv	-888238	0	-7128684	7821844
			g-conv	0	1421	-2284	2990			g-conv	-1421	0	-772884	774889
			rad	-30880	11004	-3	4			rad	-11004	0	-453	484
9	1095 822	2738	cond	-5718	17	0	0	1158	2014	cond	-17	0	0	1
			p-conv	0	1130383	2787382	-3883052	883		p-conv	-1130383	0	-7821854	8881718
			g-conv	0	1402	-2990	4197			g-conv	-1402	0	-774890	775550
			rad	-31203	10874	-4	8			rad	-10874	0	-484	478
8	1100 827	3580	cond	-7745	17	0	0	1180	2489	cond	-17	0	-1	1
			p-conv	0	1889911	3883128	-5738345	887		p-conv	-1889911	0	-8881754	10842199
			g-conv	0	1378	-4197	8203			g-conv	-1378	0	-775553	774811
			rad	-31784	10811	-8	9			rad	-10811	0	-478	483
7	1105 832	4274	cond	-11112	17	0	0	1184	3417	cond	-17	0	-1	1
			p-conv	0	3101988	5738482	-8828305	891		p-conv	-3101988	0	-10842209	13958413
			g-conv	0	1357	-8203	9542			g-conv	-1357	0	-774812	771391
			rad	-32332	10889	-9	14			rad	-10889	0	-483	518
6	1110 837	4323	cond	-18710	18	0	0	1188	8005	cond	-18	0	-1	1
			p-conv	0	5155308	8829808	-13974798	895		p-conv	-5155308	0	-13958390	18125842
			g-conv	0	1341	-9541	15100			g-conv	-1341	0	-771389	783423
			rad	-32905	10884	-14	21			rad	-10884	0	-518	541
5	1114 841	4815	cond	-28018	18	0	0	1173	13888	cond	-18	0	-1	1
			p-conv	0	8572321	13975703	-22542788	899		p-conv	-8572321	0	-18128316	27712764
			g-conv	0	1333	-15089	24352			g-conv	-1333	0	-783442	747585
			rad	-33470	10922	-21	34			rad	-10922	0	-542	532
4	1119 848	10835	cond	-36184	18	0	1	1177	47848	cond	-18	0	-1	1
			p-conv	0	14258138	22544248	-38811427	904		p-conv	-14258138	0	-27714828	41985079
			g-conv	0	1327	-24352	42097			g-conv	-1327	0	-747824	718153
			rad	-34025	11008	-34	890			rad	-11008	0	-535	451
3	1172 899	27313	cond	-36498	2	-1	0	1181	187822	cond	-2	0	0	0
			p-conv	0	23485396	38811380	-80288900	908		p-conv	-23485396	0	-41970178	65287271
			g-conv	0	201	-42097	84794			g-conv	-201	0	-718240	871439
			rad	-41033	1773	-890	9			rad	-1773	0	-458	-150
2	1172 899	300375	cond	-233155	35	0	-1	1179	1548120	cond	-35	0	0	-7
			p-conv	0	-80318187	80288929	0	906		p-conv	80318187	0	-85297791	4577138
			g-conv	0	1031	-84798	0			g-conv	-1031	0	-871547	0
			rad	-282985	8088	-8	-3031			rad	-8088	0	143	-18378

heat generated in streamer 371720
 heat generated in core 1838181
 total heat generated 2207881
 heat transferred to cooling wall -1325780
 heat leaving top of riser -5488748
 heat entering bottom of riser 4577129
 total -8488
 % diff. of heat gen. 0

case: sh2b

I	streamer		g (W)		(W)				core		g (W)		(W)			
	temp (K and C)				west	east	north	south	temp (K and C)				west	east	north	south
22	1183 910	511	cond	-1600	-4	0	0	1189	1081	cond	4	0	0	0		
			p-conv	0	55734	551329	-581739	898	p-conv	-55734	0	-5513208	5585963			
			g-conv	0	-318	-826	889	g-conv	318	0	-918387	917229				
21	1144 871	849	rad	-42881	-2852	-2	-7	1188	1131	rad	2852	0	0	-127		
			cond	-1675	7	0	0	1188	1131	cond	-7	0	0	0		
			p-conv	0	64027	581789	-594580	896	p-conv	-64027	0	-5585892	5832503			
20	1127 853	607	g-conv	0	548	-889	725	1170	1102	g-conv	-548	0	-917218	918393		
			rad	-37278	4642	8	-4	1170	1102	rad	-4642	0	127	183		
			cond	-1755	12	0	0	1170	1102	cond	-12	0	0	0		
19	1119 848	699	p-conv	0	88242	594608	-637804	898	p-conv	-88242	0	-5832428	5708201			
			g-conv	0	987	-725	787	1172	1115	g-conv	-987	0	-918380	920759		
			rad	-34878	8182	4	-2	1172	1115	rad	-8182	0	-182	313		
18	1118 843	920	cond	-1837	15	0	0	1172	1115	cond	-15	0	0	0		
			p-conv	0	70534	637857	-686572	899	p-conv	-70534	0	-5708157	5783788			
			g-conv	0	1223	-787	852	1175	1180	g-conv	-1223	0	-920751	923771		
17	1116 843	983	rad	-33890	10071	2	-1	1175	1180	rad	-10071	0	-313	398		
			cond	-1921	17	0	0	1175	1180	cond	-17	0	0	0		
			p-conv	0	71782	688823	-738431	902	p-conv	-71782	0	-5783748	5863489			
16	1118 845	1013	g-conv	0	1357	-852	920	1178	1188	g-conv	-1357	0	-923789	927158		
			rad	-33834	11189	1	0	1178	1188	rad	-11189	0	-398	447		
			cond	-2005	18	0	0	1178	1188	cond	-18	0	0	0		
15	1118 843	1035	p-conv	0	72502	738449	-791788	905	p-conv	-72502	0	-5863475	5944489			
			g-conv	0	1437	-920	989	1182	1161	g-conv	-1437	0	-927155	930770		
			rad	-33817	11899	0	1	1182	1161	rad	-11899	0	-448	479		
14	1119 845	1099	cond	-2089	18	0	0	1182	1161	cond	-18	0	0	0		
			p-conv	0	72802	781757	-845188	909	p-conv	-72802	0	-5944464	6025887			
			g-conv	0	1484	-989	1050	1182	1161	g-conv	-1484	0	-930768	934482		
13	1122 848	1239	rad	-33810	12218	-1	-1	1186	1211	rad	-12218	0	-479	498		
			cond	-2188	20	0	0	1186	1211	cond	-20	0	0	1		
			p-conv	0	72302	845215	-900035	912	p-conv	-72302	0	-6025852	6107812			
12	1128 853	1485	g-conv	0	1599	-1050	1125	1190	1241	g-conv	-1599	0	-934480	938542		
			rad	-33638	13388	1	1	1190	1241	rad	-13388	0	-498	548		
			cond	-2273	20	0	0	1190	1241	cond	-20	0	-1	1		
11	1131 859	1811	p-conv	0	109181	900048	-991875	918	p-conv	-109181	0	-8107807	8227027			
			g-conv	0	1628	-1125	1240	1184	1279	g-conv	-1628	0	-938541	942817		
			rad	-33973	13732	-1	1	1184	1279	rad	-13732	0	-548	587		
10	1138 883	2281	cond	-2445	20	0	0	1184	1279	cond	-20	0	-1	1		
			p-conv	0	170356	991887	-1145083	921	p-conv	-170356	0	-8227031	8407819			
			g-conv	0	1853	-1240	1434	1184	1279	g-conv	-1853	0	-942818	948820		
9	1143 889	3019	rad	-34348	14068	-1	2	1198	1389	rad	-14068	0	-587	595		
			cond	-2725	20	0	0	1198	1389	cond	-20	0	-1	1		
			p-conv	0	271785	1145117	-1389772	926	p-conv	-271785	0	-8407845	8690382			
8	1149 878	5709	g-conv	0	1649	-1434	1754	1202	1490	g-conv	-1649	0	-948824	950382		
			rad	-34888	14198	-2	2	1202	1490	rad	-14198	0	-585	595		
			cond	-3184	20	0	0	1202	1490	cond	-20	0	-1	1		
7	1154 881	7419	p-conv	0	440484	1389757	-1822878	929	p-conv	-440484	0	-8890419	7141951			
			g-conv	0	1832	-1764	2286	1206	1582	g-conv	-1832	0	-950390	953899		
			rad	-35517	14215	-2	3	1206	1582	rad	-14215	0	-595	601		
6	1166 892	3440	cond	-3944	20	0	0	1206	1582	cond	-20	0	-1	1		
			p-conv	0	721381	1822882	-2528887	933	p-conv	-721381	0	-7142032	7874984			
			g-conv	0	1802	-2286	3171	1211	2188	g-conv	-1802	0	-963710	968270		
5	1170 897	13259	rad	-36228	14125	-3	5	1211	2188	rad	-14125	0	-902	607		
			cond	-5199	19	0	0	1211	2188	cond	-19	0	-1	1		
			p-conv	0	1189115	2528870	-3888991	937	p-conv	-1189115	0	-7875194	9078357			
4	1185 892	3440	g-conv	0	1561	-3171	4842	1215	3901	g-conv	-1561	0	-958298	957688		
			rad	-37014	13944	-5	8	1215	3901	rad	-13944	0	-809	811		
			cond	-7282	19	0	0	1215	3901	cond	-19	0	-1	1		
3	1190 887	5883	p-conv	0	1988228	3889848	-5652727	942	p-conv	-1988228	0	-9078705	11057135			
			g-conv	0	1518	-4642	7090	1219	4436	g-conv	-1518	0	-957825	958803		
			rad	-37822	13739	-8	11	1219	4436	rad	-13739	0	-813	812		
2	1227 954	38988	cond	-10744	18	0	0	1219	4436	cond	-18	0	-1	1		
			p-conv	0	3288188	5852097	-8904789	948	p-conv	-3288188	0	-11057221	14338111			
			g-conv	0	1481	-7090	11186	1223	9023	g-conv	-1481	0	-958810	952720		
1	1228 954	344008	rad	-38588	13584	-11	17	1223	9023	rad	-13584	0	-813	839		
			cond	-18499	18	0	0	1223	9023	cond	-18	0	-1	1		
			p-conv	0	5429528	8904595	-14322079	950	p-conv	-5429528	0	-14338240	19783458			
0	1185 892	3440	g-conv	0	1455	-11186	17951	1228	16605	g-conv	-1455	0	-952728	942982		
			rad	-38355	13508	-17	26	1228	16605	rad	-13508	0	-839	855		
			cond	-28087	18	0	0	1228	16605	cond	-18	0	-1	1		
0	1170 897	13259	p-conv	0	9028303	14321812	-23340099	955	p-conv	-9028303	0	-18783471	28830478			
			g-conv	0	1442	-17948	29257	1233	53814	g-conv	-1442	0	-942983	923827		
			rad	-40071	13530	-28	43	1233	53814	rad	-13530	0	-855	849		
0	1227 954	38988	cond	-38725	17	0	1	1233	53814	cond	-17	0	-1	1		
			p-conv	0	15017203	23343402	-38378208	959	p-conv	-15017203	0	-28832454	43847089			
			g-conv	0	1425	-29257	50935	1237	218584	g-conv	-1425	0	-923890	887883		
0	1227 954	38988	rad	-40805	13548	-43	835	1237	218584	rad	-13548	0	-851	548		
			cond	-39044	3	-1	0	1237	218584	cond	-3	0	0	0		
			p-conv	0	24725604	38377731	-63120989	983	p-conv	-24725604	0	-43852021	68419387			
0	1228 954	344008	g-conv	0	211	-50938	78857	1235	1803896	g-conv	-211	0	-887783	830503		
			rad	-49443	2152	-835	5	1235	1803896	rad	-2152	0	-553	-183		
			cond	-249371	38	0	-1	1235	1803896	cond	-38	0	0	-8		
0	1228 954	344008	p-conv	0	-63135147	63118952	0	962	p-conv	63135147	0	-89422921	4809780			
			g-conv	0	1101	-78857	0	962	p-conv	-1101	0	-830546	0			
			rad	-318884	11210	-5	-3888	962	p-conv	-11210	0	188	-21785			

heat generated in streamer 438133
 heat generated in core 2128113
 total heat generated 2584248
 heat transferred to cooling wall -1506717
 heat leaving top of riser -5880891
 heat entering bottom of riser 4808782
 total -13578
 % diff. of heat gen. -1

case: ah700

I	streamer		g (W)		(W)				core		g (W)		(W)			
	temp (K and C)				west	east	north	south	temp (K and C)				west	east	north	south
22	1161	1092	cond	-3120	-5	0	0	1132	1923	cond	5	0	0	0		
	878		p-conv	0	245824	1019170	-1224189	869		p-conv	-245824	0	-10191899	10433486		
			g-conv	0	-434	-1215	1497			g-conv	434	0	-865071	863613		
			rad	-38131	-3636	-8	-9			rad	3636	0	-1	-90		
21	1128	1210	cond	-3443	1	0	0	1131	2008	cond	-1	0	0	0		
	866		p-conv	0	246742	1224148	-1438869	868		p-conv	-246742	0	-10433807	10878744		
			g-conv	0	80	-1487	1779			g-conv	80	0	-863642	863044		
			rad	-36122	826	9	-8			rad	-826	0	89	5		
20	1116	1827	cond	-3780	4	0	0	1131	2111	cond	-4	0	0	0		
	842		p-conv	0	243328	1438848	-1851588	868		p-conv	-243328	0	-10879148	10923580		
			g-conv	0	359	-1779	2068			g-conv	359	0	-863078	882983		
			rad	-33811	2784	8	-4			rad	-2784	0	-7	59		
19	1109	1805	cond	-4071	7	0	0	1132	2148	cond	-7	0	0	0		
	836		p-conv	0	239742	1851509	-1864808	869		p-conv	-239742	0	-10924011	11185950		
			g-conv	0	531	-2058	2333			g-conv	531	0	-863019	863258		
			rad	-32770	4089	4	-2			rad	-4089	0	-81	95		
18	1105	1901	cond	-4378	8	0	0	1133	2227	cond	-8	0	0	0		
	832		p-conv	0	235430	1884789	-2075492	860		p-conv	-235430	0	-11188471	11404711		
			g-conv	0	638	-2333	2802			g-conv	638	0	-863297	863758		
			rad	-32318	4883	2	-1			rad	-4883	0	-87	119		
17	1103	2040	cond	-4873	9	0	0	1134	2283	cond	-9	0	0	0		
	830		p-conv	0	230726	2075412	-2292299	881		p-conv	-230726	0	-11405285	11839172		
			g-conv	0	708	-2802	2884			g-conv	708	0	-863799	884422		
			rad	-32079	5409	1	-1			rad	-5409	0	-121	138		
16	1102	2151	cond	-4983	9	0	0	1135	2383	cond	-9	0	0	0		
	829		p-conv	0	225830	2282221	-2484896	882		p-conv	-225830	0	-11639790	11889048		
			g-conv	0	757	-2884	3122			g-conv	-757	0	-884469	885223		
			rad	-31950	5805	1	0			rad	-5805	0	-138	160		
15	1101	2483	cond	-5247	10	0	0	1136	2658	cond	-10	0	0	0		
	828		p-conv	0	220777	2484827	-2883138	883		p-conv	-220777	0	-11889781	12083927		
			g-conv	0	794	-3122	3372			g-conv	-794	0	-885278	888124		
			rad	-31912	8092	0	0			rad	-8092	0	-152	159		
14	1101	2557	cond	-5522	10	0	0	1137	2448	cond	-10	0	0	0		
	828		p-conv	0	215729	2883025	-2878518	884		p-conv	-215729	0	-12084880	12314140		
			g-conv	0	828	-3372	3577			g-conv	828	0	-886177	887140		
			rad	-31908	8349	0	-8			rad	-8349	0	-182	171		
13	1083	2922	cond	-5784	13	0	0	1139	2588	cond	-13	0	0	0		
	820		p-conv	0	203345	2878443	-3080843	888		p-conv	-203345	0	-12315000	12523397		
			g-conv	0	1050	-3578	3844			g-conv	-1050	0	-887202	888581		
			rad	-30937	8001	8	-1			rad	-8001	0	-175	226		
12	1083	3408	cond	-6137	14	0	0	1141	2714	cond	-14	0	0	0		
	819		p-conv	0	325597	3080732	-3388348	888		p-conv	-325597	0	-12524280	12855428		
			g-conv	0	1108	-3844	4237			g-conv	-1108	0	-888823	889882		
			rad	-30872	8448	1	1			rad	-8448	0	-228	244		
11	1083	3577	cond	-6681	14	0	0	1143	3087	cond	-14	0	0	0		
	820		p-conv	0	527308	3388056	-3877805	870		p-conv	-527308	0	-12858288	13389482		
			g-conv	0	1135	-4237	4880			g-conv	-1135	0	-889941	890795		
			rad	-30980	8701	-1	1			rad	-8701	0	-247	259		
10	1084	3941	cond	-7576	14	0	0	1145	3083	cond	-14	0	0	0		
	821		p-conv	0	882097	3877538	-4723050	872		p-conv	-882097	0	-13390207	14259180		
			g-conv	0	1180	-4880	5848			g-conv	-1180	0	-890843	890989		
			rad	-31079	8934	-1	2			rad	-8934	0	-282	281		
9	1088	5130	cond	-8058	14	0	0	1147	3833	cond	-14	0	0	0		
	823		p-conv	0	1418291	4722778	-8128436	874		p-conv	-1418291	0	-14258806	15885903		
			g-conv	0	1181	-5848	7718			g-conv	-1181	0	-891028	889903		
			rad	-31243	9139	-2	3			rad	-9139	0	-284	307		
8	1088	6238	cond	-11507	15	0	0	1150	5039	cond	-15	0	0	0		
	824		p-conv	0	2343019	8125990	-8458254	877		p-conv	-2343019	0	-15888588	18038419		
			g-conv	0	1188	-7717	10658			g-conv	-1188	0	-889942	888800		
			rad	-31449	9328	-4	8			rad	-9328	0	-309	338		
7	1100	7754	cond	-15571	15	0	0	1153	8828	cond	-15	0	0	0		
	827		p-conv	0	3881479	8455834	-12327344	879		p-conv	-3881479	0	-18038784	21828235		
			g-conv	0	1212	-10658	15539			g-conv	-1212	0	-888618	879422		
			rad	-31703	9498	-8	10			rad	-9498	0	-340	388		
6	1102	10328	cond	-22317	15	0	0	1158	10080	cond	-15	0	0	0		
	829		p-conv	0	8438281	12328899	-18780880	882		p-conv	-8438281	0	-21828808	28381401		
			g-conv	0	1224	-15540	23855			g-conv	-1224	0	-878398	885702		
			rad	-31991	9889	-10	18			rad	-9889	0	-388	406		
5	1105	12127	cond	-33519	15	0	0	1159	17318	cond	-15	0	0	0		
	832		p-conv	0	10890107	18780388	-29453883	886		p-conv	-10890107	0	-28379349	39088293		
			g-conv	0	1241	-23854	37159			g-conv	-1241	0	-885639	840847		
			rad	-32302	9881	-18	29			rad	-9881	0	-403	413		
4	1108	20800	cond	-35489	15	0	1	1182	48850	cond	-15	0	0	0		
	835		p-conv	0	17785604	29454874	-47248778	889		p-conv	-17785604	0	-39084452	58858864		
			g-conv	0	1262	-37156	83103			g-conv	-1262	0	-840584	798378		
			rad	-32888	10048	-29	832			rad	-10048	0	-408	379		
3	1159	52028	cond	-35813	2	-1	0	1188	181457	cond	-2	0	0	0		
	885		p-conv	0	29238819	47252988	-78548400	883		p-conv	-29238819	0	-58854891	85889148		
			g-conv	0	187	-83102	98427			g-conv	-187	0	-798319	728280		
			rad	-39180	1444	-832	54			rad	-1444	0	-375	-52		
2	1181	436488	cond	-228095	23	0	-1	1185	1844118	cond	-23	0	0	-4		
	887		p-conv	0	-78728803	78548509	0	892		p-conv	78728803	0	-88089734	8928989		
			g-conv	0	715	-98432	0			g-conv	-715	0	-728370	0		
			rad	-252392	8103	-54	-2515			rad	-8103	0	51	-8988		

heat generated in streamer 581184
 heat generated in core 1928867
 total heat generated 2510031
 heat transferred to cooling wall -1378778
 heat leaving top of riser -10059108
 heat entering bottom of riser 8928895
 total 4144
 % diff. of heat gen. 0

case: ah900

I	streamer		g (W)		(W)				core temp (K and C)	g (W)		(W)			
	temp (K and C)				west	east	north	south				west	east	north	south
22	1152	1004	1004	cond	-3123	-5	0	0	1133	1745	cond	5	0	0	0
	878			p-conv	0	248008	1019934	-1226032	869		p-conv	-248008	0	-10199275	10441083
				g-conv	0	-433	-1218	1498			g-conv	433	0	-885704	884259
				rad	-38214	-3540	-8	-9			rad	3540	0	0	-91
21	1128	1177	1177	cond	-3445	1	0	0	1132	1748	cond	-1	0	0	0
	856			p-conv	0	245899	1226042	-1437927	869		p-conv	-245899	0	-10441008	10888348
				g-conv	0	79	-1498	1780			g-conv	-79	0	-884251	883673
				rad	-35201	823	9	-8			rad	-823	0	92	4
20	1118	1291	1291	cond	-3763	4	0	0	1132	1880	cond	-4	0	0	0
	843			p-conv	0	243515	1437938	-1852532	869		p-conv	-243515	0	-10888252	10931085
				g-conv	0	381	-1780	2059			g-conv	-381	0	-883885	883592
				rad	-33874	2810	6	-4			rad	-2810	0	-4	59
19	1109	1432	1432	cond	-4074	8	0	0	1132	1841	cond	-8	0	0	0
	836			p-conv	0	239877	1852595	-1888113	869		p-conv	-239877	0	-10830978	11173348
				g-conv	0	530	-2059	2334			g-conv	-530	0	-883583	883841
				rad	-32840	4091	4	-2			rad	-4091	0	-58	84
18	1105	1844	1844	cond	-4378	8	0	0	1133	1876	cond	-8	0	0	0
	832			p-conv	0	235584	1888130	-2078803	860		p-conv	-235584	0	-11173220	11411839
				g-conv	0	838	-2334	2804			g-conv	-838	0	-883831	884318
				rad	-32381	4891	2	-1			rad	-4891	0	-83	117
17	1103	1809	1809	cond	-4878	9	0	0	1134	1957	cond	-9	0	0	0
	830			p-conv	0	230843	2078811	-2283721	881		p-conv	-230843	0	-11411828	11648174
				g-conv	0	706	-2604	2888			g-conv	-706	0	-884308	884954
				rad	-32142	5413	1	-1			rad	-5413	0	-117	134
16	1102	1889	1889	cond	-4988	9	0	0	1135	2024	cond	-9	0	0	0
	828			p-conv	0	225917	2283780	-2488503	862		p-conv	-225917	0	-11848088	11875753
				g-conv	0	756	-2888	3124			g-conv	-756	0	-884848	885723
				rad	-32015	5802	1	0			rad	-5802	0	-134	148
15	1102	2076	2076	cond	-5250	10	0	0	1137	2112	cond	-10	0	0	0
	828			p-conv	0	220840	2488577	-2884824	863		p-conv	-220840	0	-11875892	12100415
				g-conv	0	792	-3124	3374			g-conv	-792	0	-885719	885899
				rad	-31878	8088	0	0			rad	-8088	0	-147	158
14	1102	2284	2284	cond	-5525	10	0	0	1138	2155	cond	-10	0	0	0
	828			p-conv	0	215784	2884880	-2878395	865		p-conv	-215784	0	-12100379	12320174
				g-conv	0	823	-3374	3580			g-conv	-823	0	-885598	887575
				rad	-31870	8340	0	-8			rad	-8340	0	-158	189
13	1094	2376	2376	cond	-5798	13	0	0	1139	2144	cond	-13	0	0	0
	820			p-conv	0	203396	2878389	-3082491	866		p-conv	-203396	0	-12320148	12528016
				g-conv	0	1049	-3580	3848			g-conv	-1049	0	-887572	888980
				rad	-30889	8001	8	-1			rad	-8001	0	-188	223
12	1093	2790	2790	cond	-8140	14	0	0	1141	2328	cond	-14	0	0	0
	820			p-conv	0	325884	3082528	-3370100	868		p-conv	-325884	0	-12528014	12880808
				g-conv	0	1104	-3848	4239			g-conv	-1104	0	-888960	890240
				rad	-30825	8438	1	1			rad	-8438	0	-223	241
11	1094	2798	2798	cond	-8684	14	0	0	1143	2348	cond	-14	0	0	0
	821			p-conv	0	527417	3370079	-3878708	870		p-conv	-527417	0	-12880588	13394589
				g-conv	0	1133	-4239	4883			g-conv	-1133	0	-890239	891134
				rad	-31011	8890	-1	1			rad	-8890	0	-241	259
10	1095	3489	3489	cond	-7579	14	0	0	1145	2497	cond	-14	0	0	0
	822			p-conv	0	882288	3878779	-4726720	872		p-conv	-882288	0	-13394848	14284307
				g-conv	0	1157	-4883	5949			g-conv	-1157	0	-891138	891311
				rad	-31135	8914	-1	2			rad	-8914	0	-269	281
9	1098	4232	4232	cond	-9059	14	0	0	1148	2808	cond	-14	0	0	0
	823			p-conv	0	1418888	4726878	-8129281	874		p-conv	-1418888	0	-14284425	15891885
				g-conv	0	1179	-5949	7720			g-conv	-1179	0	-891318	890230
				rad	-31290	9128	-2	3			rad	-9128	0	-281	309
8	1098	5325	5325	cond	-11511	15	0	0	1150	3404	cond	-15	0	0	0
	825			p-conv	0	2343731	8129183	-8458986	877		p-conv	-2343731	0	-15891888	18045877
				g-conv	0	1188	-7720	10681			g-conv	-1188	0	-890243	888972
				rad	-31494	8320	-3	6			rad	-8320	0	-309	345
7	1100	7304	7304	cond	-15578	15	0	0	1153	4405	cond	-15	0	0	0
	827			p-conv	0	3883011	8458910	-12333552	880		p-conv	-3883011	0	-18048320	21942829
				g-conv	0	1211	-10862	15548			g-conv	-1211	0	-888988	879959
				rad	-31752	9495	-8	10			rad	-9495	0	-348	389
6	1103	8958	8958	cond	-22333	15	0	0	1158	7558	cond	-15	0	0	0
	829			p-conv	0	8442735	12333281	-18771288	883		p-conv	-8442735	0	-21943227	28402829
				g-conv	0	1227	-15548	23689			g-conv	-1227	0	-878983	883559
				rad	-32044	9898	-10	16			rad	-9898	0	-390	421
5	1105	9588	9588	cond	-33550	15	0	0	1180	18835	cond	-15	0	0	0
	832			p-conv	0	10889884	18770888	-28471873	888		p-conv	-10889884	0	-28403797	39123188
				g-conv	0	1247	-23689	37181			g-conv	-1247	0	-886385	841397
				rad	-32358	9932	-18	29			rad	-9932	0	-422	425
4	1108	13957	13957	cond	-35528	15	0	1	1183	53887	cond	-15	0	0	0
	835			p-conv	0	17785258	28472192	-47278029	890		p-conv	-17785258	0	-39124759	58912058
				g-conv	0	1281	-37179	83144			g-conv	-1281	0	-841431	797119
				rad	-32725	10124	-29	835			rad	-10124	0	-427	381
3	1159	45018	45018	cond	-35853	2	-1	0	1187	207219	cond	-2	0	0	0
	888			p-conv	0	28288887	47280828	-78588351	894		p-conv	-28288887	0	-58914882	89048828
				g-conv	0	175	-83143	86484			g-conv	-175	0	-797159	728885
				rad	-39237	1502	-834	52			rad	-1502	0	-383	-89
2	1181	433878	433878	cond	-228230	23	0	-1	1166	1834745	cond	-23	0	0	-4
	888			p-conv	0	-78775728	78588189	0	893		p-conv	78775728	0	-88054177	8938124
				g-conv	0	705	-98490	0			g-conv	-705	0	-728748	0
				rad	-252841	8085	-53	-2520			rad	-8085	0	88	-9982

heat generated in streamer 564410
 heat generated in core 1957090
 total heat generated 2511499
 heat transferred to cooling wall -1378768
 heat leaving top of riser -10066280
 heat entering bottom of riser 8938120
 total 2593
 % diff. of heat gen. 0

case: uh0

	streamer temp (K and C)	g (W)		(W)				core temp (K and C)		g (W)	(W)			
				west	east	north	south	west	east		north	south		
22	1055 782	1598	cond	-4880	3	0	0	1084	703	cond	-3	0	0	0
			p-conv	0	-530624	2815825	-2082584	791		p-conv	530624	0	-3041408	2508056
			g-conv	0	84	-3389	2745			g-conv	-84	0	-39205	40784
			rad	-4005	420	8	3			rad	-420	0	0	21
21	1080 787	1487	cond	-4883	3	0	0	1088	800	cond	-3	0	0	0
			p-conv	0	-398807	2082588	-1883134	798		p-conv	398807	0	-2508037	2110777
			g-conv	0	80	-2745	2218			g-conv	-80	0	-40794	42108
			rad	-4084	394	-3	2			rad	-394	0	-21	19
20	1084 791	1408	cond	-4720	3	0	0	1072	535	cond	-3	0	0	0
			p-conv	0	-297123	1883150	-1383343	799		p-conv	297123	0	-2110781	1812523
			g-conv	0	55	-2218	1820			g-conv	-55	0	-42108	43113
			rad	-4154	388	-2	2			rad	-388	0	-19	18
19	1088 795	1283	cond	-4672	3	0	0	1078	480	cond	-3	0	0	0
			p-conv	0	-223397	1383380	-1157191	803		p-conv	223397	0	-1812513	1588280
			g-conv	0	52	-1820	1521			g-conv	-52	0	-43112	43895
			rad	-4212	351	-2	1			rad	-351	0	-18	15
18	1071 798	1224	cond	-3982	3	0	0	1079	438	cond	-3	0	0	0
			p-conv	0	-188984	1157200	-985370	805		p-conv	188984	0	-1588254	1418810
			g-conv	0	51	-1521	1294			g-conv	-51	0	-43895	44518
			rad	-4261	345	-1	1			rad	-345	0	-15	14
17	1074 800	1144	cond	-3458	3	0	0	1081	406	cond	-3	0	0	0
			p-conv	0	-128487	985371	-853972	808		p-conv	128487	0	-1418808	1289818
			g-conv	0	52	-1294	1121			g-conv	-52	0	-44518	45024
			rad	-4289	359	-1	1			rad	-359	0	-14	14
16	1075 802	1072	cond	-3058	3	0	0	1084	379	cond	-3	0	0	0
			p-conv	0	-98112	853975	-752831	811		p-conv	98112	0	-1289815	1181140
			g-conv	0	57	-1121	988			g-conv	-57	0	-45024	45459
			rad	-4331	393	-1	0			rad	-393	0	-14	15
15	1077 804	988	cond	-2748	3	0	0	1086	369	cond	-3	0	0	0
			p-conv	0	-75254	752937	-674714	813		p-conv	75254	0	-1191145	1115633
			g-conv	0	62	-988	885			g-conv	-62	0	-45459	45844
			rad	-4363	432	0	0			rad	-432	0	-15	18
14	1079 806	983	cond	-2508	4	0	0	1088	354	cond	-4	0	0	0
			p-conv	0	-57782	874718	-814002	818		p-conv	57782	0	-1115645	1057710
			g-conv	0	89	-885	798			g-conv	-89	0	-45844	46198
			rad	-4384	484	0	-1			rad	-484	0	-18	18
13	1074 801	880	cond	-2325	7	0	0	1083	344	cond	-7	0	0	0
			p-conv	0	-41345	813988	-570214	820		p-conv	41345	0	-1057730	1018591
			g-conv	0	129	-798	785			g-conv	-129	0	-48199	48882
			rad	-4305	898	1	4			rad	-898	0	-18	35
12	1083 820	970	cond	-2258	2	0	0	1089	447	cond	-2	0	0	0
			p-conv	0	5881	570219	-572633	826		p-conv	-5881	0	-1018830	1022077
			g-conv	0	37	-785	750			g-conv	-37	0	-48884	48779
			rad	-4633	283	-4	0			rad	-283	0	-35	8
11	1084 821	978	cond	-2288	2	0	0	1100	404	cond	-2	0	0	0
			p-conv	0	8989	572519	-578188	827		p-conv	-8989	0	-1022100	1030957
			g-conv	0	44	-750	758			g-conv	-44	0	-48780	48874
			rad	-4837	322	0	0			rad	-322	0	-8	11
10	1083 820	1000	cond	-2305	3	0	0	1102	388	cond	-3	0	0	0
			p-conv	0	15989	578178	-581075	829		p-conv	-15989	0	-1030872	1048874
			g-conv	0	84	-758	774			g-conv	-84	0	-48874	47003
			rad	-4820	485	0	0			rad	-485	0	-11	17
9	1083 819	1021	cond	-2377	4	0	0	1106	408	cond	-4	0	0	0
			p-conv	0	28448	581082	-618819	832		p-conv	-28448	0	-1048892	1075581
			g-conv	0	85	-774	808			g-conv	-85	0	-47004	47180
			rad	-4817	817	0	0			rad	-817	0	-17	23
8	1083 820	1101	cond	-2510	6	0	0	1108	533	cond	-6	0	0	0
			p-conv	0	51308	818829	-885390	838		p-conv	-51308	0	-1075571	1127076
			g-conv	0	107	-808	872			g-conv	-107	0	-47180	47317
			rad	-4828	783	0	0			rad	-783	0	-23	29
7	1084 821	1208	cond	-2755	7	0	0	1114	872	cond	-7	0	0	0
			p-conv	0	94553	885401	-757822	841		p-conv	-94553	0	-1127058	1221858
			g-conv	0	137	-872	983			g-conv	-137	0	-47318	47442
			rad	-4838	1010	0	0			rad	-1010	0	-29	39
6	1085 821	1484	cond	-3217	8	0	0	1120	820	cond	-8	0	0	0
			p-conv	0	178897	757845	-833352	847		p-conv	-178897	0	-1221889	1398430
			g-conv	0	178	-883	1225			g-conv	-178	0	-47439	47458
			rad	-4853	1308	0	1			rad	-1308	0	-39	52
5	1087 824	2005	cond	-4094	12	0	0	1128	1242	cond	-12	0	0	0
			p-conv	0	334725	833398	-1287884	858		p-conv	-334725	0	-1399423	1735070
			g-conv	0	220	-1225	1689			g-conv	-220	0	-47458	47175
			rad	-4888	1688	-1	2			rad	-1688	0	-52	89
4	1101 828	2887	cond	-5189	14	0	0	1140	3188	cond	-14	0	0	0
			p-conv	0	838413	1287851	-1808465	867		p-conv	-838413	0	-1735108	2374849
			g-conv	0	288	-1889	2871			g-conv	-288	0	-47178	48178
			rad	-4787	2085	-2	37			rad	-2085	0	-89	95
3	1157 883	5185	cond	-5288	-1	0	0	1154	11950	cond	1	0	0	0
			p-conv	0	1154488	1808534	-3083708	881		p-conv	-1154488	0	-2374818	3520187
			g-conv	0	-15	-2871	4013			g-conv	15	0	-48179	43318
			rad	-5816	-128	-37	0			rad	128	0	-88	-17
2	1157 884	14280	cond	-10043	0	0	0	1151	78529	cond	0	0	0	-1
			p-conv	0	-3085182	3083893	0	878		p-conv	3085182	0	-3520185	504418
			g-conv	0	-73	-4013	0			g-conv	-73	0	-43318	0
			rad	-11101	-821	0	-148			rad	821	0	17	-759

heat generated in streamer 43926
 heat generated in core 101198
 total heat generated 145122
 heat transferred to cooling wall -181208
 heat leaving top of riser -488374
 heat entering bottom of riser 504417
 total -43
 % diff. of heat gen. 0

case: sh8

I	streamer		g (W)	(W)				core		g (W)	(W)			
	temp (K and C)			west	east	north	south	temp (K and C)			west	east	north	south
22	889	314	cond	-4541	-3	0	0	877	898	cond	-3	0	0	0
	618		p-conv	0	802283	715840	-1504388	604		p-conv	-802283	0	-7158288	7954498
			g-conv	0	-288	-411	810			g-conv	288	0	-301178	300054
21	880	519	rad	-13278	-1006	-2	-3	877	897	rad	1006	0	0	-13
	807		cond	-5812	-1	0	0	804		cond	1	0	0	0
			p-conv	0	838356	1504425	-2330808			p-conv	-838356	0	-7958357	8797442
20	877	741	g-conv	0	-73	-810	1422	804		g-conv	73	0	-300049	288889
	803		rad	-12760	-271	3	-2	877	1159	rad	271	0	13	-6
			cond	-7138	0	0	0	804		cond	0	0	0	0
19	876	852	p-conv	0	889559	2330844	-3189288	804		p-conv	-889559	0	-8797313	8888830
	801		g-conv	0	11	-1422	1952			g-conv	-11	0	-288885	287895
			rad	-12528	42	2	-1	877	1288	rad	-42	0	5	0
18	874	1323	cond	-8503	1	0	0	804		cond	-1	0	0	0
	800		p-conv	0	894292	3189388	-4073191	877	1488	p-conv	-894292	0	-8668890	10581033
			g-conv	0	56	-1952	2497	804		g-conv	-56	0	-287891	288830
17	873	1537	rad	-12412	205	1	-1	877	1802	rad	-205	0	0	4
	800		cond	-8903	1	0	0	804		cond	-1	0	0	0
			p-conv	0	811838	4073262	-4875173			p-conv	-811838	0	-10560911	11472713
16	873	1872	g-conv	0	81	-2497	3052	877		g-conv	-81	0	-288827	285774
	800		rad	-12350	289	1	-1	804		rad	-289	0	-4	7
			cond	-11323	1	0	0	877	1825	cond	-1	0	0	0
15	873	2004	p-conv	0	922010	4875209	-5887535	804		p-conv	-922010	0	-11472595	12384492
	800		g-conv	0	87	-3052	3814			g-conv	-87	0	-285771	284733
			rad	-12319	356	1	0	877	1825	rad	-356	0	-7	10
14	873	2338	cond	-12753	1	0	0	804		cond	-1	0	0	0
	800		p-conv	0	924743	5887571	-8803027	877	1488	p-conv	-924743	0	-12394389	13318824
			g-conv	0	106	-3814	4178	804		g-conv	-106	0	-284730	283710
13	873	2617	rad	-12305	391	0	0	877	2008	rad	-391	0	-10	12
	800		cond	-14181	1	0	0	806		cond	-1	0	0	0
			p-conv	0	920407	6803049	-7714298			p-conv	-920407	0	-13318708	14238828
12	873	2887	g-conv	0	112	-4178	4738	806		g-conv	-112	0	-283708	282712
	800		rad	-12303	413	0	0	877	2084	rad	-413	0	-12	14
			cond	-15597	1	0	0	806		cond	-1	0	0	0
11	873	3104	p-conv	0	908405	7714355	-8815024	877	2292	p-conv	-908405	0	-14238508	15147353
	800		g-conv	0	118	-4738	5281	806		g-conv	-118	0	-282710	281748
			rad	-12308	428	0	0	877	2507	rad	-428	0	-14	18
10	873	3581	cond	-18991	2	0	0	806		cond	-2	0	0	0
	800		p-conv	0	894237	8815089	-9500738	877	2648	p-conv	-894237	0	-15147283	16040707
			g-conv	0	122	-5291	5838	806		g-conv	-122	0	-281748	280820
9	873	3867	rad	-12311	450	0	0	877	2853	rad	-450	0	-18	18
	800		cond	-18387	2	0	0	806		cond	-2	0	0	0
			p-conv	0	886448	9500749	-10378755	877	3048	p-conv	-886448	0	-18040824	18928081
8	873	4252	g-conv	0	127	-5838	6410	806		g-conv	-127	0	-280818	288918
	800		rad	-12318	469	0	8	877	3292	rad	-469	0	-18	20
			cond	-18744	1	0	0	806		cond	-1	0	0	0
7	873	4928	p-conv	0	879519	10378833	-11249852	877	3581	p-conv	-879519	0	-18825874	17804072
	803		g-conv	0	81	-8410	8840	806		g-conv	-81	0	-289918	288903
			rad	-12508	227	-8	-14	877	3853	rad	-227	0	-20	8
6	871	567	cond	-20883	2	0	0	806		cond	-2	0	0	0
	807		p-conv	0	892071	11249702	-11834228	877	4252	p-conv	-892071	0	-17803884	18484770
			g-conv	0	197	-6840	7313	806		g-conv	-197	0	-288991	288318
5	889	598	rad	-12173	721	14	-3	880	3048	rad	-721	0	-8	34
	808		cond	-22251	3	0	0	807		cond	-3	0	0	0
			p-conv	0	1134890	11834334	-13082861			p-conv	-1134890	0	-18484678	18828768
4	887	638	g-conv	0	240	-7313	7889	807		g-conv	-240	0	-288318	287282
	594		rad	-12100	880	3	-7	881	3439	rad	-880	0	-34	44
			cond	-22810	4	0	0	807		cond	-4	0	0	0
3	887	728	p-conv	0	1878585	13082888	-14838013	807		p-conv	-1878585	0	-18828878	21507124
	594		g-conv	0	314	-7888	8131			g-conv	-314	0	-287281	285427
			rad	-11982	1148	7	-8	882	4084	rad	-1148	0	-44	62
2	884	818	cond	-22848	5	0	0	882		cond	-5	0	0	0
	591		p-conv	0	3114518	14838125	-18047854	809		p-conv	-3114518	0	-21507093	24822833
			g-conv	0	400	-9131	11038			g-conv	-400	0	-285427	282182
1	882	897	rad	-11814	1480	9	-9	883	5747	rad	-1480	0	-82	85
	588		cond	-22888	6	0	0	810		cond	-6	0	0	0
			p-conv	0	5172703	18047733	-23220807			p-conv	-5172703	0	-24822724	28797584
0	881	9296	g-conv	0	491	-11038	14224	810		g-conv	-491	0	-282183	278528
	587		rad	-11882	1789	9	-7	888	10833	rad	-1789	0	-85	113
			cond	-22882	7	0	0	812		cond	-7	0	0	0
-1	881	14150	p-conv	0	8807830	23220898	-31834841	812		p-conv	-8807830	0	-28788002	38407470
	587		g-conv	0	574	-14224	19550			g-conv	-574	0	-278530	286702
			rad	-11802	2088	7	0	889	30045	rad	-2088	0	-113	144
-2	881	15150	cond	-23035	8	0	1	889		cond	-8	0	0	0
	587		p-conv	0	14354094	31834581	-48204633	815		p-conv	-14354094	0	-38408403	52752447
			g-conv	0	841	-19550	29799			g-conv	-841	0	-288708	248885
-3	889	25224	rad	-11802	2351	0	300	892	112849	rad	-2351	0	-144	189
	818		cond	-23341	1	-1	0	819		cond	-1	0	0	0
			p-conv	0	23446078	48204478	-68875338			p-conv	-23446078	0	-52753855	78113938
-4	890	248801	g-conv	0	77	-29800	42887	892		g-conv	-77	0	-248882	223488
	817		rad	-13284	289	-300	22	819		rad	-289	0	-170	-8
			cond	-148382	8	0	0	892	847735	cond	-8	0	0	-1
-5	890	248801	p-conv	0	-89835457	68874774	0	819		p-conv	89835457	0	-78114357	8372884
	817		g-conv	0	278	-42887	0			g-conv	-278	0	-223480	0
			rad	-85428	1088	-22	-802			rad	-1088	0	6	-1841

heat generated in streamer 339885
 heat generated in core 841345
 total heat generated 1181010
 heat transferred to cooling wall -808831
 heat leaving top of riser -8744018
 heat entering bottom of riser 8372883
 total 822
 % diff. of heat gen. 0